PATHOGENESIS OF ANTI-GRP78 AUTOANTIBODIES IN PROSTATE CANCER

CHARACTERIZING THE ROLE OF ANTI-GRP78 AUTOANTIBODIES IN PROSTATE CANCER AND THEIR CONTRIBUTION TO TUMOUR PROLIFERATION

By

Ali Al-Hashimi, Hons. B.Sc.

A Thesis

Submitted to the School of Graduate Studies

in Partial Fulfilment of the Requirements for the Degree Doctor of Philosophy

DOCTOR OF PHILOSOPHY (Ph.D.) (2016) McMaster University

Department of Medical Sciences Hamilton, Ontario, Canada

TITLE: Characterizing the role of anti-GRP78 autoantibodies in prostate cancer and their contribution to tumour proliferation.

AUTHOR: Ali Al-Hashimi (H. B.Sc. McMaster University)

SUPERVISOR: Dr. Richard C. Austin, Ph.D.

PAGES: xiv, 213

ABSTRACT

Prostate Cancer Canada estimates that sixty-five Canadian men will be diagnosed with prostate cancer (PC) daily, thus, PCa is the most frequently diagnosed cancer and the second leading cause of caner-related deaths in men. Currently, the etiology of PC remains under investigation and mechanisms of its growth and proliferation are yet to be fully characterized. This gap in knowledge places patients diagnosed with PC at risk of being under- or over-treated, and thus this thesis was dedicated to better understand the pathology of this disease.

We and others had demonstrated that the endoplasmic reticulum (ER)-resident molecular chaperone, termed GRP78, can translocate to the cell surface in some cancer cells, including PC, bladder, breast and leukaemia malignancies. In PC, cell surface GRP78 can bind to different ligands and elicit new functions such as activation of pro-survival and/or pro-apoptotic pathways. Furthermore, studies have found that cell surface GRP78 acts as an antigenic receptor leading to production of anti-GRP78 autoantibodies.

The overall objective of my PhD thesis was to study and identify new functions for cell surface GRP78 and define its impact PC tumour growth and proliferation. Based on my findings, we report a new function of cell surface GRP78 where it can modulate the activity of the major initiator of the coagulation cascade, tissue factor (TF), following the binding of anti-GRP78 autoantibodies to cell surface GRP78. Here, we demonstrated that the binding of anti-GRP78 autoantibody to cell surface GRP78 elicits an increase in cytosolic Ca^{2+} concentration, and leads to TF activation

on intact bladder carcinoma cells (T24/83). This finding was preceded by establishing a new technique of real-time measurement of TF activity in a continuous manner on intact cells.

In addition to its function as the major initiator of the coagulation cascade, TF contributes to angiogenesis in cancer biology. This raises the question whether anti-GRP78 autoantibodies can activate TF and contribute to enhanced tumour progression. Using the NOD/SCID mouse model, anti-GRP78 autoantibodies were shown to accelerate tumour growth of implanted DU145 PC cell line xenograft. This observed accelerated rate of tumour growth was reversed using a TF knock down DU145 cell line, emphasizing the requirement of TF expression to mediate this process. Finally, we demonstrate the ability of heparin and low molecular weight heparin molecules to interfere with the binding of anti-GRP78 autoantibodies to cell surface GRP78; *in vitro* and *in vivo* investigations demonstrate reduced TF activity and tumour progression, respectively. This likely involves the ability of heparin and low molecular weight heparin to bind to a reported heparin binding region in cell surface GRP78 that is also known to harbor the epitope for the anti-GRP78 autoantibodies. To our knowledge, this novel finding is the first to show a direct role for an autoantibody produced by the host immune system as the driver for tumour progression via TF. These findings have the potential to improve management of this disease which will help in improving quality of life for patients affected with PC.

ACKNOWLEDGMENT

This work would not be complete without the sincere acknowledgement of the indviduals who guided me along this rewarding academic journey.

First and foremost, I would like to thank my supervisor and scientific father, Dr. Richard Carl Austin, for coaching me and creating a positive collaborative environment in the lab which helped me grow into the scientist I am today. You helped me progress and grow into a collaborative and successful team player. When things got tough, you always made research interesting and found a way to help us overcome obstacles in our path. You provided me with many amazing opportunities, from conference presentations, book chapters publications, original scientific publications, and most importantly the independence to think, design experiments, problem-solve and perform experiemts. Your outlook on research is always optimistic, and incredibly motivating; whether it is a lunch out, an ice fishing adventure or a camping trip to the French River! To my committee members, Drs. Patricia Liaw and Peter Gross, thank you for your swift and firm direction. To Dr. Bobby Shayegan, thank you for your support and relaying your clinical experitise to drive this project into the success that it is today.

To members of the Austin laboratory, Sana Basseri, Sudesh Sood, Gabriel Gyulay, Sarka Lhotak, Edward Lynn, Elizabeth Crane, Celeste Collins, Celeste Bouchard, and Paul Francois-Burridge Lebeau, your friendship and technical support were imperative for the completion of this degree. It has been an enjoyable research and learning environment! You are the best research team a student can ask for!

To my parents, thank you for believing in me and supporting my decisions. Your support and kindness, dedication and hard work are the roots of my success and source of my inspiration. Without your guidance, sacrifices, and endless love and patience, I would not be where I am today. You taught me to be resourceful and confident in times of doubt. To my sisters, Dina, Asmaa, and Nancy your generosity, direction and support throughout this degree have been outstanding. I could not have completed this degree without you. Thank you for always being there and standing by my side. To my second family, Salma and Matthew, thank you for your advice and taking care of me during this degree. To Adam, ADAH! To Danya, thank you for your kind support and friendship. To Paul, our trips and adventures were really once-in-a-lifetime experiences! I look forward to many more camping trips (Hudson and Caspar are attending, of course) and world travel adventures. To Celeste Bouchard, your friendship, technical support and having a positive outlook on this world were much appreciated. To Bashar, after being away for so long, you are finally here! Thanks for your friendship and support from overseas. To Michelle, thanks for your support and sharing your rants about graduate school.

PREFACE

This thesis is prepared in the "sandwich" format as outlined in the "Guide for the preparation of Master's and Doctoral Theses" available through the School of Graduate Studies, McMaster University, Hamilton, ON. Chapter 1 of this thesis is a comprehensive general introcduction. The body of this thesis consists of 3 chapters (Chapter 2-4), each one an independent study, two of which are published and one is submitted for publication or under review at the time of the thesis submission. All submitted and published studies and manuscripts included in this thesis were written by the author of this thesis. The preamble section preceding each chapter describes the contributions of other authors to the multi-authored work. Finally, the discussion sections (Chapter 5-7) summarizes the conclusions of this thesis and draws out the overall implications.

TABLE OF CONTENTS

LIST OF ABBREVIATIONS

α_2M(*)	α_2-macroglobulin (activated)
α_2M BD	α_2-macroglobulin binding domain
Ad-βgal	β-galactosidase adenovirus
Ad-GRP78	GRP78 adenovirus
AMP	adenosine monophosphate
ANOVA	analysis of variance
APC	allophycocyanin
ATP	adenosine triphosphate
BAPTA	1,2-bis(2-aminophenoxy)ethane-N.N,N',N'-tetraacetic acid
BiP	binding protein
BSA	bovine serum albumin
Ca^{2+}	calcium
COX-A9	coxsackievirus A9
DIC	disseminated intravascular coagulapathy
DMSO	dimethyl sulfoxide
DNA	deoxyribonucleic acid
dsRNA	double stranded ribonucleic acid
DTT	dithiothreitol
EC	endothelial cell

EDTA	ethylenediaminetetraacetic acid
EGF1/2	epidermal growth factor-1/2
ELISA	enzyme linked immuno-sorbent assay
ER	endoplasmic reticulum
FACS	fluorescence-activated cell sorting
FBS	fetal bovine serum
FI(a)	factor I (activated)
FII(a)	factor II (activated)
FV(a)	factor V (activated)
FVII(a)	factor VII (activated)
FVIII(a)	factor VIII (activated)
FIX(a)	factor IX (activated)
FX(a)	factor X (activated)
FXI(a)	factor XI (activated)
FXII(a)	factor XII (activated)
GRP78	78 kDa glucose-regulated protein
GRP94	94 kDa glucose-regulated protein
HBSS	hanks basic salt solution
HEPES	4-(2-hydroxyethyl)-1-piperazineethanesulfonic acid
hr	human recombinant
HRP	horseradish peroxidase

HSP70	heat shock protein 70
IP_3	inositol triphosphate
K5	kringle 5
KDEL	lysine-aspartate-glutamate-leucine
LDL	low-density lipoprotein
LMWH	low molecular weight heparin
LPS	lipopolysaccharide
LRP	low-density lipoprotein receptor-related protein
MAP-70	70 kDa MHC-1 associated protein
MAPK	mitogen-activated protein kinase
MHC-1	major histocompatibility complex class I
micro Pg	microplasminogen
mini Pg	miniplasminogen
MTJ-1	murine tumor cell dnaJ-like protein-1
PAGE	polyacrylamide gel elecrophoresis
PAR	protease activated receptor
PBS	phosphate-buffered saline
PCA	procoagulant activity
PDI	protein disulfide isomerase
pfa	paraformaldehyde
Pg	plasminogen

PI_3	phosphatidylinositol 3
PS	phosphatidylserine
RBT	rabbit brain tromboplastin
RIPA	radioimmunoprecipitation
RNA	ribonucleic acid
ROS	reactive oxygen species
SEM	standard error of the mean
SERCA	sarco-(endo)plasmic reticulum Ca^{2+}-ATPase
SDS	sodium dodecyl sulfate
SMC	smooth muscle cell
TBS	tris-buffered saline
TBST	tris-buffered saline with tween-20
TF	tissue factor
TFPI	tissue factor pathway inhibitor
Tg	thapsigargin
Tm	tunicamycin
TNF-α	tumor necrosis factor-α
UPR	unfolded protein response
VEGF	vascular endothelial growth factor
VTE	venous thromboembolism

CHAPTER 1

GENERAL INTRODUCTION AND OBJECTIVES

1.0 Introduction

Prostate cancer (PC) is the second leading cause of death in Canadian men, and accounts for 25% of newly diagnosed cancer cases among Canadian men (Center et al., 2012; Jemal, Siegel et al. 2009). In addition to the inherent pathologies associated with PC, patients are prone to a hypercoagulable state that can contribute to worse prognoses and disabilities among cancer patients (Sousou and Khorana 2009; Sud and Khorana, 2009). Current evidence indicates that this prothrombotic state occurs on the surface of cancer cells due to the inherent overexpression and/or procoagulant activity (PCA) of tissue factor (TF) (Callander, Varki et al. 1992). In addition to its critical role in hemostasis and clot formation, TF also promotes tumour growth and metastasis (Rak, Milsom et al. 2006, Milsom and Rak 2008, Milsom, Yu et al. 2008). In fact, it is well-established that enhanced TF expression and/or procoagulant activity correlates with PC progression, angiogenesis and malignant phenotype (Abdulkadir, Carvalhal et al. 2000, Kaushal, Mukunyadzi et al. 2008).

1.1 Tissue Factor (TF)

1.1.1 The Role of TF in Hemostasis

In cases where injury is incurred, the body is equipped with a coagulation system to control bleeding by formation of a fibrin clot, the first step in repairing injury to the vasculature. Clot formation can be initiated via two main pathways, the intrinsic and extrinsic coagulation pathway (Figure 1) that merge into a common final pathway leading to fibrin polymerization and cross-linking. A cascade of zymogen

activations amplifies the coagulation cascade with the activated form of one clotting factor catalyzing the activation of the next clotting factor resulting in amplification of the clotting pathway (Berg, Tymoczko, & Stryer, 2002).

The intrinsic clotting pathway can be initiated by activated platelets phosphates and, the release of nucleic acids (DNA and RNA) by activated neutrophils and the exposure of anionic surfaces due to injury, such as the exposure of phosphotidylserine molecules, of the vasculature and results in the activation of factor XII (FXII). This anionic surface provides a binding site for the factors involved in the coagulation cascade. Once the intrinsic pathway is initiated, FXIIa activates factor XI (FXI), which in turn activates factor IX (FIX). Factor VIIIa (FVIIIa), Ca^{2+} and platelet factor, FIXa can activate factor X (FX). FXa generation is the first step of the common final pathway shared by both the intrinsic and extrinsic pathways. FXa and the Ca^{2+} cofactor, factor Va (FVa) and platelet factor, cleaves prothrombin (factor II) into its active form thrombin (factor IIa). Thrombin can then cleave fibrinogen (factor I) into fibrin monomers (Factor Ia), which have the ability to spontaneously polymerize into an ordered fibrin clot (Berg *et al.*, 2002).

Figure 1. The Coagulation Cascade

The coagulation cascade is comprised of the intrinsic and extrinsic pathways, which both merge into a common final pathway leading to fibrin polymerization and cross-linking. The intrinsic clotting pathway is initiated by the exposure of FXII and exposure of the anionic phosphotidylserine molecules due to injury of the vasculature and results in the activation of FXII. The extrinsic clotting pathway is initiated by the de-encryption of TF and the activation of FVIIa from damaged tissue as a result of trauma. FXa generation is the first step of the final common pathway which leads to thrombin and ultimately fibrin generation and crosslinking to form a clot.

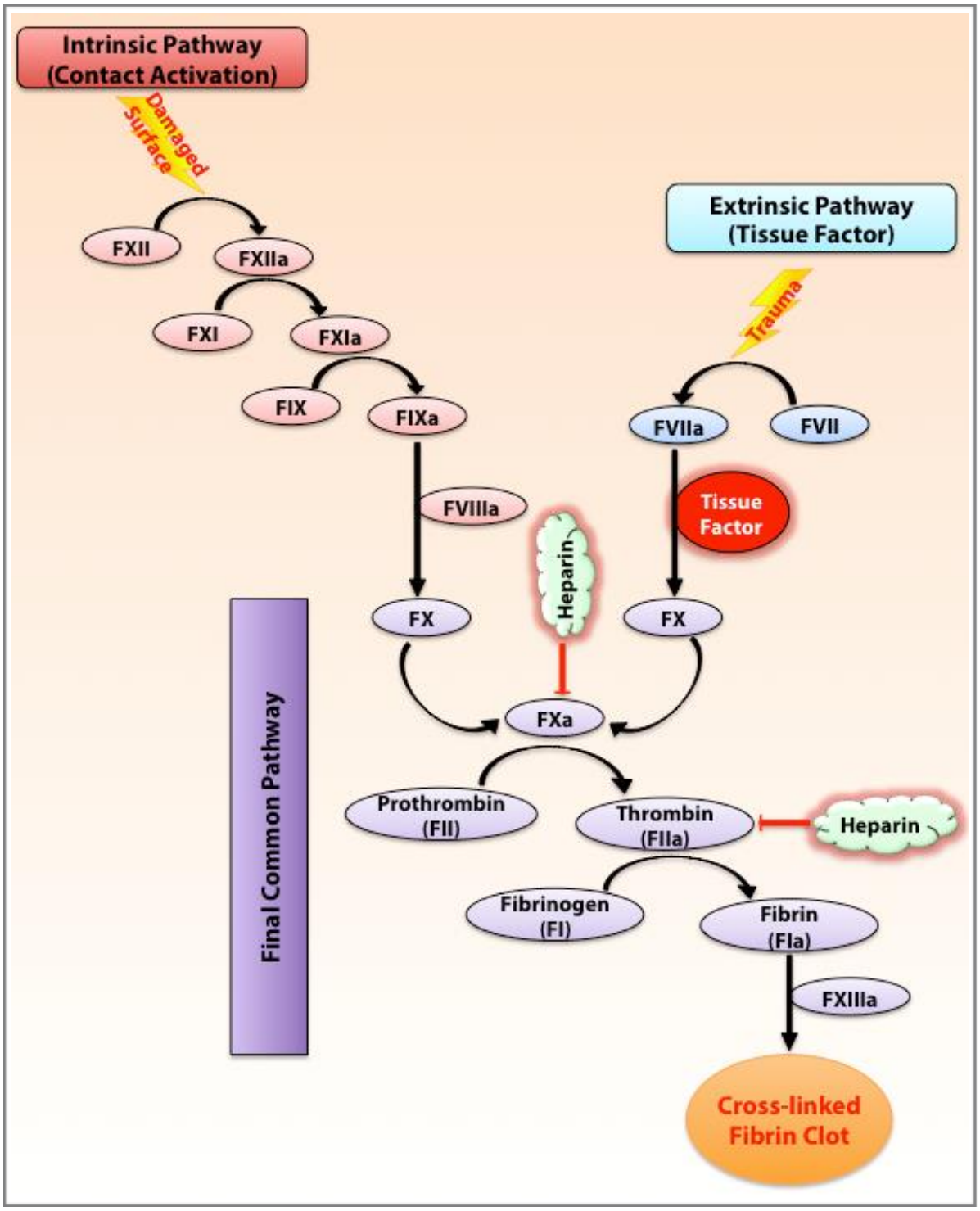
Intrinsic Pathway
(Contact Activation)
Damaged Surface
FXII
FXIIa
FXI
FXIa
FIX
FIXa
FVIIIa
FX
Extrinsic Pathway
(Tissue Factor)
Trauma
FVIIa
FVII
Tissue Factor
FX
Heparin
FXa
Final Common Pathway
Prothrombin
(FII)
Thrombin
(FIIa)
Heparin
Fibrinogen
(FI)
Fibrin
(Fia)
FXIIIa
Cross-linked
Fibrin Clot

The extrinsic clotting pathway is initiated by the de-encryption of tissue factor (TF) (factor III) and the activation of factor VIIa (FVIIa) from damaged tissue as a result of trauma. FVIIa then binds its receptor TF and becomes allosterically activated. TF also enhances the proteolytic capacity and amidolytic activity of FVIIa within the TF-FVIIa complex. TF-FVIIa complex formation decreases FVIIa flexibility and increases FVIIa catalytic site exposure, thereby significantly increasing the catalytic efficiency by greater than one million fold (Morrissey, 2001; Konigsberg *et al.*, 2001). FVIIa is a plasma serine protease coagulation factor that functions to activate FIX and FX (Ruf & Dickinson, 1998). The activated TF-FVIIa complex recruits FX to form the coagulation-initiation complex responsible for FXa generation and ultimately thrombin generation and fibrin clot formation (Berg *et al.*, 2002). The TF-FVIIa complex is able to activate FVII resulting in additional coagulation initiation complexes (Ruf & Dickinson, 1998).

The TF-FVIIa complex also plays a minor role in the intrinsic pathway of coagulation through its capability of activating FIX albeit at a slower rate (Ruf & Dickinson, 1998). Together with its cofactor FVIIIa, FIX can generate FXa (Berg *et al.*, 2002).

TF procoagulant activity (PCA) is defined as the ability of the TF-FVIIa complex to initiate coagulation leading to FX activation and ultimately thrombin generation. There are a number of systems in place to regulate TF PCA, with the most notable being TF pathway inhibitor (TFPI). Circulating TFPI can interact with FXa and this complex binds to the TF-FVIIa complex with a higher affinity creating a quaternary

complex of TF-FVIIa-TFPI-FXa (Hamamoto *et al.*, 1993). TFPI not only blocks TF-FVIIa coagulant activity within the quaternary complex (Hamamoto *et al.*, 1993), but it also promotes the internalization and degradation of TF-FVIIa (Iakhiaev *et al.*, 1999).

1.1.2 TF Structure

TF consists of 263 amino acids and is a member of the type II cytokine receptor family. TF is responsible for the initiation of the extrinsic pathway of the coagulation cascade (Martin, Boys, & Ruf, 1995). Due to post-translational N-linked glycosylation, the molecular mass of TF is 45 kDa (Spicer *et al.*, 1987). TF is encoded by a six exon, five intron 12.4 kb gene located on chromosome 1 of locus 1p22-23 (Mackman *et al.*, 1989). This cell surface glycoprotein is predominantly extracellular with a single pass transmembrane domain and a short cytoplasmic tail(Martin *et al.*, 1995). The N-terminal extracellular domain displays characteristics consistent with other cytokine receptors including a ligand binding site composed of two fibronectin type III domains and intracellular signalling capacity (Harlos *et al.*, 1994; Muller *et al.*, 1994). In terms of its signalling capacity, TF plays a role in tumour metastasis and angiogenesis which are unrelated to coagulation (Versteeg *et al.*, 2003; Bromberg *et al.*, 1995). The ligands capable of interacting with the fibronectin type III domains include epidermal growth factor-1 (EGF1), EGF2, the Gla domain and the protease domains on FVII (Banner *et al.*, 1996; Morrissey, 2001). TF also contains two disulfide bonds in the extracellular domain bridging Cys49 with Cys57 and Cys186 with Cys209 (Harlos *et al.*, 1994). The transmembrane domain of TF is

not specifically required for TF function, however membrane association is. Substitution of the TF transmembrane domain with other lipid domains, such as a phosphatidylinositol anchor, preserves TF function (Paborsky *et al.*, 1991). Although the cytoplasmic tail is essential for TF-FVIIa signalling (Ott *et al.*, 2005), it is not required for coagulation (Paborsky *et al.*, 1991) or TF encryption (Wolberg *et al.*, 2000).

1.1.3 TF Distribution, Cellular Localization and Expression

TF is expressed throughout the body, most notably in organ capsules, the adventitia of the vasculature including fibroblasts, pericytes and smooth muscle cells, and in epithelial layers as well as tumour cells (Drake, Morrissey, & Edgington, 1989). Typically TF is not expressed in vascular cells or other cells that come in contact with blood, however under certain thrombotic conditions such as sickle cell disease, hyperhomocysteinemia and vascular injury, or stimulation with lipopolysaccharides (LPS), IL-1β or tumour necrosis factor-α (TNF-α), TF expression is increased in monocytes and endothelial cells (EC) (Fryer, Wilson, Gubler, Fitzgerald, & Rodgers, 1993; Marmur *et al.*, 1993; Solovey, Gui, Key, & Hebbel, 1998; Eilertsen & Bjarne, 2004). The TF pathway may be involved in coronary artery diseases including atherosclerosis. TF is expressed on cells throughout atherosclerotic plaque, including smooth muscle cells (SMCs), monocytes, macrophages/foam cells, and within the extracellular matrix and the necrotic core (Wilcox *et al.*, 1989; Marmur *et al.*, 1996; Thiruvikraman *et al.*, 1996).

The highest level of TF expression is found in the placenta, lungs and brain and more specifically on cell types within these organs (trophoblasts, alveolar cells and astrocytes respectively) as well as epithelial cells surrounding organs, and adventitial fibroblasts surrounding blood vessels (Drake *et al.*, 1989b; Faulk *et al.*, 1990; Mackman *et al.*, 1993; Fleck *et al.*, 1990; Eddleston *et al.*, 1993; Flossel *et al.*, 1994; Luther *et al.*, 1996). This distribution provides a hemostatic envelope protecting these vital organs from exsanguination (Drake *et al.*, 1989b; Maly *et al.*, 2007). Intermediate levels of TF are found in the uterus, testes, intestine, kidneys and heart (Drake *et al.*, 1989b; Mackman *et al.*, 1993). Low level TF expression is found in the liver, skeletal muscle, thymus and spleen (Drake *et al.*, 1989b; Mackman *et al.*, 1993). These organs expressing low levels of TF rely on FVIIIa/FIXa of the intrinsic pathway of coagulation to prevent bleeding (Maly *et al.*, 2007). Cardiac myocytes but not skeletal myocytes constitutively express TF (Drake *et al.*, 1989b).

TF is required for embryonic development. TF knock-out mutations are embryonic lethal in the mouse, also there are no known TF-deficient human diseases (Bugge *et al.*, 1996; Carmeliet *et al.*, 1996). TF knock-out is lethal due to the loss of both hemostatic and non-hemostatic pathways (Carmeliet *et al.*, 1996). TF-deficient murine models (1% TF mouse model) do survive embryonic development, however these mice are prone to fatal spontaneous hemorrhages in the heart indicating the critical hemostatic role played by TF in this organ (Parry *et al.*, 1998; Pawlinski *et al.*, 2002).

Blood-borne TF or plasma TF is an additional source of TF contributing to and essential for rapid thrombus formation (Hathcock & Nemerson, 2004). Typical blood-borne TF levels in healthy patients are between 149 and 172 pg/ml which is significantly less than TF levels in the vessel wall (Koyama *et al.*, 1994; Albrecht *et al.*, 1996; Mackman, 2004). Studies have demonstrated that various diseases including sepsis, atherosclerosis, sickle cell disease and diabetes can increase blood-borne TF levels (Nieuwland *et al.*, 2000; Mallat *et al.*, 1999; Diamant *et al.*, 2002). Blood-borne TF typically occurs in the form of cell-derived microparticles (Berckmans *et al.*, 2001), however others have suggested that platelets contain TF (Siddiqui *et al.*, 2002) and that the major source of blood-borne TF is an alternatively spliced form of soluble TF (Bogdanov *et al.*, 2003).

1.1.4 TF and Cancer

The role of TF in malignant disease progression is an exciting new area in cancer research. A variety of hemostatic proteins including TF participate in tumour progression including angiogenesis, metastasis, and improved tumour survival. Although the molecular mechanisms are still unknown, TF signalling is emerging as a major player resulting in pro-tumourigenic gene upregulation and protein synthesis (Rak et al. 2006, Milsom et. al. 2008).

Aberrant TF expression is characteristic of a variety of human tumors including breast cancer, pancreatic cancer (Vrana *et al.*, 1996), lung cancer (Koomagi & Volm, 1998), colorectal cancer (Lykke & Nielsen, 2003), glioma (Hamada *et al.*, 1996), and prostate cancer (Adbulkadir *et al.*, 2000). Furthermore, TF expression correlates

with tumour invasiveness and metastatic potential (Lykke & Nielsen, 2003). Normally, constitutive TF expression is confined to the subendothelium, and only interacts with blood after vascular injury, however is apparent that with tumour progression the regulation of TF expression is lost (Drake, Morrissey, & Edgington, 1989b).

Hypoxia, and the loss of the tumour suppressor gene phosphatase and tensin homolog (PTEN) results in TF upregulation and TF PCA in malignant gliomas (Rong *et al.*, 2005). Additionally, the activation of K-ras oncogene and loss of the p53 tumour suppressor gene controlled TF expression in colorectal cancer cells *in vitro* (Yu *et al.*, 2005). Furthermore, the control of TF expression was dependent on mitogen-activated protein kinase (MAPK) and phosphatidylinositol 3-kinase (PI_3K) (Yu *et al.*, 2005).

-TF and Hypercoagulability

Hypercoagulability is common in cancer patients resulting in an increased risk of venous thromboembolism (VTE), pulmonary embolism, disseminated intravascular coagulapathy (DIC) and haemorrhage (Prandoni *et al.*, 2002). Moreover, this hypercoagulable state can contribute to tumorigenesis by supporting angiogenesis. This hypercoagulability is dependent on TF as demonstrated in human breast cancer cell lines; clot formation was FVIIa dependent and attenuated by anti-TF antibodies (Hu *et al.*, 1994). Additionally, the upregulation of TF is an independent predictor of VTE in ovarian cancer (Uno *et al.*, 2007) and is associated with VTE in

pancreatic cancer (Khorana *et al.*, 2007). Furthermore, the upregulation of TF has also been demonstrated to lead to the systemic release of TF positive microparticles (Yu *et al.*, 2005). TF positive microparticle levels can predict deep vein thrombosis DVT (Tesselaar *et al.*, 2007) and correlate with D-dimer levels (which strongly predict VTE in cancer patients) (Hron *et al.*, 2007).

Unfortunately, chemotherapy and radiotherapy worsen the prothrombotic events in cancer patients. Eleven percent of patients receiving chemotherapy have VTE every year, and hormone therapies (such as tamoxifen) increase this risk by an additional 2-3 fold (Goldhaber, 2005). Moreover, anti-angiogenic drugs are unexpectedly associated with a high incidence of thrombosis; however these results may be confounded since a number of clinical trials employed both anti-angiogenics and chemotherapeutics in combination (Marx *et al.*, 2002; Zangari *et al.*, 2004). While the effect of cancer therapies on the hypercoagulable state of patients is evident, the mechanisms are unknown; Lysov and colleagues had shown that an increase in tumour-secreted microparticles and cell-free DNA can be a contributor to this phenotype (Lysov *et al.* 2016). However, TF and TFPI are likely involved (Ma *et al.*, 2005). Treatment of endothelial cells *in vitro* with an inhibitor to vascular endothelial growth factor receptor-2 (VEGFR-2) in combination with chemotherapeutics (especially cisplatin and gemcitabine, at the traditional maximum-tolerated dose) triggered a significant increase in surface TFPI expression suggesting a procoagulant conversion of the ECs, however this

conversion was attenuated when the chemotherapeutics were administered at a lower metronomic dose (Ma *et al.*, 2005).

-TF and Angiogenesis

Angiogenesis is the process through which new blood vessels form from the existing vasculature and is essential for tumour growth since diffusion is insufficient beyond 2 mm (Folkman, 1990). TF-mediated angiogenesis occurs indirectly through clotting (Rak *et al.*, 2006) or through the release of proangiogenic factors (Zhang *et al.*, 1994) and directly through clotting-independent mechanisms (Hembrough *et al.*, 2003).

The TF indirect regulation of angiogenesis through clotting is partially mediated through TF-induced thrombin generation. The resulting fibrin clot creates a proangiogenic matrix facilitating blood vessel infiltration (Rak *et al.*, 2006). Coagulation also results in the release of proangiogenic factors from the granules of activated platelets. This engages additional angiogenic pathways that are dependent on FXa generation, thrombin, and protease activated receptor (PAR) -1 and -2 signalling (Griffin *et al.*, 2001; Zhang *et al.*, 1994). The overexpression of TF has been demonstrated to decrease the expression of thrombospondin (antiangiogenic) while increasing the expression of VEGF (proangiogenic) in melanoma cells (Abe *et al.*, 1999), fibrosarcomas (Zhang *et al.*, 1994), and gastric cancer cells (Zhang *et al.*, 2005). There is some controversy over whether TF overexpression regulates thrombospondin expression (Yu *et al.*, 2005; Zhang *et al.*,

1994), however it is well established that the cytoplasmic domain of TF is required for VEGF production in melanomas (Abe *et al.*, 1999) and in gastric cancer (Zhang *et al.*, 1994). A positive feedback loop exists which can drive additional TF expression with TF induction of VEGF on tumour cells and further promoting tumourigenesis (Zhang *et al.*, 1994).

The direct TF regulation of angiogenesis is proposed to involve TF's intracellular functions including PAR-2 signalling and activation of the MAPK family of proteins. TF plays a direct role in blood vessel formation since $TF^{-/-}$ mice are embryonic lethal due to hemorrhage from embryonic and extraembryonic vessels (Carmeliet *et al.*, 1996). Interestingly, inhibitors specific to the TF-FVIIa-FXa complex and to FXa revealed that angiogenesis is dependent on TF-FVIIa and independent of FXa, suggesting TF-FVIIa signalling is imperative to this function (Hembrough *et al.*, 2003). Furthermore, exposure of breast cancer cells to FVIIa induced the expression of various proangiogenic genes including VEGF (Albrektsen *et al.*, 2007; Ollivier *et al.*, 1998), urokinase-type plasminogen activator receptor (Taniguchi *et al.*, 1998), early growth response gene 1 (Camerer *et al.*, 1999), IL-8 (Albrektsen *et al.*, 2007; Hjortoe *et al.*, 2004) cysteine-rich angiogenic inducer (Ge *et al.*, 2003) and connective tissue growth factor (Albrektsen *et al.*, 2007). These proteins facilitate angiogenesis through cell adhesion, proliferation and migration (Bluff *et al.*, 2008).

Activation of the PAR-2 signalling pathway by TF-FVIIa has been suggested as a mechanism through which TF directly induces tumour angiogenesis. TF-FVIIa activation of PAR-2 is well established (reviewed in Rao & Pendurthi, 2005) and

recent data suggests this signalling is integral to breast tumour growth *in vivo* (Versteeg *et al.*, 2008). Moreover, angiogenesis mediated by TF-FVIIa signalling through PAR-2 is negatively regulated by the TF cytoplasmic domain. Deletion of the TF cytoplasmic domain resulted in accelerated angiogenesis in a murine model (Belting *et al.*, 2004). PAR-2 signalling has been demonstrated to specifically target the TF cytoplasmic domain for phosphorylation (Ahamed & Ruf, 2004) at Ser253 by protein kinase C and ser258 by a proline-directed kinase (Dorfleutner & Ruf, 2003). Additionally, PAR-2 signalling activates Rac which promotes cell motility through the recruitment of the β-arrestin scaffolding complex (Ge *et al*, 2003).

Finally, the proteolytic activity of TF-FVIIa has been demonstrated to activate the MAPK family including p42/p44 MAPK, p38 MAPK and c-jun N-terminal kinase (Versteeg *et al.*, 2000). Additionally, the MAPK pathway has been implicated in the VEGF upregulation of TF, since MAPK inhibitors attenuated this process (Guba *et al.*, 2005). While the exact mechanism of MAPK induced angiogenesis is unclear, MAPK has been associated with cell proliferation, however, the more probable mechanism involves MAPK phosphorylation of transcription factors responsible for inducing angiogenesis stimulating proteins (Bluff *et al.*, 2008).

-TF and Metastasis

Metastasis is the process through which tumour cells infiltrate the bloodstream or lymphatic vessels and migrate to distant sites to establish secondary tumors. This process is vastly dependent on the coagulation cascade, most notably on thrombin

generation (Palumbo *et al.*, 2007, Booden *et al.*, 2004). TF has been demonstrated to play a supporting role through fibrinogen-dependent and platelet-dependent restriction of natural killer cells (mediate micrometastase clearance) (Palumbo *et al.*, 2007). Interestingly, while the mechanisms are unclear, non metastatic breast cancer cells demonstrate low TF expression however metastatic breast cancer cells have abundant cell surface TF (Bluff *et al.*, 2006). Perhaps the TF-FVIIa generation of downstream coagulation factors plays a role; however, a promising hypothesis suggests that TF-FVIIa signalling stimulates cell motility.

Many studies have linked TF-FVIIa signalling to cell motility. Cleaving of the TF extracellular domain was demonstrated to result in the interaction of the TF cytoplasmic domain with actin-binding protein 280 which is involved in cell adhesion and migration *in vitro* (Ott *et al.*, 1998). Moreover, the PARs were implicated in conjunction with tyrosine kinase receptors in a study linking TF-FVIIa signalling and migration stimulated by platelet derived growth factor BB (Siegbahn *et al.*, 2000). PAR-1 is highly expressed and is activated by thrombin in invasive breast cancers but is absent in healthy breast tissue or non-invasive cancers (Booden *et al.*, 2004). A PAR-2 mechanism is involved in the migration of breast cancer cells *in vitro* independent of TF-FVIIa signalling (Jiang *et al.*, 2004); anti-PAR-2 antibodies inhibit IL-8 mediated migration in breast cancer cells (Hjortoe *et al.*, 2004). To further decipher the role of PARs in migration, siRNA determined that knockdown of PAR-2 but not PAR-1 impaired the migration of invasive breast cancer cells (Morris *et al.*, 2006).

The cytoplasmic domain of TF proves to be critical in the migration of porcine aortic ECs (Siegbahn *et al.*, 2005) and human bladder carcinoma cells (Ott *et al.*, 2005). TF seems to function as a negative regulator of chemotaxis through the suppression of $\alpha_3\beta_1$-dependent migration on laminin 5, however PAR-2-dependent phosphorylation of the TF cytoplasmic domain reversed this effect (Dorfleutner *et al.*, 2004). This suggests that TF-mediated cell motility is regulated by phosphorylation. Furthermore, TF is constitutively associated with $\alpha_3\beta_1$ on the surface of highly aggressive breast cancer cells (Versteeg *et al.*, 2008).

Finally, many *in vivo* models of human cancers support the role of TF in metastasis (Ngo *et al.*, 2007; Amarzguioui *et al.*, 2006; Bromberg *et al.*, 1995; Mueller *et al.*, 1992). The level of TF was found to correlate with the metastatic potential of melanoma cells injected into severe combined immunodeficiency mice (Bromberg *et al.*, 1995). Additionally, blocking of TF with anti-TF antibodies (Mueller *et al.*, 1992; Ngo *et al.*, 2007), the Fab fragment of TF antibodies (Mueller *et al.*, 1992), and siRNA (Amarzguioui *et al.*, 2006) all significantly inhibited the metastasis of melanomas and breast cancer. Interestingly, cytoplasmic TF signalling (Bromberg *et al.*, 1995; Mueller *et al.*, 1998) as well as the proteolytic activity of TF-FVIIa on the cell surface (Bromberg *et al.*, 1995) both proved to be integral.

-TF and Tumor Cell Survival

Resistance to apoptosis is a well-documented mechanism of malignant cell survival, and activation of anti-apoptotic pathways as well as defects in apoptosis promote

tumorigenesis and metastasis (Rao & Pendurthi, 2005). FVIIa is an established inducer of the anti-apoptotic pathways P42/44 MAPK and protein kinase B signalling (Dimmeler & Zeiher, 2000). Interestingly, studies overexpressing TF in human breast cancer cells (MCF-7) have demonstrated that the formation of the TF-FVIIa complex prevented apoptosis in a thrombin dependent pathway which initiated the phosphorylation of both P42/44 MAPK and protein kinase B/Akt resulting in survivin expression (anti-apoptotic protein) (Jiang, Guo & Bromberg, 2006). Additional data suggests that serum deprived baby hamster kidney and Chinese hamster ovary cells overexpressing TF demonstrate increased cell survival when supplemented with FVIIa (Sorensen *et al.*, 2003). Furthermore, loss of adhesion may be responsible for the anti-apoptotic properties induced by FVIIa since TF-FVIIa signalling has been demonstrated in the production of STAT5-dependent BclxL production and Jak2-dependent activation of protein kinase B (Versteeg *et al.*, 2004).

An additional mechanism through which TF promotes tumour cell survival is through protection against immune recognition and cytotoxicity. TF expressing colon cancer cells demonstrated a 40% invasion rate from peripheral blood monocytes dependent on the TF cytoplasmic domain (Li *et al.*, 2006). This could lead to increased cell survival and metastasis, however, the exact mechanism is not known.

1.1.5 TF Inactivation (Encryption)

Cell surface levels of TF do not directly correlate with TF PCA suggesting that TF exists on the cell surface in two distinct classes: encrypted and de-encrypted (Bach & Rifkin, 1990). Encrypted TF, while capable of binding factor VIIa, is unable to activate factor X effectively (Le, Rapaport, & Rao, 1992). TF encryption provides the cell with a mechanism of rapid hemostatic response without transcriptional upregulation of the TF gene. Many agents can significantly increase TF PCA including detergents (Carson, 1996; Carson *et al.*, 1996), Ca^{2+} ionophores (Bach & Moldow, 1997), and oxidants (Greeno *et al.*, 1996; Penn *et al.*, 1999; Penn *et al.*, 2000). TF expression and activity are independently regulated where some agents such as lipoproteins regulate the synthesis of *de-novo* TF, while other agents including oxidants promote the post-translational modification of encrypted TF to its active form (Penn *et al.*, 1999; Penn *et al.*, 2000). For example, the increase in TF PCA associated with oxLDL treatment also drives the transcription of TF mRNA while treatment with hydrogen peroxide (H_2O_2) only results in increased TF PCA (Penn *et al.*, 1999; Penn *et al.*, 2000; Bochkov *et al.*, 2002).

Since a large portion of expressed TF is exposed on the cell surface, various regulatory pathways are needed to maintain TF in an encrypted state to prevent unprovoked widespread coagulation (Drake *et al.*, 1989a). There are several proposed mechanisms regulating cell surface TF encryption including the formation of TF homodimers, the phospholipid microenvironment including phosphatidylserine (PS) exposure, TF compartmentalization in lipid rafts, the

endocytosis and degradation of the TF-FVIIa complex, and isomerization of the TF disulfide bond (Figure 2) (Kunzelmann-Marche *et al.*, 2000; Bjorklid & Storm, 1977; Sevinsky *et al.*, 1996; Roy *et al.*, 1991; Iakhiaev *et al.*, 1999). Although there are several proposed mechanisms of TF post-translational regulation, the mode of TF encryption varies between cell systems. Additionally, the mechanisms through which TF is decrypted are poorly understood and highly controversial.

Figure 2. Models of TF Inactivation (Encryption)

The five major models of TF encryption include TF dimerization, altered phospholipid asymmetry, TF compartmentalization in caveolae, TF-FVIIa Endocytosis, and TF disulfide bond isomerization. Panel A, the homodimerization of TF on the cell surface is proposed to maintain TF in a latent or encrypted state, TF is activated by the dissociation of the complex. Panel B, Anionic phospholipids are normally maintained on the inner leaflet of the plasma membrane creating a non-coagulant cell surface, however disruption to this asymmetry allows the exposure of anionic phospholipids on the outer leaflet resulting in TF de-encryption through a TF conformational change. Panel C, the sequestering of TF within caveolae is thought to increase self-associations thereby encrypting TF. TF not sequestered within caveolae is thought to be active however how TF escapes the caveolae is unknown. Panel D, TF-FVIIa endocytosis mediated by LRP and TFPI results in the degradation of the coagulation initiation complex thereby decreasing TF PCA. TF may also be recycled back to the cell surface however the mechanism is unknown. Panel E, TF with unpaired Cys186-Cys209 on the extracellular domain is thought to be encrypted, while disulfide bond formation is thought to de-encrypt TF. PDI is proposed to regulate TF PCA through disulfide bond formation and cleavage.

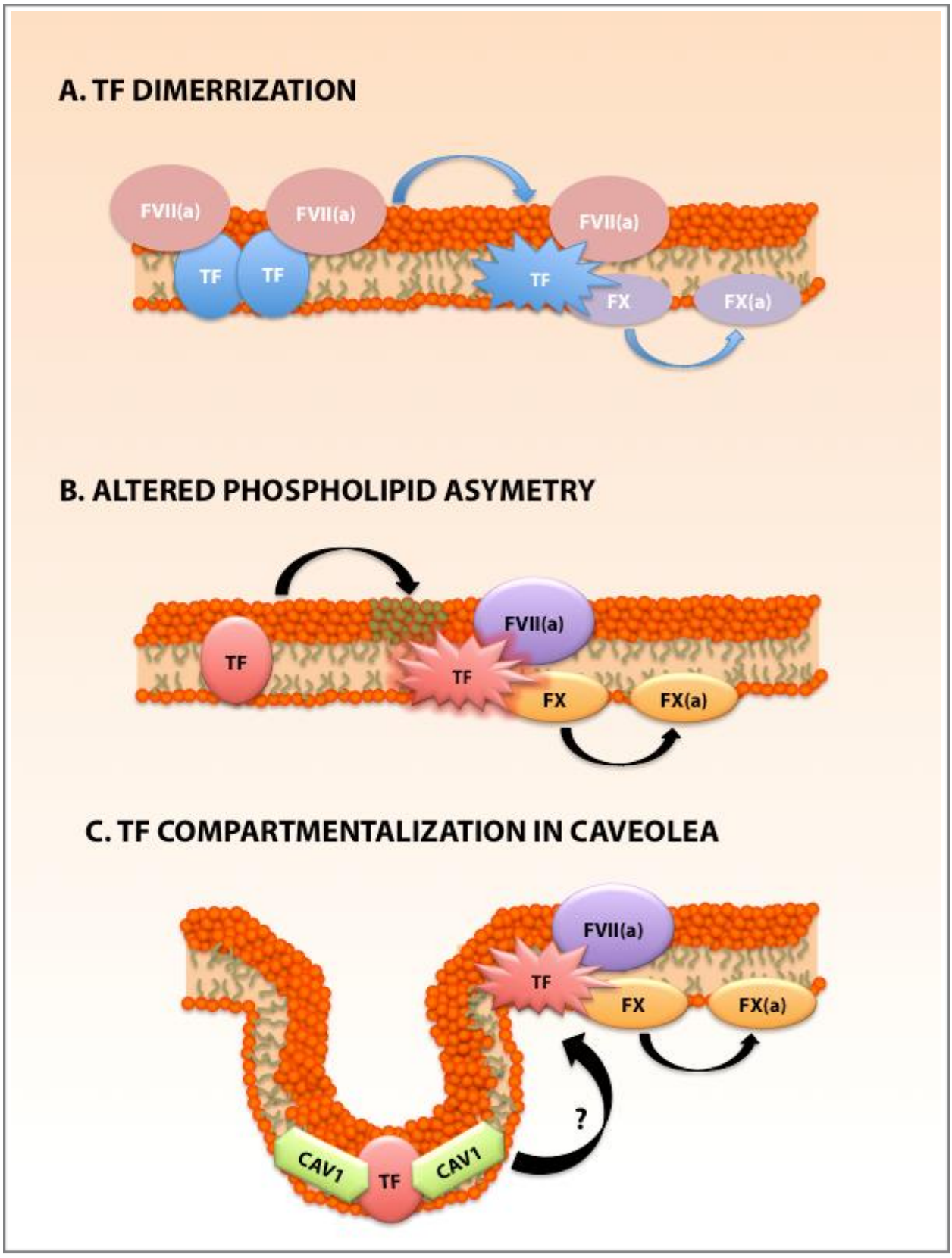
A. TF DIMERRIZATION
FVII(a)
FVII(a)
FVII(a)
TF
TF
TF
FX
FX(a)
B. ALTERED PHOSPHOLIPID ASYMETRY
TF
FVII(a)
TF
FX
FX(a)
C. TF COMPARTMENTALIZATION IN CAVEOLEA
FVII(a)
TF
FX
FX(a)
?
CAV1
TF
CAV1

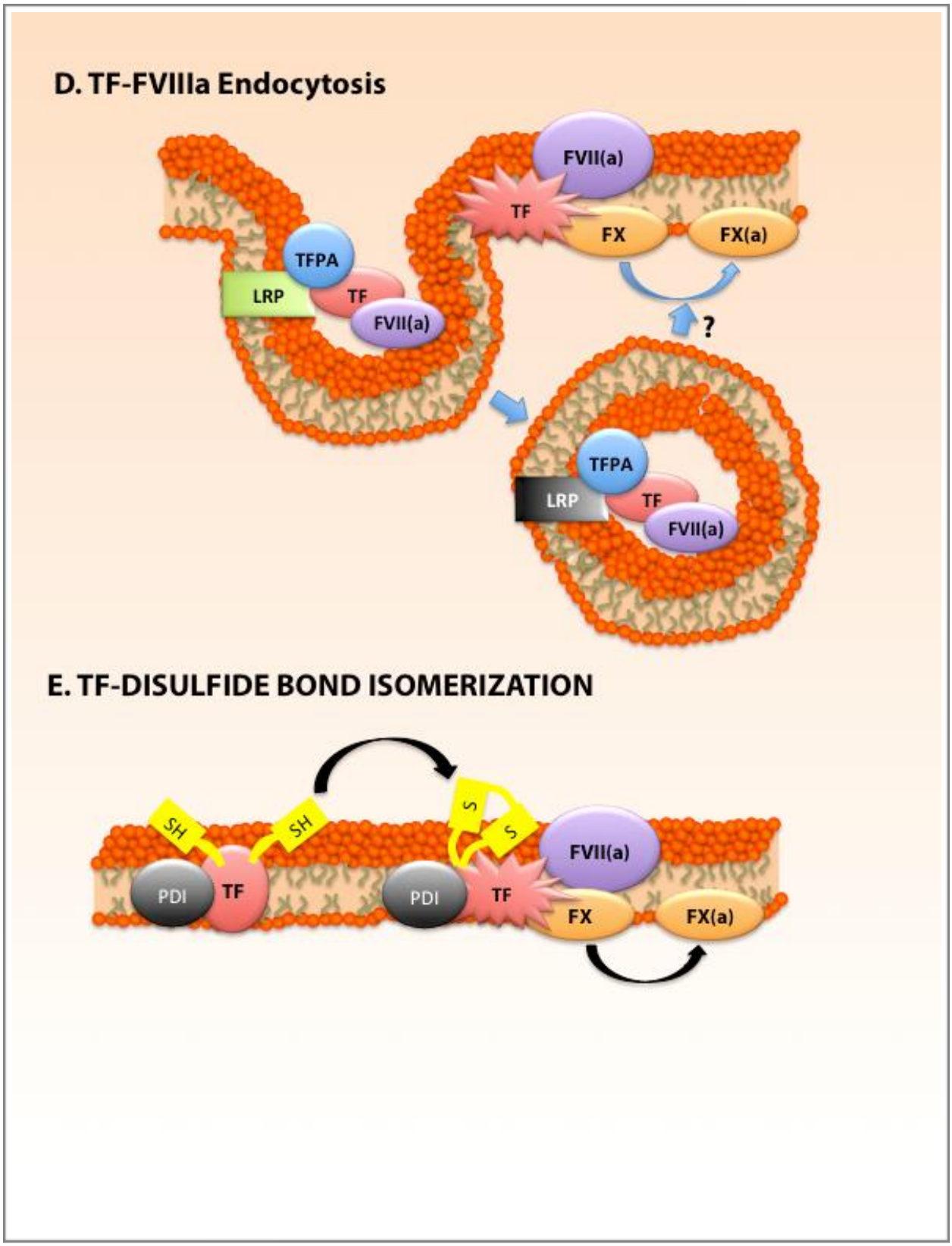
D. TF-FVIIIa Endocytosis
FVII(a)
TF
FX
FX(a)
TFPA
LRP
TF
FVII(a)
?
TFPA
LRP
TF
FVII(a)
E. TF-DISULFIDE BOND ISOMERIZATION
SH
SH
S
S
FVII(a)
PDI
TF
PDI
TF
FX
FX(a)

-TF Dimerization

The dimerization of exposed TF or the clustering of TF at the cell surface has been proposed as a mechanism of TF activation, and that deencryption requires the dissociation of TF homodimers into monomers (Bach & Moldow, 1997). Although TF dimers are still capable of binding FVIIa, proponents hypothesize that dimerization may sterically hinder the other binding sites on TF thus preventing the formation of the coagulation initiation complex and maintaining TF proteolytic inactivity (Bach & Moldow, 1997). Studies have demonstrated the ability of TF to form homodimers on the cell surface using chemical cross-linking studies (Roy, Paborsky, & Vehar, 1991). Additionally, an increase in cytosolic Ca^{2+} has been demonstrated to reverse TF dimerization (Bach & Moldow, 1997). Furthermore, it has been demonstrated that the extracellular domain of TF dimerizes in a purified *in vitro* system, and that this does not influence FXa generation, however it did increase FVIIa autoactivation (Donate *et al.*, 2000). Additionally, the observation that TF dimerization does not decrease FXa generation is contradictory to the TF dimerization model. Although this suggested model of TF regulation could aid in TF encryption, studies suggests that alone, TF dimerization likely does not influence TF activity (Donate *et al.*, 2000).

-Altered Phospholipid Asymmetry

The plasma membrane lipid-bilayer is composed of phospholipids distributed asymmetrically between the inner and outer leaflets. Typically, anionic phospholipids including phosphatidylserine (PS) and phosphatidylethanolamine (PE) are retained on the inner leaflet and choline-containing phospholipids such as phosphatidylcholine (PC) and sphingomyelin reside on the outer leaflet (Diaz & Schroit, 1996). The lipid transporters flippase, floppase and scramblase all perform independent functions resulting in the net inward movement of anionic phospholipids to the inner leaflet in quiescent cells dependent on ATP hydrolysis. Flippase is an aminophospholipid translocase that specifically traffics PS inward (Diaz & Schroit, 1996). Floppase is somewhat less specific and traffics phospholipids outward (Diaz & Schroit, 1996). Scramblase is Ca^{2+} dependent and traffics lipids bidirectionally (Zwaal, Comfurius & Bevers, 2005). When cells are perturbed and these proteins become enhanced or inhibited, the PS asymmetry can shift outward. A well established mechanism of cell surface TF regulation is the composition of the phospholipid microenvironment and the availability of anionic phospholipids, most notably PS, on the outer leaflet in close proximity to TF (Kunzelmann-Marche *et al.*, 2000; Bjorklid & Storm, 1977). Studies suggest that PS interacts with the TF-FVIIa complex aiding in the localization of the complex with FX resulting in a more rapid conversion of FX to FXa (Ruf *et al.*, 1991). Additionally, the calcium cations bound to the Gla domain of FX and other coagulation factors interact with the anionic charge of PS (Sunnerhagen *et al.*, 1995; Morrissey, 2001). Furthermore, blocking PS with

annexin V has been demonstrated to attenuate Ca^{2+} ionophore induced TF PCA (Wolberg *et al.*, 1999).

In addition to Ca^{2+} ionophores, other biologically relevant events including platelet activation by collagen and thrombin can disrupt PS asymmetry (Zwaal & Schroit, 1997; Thiagarajan & Tait, 1991). Apoptosis also induces PS asymmetry and TF PCA (Fadok *et al.*, 1992; Greeno *et al.*, 1996). Furthermore, many human diseases associated with increased risks of thrombotic events display increased PS exposure including: cancer, antiphospholipid antibody syndrome, diabetes, viral and bacterial infections, sickle cell anemia, malaria, thalassemia, and preeclampsia (Reviewed by Zwaal, Comfurius & Bevers, 2005). It is evident that PS accelerates coagulation on the cell surface, and there is no doubt that mechanisms resulting in the loss of PS asymmetry are directly linked to increased TF PCA, however whether PS functions to increase the associate of FX with the TF-FVIIa complex or functions to decrypt TF is unknown. Either way, maintenance of phospholipid asymmetry is a rational mechanism by which the cell maintains TF encryption.

-TF Compartmentalization in Caveolae

First proposed in 1975, TF compartmentalization within caveolae or lipid rafts provides an additional mechanism by-which TF encryption is governed (Maynard *et al.*, 1975). These caveolae are microdomains on the plasma membrane rich in glycosphingolipids and cholesterol, poor in anionic phospholipids, and contain caveolin-1 expression (Mulder *et al.*, 1996; Hofer & Brown, 2003; Fielding & Fielding,

2000). Lipid rafts are also microdomains rich in sphingomyelin and cholesterol and can exist as caveolae (Lupu *et al.*, 2005). Proponents of this theory suggest that this mechanism functions by sequestering TF, thereby increasing self-association and decreasing PCA (Bach, 2006) while also providing an environment non-conducive to TF activation (Mulder *et al.*, 1996). Evidence supporting this theory is the phenomenon by which TF PCA is greatly enhanced by the freeze-thawing of cells which in turn has been demonstrated to disrupt caveolae (Giesen & Nemerson, 2000). Additionally, the localization of TF to caveolae has been demonstrated in a number of cell types including SMCs (Mulder *et al.*, 1996a), ECs (Mulder *et al.*, 1996b), and fibroblasts (Mandal *et al.*, 2005). One major flaw in this theory is that FVIIa and TF antibodies are still capable of binding caveolae sequestered TF (Giesen & Nemerson, 2000), however the TF-FVIIa complexes formed within these microenvironments are not able to activate FX suggesting that TF is encrypted (Sevinsky *et al.*, 1996). TF encryption within these caveolae may be due to glycosphingolipid-rich environment and not due to physical sequestering of TF and self-associations (Sevinsky *et al.*, 1996). It has been demonstrated that TF expression is not uniform across the plasma membrane and that the distribution is not random (Maynard *et al.*, 1975). While the exact distribution of encrypted TF and decrypted TF is unknown, this theory would suggest that TF within lipid rafts is encrypted while TF elsewhere on the cell surface is de-encrypted (Bach, 2006). TF acylation at Cys245 on the cytoplasmic tail may target TF to lipid rafts (Bach *et al.*, 1988; Zacharias *et al.*, 2002). Some have suggested that TF acylation is the key to TF

encryption and that localization within the lipid raft is circumstantial (Bach, 2006). However several studies have demonstrated that the cytoplasmic tail of TF is not required for TF encryption or de-encryption (Carson & Bromberg, 2000; Wolberg *et al.*, 2000). Interestingly, cholesterol depletion independent of caveolae disruption has been demonstrated to attenuate TF PCA suggesting that cholesterol and not caveolae is integral to TF PCA (Lupu *et al.*, 1997; Crawley *et al.*, 2000; Westmuckett *et al.*, 2000). Additionally, TFPI has been localized to caveolae (Lupu *et al.*, 1997; Crawley *et al.*, 2000; Westmuckett *et al.*, 2000) however its role in TF PCA inhibition within the caveolae is ambiguous and controversial. Studies have demonstrated that within the caveolae TFPI attenuates TF PCA (Lupu *et al.*, 2005) while others reveal that TFPI is not required within this microdomain to decrease TF PCA (Dietzen *et al.*, 2003).

-TF-FVIIa Endocytosis

Another microdomain of the cell surface that may play a role in TF encryption in addition to lipid rafts and caveolae are clathrin-coated pits. Clathrin-coated pits are basket-like structures composed of clathrin and other specific cell surface receptors involved in receptor-mediated endocytosis (Alberts *et al.*, 1994). Ligand binding to the receptors initiates the invagination and pinching off of the pits forming clathrin-coated vesicles targeted to late endosomes for degradation (Alberts *et al.*, 1994; Iakhiaev *et al.*, 1999).

Clatherin-coated pits were suggested as a mechanism of TF encryption when TF was observed to co-localize with α-adaptin, a common protein composing clathrin-coated pits, upon the addition of FVIIa and TFPI. The result was a decrease in TF levels on the cell surface suggesting endocytosis of the coagulation initiation complex (Hamik *et al.*, 1999). Furthermore, blocking of the LDL receptor-related protein (LRP) prevented the decrease in TF cell surface levels suggesting that TFPI induces LRP-mediated endocytosis of TF at clathrin-coated pits (Hamik *et al.*, 1999). Additional studies in fibroblasts confirm that the TFPI-FXa complex induces LRP-mediated degradation of FVIIa complimented with a decrease of cell surface TF (Iakhiaev *et al.*, 1999). Interestingly, TF-FVIIa can be internalized in the absence of TFPI, however in this case TF is recycled back to the cell surface resulting in no change to total protein expression (Iakhiaev *et al.*, 1999). This second mechanism of TF-FVIIa endocytosis is suggested to be independent of LRP and mediated by non-clathrin coated pits (possibly caveolae). Transport of TF-FVIIa to early endosomes results in the dissociation of the complex and FVIIa is degraded while TF is recycled back to the cell surface (Iakhiaev *et al.*, 1999). Moreover, due to the differential expression of LRP in various cell types, these effects seem to be cell specific (Rao & Pendurthi, 2003).

-TF Disulfide Bond Isomerization

A novel controversial mechanism of TF encryption suggests that cryptic TF contains unpaired cysteine thiols on the extracellular domain at Cys186 and Cys209

and that decryption requires the formation of a Cys186-Cys209 disulfide bond (Ahamed *et al.*, 2006). TF contains four cysteine residues on the extracellular domain and the disulfide bond between Cys186 and Cys209 is allosteric since it bonds cysteines on adjacent stands of a single β-sheet (Chen *et al.*, 2006). It is well established that encrypted TF has a much lower affinity for FVIIa than active TF and many have reasoned that this change in affinities is due to a conformational change in TF. The post-translational modification of disulfide bond formation between Cys186 and Cys209 satisfies this reasoning and has been shown to be required for the activation of coagulation (Rehemtulla, Ruf & Edgington, 1991). Recent data supports the integral role played by the Cys186-Cys209 disulfide bond in maintaining the state of TF encryption (Chen *et al.*, 2006; Ahamed *et al.*, 2006). Additionally, adenoviral transduction of human umbilical vein endothelial cells (HUVECs) with alanine substitutions at Cys186 and Cys209 prevented disulfide bond formation demonstrating impairment in coagulation. However, TF signalling remained intact (Rehemtulla, Ruf & Edgington, 1991). Cryptic TF does maintain signalling function in conjunction with FVIIa, suggesting that disulfide bond isomerization is critical in the determination between TF signalling and coagulation (Ahamed *et al.*, 2006). Furthermore, treatment with thiol-oxidizing agents results in increased TF PCA suggesting the reduction-oxidation state of the disulfide bond is integral to TF encryption/decryption (Chen *et al.*, 2006). Oxidation of the disulfide bond has been demonstrated to alter the quaternary structure of TF and improve substrate binding to TF (Chen *et al.*, 2006).

Protein disulfide isomerase (PDI) is an oxidoreductase chaperone that functions in the ER to shuffle disulfide bonds during nascent polypeptide folding (Freedman, 1989; Gethind & Sambrook, 1992; Sitia & Braakman, 2003). Interestingly, co-localization of PDI and TF on the cell surface has been demonstrated using biotinylation assays and immunoprecipitation. PDI has been proposed as the switch responsible for TF disulfide bond oxidation and reduction resulting in TF PCA or TF encryption and cell signalling respectively (Ahamed *et al.*, 2006). The controversy surrounding this hypothesis is again worth mentioning since other groups have published recently with contradictory results. These studies could not show cell surface PDI or co-localized of PDI with TF (Pendurthi *et al.*, 2007). Additionally, shRNA knock-down of PDI showed no effect on TF signalling or coagulant function (Pendurthi *et al.*, 2007). Opponents of this hypothesis call attention to PDI being predominantly ER resident without a proper membrane attachment site (Turano *et al.*, 2002) inferring that cell surface levels of PDI would be in trace amounts at best (Pendurthi *et al.*, 2007).

1.1.6 Cellular Pathways Regulating TF PCA

There are many proposed mechanisms of TF de-encryption including elevated levels of intracellular Ca^{2+}, oxidative stress and apoptosis. These mechanisms are not entirely distinct as some overlap with the induction of anionic phospholipid asymmetry, and the oxidation of the TF disulfide bond. Once decrypted, TF binds FVIIa with higher affinity and this complex can catalyze FXa generation with efficiency (Le, Rapaport, & Rao, 1992).

-Intracellular Free Ca^{2+}

The availability of intracellular Ca^{2+} is a well established inducer of TF PCA (Bach & Rifkin, 1990; Carson *et al.*, 1994; Greeno *et al.*, 1996; Bach & Moldow, 1997; Wolberg *et al.*, 2000). In quiescent cells cytosolic Ca^{2+} levels are maintained around 100 nM by Ca^{2+} pumps and channels on organelle and plasma membranes (Orrenius *et al.*, 1989). Treatment of intact cells with Ca^{2+} ionophores will cause a rapid increase in TF PCA of approximately 100-fold over basal levels (Bach & Rifkin, 1990). Upon ionophore treatment, Ca^{2+} can be released from internal stores within the endoplasmic reticulum (ER) and/or through an influx of extracellular Ca^{2+} crosses the plasma membrane (Bakanay, Key & Bach, 2001). Ionophores including ionomycin and A23187 inhibit the plasma membrane Ca^{2+}-ATPase pumps preventing the export of Ca^{2+}. Other Ca^{2+} agonists including thapsigargin function to release Ca^{2+} stores into the cytosol by specifically inhibiting the sarco-(endo)plasmic reticulum Ca^{2+}-ATPase (SERCA) pumps (Thastrup *et al.*, 1990). Once cytosolic Ca^{2+} levels reach 4-fold over basal level, TF becomes de-encrypted and TF PCA is induced within 30 sec (Bakanay, Key & Bach, 2001; Bach & Moldow, 1997). While the impact of Ca^{2+} on TF decryption is undeniable, the mechanism is not distinct and involves membrane rearrangement and vesicular shedding (Carson, Perry & Pirruccello, 1994).

The same Ca^{2+} ionophore treatment that results in TF PCA also results in a disturbance in PS asymmetry. This phenomenon suggests that these two mechanisms may be coupled to collectively increase TF PCA (Bach & Rifkin, 1990;

Bach & Moldow, 1997; Wolberg et al., 1999; Bakanay, Key & Bach, 2001). As described previously, increased cytosolic Ca^{2+} levels inhibit flippase activity (responsible for inward PS trafficking) while also enhancing scramblase activity (bidirectional lipid movement). This results in a net outward movement of PS and therefore an increase in TF de-encryption and PCA (Zwaal & Schroit, 1997; Zwaal, Comfurius & Bevers, 2005). However, annexin V does not attenuate all Ca^{2+} ionophore-induced TF PCA suggesting that TF activation by Ca^{2+} ionophores is not solely regulated by anionic phospholipids (Wolberg *et al.*, 1999; Wolberg *et al.*, 2000). Ionomycin-induced TF PCA also results in the dissociation of TF dimers providing evidence for the TF dimerization model (Bach & Moldow, 1997). Also, some have demonstrated that Ca^{2+}-mediated TF PCA is calmodulin-dependent (Bach & Moldow, 1997; Bach & Rifkin, 1990).

Reactive oxygen species (ROS) have also been demonstrated to mediate the effect of increased cytosolic Ca^{2+} on TF PCA. Ca^{2+} efflux from the ER is known to increase the peroxidase activity of various enzymes including lipoxygenases and cyclooxygenases which both lead to the generation of ROS as a by-product (Pahl, 1999). High levels of cytosolic Ca^{2+} are also responsible for increased mitochondrial Ca^{2+} uptake resulting in oxidative stress due to disruption of the mitochondrial membrane potential and the electron transport chain (Dykens, 1994; Kowaltowski *et al.*, 1995). A cytotoxic cycle ensues whereby ROS leads to membrane peroxidation and increased permeability to Ca^{2+} resulting in a further influx (Orrenius *et al.*, 1989; Liu *et al.*, 1997; Liu *et al.*, 1998).

-*Oxidative Stress*

Many oxidants have the ability to increase TF PCA and some also induce *de novo* TF synthesis. Treatment of cells with aldehydes (Cabre *et al.*, 2004), oxidized phospholipids (Bochkov *et al.*, 2002) or oxLDL (Penn *et al.*, 2000) all increase TF PCA and TF protein levels on the cell surface. Interestingly, TF has been demonstrated to co-localize with oxLDL on the cell surface of macrophages (Lewis *et al.*, 1995). Increases in TF activity but not TF protein levels are the result of treatment with H_2O_2 (Penn *et al.*, 1999) and oxidized phospholipids (Weinstein *et al.*, 2000; Bochkov *et al.*, 2002). Additionally, TF PCA induced by oxLDL, thrombin and copper is attenuated by antioxidants (Crutchley & Que, 1995; Rota *et al.*, 1998; Penn *et al.*, 2000; Herket *et al.*, 2002; Banfi *et al.*, 2003). It is evident that the mechanisms responsible for TF expression and TF PCA in response to ROS are independently regulated.

The mechanisms through which TF PCA is induced by ROS are unclear, however lipid peroxidation, plasma membrane composition alteration and substrate binding site modification have all been suggested (Penn *et al.*, 2000). TF PCA induction by ROS is likely mediated through Ca^{2+}. It is well established that ROS inhibit ER Ca^{2+}-ATPases which results in increased cytosolic Ca^{2+} levels (Liu *et al.*, 1998; Stevens *et al.*, 2000). ROS can cause lipid peroxidation of the plasma and ER membranes resulting in increased permeability to Ca^{2+} and ultimately higher levels of intercellular free Ca^{2+} (Orrenius *et al.*, 1989; Liu *et al.*, 1997; Liu *et al.*, 1998). Additionally, lipid peroxidation of cardiolipin (a component of the mitochondrial

membrane) results in the dissociation of cytochrome c, triggering apoptosis and ultimately a Ca^{2+} influx (Ott *et al.*, 2002).

-Apoptosis

Apoptosis, or programmed cell death, begins with cell shrinkage and chromatin condensation followed by nuclear condensation and fragmentation (Saraste & Pulkki, 2000). Cellular extensions form and develop into apoptotic bodies which are pinched off from the plasma membrane in a process called blebbing (Saraste & Pulkki, 2000). Apoptosis can be induced by a number of agents including Ca^{2+} ionophores, cyclohexamides (Greeno *et al.*, 1996), and chemotherapeutic agents (Paredes *et al.*, 2003) all of which lead to increased TF PCA. One of the mechanisms through which apoptosis likely causes TF PCA is through the loss of anionic phospholipid asymmetry which is characteristic of early apoptosis (Martin *et al.*, 1995). As described previously, anionic phospholipids exposed on the outer leaflet increase interactions between TF and coagulation factors resulting in increased TF PCA (Carson, 1996; Hansen *et al.*, 1999; Barrowclife *et al.*, 2002; Sato *et al.*, 2004).

Both calcium agonists and oxidative stress can lead to apoptosis and are well established inducers of TF de-encryption. Increases in cytosolic Ca^{2+} from ER stores and influxes across the plasma membrane induce apoptosis and mediate increases in TF PCA through apoptotic pathways (Rizzuto *et al.*, 1993). Oxidative stress causes lipid peroxidation resulting in both apoptosis and increases in intracellular Ca^{2+} (Slater *et al.*, 1995). An example of this is the apoptotic agent

staurosporine which increases cytosolic Ca^{2+} and ROS leading to lipid peroxidation of the membranes and loss of mitochondrial membrane potential, resulting in increased TF PCA (Kruman *et al.*, 1998). It is obvious that the intricacies of Ca^{2+}, ROS, membrane disruption and apoptosis are all interconnected making it difficult to differentiate their individual effects on TF.

Interestingly, TF-FVIIa signalling displays anti-apoptotic effects (Sorensen *et al.*, 2003; Versteeg *et al.*, 2003). The addition of FVIIa to serum deprived cells has been demonstrated to inhibit apoptosis dependent on TF but independent of FXa or thrombin generation (Sorensen *et al.*, 2003; Versteeg *et al.*, 2003). The anti-apoptotic properties of TF signalling seem to be mediated through the PI3 kinase/Akt pathway (Sorensen *et al.*, 2003; Versteeg *et al.*, 2003). The TF overexpression associated with cancer likely results in the increased survival and enhanced metastasis observed in these cells (Versteeg *et al.*, 2003).

1.2 The Endoplasmic Reticulum (ER)

1.2.1 ER Function

The ER is a network of interconnected membrane bound vesicles responsible for processing secretory and cell surface proteins. This organelle provides a unique environment for nascent polypeptide folding, post-translational modifications, and quality control before transport to the Golgi apparatus for further modification. Nascent polypeptides translocate into the ER from ER membrane-bound ribosomes through the Sec61 complex (Sitia & Braakman, 2003). The redox potential of the ER lumen is oxidizing which is optimal for Cys-Cys disulfide bond formation (Sitia &

Braakman, 2003; Ma & Hendershot, 2004). Additionally, the ER contains a resting Ca^{2+} concentration of 400 μM making it the largest calcium store in the cell (Rizzuto *et al.*, 2003; Michalak *et al.*, 1999). Ca^{2+} is required for proper chaperone-nascent polypeptide and chaperone-chaperone interactions (Vassilakos *et al.*, 1998; Corbett *et al.*, 1999). Additionally, ER Ca^{2+} depletion from treatment with Ca^{2+} ionophores inhibits the secretion of various proteins from the ER further highlighting the importance of high Ca^{2+} concentrations (Lodish & Kong, 1990). The post-translational modification N-linked glycosylation is also catalyzed within the ER lumen. Interestingly, hypoglycosylated proteins (likely due to protein misfolding) have increased affinity for molecular chaperones supporting their role in post-translational modification (Dorner *et al.*, 1987). Mature, properly folded and modified proteins are transported out of the ER to the Golgi cis-face in coatomer protein (COP) II coated vesicles (Ellgaard & Helenius, 2003). Irrevocably damaged or misfolded proteins are disposed of through the ER-associated degredation (ERAD) pathway which involves the retro-translocation of proteins via the Sec61 translocon into the cytosol (Wiertz *et al.*, 1996). Damaged and misfolded proteins in the cytosol are targeted for degradation in the proteasome with ubiquitin (Meerovitch *et al.*, 1998).

1.2.2 ER Chaperone Proteins

Molecular chaperones within the ER lumen assist in correct protein folding as well as regulating protein quality control. These chaperones include PDI, ERpTZ, calreticulin, calnexin and the glucose-regulated protein (GRP) 78 and 94 (Ruddon &

Bedows, 1997). Unfolded or misfolded proteins are targeted by the chaperones to prevent the aggregation of misfolded proteins and maintain them in a conformation compatible with correct protein folding. Interestingly, multimers of GRP78, GRP94, and PDI have been found in association with immature immunoglobulins, however calreticulin and calnexin are not involved suggesting separate chaperone systems that are possibly governed by a functional or temporal basis (Meunier *et al.*, 2002). Molecular chaperones are typically attracted to misfolded proteins that are underglycosylated or have exposed hydrophobic domains to aid in correct protein folding (Ruddon & Bedows, 1997; Sitia & Braakman, 2003).

The glycoprotein folding chaperones calnexin and calreticulin recognize underglycosylated glycoproteins. Nascent glycoproteins are retained in the ER until they are properly folded by the addition of a glucose moiety which provides a binding site for calreticulin and calnexin (Vassilakos *et al.*, 1998; Spiro *et al.*, 1996). Glycoproteins are released from calnexin and calreticulin, allowing for proper protein folding, by the removal of the glucose moiety by glucosidase I and II (Michalak *et al.*, 1999). Once released, the oxidoreductase PDI catalyzes correct disulfide bond formation by reshuffling incorrect bonds and also ensures disulfide bond flexibility until correct protein folding is complete (Freedman, 1989; Gething & Sambrook, 1992; Sitia & Braakman, 2003). Interestingly, low Ca^{2+} levels (100 μM) in the ER result in PDI:calreticulin complex formation causing the dissociation of unfolded proteins. However, when Ca^{2+} levels return to normal (>400 μM) the chaperone complex dissociates thereby exposing the binding sites and encouraging

binding to unfolded proteins (Corbett *et al.*, 1999). This mechanism provides insight into how Ca^{2+} ionophores cause ER stress through the accumulation of unfolded proteins. Once released from calreticulin or calnexin, correctly folded proteins are transported to the Golgi apparatus, whereas unfolded proteins are re-glycosylated by UDP-glucose-glycoproteins glucosyltransferase (UGGT) thereby recreating the chaperone binding site (Michalak *et al.*, 1999).

The heat shock 70 (HSP70) family of ER chaperones recognize the inappropriate exposure of hydrophobic domains and includes GRP78 and GRP94 (Flynn *et al.*, 1991). Using ATP hydrolysis, GRP78 repeatedly binds unfolded proteins until no hydrophobic domains remain exposed (Gething, 1999). ATP binding to GRP78 opens the substrate binding domain allowing the interaction with hydrophobic domains (Zhu *et al.*, 1996; Gething, 1999). The DnaJ family of co-chaperones ER-localized DnaJ-domain containing proteins 1-5 (ERdj1, ERdj2 ERdj3, ERdj4, ERdj5) associate with GRP78 stimulating the hydrolysis of ATP to ADP (Chevalier *et al.*, 2000; Shen *et al.*, 2002; Cunnea *et al.*, 2003; Shen & Hendershot, 2005). The release of the protein from the substrate binding domain is mediated by the nucleotide exchange factor BiP-associated protein (BAP) which stimulates the conversion of ADP to ATP (Chung *et al.*, 2002). Moreover, mutations in the ATPase domain of GRP78 (Hendershot *et al.*, 1996) or low levels of ATP in the cell (Dorner *et al.*, 1990) blocks the dissociation of proteins from GRP78 thereby preventing their secretion. Dissociation of proteins from GRP78 allows correct protein folding and and

transport to the Golgi apparatus, however, if hydrophobic domains remain exposed then GRP78 will rebind until the protein is correctly folded (Hendershot *et al.*, 1996).

1.3 Glucose Regulated Protein of 78 kDa (GRP78)

1.3.1 GRP78 Structure

GRP78 is a member of the heat shock 70 family of proteins (Ron et. al. 2003, Misra, Gonzalez-Gronow, Gawdi, & Pizzo, 2005, Lee 2009). This soluble protein has two functional domains: an N-terminal domain with ATPase activity, and a C-terminal polypeptide binding domain containing an ER localizing KDEL sequence (Figure 3A) (Chevalier, Rhee, Elguindi, & Blond, 2000a; Misra *et al.*, 2005; Xiao, Chung, Pyun, Fine, & Johnson, 1999). The substrate binding domain of GRP78 contains two β sheets each composed of four antiparallel β strands as revealed by x-ray crystallography of the E. coli homologue DnaK. Together the β sheets form a sandwich containing five helical elements (Zhu *et al.*, 1996). Polypeptides bind to the channel formed by the β sandwich and are maintained within the binding domain by the helical elements which form a "hinged-lid" (Zhu *et al.*, 1996; Gething, 1999). The KDEL sequence, lysine-aspartate-glutamate-leucine, occupies the tip of the C-terminus and is expressed by many ER chaperones (Monro & Pelham, 1987). If found outside the ER, KDEL receptors on the cytosolic side of the ER membrane interacts with GRP78 molecules at the KDEL site to be transported back to the ER lumen (Munro & Pelham, 1987). Interestingly, GRP78 contains two putative transmembrane domains displaying significant hydrophobicity and trypsin sensitivity (Figure 3B) (Reddy *et al.*, 2003).

Figure 3. The Structure of GRP78

Representation of the 653 amino acid peptide sequence. The N-terminal ATPase domain and C-terminal substrate binding domain both contribute to the protein function. In addition to these, GRP78 contains two putative transmembrane domains as well as an N-terminal signalling domain which maintains signalling capacities. GRP78 is typically maintained within the ER lumen, however, if GRP78 escapes the ER, KDEL receptors on the ER can help being GRP78 molecules by interaction with their KDEL tag.

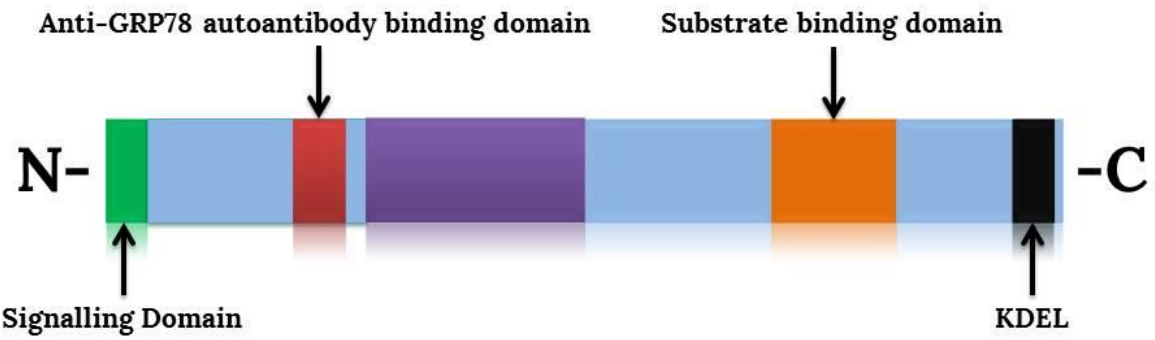
Anti-GRP78 autoantibody binding domain
Substrate binding domain
N-
-C
Signalling Domain
KDEL

While the function of GRP78 is most notably an ER resident molecular chaperone, many recent studies have shown the expression of GRP78 on the cell surface of relevant cell types during many pathological conditions including cancer (Arap *et al.*, 2004; Corrigall *et al.*, 2001; Liu, Bhattacharjee, Boisvert, Dilley, & Edgington, 2003; Misra *et al.*, 2005).

1.3.3 Cellular Localization of GRP78

-ER Stress and Cell Surface GRP78

GRP78 is typically maintained within the ER lumen by the KDEL ER retention sequence, however various KDEL-expressing chaperones such as PDI and calreticulin have been documented on the cell surface (Wiest *et al.*, 1997; Xiao *et al.*, 1999b; Shin *et al.*, 2003). Numerous studies have demonstrated the presence of GRP78 on the cell surface as well as GRP78 in cell culture medium and in the circulation (Xiao *et al.*, 1999a; Delpino & Castelli, 2002; Shin *et al.*, 2003; Liu *et al.*, 2003; Arap *et al.*, 2004). Additionally, cell surface GRP78 contains its KDEL sequence suggesting that preferential cleavage of this sequence is not a requirement for surface expression (Xiao *et al.*, 1999a). Interestingly, these studies were all performed using cancer cells or cells overexpressing GRP78 suggesting that cell surface GRP78 may only occur in under conditions where the protein is overexpressed (Delpin & Castelli, 2002; Shin *et al.*, 2003; Arap *et al.*, 2004). While cell surface GRP78 is well documented, the orientation of GRP78 on the cell surface is unknown. Further, there are no structural differences between cytosolic and cell

surface GRP78 proteins, however whether GRP78 is a true integral membrane protein or is dependent on associations with other cell surface proteins remains unclear (Reddy *et al.*, 2003). Additionally, the mechanism through which GRP78 translocates to the plasma membrane remains unknown since cell surface GRP78 is documented to retain the KDEL sequence (Xiao *et al.*, 1999a). There are three possible theories as to how cell surface GRP78 escapes the KDEL ER retrieval system. Firstly, during ER stress and GRP78 upregulation, the KDEL receptor may become saturated allowing excess GRP78 to translocate to the cell surface. Secondly, the down regulation of the KDEL receptor may occur under certain conditions thereby allowing GRP78 to move to the cell surface. Finally, a large body of evidence is suggestive of another protein aiding in the translocation of GRP78 to the cell surface (Misra *et al.*, 2005). This other protein could mask the KDEL sequence allowing GRP78 to escape ER retrieval.

-The Regulation of Cell Surface Levels of GRP78

Although the exact mechanisms are not known, hypoxia (Davidson *et al.*, 2005), ER stress (Delpino & Castelli, 2002) and the cochaperone murine tumour cell DnaJ-like protein 1 (MTJ-1) (Misra *et al.*, 2005) have all been shown to regulate cell surface levels of GRP78. Hypoxia has been identified as a mechanism of increasing cell surface levels of GRP78 (Davidson *et al.*, 2005). One study showed that when HT1080 human fibrosarcoma cells were starved for oxygen for 24 hours cell surface levels of GRP78 increased over 4-fold as determined by immunohistochemical

analysis (Davidson *et al.*, 2005). Endoplasmic reticulum stress has also been shown to increase not only ER resident GRP78 but also cell surface and secreted levels of GRP78 (Delpino & Castelli, 2002). Induction of ER stress with thapsigargin demonstrated a marked increase in cell surface GRP78 and secreted GRP78 as measured by a biotinylation assay and ELISA respectively (Delpino & Castelli, 2002). However, the mechanism of ER stress induced GRP78 transport to the cell surface, as well as its release into the media are not understood (Delpino & Castelli, 2002).

In addition to hypoxia and ER-stress, recent studies have demonstrated that the GRP78 cochaperone murine tumour cell DnaJ-like protein 1 (MTJ-1) also has the ability to regulate cell surface levels of GRP78 (Misra *et al.*, 2005). MTJ-1 increases the catalytic activity of GRP78 in addition to acting as a cochaperone to aid GRP78 in the translocation and correct folding of nascent polypeptides (Chevalier, Rhee, Elguindi, & Blond, 2000b). MTJ-1 is thought to be responsible for the translocation of GRP78 to the cell surface (Misra *et al.*, 2005). GRP78 and MTJ-1 associate together on the cell surface as established by co-immunoprecipitation assays of plasma membrane lysates (Misra *et al.*, 2005). Furthermore, silencing of the MTJ-1 gene by RNA interference blocks GRP78 from reaching the cell surface (Misra *et al.*, 2005).

1.3.3 Non-Chaperone Functions of GRP78

-Calcium Binding Protein

Like most molecular chaperones, GRP78 is a major Ca^{2+} binding protein that aids in maintaining ER Ca^{2+} balance (Lee, 2001; Lievremont *et al.*, 1997). GRP78, as well as other major Ca^{2+} binding chaperones, does not contain a putative Ca^{2+} binding

domain; however Ca^{2+} binds to paired anionic amino acids within the chaperone's structure (Lucero *et al.*, 1994). Although GRP78 contains the greatest number of anionic residues (111) it has few paired anionic residues (19) making its Ca^{2+} binding capacity 1-2 mole Ca^{2+}/mole GRP78 compared to PDI (23 mole Ca^{2+}/mole GRP78) and calreticulin (20 mole Ca^{2+}/mole GRP78) (Lucero *et al.*, 1994; Lievremont *et al.*, 1997). Interestingly, the overexpression of GRP78 increases the Ca^{2+} storage capacity of the ER (Lievremont *et al.*, 1997) and attenuates oxidant-induced fluctuations in Ca^{2+} and subsequent apoptosis (Liu *et al.*, 1998; Aoki *et al.*, 2001). Additionally, knock-down of GRP78 using anti-sense causes increases in intracellular free Ca^{2+} in response to H_2O_2 (Aoki *et al.*, 2001) or glutamate (Yu *et al.*, 1999) supporting the role of GRP78 in maintaining cellular Ca^{2+} homeostasis and preventing Ca^{2+} induced apoptosis.

The binding of Ca^{2+} to GRP78 may also influence the ATP/ADP binding domain (Lamb *et al.*, 2006). Ca^{2+} binding to GRP78 allows for quicker dissociation of ADP resulting in more efficient ATP binding (Lamb *et al.*, 2006). Since the binding of GRP78 to caspases is ATP dependent (Reddy *et al.*, 2003), Ca^{2+} binding to GRP78 may have consequences on its cytoprotective properties as discussed in the next section (Lamb *et al.*, 2006).

-GRP78 is The Primary Receptor for the α_2-Macroglobulin Signaling Pathway

α_2M is a class of proteinase inhibitors that target a variety of proteinases in the metallo-, serine-, aspartic acid and thiol- families (Cheng, Grima, & Stahler, 1990;

Misra *et al.*, 2002). When α_2M becomes irreversibly bound to a proteinase, α_2M undergoes a conformational change and is converted to its active state α_2M* (Gettins, 1995; Misra *et al.*, 2002). α_2M* then binds to and triggers a cellular receptor which results in a signalling cascade mediated by an influx of intracellular calcium, and elevates inositol phosphates as well as cyclic AMP (Howard *et al.*, 1996; Howard, Misra, DeCamp, & Pizzo, 1996; Misra, Chu, Rubenstein, Gawdi, & Pizzo, 1993; Misra, Gawdi, Gonzalez-Gronow, & Pizzo, 1999; Misra & Pizzo, 2002). This signalling pathway regulates cell survival and proliferation (Misra *et al.*, 2002; Misra *et al.*, 2004; Misra *et al.*, 2005). Additionally, α_2M* signalling through GRP78 regulates macrophage cell mobility by recruiting p21-activated protein kinase-2 (PAK-2) with the aid of the adaptor protein NCK to the plasma membrane for activation by tyrosine phosphorylation (Misra *et al.*, 2005). Activated PAK-2 in turn increases LIM kinase activity resulting in cofilin phosphorylation (actin binding protein), thereby inhibiting its depolymerization and regulating actin assembly and motility (Misra *et al.*, 2005). When this pathway was first described by Pastan and colleagues in the 1980's, two classes of receptors with different binding affinities were identified (Dickson, Willingham, Gallo, & Pastan, 1981; Hanover, Cheng, Willingham, & Pastan, 1983; Hanover, Willingham, & Pastan, 1983). A decade later, the lower affinity binding site was identified as the low density lipoprotein receptor-related protein (LRP) (Strickland *et al.*, 1990).

The LRP pathway is activated by numerous ligands and results in the transcriptional regulation of various proteins (Misra, Chu, Gawdi, & Pizzo, 1994a).

The LRP pathway is mediated by the activation of the pertussis toxin-sensitive G protein (Goretzki & Mueller, 1998; Misra, Chu, Gawdi, & Pizzo, 1994a; Misra, Chu, Gawdi, & Pizzo, 1994b; Misra, Gawdi, & Pizzo, 1999; Misra *et al.*, 2002). α_2M* has been shown to bind to LRP, however the signalling mechanism that results from α_2M activation is distinct from the mechanism observed with the binding of other LRP ligands suggesting that the primary receptor for α_2M* is independent of LRP (Goretzki & Mueller, 1998; Misra *et al.*, 1993; Misra, Chu, Gawdi, & Pizzo, 1994a; Misra, Chu, Gawdi, & Pizzo, 1994b; Misra, Gawdi, & Pizzo, 1999; Misra *et al.*, 2002). Differences include the activation of a unique G protein as well as the absence of receptor-associated protein (RAP) or Ni^{2+} antagonism observed with all other LRP ligands (Goretzki & Mueller, 1998; Misra *et al.*, 1993; Misra, Chu, Gawdi, & Pizzo, 1994a; Misra, Chu, Gawdi, & Pizzo, 1994b; Misra, Gawdi, & Pizzo, 1999; Misra *et al.*, 2002; Odom, Misra, & Pizzo, 1997). These results have allowed for the elucidation of the true receptor for α_2M* signal transduction.

Recent studies have shown that GRP78 has the highest binding affinity for the α_2M signalling pathway (Misra *et al.*, 2002; Misra *et al.*, 2004). Cell surface GRP78 has been shown to be necessary and sufficient for α_2M* signal transduction, while LRP is not (Misra *et al.*, 2002; Misra *et al.*, 2004). Antibodies directed against GRP78 compete for α_2M* binding sites, thereby abolishing the α_2M* increase in $[Ca^{2+}]$ and resulting signalling cascade (Misra *et al.*, 2002). GRP78 gene silencing through dsRNA homologs effectively attenuates α_2M* induced $[^3H]$ thymidine uptake, IP_3 and $[Ca^{2+}]$ increases, induction of Grb2, Sos, Shc and Raf-1, as well as the activation

of MEK1/2, ERK 1/2, p38 MAPK and JNK (Misra *et al.*, 2004). LRP ablation does not attenuate α_2M* signalling; α_2M* is still capable of eliciting a calcium response in these cells (Misra *et al.*, 2002).

-GRP78 and Pathology

The majority of studies assessing cell surface GRP78 have been performed using cancer cells or cells overexpressing GRP78, suggesting that cell surface GRP78 may be a phenomenon only observed under pathological conditions (Delpin & Castelli, 2002; Shin *et al.*, 2003; Arap *et al.*, 2004). Additionally, cell surface GRP78 levels correlate with various pathological conditions such as rheumatoid arthritis (Bläss *et al.*, 2001; Corrigall *et al.*, 2001), atherosclerosis (Liu *et al.*, 2003), and many cancers including prostate cancer, and melanomas (Arap *et al.*, 2004; Mintz *et al.*, 2003; Shin *et al.*, 2003). Patients with these various pathologies mount an autoimmune response to cell surface GRP78, and these GRP78 autoantibodies demonstrate important biological functions (Lee *et al.*, 2007; Dong *et al.*, 2008; Pfaffenbach *et al.*, 2011).

Rheumatoid arthritis is characterized by the chronic inflammation of the synovial joints and is a leading crippling autoimmune disease (Corrigall *et al.*, 2001). GRP78 has been identified on the cell surface of synovial cells and was demonstrated to be highly antigenic (Bläss *et al.*, 2001; Corrigall *et al.*, 2001). One study demonstrated that 63% of rheumatoid arthritis patients tested positive for GRP78 autoantibodies, while none of the healthy volunteers had GRP78 autoantibodies (Blass *et al.*, 2001). Furthermore, mouse models of arthritis develop GRP78 autoantibodies, however

intravenous injection of GRP78 into these mice prior to arthritis development completely inhibited arthritis (Corrigall *et al.*, 2001).

A recent study identifying unique molecular targets on the surface of atherosclerotic lesions demonstrated the presence of cell surface GRP78 (Liu *et al.*, 2003). Using phage biopanning in the atherosclerotic mouse model (ApoE protein knock out mouse model) *in vivo* and human lesions *ex vivo*, phage preferentially binding to cell surface GRP78 were identified (Liu *et al.*, 2003). Interestingly, unpublished data from our laboratory have demonstrated a significant increase in GRP78 autoantibodies in 25 week old $ApoE^{-/-}$ mice compared to younger $ApoE^{-/-}$ mice.

-Anti-GRP78 Autoantibodies and Cancer Pathologies

GRP78 is expressed on the cell surface of many different human cancers (Arap *et al.*, 2004; Mintz *et al.*, 2003; Shin *et al.*, 2003). Employing a phage biopanning technique, one study identified GRP78 as a tumourspecific cell surface antigen (Arap *et al.*, 2004). Biotinylation of cell surface proteins revealed GRP78 on the cell surface of neuroblastoma cells (SH-SY5Y), lung adenocarcinoma cells (A549), colon adenocarcinoma cells (LoVo), lymphoblastic leukemia-B cells (Sup-B15), ovarian tumourcells (Shin *et al.*, 2003), human rabdomiosarcoma cells (Delpino & Castelli, 2002), NG108-15 cells (Xiao et al., 1999), and thymic lymphoma cells (Wiest *et al.*, 1997). Immunofluorescence was also used to demonstrate cell surface GRP78 on the prostate adenocarcinoma cell lines 1-LN, PC-3 and DU145 as well as the melanoma

cell line DM413 (Gonzalez-Gronow *et al.*, 2006). Moreover, GRP78 autoantibodies have been isolated from the blood of patients with prostate cancer (Gonzalez-Gronow *et al.*, 2006) or kidney cancer (Pinthus & Austin, unpublished data), and autoantibody titers are correlated with advancing disease and poorer prognosis (Gonzalez-Gronow *et al.*, 2006). GRP78 autoantibody titers from healthy volunteers average ~7 μg/mL while the average prostate cancer patient displays titers of ~60 μg/mL with some individual patients expressing as high as 250 μg/ml (Gonzalez-Gronow *et al.*, 2006). Interestingly, the majority of GRP78 autoantibodies map to a specific N-terminal tertiary epitope on GRP78 (Leu98-Leu115) (Gonzalez-Gronow *et al.*, 2006). Recent studies have demonstrated that the autoantibodies are biologically important since they increase prostate cancer cell proliferation and survival *in vitro* (Gonzalez-Gronow et al., 2006). While the mechanisms are still not understood, it is clear that during the progression of atherosclerosis and cancer that GRP78 is expressed on the cell surface, and that GRP78 autoantibodies play a significant biological function in tumorgenesis. However, the role of GRP78 autoantibodies in atherosclerotic lesion development, and in thrombosis still remains unknown.

-GRP78 and Thrombosis

Recent work with cell surface GRP78 suggests a role for GRP78 in thrombosis (Bhattacharjee *et al.*, 2005). One study identified GRP78 on the cell surface and demonstrated that treatment with GRP78 antibodies induced an increase in TF PCA

(Bhattacharjee *et al.*, 2005). This study also showed evidence of a TF-GRP78 direct interaction using co-immunoprecipitation, however the association of TF and GRP78 was only possible when TF was overexpressed and whole cell lysates were employed, not purified plasma membrane extracts (Bhattacharjee *et al.*, 2005). In response to this data, a direct interaction between TF and GRP78 has been proposed as the mechanism through which GRP78 modulates TF PCA. In this report we show that GRP78 may in fact interact with TF, however, modulation of TF PCA occurs via an intracellular pathway. Moreover, Cytoscape® was used to visualize interactions between GRP78 and TF; no interaction was demonstrated between the two proteins (Figure 4).

Our previous study demonstrated that GRP78 overexpression inhibits TF PCA in a prothrombotic cell line (Watson *et al.*, 2003). Stable overexpression of GRP78 attenuates TF mediated thrombin generation without decreasing cell surface levels of TF (Watson *et al.*, 2003). These findings suggest that GRP78 inhibition of TF PCA is not due to ER retention, but rather an indirect Ca^{2+} mediated mechanism since the overexpression of GRP78 was also capable of decreasing TF PCA induced by ionomycin, H_2O_2 and adenoviral infection (Watson *et al.*, 2003).

Figure 4: Protein interaction for GRP78 and TF generated using Cytoscape®.

The molecular interaction network demonstrated that GRP78 and TF can interact with many proteins, however there was no direct interaction between each other. The figure was generated using InAct and InnctoDB-AII databases; GRP78 and TF were shown to interact with 220 and 87 proteins, respectively.

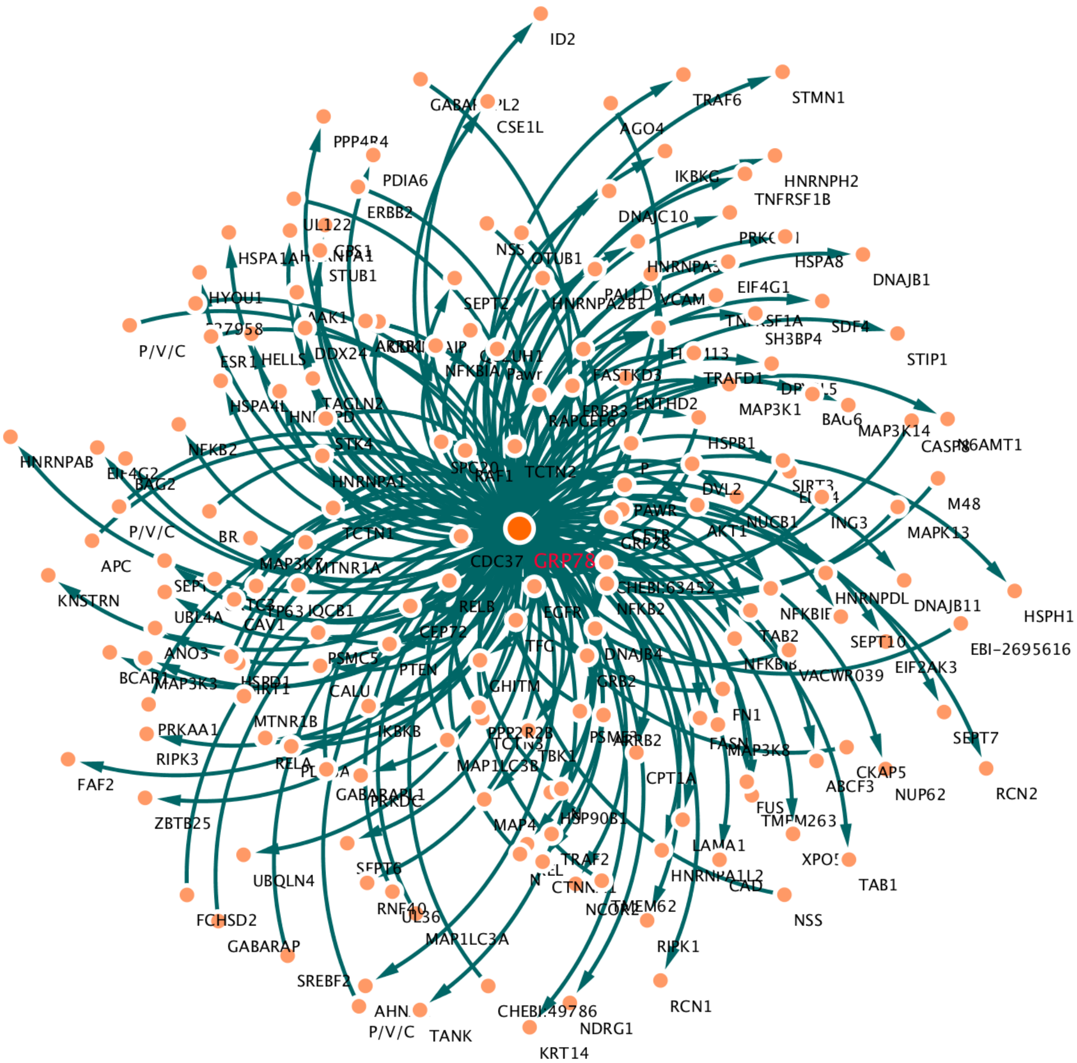
GRP78
CDC37
ID2
STMN1
TRAF6
AGO4
CSE1L
PPP4R4
PDIA6
ERBB2
IKBKG
HNRNPH2
TNFRSF1B
DNAJC10
PRKC
HSPA8
DNAJB1
EIF4G1
SDF4
STIP1
SH3BP4
HSPA1A
STUB1
HYOU1
P/V/C
HELLS
DDX24
SEPT2
NFKBIA
FASTKD3
ENTHD2
TRAFD1
MAP3K1
BAG6
MAP3K14
CASP8
N6AMT1
HSPA4L
TAGLN2
NFKB2
HNRNPAB
BAG2
HNRNPA1
STK4
SPC20
RAF1
TCTN2
HSPB1
DVL2
SIRT3
ING3
NUCB1
AKT1
PAWR
M48
MAPK13
HSPH1
DNAJB11
EBI-2695616
HNRNPDL
APC
TCTN1
MTNR1A
KNSTRN
UBL4A
CAV1
IQCB1
SEPT2
RELB
EGFR
NFKB2
TAB2
SEPT10
EIF2AK3
VACWR039
ANO3
BCAR
MAP3K3
PSMC5
PTEN
CALU
GHITM
DNAJB4
GRB2
FN1
SEPT7
RCN2
PRKAA1
RIPK3
MTNR1B
IKBKB
RELA
FAF2
ZBTB25
GABARAPL1
PRKDC
MAP1LC3B
CPT1A
ARRB2
MAP3K8
CKAP5
NUP62
ABCF3
FUS
TMEM263
XPO5
TAB1
UBQLN4
MAP4
HSP90B1
TRAF2
LAMA1
HNRNPA1L2
CAD
NSS
FCHSD2
GABARAP
RNF40
UL36
MAP1LC3A
TMEM62
RIPK1
RCN1
SREBF2
AHN
P/V/C
TANK
CHEBI:49786
NDRG1
KRT14

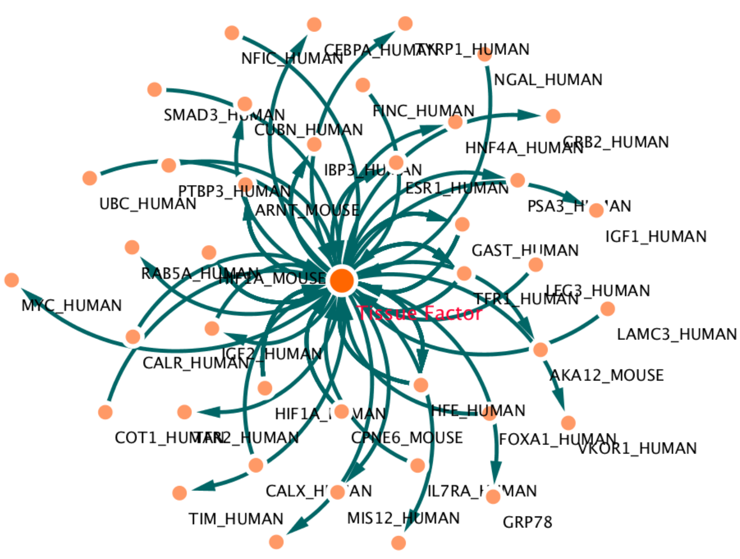
Tissue Factor
NFIC_HUMAN
CEBPA_HUMAN
TXRP1_HUMAN
NGAL_HUMAN
SMAD3_HUMAN
FINC_HUMAN
CUBN_HUMAN
HNF4A_HUMAN
GRB2_HUMAN
ESR1_HUMAN
UBC_HUMAN
PTBP3_HUMAN
ARNT_MOUSE
IGF1_HUMAN
GAST_HUMAN
RAB5A_HUMAN
HIF1A_MOUSE
TFR1_HUMAN
LEG3_HUMAN
MYC_HUMAN
LAMC3_HUMAN
CALR_HUMAN
IGF2_HUMAN
AKA12_MOUSE
HFE_HUMAN
COT1_HUMAN
TAR2_HUMAN
CPNE6_MOUSE
FOXA1_HUMAN
VKOR1_HUMAN
CALX_HUMAN
IL7RA_HUMAN
TIM_HUMAN
MIS12_HUMAN
GRP78

1.4 Hypothesis and Research Overview:

While it is clear that the expression of GRP78 on the cell surface of cancer cells is not coincidental, its actual function as a cellular receptor is still unclear. Cell surface GRP78 seems to have functions that are distinct from its chaperone activity. Some studies deemed that cell surface GRP78 possesses pro- and/or anti-tumourigenic properties, others have concluded that its an antigenic molecule leading to production of anti-GRP78 autoantibodies. Such functions were shown to depend on cell surface GRP78 binding partner. However, current knowledge lacks the understanding of the mechanism or consequence when physiological concentrations of these ligands are bound to cell surface GRP78.

Previously, Bhattacharjee and colleagues had determined that cell surface GRP78 can regulate TF and its proculagulant activity via direct interaction (Bhattacharjee, Ahamed et al. 2005); disruption of TF and GRP78 interaction resulted in increased TF activation. These findings, combined with the discovery of anti-GRP78 autoantibodies (Mintz, Gibo et al. 2003), have lead us to hypothesize that pathological concentrations of anti-GRP78 autoantibodies (60μg/mL) modulate TF actvity. This increased TF activation can results in enhanced tumour progression. To test this hypothesis, we pursued the following objectives: (1) To define the intracellular mechanism by which anti-GRP78 autoantibodies increase TF activation. (2) To determine how increased TF activation can affect tumour growth. (3) To identify means to alleviate the effect of anti-GRP78 autoantibodies on increased TF activation. These objectives were evaluated in the following chapters:

1.4.1 *Chapter 2*: Development of a continuous assay for the measurement of tissue factor procoagulant activity on intact cells

Published in: Laboratory Investigation (2010) **90,** 953–962; doi:10.1038/labinvest.2010.59; published online 8 March 2010.

Summary: To accurately measure TF activity, we established a new technique to where tissue factor activity can be measured in a continuous manner in real time on intact cells. This allowed us to identify molecules that may have delayed TF activation.

1.4.2. *Chapter 3*: Binding of Anti-GRP78 Autoantibodies to Cell Surface GRP78 Increases Tissue Factor Procoagulant Activity via the Release of Calcium from Endoplasmic Reticulum Stores

Published in: Journal of Biological Chemistry (2010). **285**, 28912-28923. doi: 10.1074/jbc.M110.119107; published online on 6 July 2010.

Summary: In this publication, the mechanism by which the binding of anti-GRP78 autoantibodies to cell surface GRP78 can increase TF activation in the bladder carcinoma cell line, T24/83. This involves activation of an intracellular mechanism where an increase in insisitol-triphosphate (IP3) molecules leads to increased cytosolic Ca^{2+} concentration, and subsequent membrane change resulting in increased TF activity.

1.4.3. Chapter 4: Cell Surface GRP78 Activation by Anti-GRP78 Autoantibodies Confers Tumor Growth via Tissue Factor, submitted to Cancer Cell.

Summary: In this publication, anti-GRP78 autoantibodies were shown to accelerate tumour growth in vivo. The expression of the TF protein was required for this process. Finally, heparin and low molecular weight heparin molecules were shown to interrupt the binding of anti-GRP78 autoantibodies to cell surface GRP78, subsequently, the effect of anti-GRP78 autoantibodies on accelerated tumour growth was reversed.

CHAPTER 2

LABORATOY INVESTIGATION PUBLICATION

Preamble

This chapter is an orginal published in the Laboratory Investigation journal

Lab Invest. 2010 Jun;90(6):953-62. doi: 10.1038/labinvest.2010.59. Epub 2010 Mar 8.

Authors' Contribution

J. Caldwell, J. Dickhout, A. Al-Hashimi and R.C. Austin designed the study. J. Caldwell and A. Al-Hashimi performed experiments and related analyses, performed Western blotting, conducted. R.C. Austin provided intellectual input. A. Al-Hashimi and R.C. Austin reviewed and edited the manuscript and all authors approved of the final submission.

Laboratory Investigation (2010) 90, 953–962

Development of a continuous assay for the measurement of tissue factor procoagulant activity on intact cells

Jennifer A Caldwell, Jeffrey G Dickhout, Ali A Al-Hashimi and Richard C Austin

Tissue factor (TF) is the major physiological initiator of the coagulation cascade and has an important function in the morbidity and mortality associated with many disease states, including cancer-associated thrombosis and atherosclerosis. TF normally exists in a partially encrypted state and its de-encryption on circulating monocytes, platelets or endothelial cells by inflammatory mediators can lead to thrombosis. Furthermore, many cancer cells express large amounts of TF and these cells communicate readily with the circulation through the fenestrated tumor endothelium. To assess agents or conditions that modulate the encryption state of TF, we developed a continuous assay for the determination of TF procoagulant activity (PCA) in a cell-based system. We have shown the use of this assay at detecting agents that de-encrypt TF thereby leading to an increase in TF PCA in three cancer cell lines, namely, T24/83 bladder carcinoma cells and PC-3 and DU145 prostate cancer cells. Further, through use of this assay, we have shown that the endoplasmic reticulum calcium pump inhibitor, thapsigargin, stimulates the de-encryption of TF. The continuous assay for the determination of TF PCA proved to have inherently less intra- and inter-assay variability than the widely used discontinuous assay and is considerably less labor intensive. Further, the continuous assay produced progress curves that were compatible with curve fitting to allow for the determination of the nature of reaction as well as rate constants for the underlying enzymes, TF/FVIIa and FXa. The continuous assay for the assessment of TF PCA on intact cells is applicable for high-throughput screening to allow for the determination of compounds that modulate TF PCA.
Laboratory Investigation (2010) **90,** 953–962; doi:10.1038/labinvest.2010.59; published online 8 March 2010

KEYWORDS: tissue factor; enzyme kinetics; thrombosis; encryption; chromogenic assay

Tissue factor (TF) is an integral membrane protein considered to be the major physiological initiator of the coagulation cascade. Induction of TF procoagulant activity (PCA) has direct implications in many diseases that increase the risk of thrombosis, including cancer[1] and atherosclerosis.[2] The coagulation cascade has been described as consisting of two pathways that lead to the formation of the fibrin clot: the intrinsic and extrinsic pathways.[3] The intrinsic clotting pathway is activated by the contact activation of FXII either through the exposure of blood to prosthetic devices or foreign substances.[4] The extrinsic clotting pathway is initiated by the de-encryption of TF and the activation of FVII to FVIIa. This description of the coagulation cascade has proven useful in diagnostic tools. However, the division between these pathways does not occur *in vivo* where clotting is initiated through the action of TF whereas the intrinsic pathway may behave as an important amplifier of the coagulation system.[5]

Cell-surface levels of TF do not directly correlate with TF PCA, suggesting that TF exists on the cell surface in two distinct forms: encrypted (dormant) and de-encrypted (active).[6] TF encryption provides the cell with a mechanism to elicit a rapid hemostatic response without transcriptional upregulation of the TF gene while minimizing deleterious clot formation. Many agents, including detergents,[7] Ca^{2+} ionophores[8] and oxidants,[9] can significantly increase TF de-encryption leading to the amplification of TF PCA. Because a large portion of expressed TF is exposed on the cell surface, various regulatory pathways are necessary to maintain TF in an encrypted state to prevent unprovoked

Division of Nephrology, Department of Medicine, St Joseph's Healthcare Hamilton and Hamilton Centre for Kidney Research, McMaster University, Hamilton, ON, Canada
Correspondence: Professor RC Austin, PhD, Division of Nephrology, Department of Medicine, St. Joseph's Healthcare Hamilton and Hamilton Centre for Kidney Research, McMaster University, 50 Charlton Ave. E, Hamilton, ON L8N 4A6, Canada.
E-mail: raustin@thrombosis.hhscr.org

Received 31 August 2009; revised 20 November 2009; accepted 12 January 2010

widespread coagulation.[10] There are several proposed mechanisms for regulating cell-surface TF encryption including the formation of TF homodimers, the phospholipid microenvironment (phosphatidylserine exposure), TF compartmentalization in lipid rafts, the endocytosis and degradation of the TF/FVIIa complex and isomerization of the TF disulfide bond.[11–13] Although several mechanisms of TF post-translational regulation have been proposed, the mode of TF encryption varies between different cell systems. In addition, the mechanisms through which TF is de-encrypted are poorly understood and highly controversial.

In this context, direct measurement of TF protein expression may not accurately represent the thrombogenicity associated with TF due to post-translational modifications that influence TF PCA.[14] Measuring TF PCA can be achieved by using a two-stage (discontinuous) clotting assay.[15–17] In this assay, cells are treated for a predetermined period of time with a test agent followed by incubation with a cocktail solution containing FX and FVIIa. After incubation, the reaction is terminated at a set time point and TF PCA is determined by measuring product formation. This two-step clotting assay is the gold standard methodology for measuring TF PCA. However, it is a labor-intensive method limiting the number of samples that can be run simultaneously and uses a single end point determination of product formation occurring during the putative exponential phase of the progress curve. This approach allows for variations in reaction time occurring during the first stage to produce wide variability in product output in the second stage. Further, the arbitrary assignment of the test agent's incubation time in the first stage, especially if the effects of the agent on TF PCA are unknown, makes the assay prone to false-negative results if used as a screening tool.

In this report, we propose a modified version of this gold standard assay: the continuous kinetic assay. Thus, we have combined both steps of the discontinuous assay into a single-step kinetic assay. This technique produces a progress curve of product formation over time where the rate constants of the TF/FVIIa complex and FXa action can be determined. Further, due to its single-step nature the assay is applicable for use in high-throughput screening of test substances with unknown effects or durations of action on TF PCA. In this assay, measuring TF PCA is dependent on a series of cleavages mediated by serine proteases. However, we acknowledge that certain limitations may arise from the introduction of a test agent that can either cleave the chromogenic substrate directly, independent of TF activation, giving a false-positive result, behave as a serine protease inhibitor and therefore interfere with the action of the TF/FVIIa complex or that of FXa on the chromogenic substrate, or result in cell lysis. However, in light of the fact this method is composed of only one step combined with the automative nature of the assay, it can be applied in high-throughput screening format that can be used to determine both activators and inhibitors of TF PCA.

MATERIALS AND METHODS

Cell Culture

The human bladder carcinoma cell line T24/83 was obtained from American Tissue Culture Collection (ATCC) (Rockville, MD, USA) and was cultured in M199 medium supplemented with 10% fetal bovine serum (FBS), 100 μg/ml penicillin and 100 μg/ml streptomycin. The prostate cancer cell lines, PC-3 and DU145, were obtained from ATCC. PC-3 cells were grown in F-12K medium containing 10% FBS, 100 μg/ml penicillin and 100 μg/ml streptomycin. DU145 cells were grown in Eagle's minimum essential medium containing 10% FBS, 100 μg/ml penicillin and 100 μg/ml streptomycin. Cells were cultured at 37°C in humidified air with 5% CO_2. The 7-aminoactinomycin D (7-AAD) (Beckman Coulter, Fullerton, CA, USA) viability dye was used to determine the percentage of cell survival after treatment with various agonists used in the TF PCA assay according to the manufacturer's instructions.

TF PCA Agonists

Ionomycin (Sigma-Aldrich, St Louis, MO, USA) was diluted to a final concentration of 1–20 μM. Ionomycin is a known inducer of TF PCA for the discontinuous assay and was diluted and incubated on cells for 10 min as well as used in the continuous assay. Hydrogen peroxide (Sigma-Aldrich) was diluted to a final concentration of 1–20 mM and incubated on the cells for 1 h in the discontinuous assay and also used in the continuous assay. Thapsigargin (Sigma-Aldrich) was diluted to a final concentration of 1–20 μM and determine by the continuous assay to increase TF PCA. The nonionic detergent Triton X-100 (0.01% v/v) was also used as a TF PCA agonist in the continuous assay for curve fitting experiments.

Discontinuous TF PCA Assay

Cell-surface TF PCA was measured using the chromogenic reporter substrate S-2765, as described previously by Watson *et al*.[15] Briefly, cells were seeded into a 24-well plate and upon reaching confluence washed in 1 × Tris-buffered saline (TBS). Treatment times and concentrations varied according to the reagent used; however, all treatments were diluted in cell culture media lacking FBS and antibiotics. The plates were maintained at 37°C and a cocktail containing 0.5 nM of FVIIa (Enzyme Research Laboratories, South Bend, IN, USA) and 15 nM of FX (Enzyme Research Laboratories) in 1 × TBS was added to each well to a final volume of 304 μl. At timed intervals, 15 μl of 100 mM $CaCl_2$ was added to each well and allowed to incubate for 30 min. After incubation, 250 μl of the reacting solution was transferred to a 96-well plate containing 25 μl of 0.2 mM S-2765 (Chromogenix, Lexington, MA, USA) and incubated for 3 min. The reaction was terminated with 20 μl of 50% acetic acid. The absorbance at 405 nm was determined using a spectrophotometer (Spectromax PLUS) and SOFTmax Pro software (Molecular Device, Sunnyvale, CA, USA). A standard curve was generated

where 100 U of TF activity was defined as the amount of activity in 3 μl of purified rabbit brain thromboplastin (Dade Behring, Deerfield, IL, USA), which is equivalent to 900 μg of TF (as determined by the American Diagnostica ELISA, Stamford, CT, USA). Each well was lysed with RIPA buffer (0.1% SDS). Total protein was calculated using the DC Protein Assay (Bio-Rad, Richmond, CA, USA) according to the manufacturer's instructions and described below. Cell-surface TF PCA was calculated as the amount of FXa generated per μg of total cell protein (U/μg).

Continuous TF PCA Assay

The chromogenic reporter substrate S-2765 was used to measure factor Xa generation as an indirect way of assaying cell-surface TF PCA. An equivalent number of cells were seeded into a 96-well plate and upon reaching confluency (1×10^4 cells per well) rinsed once with $1\times$ TBS before analysis. Cocktail (90 μl) containing 1 nM of FVIIa (Enzyme Research Laboratories), 30 nM of FX (Enzyme Research Laboratories), 10 mM $CaCl_2$ and 0.4 nM of S-2765 in TBS was added to each well. Each testing agent was diluted in TBS, and the given dose was added by a 10 μl addition to each well in eight replicates. The absorbance at 405 nm was then measured kinetically every 2 min for 3 h at 37°C. Maximum kinetic rate (Vmax) was calculated in each well using SOFTmax Pro and compared against the standard curve to determine TF PCA. The standard curve was generated where 100 U of TF activity was defined as the amount of activity in 1.5 μl of purified human recombiplastin (Dade Behring), which is equivalent to 450 μg of TF (as determined by the American Diagnostica ELISA). Cell-surface TF PCA was calculated as the amount of FXa generated per 1×10^4 cells (U per 1×10^4 cells). To assess the specificity of the assay for TF, the rabbit anti-human TF antibody (American Diagnostica, #4502) was used as an inhibitory antibody over a concentration range of 0–10 μg/ml while a rabbit anti-green fluorescent protein (GFP) antibody (10 μg/ml) (Affinity BioReagents, Rockford, IL, USA, #PA1-980) was used as a nonspecific antibody control.

Quantitation of Total Cellular Protein

To determine the amount of protein in each test well of the discontinuous assay, we performed the DC Protein Assay (Bio-Rad) in triplicate. Lysates in RIPA buffer were passed through a 21 1/2; gauge needle and centrifuged at 10 000 r.p.m. for 2 min. Triplicate aliquots of 5 μl of lysates were each incubated with 24.5 μl of Reagent A, 0.5 μl of Reagent S and 200 μl of Reagent B in a 96-well plate for 15–30 min. The reference standard used in this procedure was a dilution series of Bio-Rad Protein Assay Standard II. Absorbance was measured at 750 nm on a spectrophotometer using SOFTmax Pro.

Immunoblot Analysis

Total protein lysates were prepared using $4\times$ Laemmli sample buffer (50 mM Tris (pH 6.8), 2% SDS, 10% glycerol, 0.01% bromophenol blue and 50 mM DTT). Lysates were boiled for 5 min before separation by electrophoresis under reducing conditions on a 10% SDS–polyacrylamide gel. Proteins were transferred onto a nitrocellulose membrane (Bio-Rad) using the Trans-Blot Semi-Dry transfer apparatus (Bio-Rad). Membranes were blocked overnight in 5% milk (from powder) in $1\times$ TBST followed by incubation with the primary rabbit anti-human TF antibody then horseradish peroxidase-conjugated secondary antibodies (Upstate Biotechnology, Lake Placid, NY, USA) diluted in 1% milk (from powder) in $1\times$ TBST. Membranes were visualized using the Western Lighting Chemiluminescence Reagent (PerkinElmer, Boston, MA, USA) and Kodak X-OMAT Blue XB-1 film (PerkinElmer) was exposed and developed using a Kodak X-OMAT 1000A Processor. To control for protein loading, immunoblots were re-probed with a mouse monoclonal anti-β-actin antibody (Sigma-Aldrich) after re-blocking overnight in 5% milk (from powder) in $1\times$ TBST. All reagents used to make the polyacrylamide gel as well as the electrophoresis apparatus were purchased from Bio-Rad.

Statistical Analysis

The standard error of the mean for each treatment replicate was established using Excel software (Mississauga, ON, Canada). Significance of differences between control and various treatments was determined by analysis of variance (ANOVA). On finding significance with ANOVA, an unpaired Student's *t*-test was performed. For all analyses, $P \leq 0.05$ was considered significant. To compare the reproducibility of results produced by both the discontinuous and continuous assays, we calculated the intra- and inter-assay coefficient of variation (CV) for both the discontinuous and continuous assay determinations of TF PCA using the methodology described by Grotjan and Keel.[18] Further, to determine the predicted nature of the enzymatic reaction with progress curves obtained from the continuous assay, we performed enzymatic kinetic curve fitting using Table Curve 2D software version 5.01 (Systat Software Inc.), where 58 total kinetics equations were fit and best fit was determined by maximizing the R^2 value.

RESULTS

Comparison of Discontinuous *vs* Continuous Measurement of TF PCA

Schematic diagrams of the procedure for the discontinuous and continuous FXa generation assays are described in Figure 1a. To determine if the continuous assay developed to measure TF PCA was able to measure increases in TF PCA produced by the known TF agonists ionomycin and hydrogen peroxide, we examined and compared dose responses of these substances to the discontinuous assay system. As previously reported,[15] the discontinuous assay showed a significant increase in TF PCA due to treatment of T24/83 cells with the agonists ionomycin (1–20 μM) or hydrogen peroxide

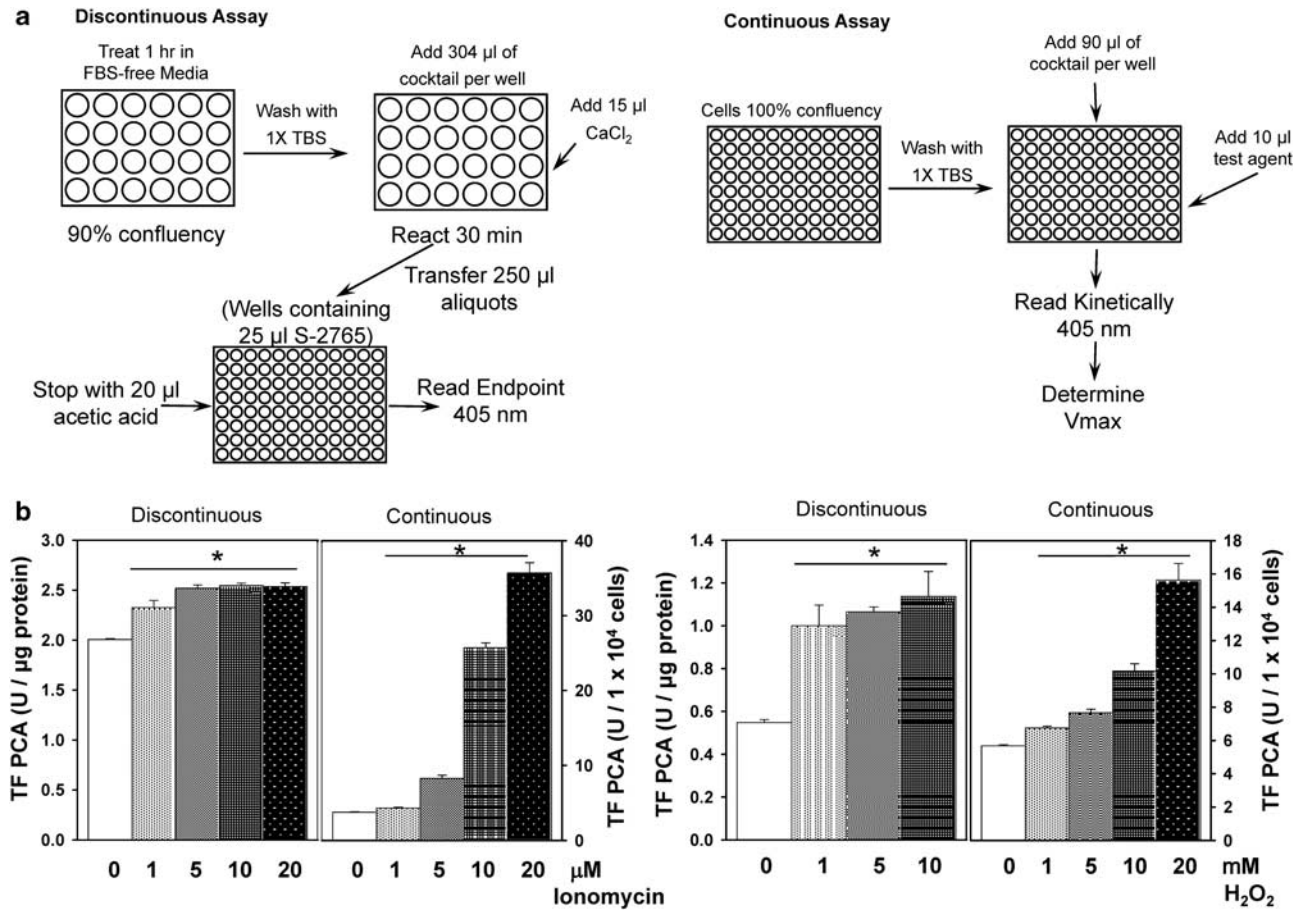

Figure 1 Continuous *vs* discontinuous measurement of TF PCA. (**a**) Schematic diagram of the procedure for the discontinuous and continuous FXa generation assays. (**b**) TF PCA measured both discontinuously and continuously on T24/83 cells in response to the agonists, ionomycin (1–20 μM) or hydrogen peroxide (1–20 mM). *$P<0.05$ *vs* vehicle control.

(1–20 mM). The continuous assay was also able to detect the dose-dependent increase in TF PCA produced in T24/83 cells in response to these agonists (Figure 1b).

Specificity of the Continuous Assay for the Measurement of TF PCA

To determine if the response measured in the continuous TF PCA assay was specific for TF activation, we used an inhibitory anti-TF antibody to determine if the assay response could be abolished (Figure 2). A nonspecific anti-GFP antibody was used as its control. Progress curves are shown in Figure 2a for the product of FXa's cleavage of the chromogenic substrate, *p*-nitroanilide (pNA), due to stimulation with the endoplasmic reticulum (ER) calcium-releasing substance thapsigargin, drug vehicle control, as well as thapsigargin treatment combined with preincubation of the cells with the anti-TF inhibitory antibody or the nonspecific anti-GFP antibody. Thapsigargin treatment increased TF PCA in T24/83 cells over vehicle control; however, this effect was abolished by preincubation with the anti-TF inhibitory antibody. The nonspecific anti-GFP antibody produced little inhibition of the thapsigargin response. To determine if the Vmax responses to the agonists thapsigargin and ionomycin were specific for TF, preincubation with the anti-TF antibody or the anti-GFP control were used. Both thapsigargin and ionomycin significantly increased the response in Vmax over vehicle control; however, this was significantly inhibited by the anti-TF antibody. The anti-GFP antibody had no significant effect on Vmax (Figure 2b). The fitting of Vmax to standards of purified human recombiplastin allowed the determination of TF PCA (U per 1×10^4 cells) generated by ionomycin (10 μM), hydrogen peroxide (10 mM) and thapsigargin (10 μM). These were all found to be dose dependently inhibited by increasing the concentration of the anti-TF inhibitory antibody (0–10 μg/ml) (Figure 2c). Further, the assay was performed with the stepwise removal of critical components of the cocktail mix, namely, calcium, chromogenic substrate (S-2765), FX, FVIIa or the cells where ionomycin (10 μM) and thapsigargin (15 μM) were used as agonists. The reaction was unable to proceed unless all critical components were present and the agonist had no effect with a complete cocktail in the absence of cells,

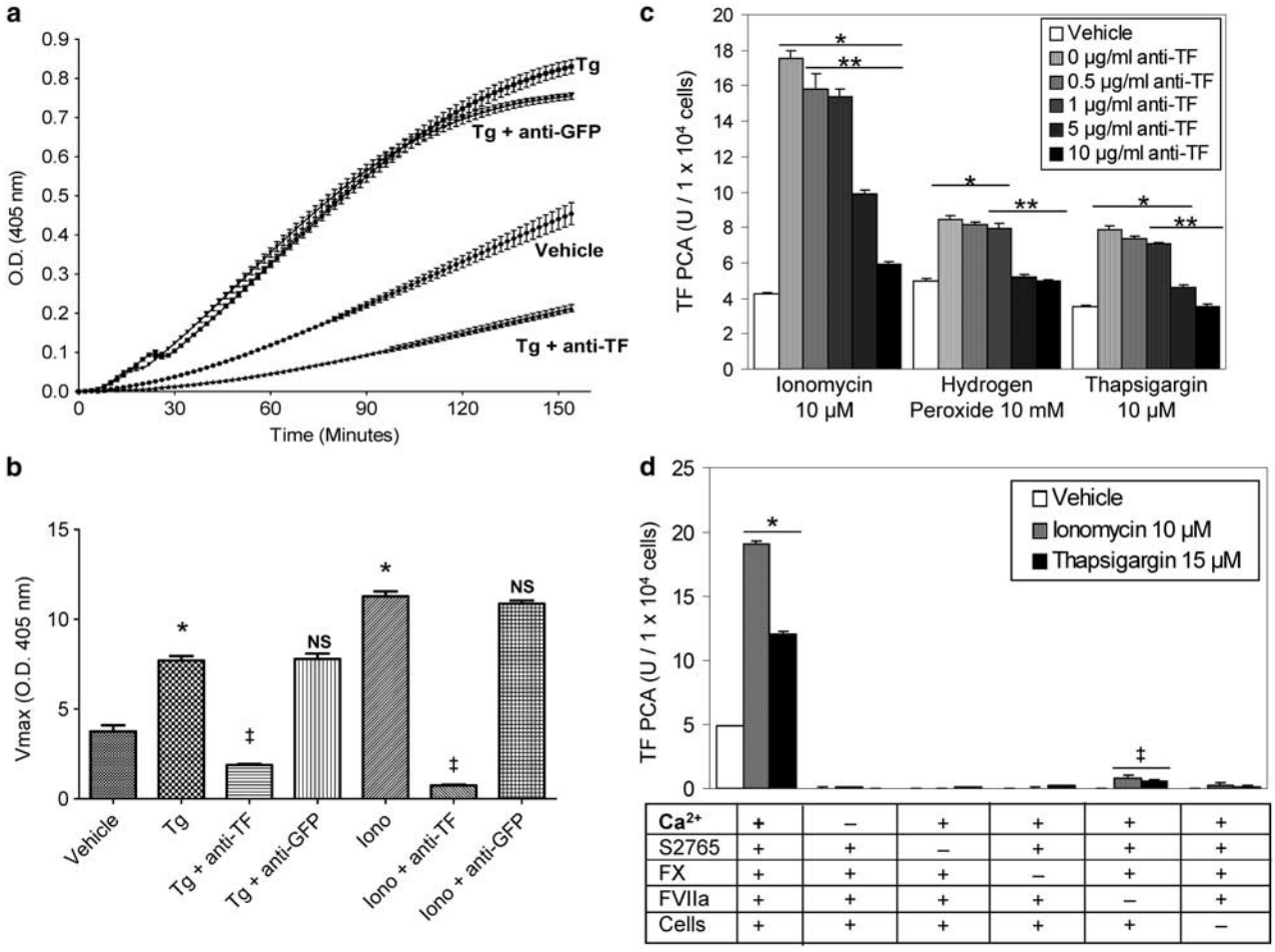

Figure 2 Determination of the specificity of the continuous assay for the measurement of TF PCA. (**a**) Progress curves for the continuous assay performed on T24/83 cells showing response of vehicle control *vs* 10 μM thapsigargin (Tg), 10 μM thapsigargin pretreated with 10 μg/ml anti-TF neutralizing antibody (Tg + anti-TF) and 10 μM thapsigargin pretreated with 10 μg/ml anti-GFP antibody (Tg + anti-GFP) as a control for the specificity of the TF neutralizing antibody effect. (**b**) Maximum rate of kinetic reaction (Vmax) derived from progress curves on T24/83 cells showing significant increases in Vmax produced by 10 μM Tg and 10 μM ionomycin (iono) treatment (*$P<0.05$ *vs* vehicle control), significant inhibition of this effect by TF neutralizing antibody (‡$P<0.05$ *vs* agonist, Tg and Iono) and no significant effect on Vmax of nonspecific antibody control, anti-GFP. (**c**) TF PCA of T24/83 cells pre-treated with the anti-TF neutralizing antibody (anti-TF, 1–10 μg/ml) followed by treatment with agonist ionomycin (10 μM), hydrogen peroxide (10 mM) or thapsigargin (10 μM). *$P<0.05$ *vs* vehicle control. ** represent significant decrease in agonist response due to pretreatment with anti-TF neutralizing antibody, $P<0.05$. (**d**) On cell controls using T24/83 cells where each component of the cocktail is absent without stimulation or with ionomycin (10 μM) or thapsigargin (15 μM) treatment. *$P<0.05$ *vs* vehicle control (‡ over 0).

indicating that the source of TF PCA increase to be from the test cells (Figure 2d).

Continuous Measurement of TF PCA in Different Cell Lines

To determine if the continuous assay was able to distinguish different levels of TF PCA between cell lines having different amounts of total TF, we used two prostate cancer cell lines (PC-3 and DU145) in the assay. Western blot analysis was performed to determine the expression of total TF in these cell lines. It was found that T24/83 cells had an intermediate level of total TF protein expression, whereas PC-3 cells had the lowest level and DU145 had the greatest level of expression (Figure 3a). Stimulation of PC-3 and DU145 cells with ionomycin, hydrogen peroxide or thapsigargin showed that both cell lines displayed a dose-dependent increase in TF PCA to these agonists (Figure 3b and c). However, TF PCA activity responses in DU145 cells with the greatest amount of TF expression were approximately 50-fold higher than that in PC-3 cells with the lowest amount of TF protein expression. These findings indicate the ability of the continuous assay to distinguish between biologically relevant levels of TF expression in different cell lines.

Agonists Potentially Interfering with the Continuous TF PCA Assay

In the discontinuous assay, agonists are removed before a determination of TF PCA is made. This allows the assay to be

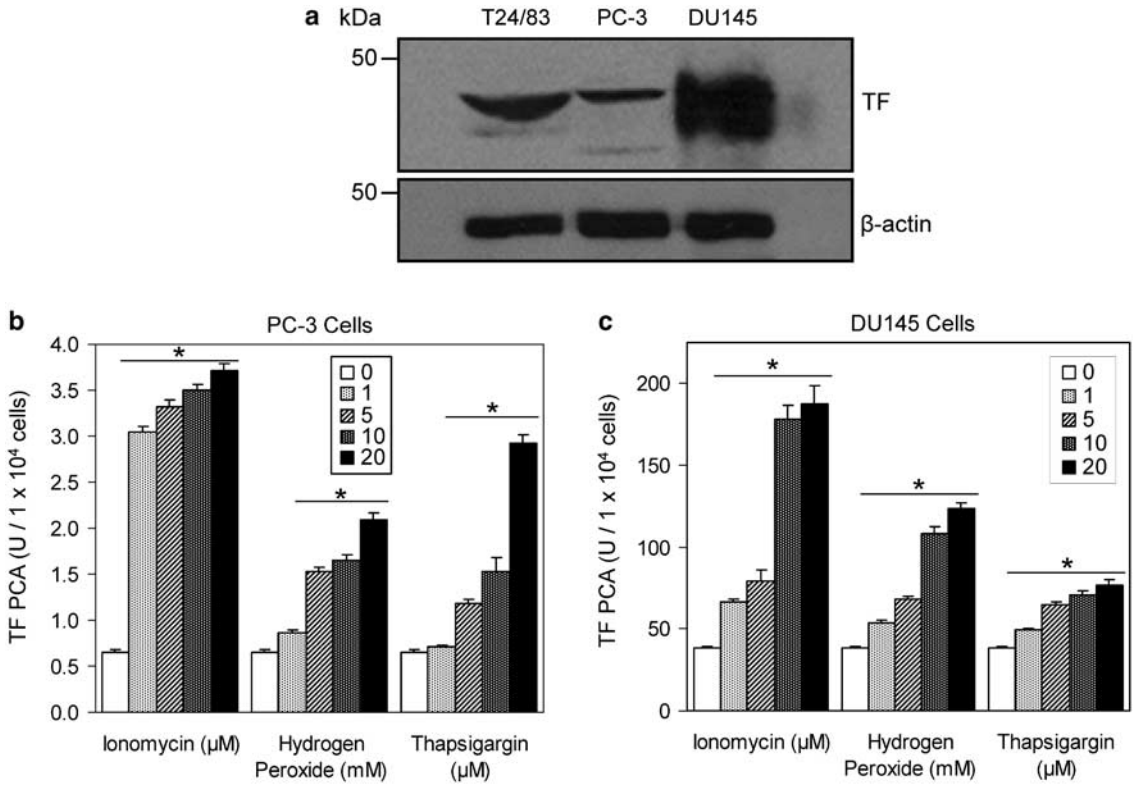

Figure 3 Continuous measurement of TF PCA in cell lines expressing different levels of total TF. (**a**) Western blot of whole-cell lysates from T24/83, PC-3 and DU145 cells showing levels of TF protein expression. To control for equivalent protein loading, blots were reprobed with anti-β-actin antibody. Treatment of (**b**) PC-3 and (**c**) DU145 cells with ionomycin (1–20 μM), hydrogen peroxide (1–20 mM) or thapsigargin (1–20 μM). *$P<0.05$ *vs* vehicle control.

run for only one fixed time point, thereby preventing the generation of kinetic progress curves. However, it does have the advantage of removing test substances that could potentially interfere with the cleavage of FX and/or the chromogenic substrate. α_2-Macroglobulin (α_2M) is a known mobilizer of intracellular calcium through its binding to the cell-surface GRP78 receptor.[19] However, it is also a broad spectrum proteinase inhibitor capable of inhibiting the serine proteinases found in the continuous TF PCA assay. Use of α_2M as a TF PCA agonist in T24/83 cells in the discontinuous assay showed a dose-dependent increase in TF PCA (Figure 4a). However, the same doses of α_2M in the continuous assay produced no increase in TF PCA whereas thapsigargin did significantly increase TF PCA (Figure 4b). Examination of doses of α_2M on the effect of preactivated FXa's cleavage of the chromogenic substrate S-2765 in a cell-free system showed that α_2M dose dependently inhibited FXa's cleavage of the substrate as shown by a significant reduction in the area under the progress curve response (Figure 4c). These findings indicate that TF PCA agonists that also interfere with TF/FVIIa or FXa enzymatic activity will not be recognized by the continuous assay as opposed to the discontinuous assay system. Agonists resulting in cytotoxicity may also lead to an increase in TF PCA. To show this effect, we used the nonionic detergent Triton X-100 to disrupt the plasma membrane. This resulted in complete cell death after treatment as measured by the 7-AAD viability dye (Figure 4d). Triton X-100 was also shown to increase TF PCA (Figure 5a). However, treatment with agonists that increase TF PCA in the continuous assay system, including thapsigargin (10 μM) and ionomycin (10 μM) (Figure 5a), did not result in a decrease in cell survival (Figure 4d).

Fitting of Kinetic Equations to Progress Curves

The ability of the continuous assay to generate progress curves of product formation allows the data generated by this assay to be subjected to further analysis through curve fitting and the determination of the rate constants of the enzymatic reaction. Progress curves for TF PCA agonists of widely varying modes of action, including the SERCA calcium pump inhibitor thapsigargin, calcium ionophore ionomycin and nonionic detergent Triton X are shown in Figure 5a. The maximum rate of product formation (Vmax) for each agonist was then fit to the standard curves of TF PCA produced by known units of recombinant TF which allowed the determination of TF PCA for each substance in T24/83 cells (Figure 5b). Curve fitting to the progress curves shown in Figure 5a determined the fitted curves shown in Figure 5c. Goodness of curve fit determined by maximum R^2 value of the fit allowed the selection of the kinetic model of enzymatic

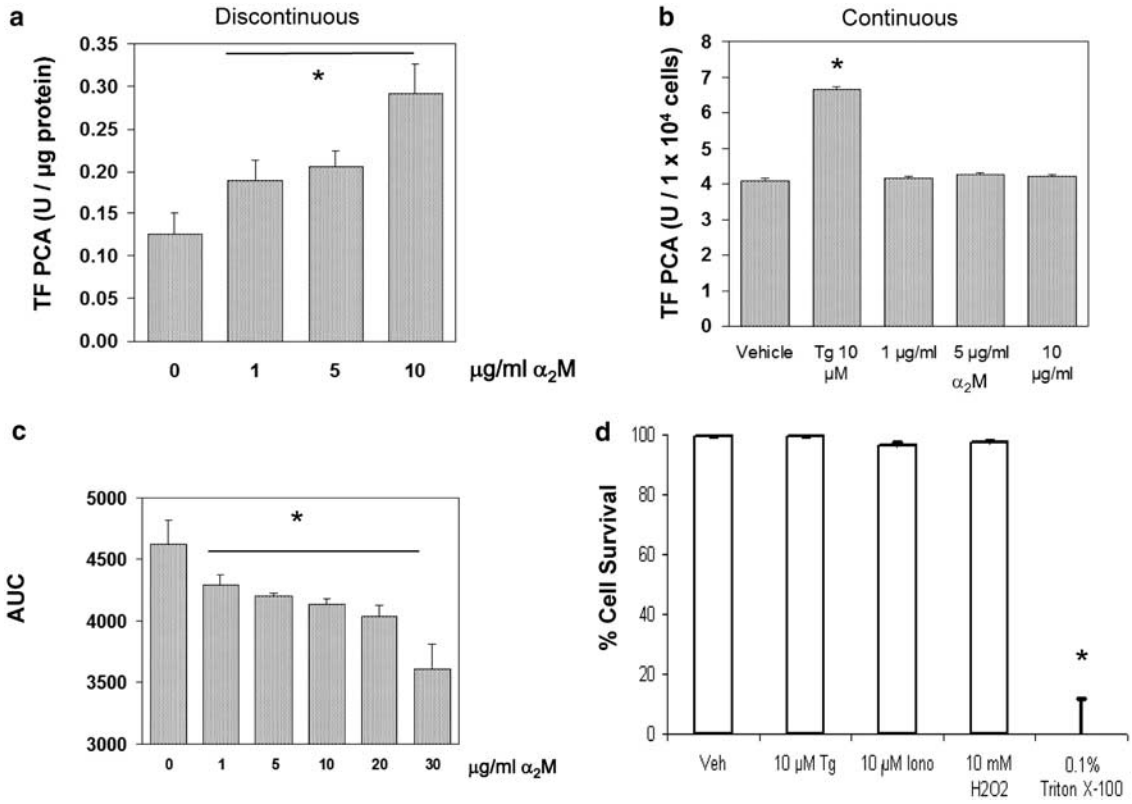

Figure 4 Agonists potentially interfering with the continuous TF PCA assay. (**a**) The proteinase inhibitor α_2-macroglobulin (α_2M) produced a significant increase in TF PCA as measured in the discontinuous assay. *$P<0.05$ *vs* vehicle control. (**b**) α_2M produced no significant response *vs* vehicle control in the continuous assay, whereas 10 μM thapsigargin (Tg) did generate a significant response. *$P<0.05$ *vs* vehicle control. (**c**) Area under the progress curve (AUC) for the continuous assay in cell-free system where FXa was added in the presence of the chromogenic substrate S-2765 and increasing concentration of α_2M produced dose-dependent reduction in the area under the progress curve. *$P<0.05$ *vs* vehicle control. (**d**) Percentage cell survival resulting from treatment with the agonists used in the continuous assay system *vs* vehicle control. Triton X-100 treatment produced a significant decrease in percentage cell survival as measured by the 7-AAD cell viability assay. *$P<0.05$ *vs* vehicle control.

product formation that best described the progress curves in Figure 5a. Despite the widely varying modes of activity of the agonists tested, all test substances accurately allowed the prediction of the mode of product formation in the continuous assay as first-order sequential formation (Figure 5d). Where two enzymes, TF/FVIIa complex and FXa lead to the sequential formation of the product, pNA, from the chromogenic substrate allowing for the determination of first-order rate constants k_1 (TF/FVIIa rate) and k_2 (FXa rate) from the equation of the fitted curve (Equation (1)).

$$y = a\left(1 + \frac{k_1^{(-k_2 x)} - k_2^{(-k_1 x)}}{k_2 - k_1}\right) \qquad (1)$$

The first-order rate constants determined for the drug vehicle ($k_1 = 0.011134$, $k_2 = 0.011103$), 10 μM thapsigargin ($k_1 = 0.023933$, $k_2 = 0.023885$), 10 μM ionomycin ($k_1 = 0.050873$, $k_2 = 0.050867$) and 0.01% Triton X ($k_1 = 0.068506$, $k_2 = 0.068504$) are in close agreement with the resultant TF PCA calculated from standard curves and show that the rate of TF/FVIIa formation closely determines the rate of FXa through the sequential formation of FXa as product of the first enzymatic reaction.

Reproducibility of the Discontinuous and Continuous Assays

To assess the reproducibility of both the discontinuous and continuous assays for the determination of TF PCA, we ran the assays both in a cell-free system where known amounts of TF were added to the reaction mixture and in a cell-based assay where the known agonist 10 μM ionomycin was used to stimulate a response in T24/83 cells. Replication of these assays within the plate as well as multiple assay runs over many plates with the same agonists allowed the calculation of both the intra- and inter-assay CV for the discontinuous and continuous assays. It was found that in a cell-free system as well as in the cell-based system both the intra- and inter-CV were dramatically lower for the continuous assay (Table 1).

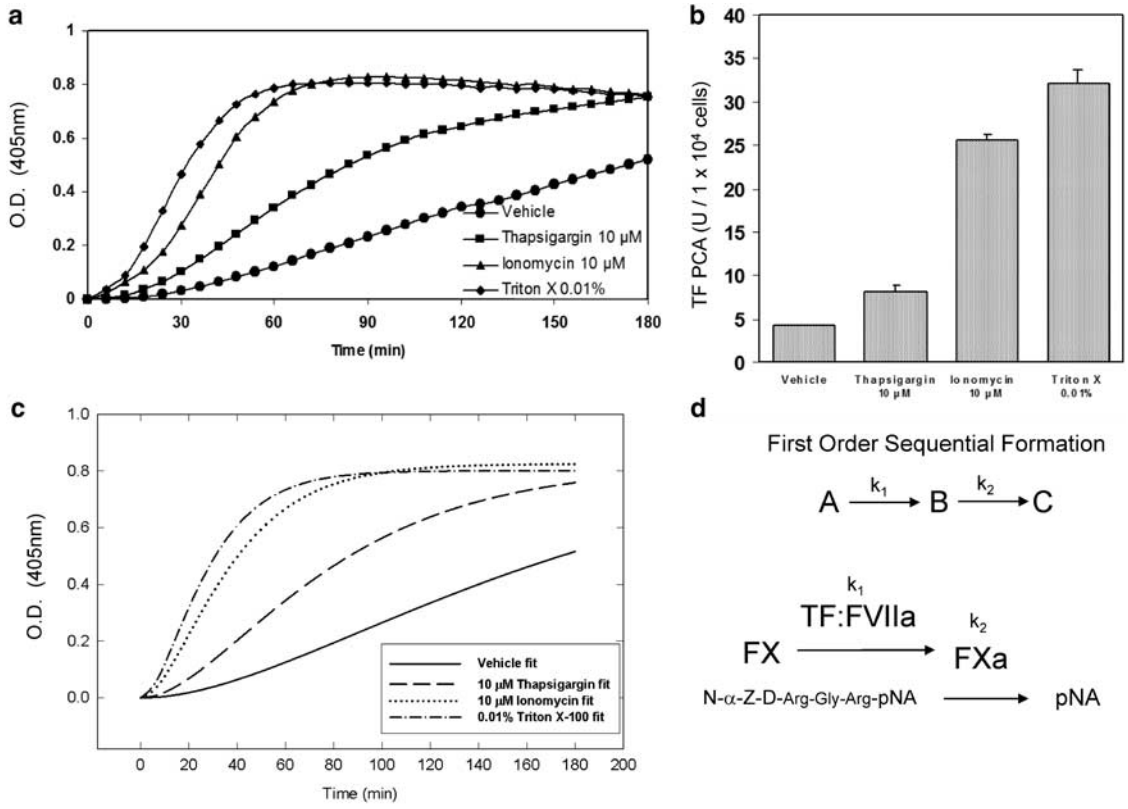

Figure 5 Fitting of progress curves generated by the continuous assay to kinetic equations for product formation to determine form and rate constants of the reaction. (**a**) Raw progress curve produced by the continuous assay in response to different agonists, thapsigargin (10 μM), ionomycin (10 μM) or Triton X-100 (0.01% v/v) known to increase TF PCA. (**b**) TF PCA determined from the progress curves of known agonists by fitting maximum rate of product production (Vmax) to maximum rates produced (Vmax) of known units (U) of recombinant TF. (**c**) Best curve fits of enzymatic kinetic equations as determined by maximum R^2 to progress curves shown in **a**. (**d**) Nature of reaction determined by curve fitting to the agonists thapsigargin, ionomycin and Triton X-100, first-order sequential formation, with concomitant rate constant determinations, k_1 and k_2, by curve fitting in **c**. Nature determined by progress curve fitting correctly predicted known reaction nature, first-order sequential formation with two enzyme complexes, TF/FVIIa and FXa leading to chromogenic product formation, pNA.

Table 1 Comparison of the intra- and inter-assay CV in discontinuous and continuous tissue factor procoagulant activity assays

	Discontinuous			Continuous		
	Dose	Intra-assay CV (%)	Inter-assay CV (%)	Dose	Intra-assay CV (%)	Inter-assay CV (%)
Cell free system	85[a]	24.5	24.5	85[a]	4.6	2.9
	170[a]	17.0	23.3	42[a]	5.0	2.3
Cell-based system	10 μM ionomycin	51.7	50.3	10 μM ionomycin	8.8	22.1

[a]Tissue factor (μg) added to cell-free system.

DISCUSSION

This study shows the use of a continuous assay for the measurement of TF PCA in a cell-based system. The previously used discontinuous assay, although able to identify agonists of TF PCA, suffers from a greater intra- and inter-assay variability. This was likely due to the requirement to determine TF PCA from a single end point determination at an arbitrarily determined time. Small differences in the time run during the first step of the discontinuous assay may have resulted in large differences in product formation in the second step due to the steep exponential rate of TF/FVIIa formation induced by many agonists in the first step. In

contrast, the continuous assay does not rely on a single end point determination of product formation. Instead, determination of the Vmax over the time course of the assay is used that appears to be inherently less subjective to random error variability. Further, the generation of progress curves in the continuous assay, unobtainable in the discontinuous measurement, allowed the application of curve fitting to accurately determine the nature of the reaction understudy, independent of the agonist used, as well as determining the rate constants for the two enzyme components of the assay, namely TF/FVIIa and FXa. It should be noted, however, inter-assay variability of 22% was observed in the continuous assay (Table 1). This effect may have arisen due to the variable expression of TF in the T24/83 cells used in the inter-assay variability calculation over time in the cell culture environment because inter-assay variability in the cell-free system for the continuous assay was in the 2–3% range (Table 1).

Indeed, the continuous assay was very sensitive to changes in TF expression in different cell types. This is indicated by the ability of the continuous assay to accurately determine in magnitude the TF PCA responses of the cell lines PC-3 and DU145 that possess widely varying amounts of total TF. Inter-assay variability is the main form of error confounding the comparison of inter-group data from different cell types over time. The continuous assay for the measurement of TF PCA has been used to compare the change in TF PCA produced by HeLa cells over time in culture. It was found that increase in cell density of HeLa cells reduced the units of TF generation per cell.[20] This effect may contribute to the inter-assay variability we observed in the continuous TF PCA assay in the cell-based system.

The assay described in this paper appears to be first conceptually established by Carson[21] based on earlier work by Kosow *et al*[22] with FX activation by Russel's viper venom. Carson showed progress curves produced from the addition of TF to a single-step assay containing a cocktail similar to that used in this paper.[21] The assay was further established in a cell-based system using HeLa cells to show the substantial differences in TF PCA of nondisrupted *vs* disrupted cells,[20] contributing to the concept that TF encryption/de-encryption is an important factor in mediating its biological effect on coagulation. The assay was further used to show detergent induced increases in TF PCA on cultured fibroblasts thereby indicating a function for phospholipid asymmetry in the regulation of TF PCA.[7]

TF encryption/de-encryption appears to be an important point in the coagulation cascade to interfere with the pathological consequences of thrombosis. Increases in cytosolic calcium are believed to result in TF de-encryption through a mechanism involving phospholipid asymmetry.[23] Indeed we have shown using the continuous assay that a calcium ionophore, ionomycin, increases TF PCA similarly to results shown by Carson and Bromberg.[24] Further, we have shown in the continuous assay that the ER calcium pump inhibitor, thapsigargin, increases TF PCA in a dose-dependent manner in a variety of cell types that include T24/83, PC-3 and DU145. This effect appeared to be specific for TF activation because it was inhibited by the anti-TF antibody, but not by a control anti-GFP antibody, and thapsigargin treatment resulted in no cytotoxic effects.

The continuous TF PCA assay as presented here is applicable for the high-throughput screen of agents that lead to the de-encryption of TF. It should be noted, however, that unknown agents might have differing effects in the discontinuous *vs* the continuous TF PCA assay systems. As we have reported, α_2M previously showed to mobilize intracellular calcium,[19] increases TF PCA in the discontinuous assay system whereas in the continuous system it had no effect. This discrepancy in results appears to be due to α_2M effect as a serine proteinase inhibitor, because we have shown that α_2M dose dependently inhibits the cleavage of the chromogenic substrate by activated FX. It is tempting to speculate which assay system more accurately reflects the physiological action of α_2M on coagulation. Because the continuous assay combines all relevant components of the system simultaneously, unlike the discontinuous system, the continuous system seems to more accurately reflect the physiological system. In this context, it should be noted that α_2M functions as a blood coagulation inhibitor.[25]

In conclusion, we describe a continuous assay for the measurement of TF PCA that shows less intra- and inter-assay variability than the commonly used discontinuous assay we as well as others have used previously.[15] This assay has the advantage of being applicable to the screening of large numbers of compounds for the induction of TF PCA as well as inhibitors of TF PCA stimulated by our test substance thapsigargin, ionomycin or hydrogen peroxide. The state of TF encryption/de-encryption measured by this assay appears to be a critical factor in determining the pathological consequences of unregulated thrombosis observed in many disease states, including cancer-related thrombosis and atherosclerosis. In this context, the continuous assay system offers promise for the elucidation of agents/conditions that may interfere with the de-encryption of TF and thus reduce the morbidity and mortality associated with the pathological manifestation of thrombotic disease.

ACKNOWLEDGEMENTS

This work was supported in part by research grants to Richard Austin from the Heart and Stroke Foundation of Ontario (T-6146), the Canadian Institutes of Health Research (MOP-74477) and the Ontario Research and Development Challenge Fund. Financial support from St Joseph's Healthcare Hamilton and a CIHR Team Grant in Thromboembolism (FRN-79846) is acknowledged. Jeffrey G. Dickhout was supported by the St Joseph's Healthcare Hamilton Division of Nephrology Junior Research Award. Richard C. Austin is a Career Investigator of the Heart and Stroke Foundation of Ontario and holds the Amgen Canada Research Chair in the Division of Nephrology at St Joseph's Healthcare and McMaster University.

DISCLOSURE/CONFLICT OF INTEREST

The authors declare no conflict of interest.

1. Carson SD, Brozna JP. The role of tissue factor in the production of thrombin. Blood Coagul Fibrinolysis 1993;4:281–292.
2. van der Wal AC, Li X, de Boer OJ. Tissue factor expression in the morphologic spectrum of vulnerable atherosclerotic plaques. Semin Thromb Hemost 2006;32:40–47.
3. Berg JM, Tymoczko JL, Stryer L. Biochemistry, 5th edn. WH Freeman and Company: New York, 2002.
4. Gailani D, Renne T. Intrinsic pathway of coagulation and arterial thrombosis. Arterioscler Thromb Vasc Biol 2007;27:2507–2513.
5. Rock G, Wells P. New concepts in coagulation. Crit Rev Clin Lab Sci 1997;34:475–501.
6. Bach R, Rifkin DB. Expression of tissue factor procoagulant activity: regulation by cytosolic calcium. Proc Natl Acad Sci USA 1990;87: 6995–6999.
7. Carson SD. Manifestation of cryptic fibroblast tissue factor occurs at detergent concentrations which dissolve the plasma membrane. Blood Coagul Fibrinolysis 1996;7:303–313.
8. Bach RR, Moldow CF. Mechanism of tissue factor activation on HL-60 cells. Blood 1997;89:3270–3276.
9. Penn MS, Cui MZ, Winokur AL, *et al.* Smooth muscle cell surface tissue factor pathway activation by oxidized low-density lipoprotein requires cellular lipid peroxidation. Blood 2000;96:3056–3063.
10. Drake TA, Ruf W, Morrissey JH, *et al.* Functional tissue factor is entirely cell surface expressed on lipopolysaccharide-stimulated human blood monocytes and a constitutively tissue factor-producing neoplastic cell line. J Cell Biol 1989;109:389–395.
11. Kunzelmann-Marche C, Satta N, Toti F, *et al.* The influence exerted by a restricted phospholipid microenvironment on the expression of tissue factor activity at the cell plasma membrane surface. Thromb Haemost 2000;83:282–289.
12. Iakhiaev A, Pendurthi UR, Voigt J, *et al.* Catabolism of factor VIIa bound to tissue factor in fibroblasts in the presence and absence of tissue factor pathway inhibitor. J Biol Chem 1999;274:36995–37003.
13. Roy S, Paborsky LR, Vehar GA. Self-association of tissue factor as revealed by chemical crosslinking. J Biol Chem 1991;266: 4665–4668.
14. Egorina EM, Sovershaev MA, Osterud B. Regulation of tissue factor procoagulant activity by post-translational modifications. Thromb Res 2008;122:831–837.
15. Watson LM, Chan AK, Berry LR, *et al.* Overexpression of the 78-kDa glucose-regulated protein/immunoglobulin-binding protein (GRP78/BiP) inhibits tissue factor procoagulant activity. J Biol Chem 2003;278:17438–17447.
16. Osterud B. Platelet activating factor enhancement of lipopoly-saccharide-induced tissue factor activity in monocytes: requirement of platelets and granulocytes. J Leukoc Biol 1992;51:462–465.
17. Sovershaev MA, Egorina EM, Gruber FX, *et al.* High tissue factor-expressing human monocytes carry low surface CD36: application to intersubject variability. J Thromb Haemost 2007;5:2453–2460.
18. Grotjan HE, Keel BA. Data interpretation and quality control. In: Diamandis EP, Christopoulos TK (eds). Immunoassay, 1st edn. Academic Press: Toronto, 1996.
19. Gonzalez-Gronow M, Cuchacovich M, Llanos C, *et al.* Prostate cancer cell proliferation *in vitro* is modulated by antibodies against glucose-regulated protein 78 isolated from patient serum. Cancer Res 2006;66:11424–11431.
20. Carson SD, Archer PG. Tissue factor activity in HeLa cells measured with a continuous chromogenic assay and ELISA reader. Thromb Res 1986;41:185–195.
21. Carson SD. Computerized analysis of enzyme cascade reactions using continuous rate data obtained with an ELISA reader. Comput Programs Biomed 1985;19:151–157.
22. Kosow DP, Furie B, Forastieri H. Activation of factor X: kinetic properties of the reaction. Thromb Res 1974;4:219–227.
23. Bach RR. Tissue factor encryption. Arterioscler Thromb Vasc Biol 2006;26:456–461.
24. Carson SD, Bromberg ME. Tissue factor encryption/de-encryption is not altered in the absence of the cytoplasmic domain. Thromb Haemost 2000;84:657–663.
25. Bikfalvi A, Beress L. Natural proteinase inhibitors: blood coagulation inhibition and evolutionary relationships. Comp Biochem Physiol B 1987;87:435–441.

CHAPTER 3

JOURNAL OF BIOLOGICAL CHEMISTRY PUBLICATION

.

Preamble

This chapter is an orginal published in the Journal of Biological Chemistry

J Biol Chem. 2010 Sep 10;285(37):28912-23. doi: 10.1074/jbc.M110.119107. Epub 2010 Jul 6.

Authors' Contribution

A. Al-Hashimi and R.C. Austin designed the study. A. Al-Hashimi performed all the cell culture experiments and related analyses, performed Western blotting, conducted. Figure 1 includes work that was conducted by Lindsay Pozza and Jennifer Caldwell. A. R.C. Austin provided intellectual input. A. Al-Hashimi and R.C. Austin reviewed and edited the manuscript and all authors approved of the final submission.

THE JOURNAL OF BIOLOGICAL CHEMISTRY VOL. 285, NO. 37, pp. 28912–28923, September 10, 2010

Binding of Anti-GRP78 Autoantibodies to Cell Surface GRP78 Increases Tissue Factor Procoagulant Activity via the Release of Calcium from Endoplasmic Reticulum Stores*[S]

Received for publication, March 2, 2010, and in revised form, June 16, 2010 Published, JBC Papers in Press, July 6, 2010, DOI 10.1074/jbc.M110.119107

Ali A. Al-Hashimi[‡], Jennifer Caldwell[‡], Mario Gonzalez-Gronow[§], Salvatore V. Pizzo[§], Danya Aboumrad[‡], Lindsay Pozza[‡], Hiam Al-Bayati[‡], Jeffrey I. Weitz[§¶], Alan Stafford[¶], Howard Chan[¶], Anil Kapoor[‖], Donald W. Jacobsen[‡‡3], Jeffrey G. Dickhout[§1], and Richard C. Austin[‡¶2]**

*From the [‡]Department of Medicine and Division of Nephrology and the [‖]Department of Surgery and Division of Urology, St Joseph's Hospital and McMaster University, Hamilton, Ontario L8N 4A6, Canada, the [¶]Thrombosis and Atherosclerosis Research Institute, Hamilton General Hospital and McMaster University, Hamilton, Ontario L8L 2X2, Canada, the [§]Department of Pathology, Medical Center, Duke University, Durham, North Carolina 27710, the **Department of Cell Biology, Lerner Research Institute, Cleveland Clinic, Cleveland, Ohio 44195, and the [‡‡]Department of Molecular Medicine, Cleveland Clinic Lerner College of Medicine, Case Western Reserve University, Cleveland, Ohio 44106*

The increased risk of venous thromboembolism in cancer patients has been attributed to enhanced tissue factor (TF) procoagulant activity (PCA) on the surface of cancer cells. Recent studies have shown that TF PCA can be modulated by GRP78, an endoplasmic reticulum (ER)-resident molecular chaperone. In this study, we investigated the role of cell surface GRP78 in modulating TF PCA in several human cancer cell lines. Although both GRP78 and TF are present on the cell surface of cancer cells, there was no evidence of a stable interaction between recombinant human GRP78 and TF, nor was there any effect of exogenously added recombinant GRP78 on cell surface TF PCA. Treatment of cells with the ER stress-inducing agent thapsigargin, an inhibitor of the sarco(endo)plasmic reticulum Ca^{2+} pump that causes Ca^{2+} efflux from ER stores, increased cytosolic $[Ca^{2+}]$ and induced TF PCA. Consistent with these findings, anti-GRP78 autoantibodies that were isolated from the serum of patients with prostate cancer and bind to a specific N-terminal epitope (Leu^{98}–Leu^{115}) on cell surface GRP78, caused a dose-dependent increase in cytosolic $[Ca^{2+}]$ and enhanced TF PCA. The ability to interfere with cell surface GRP78 binding, block phospholipase C activity, sequester ER Ca^{2+}, or prevent plasma membrane phosphatidylserine exposure resulted in a significant decrease in the TF PCA induced by anti-GRP78 autoantibodies. Taken together, these findings provide evidence that engagement of the anti-GRP78 autoantibodies with cell surface GRP78 increases TF PCA through a mechanism that involves the release of Ca^{2+} from ER stores. Furthermore, blocking GRP78 signaling on the surface of cancer cells attenuates TF PCA and has the potential to reduce the risk of cancer-related venous thromboembolism.

Venous thromboembolism and other hypercoagulable states are major contributors to death and disability in cancer patients (1, 2). Although the prothrombotic state of cancer can be influenced by the activation of specific oncogenes (3), current evidence suggests that the major impact involves the enhanced expression and/or procoagulant activity (PCA)[4] of tissue factor (TF) on the surface of cancer cells (4).

TF is a 47-kDa transmembrane glycoprotein, and the major physiological initiator of the coagulation cascade (5). TF is normally expressed on the cell surface in a latent or "encrypted" form (6). Following exposure of cells to a number of pathophysiological agents/conditions, including cytokines (7), endotoxin (8), apoptosis (9, 10), hypoxia (11), and/or changes in intracellular $[Ca^{2+}]$ (12, 13), TF is converted into an active or "de-encrypted" form (14). De-encrypted TF on the cell surface binds circulating factor VIIa, and the resulting complex acts as a catalyst for the conversion of factors IX and X to IXa and Xa, respectively. This triggers thrombin generation leading to the formation of a fibrin clot. It is believed that TF de-encryption provides a mechanism by which cells initiate a rapid hemostatic response without the necessity of transcriptional up-regulation of TF. Some proposed mechanisms for modulating TF PCA include the formation of TF homodimers, the phospholipid microenvironment, including phosphatidylserine (PS) exposure, TF compartmentalization in lipid rafts, endocytosis and

* This work was supported in part by research grants from the Heart and Stroke Foundation of Ontario (T-6146), the Canadian Institutes of Health Research (MOP-74477), and the Ontario Research and Development Challenge Fund (to R. C. A.). This work was also supported by St Joseph's Healthcare Hamilton and by a Canadian Institutes of Health Research Team Grant in Thromboembolism (FRN-79846).

[S] The on-line version of this article (available at http://www.jbc.org) contains supplemental Fig. 1 and references.

[1] Supported by a St Joseph's Healthcare Hamilton Division of Nephrology Junior Research Award.

[2] A Career Investigator of the Heart and Stroke Foundation of Ontario and holder of the Amgen Canada Research Chair in the Division of Nephrology at St Joseph's Healthcare and McMaster University. To whom correspondence should be addressed: 50 Charlton Ave. East, Rm. T-3313, Hamilton, Ontario L8N 4A6, Canada. Tel.: 905-522-1155 (ext. 35175); Fax: 905-540-6589; E-mail: austinr@taari.ca.

[3] Supported in part by the National Heart, Lung and Blood Institute of the National Institutes of Health (HL52234).

[4] The abbreviations used are: PCA, procoagulant activity; ER, endoplasmic reticulum; GRP78, 78-kDa glucose-regulated protein; PLC, phospholipase C; SPR, surface plasmon resonance; TF, tissue factor; Tg, thapsigargin; Tm, tunicamycin; UPR, unfolded protein response; PS, phosphatidylserine; HBSS, Hanks' balanced salt solution; RU, response units; BAPTA, 1,2-bis(2-aminophenoxy)ethane-*N*,*N*,*N*′,*N*′-tetraacetic acid; IP_3, inositol 1,4,5-trisphosphate.

degradation of the TF-FVIIa complex, and isomerization of the TF disulfide bond by protein disulfide isomerase (15, 16).

Besides its critical role in thrombosis and hemostasis, recent studies indicate that TF also promotes cancer growth and metastasis (17–20). It is well established that enhanced TF expression/PCA correlates with cancer progression, angiogenesis, and a malignant phenotype (21, 22). It is believed that TF modulates cancer growth and metastasis by activating the coagulation system at the cell surface or through coagulation-independent signals. In addition, the release of TF-bearing microvesicles from the surface of tumor cells into the circulation can enhance systemic coagulation (23). Despite the causal role of TF in tumorigenesis, the cellular factors that modulate TF expression/PCA in cancer are poorly understood.

Recent studies have reported that TF expression/PCA can be modulated by GRP78, an endoplasmic reticulum (ER)-resident molecular chaperone that facilitates the correct folding and assembly of newly synthesized proteins (24). Overexpression of ER lumenal GRP78 inhibits TF PCA by protecting cells from changes in intracellular Ca^{2+} levels and/or the generation of reactive oxygen species (24). Furthermore, cell surface expression of GRP78 in cultured endothelial cells negatively regulates TF PCA through a direct GRP78/TF interaction (25). However, antibody-mediated GRP78 inhibition on the cell surface resulted in a significant increase in TF PCA. GRP78 is also highly expressed on the surface of many human cancers (26–31), where it functions as a unique signaling receptor to promote cell proliferation and survival (32). Furthermore, exposure of GRP78 on the surface of cancer cells stimulates the production of anti-GRP78 autoantibodies, high levels of which are correlated with accelerated cancer progression, enhanced metastatic potential, and reduced survival (33). We now report that anti-GRP78 autoantibodies isolated from the serum of patients with prostate cancer bind to GRP78 on the surface of cancer cells and enhance TF PCA. Mechanistically, engagement of the autoantibodies with cell surface GRP78 causes PLC-mediated release of Ca^{2+} from ER stores, thereby increasing cytosolic [Ca^{2+}]. The increase in cytosolic [Ca^{2+}] alters plasma membrane asymmetry resulting in enhanced TF PCA. Based on these findings, the engagement of anti-GRP78 autoantibodies with cell surface GRP78 may explain how TF is activated on cancer cells and contributes to the hypercoagulable state observed in cancer patients.

EXPERIMENTAL PROCEDURES

Cell Culture—Cancer cell lines were purchased from the American Tissue Culture Collection (Manassas, VA). The human bladder carcinoma cell line T24/83 was cultured in M199 media (Invitrogen), whereas the prostate cancer cell line PC-3 was cultured in F-12 media (Invitrogen). All media was supplemented with 10% fetal bovine serum (Sigma-Aldrich) containing 100 units/ml penicillin and 100 μg/ml streptomycin (Invitrogen). Cells were maintained at 37 °C in a humidified atmosphere of 5% CO_2/95% air.

Production and Purification of Recombinant Human GRP78 in Bacteria—High level expression of recombinant human GRP78 was achieved in bacteria (see supplemental Fig. S1). Briefly, transformed Rosetta (DE3) cells containing the GRP78-pET-28b construct were grown at 16 °C in LB media and treated with isopropyl β-D-1-thiogalactopyranoside to induce GRP78 expression. GRP78 protein was purified by using a nickel affinity fast protein liquid chromatography (FPLC) system, as described previously (34). Integrity and purity of the recombinant GRP78 protein was assessed by SDS-PAGE (supplemental Fig. S1*A*) and immunoblotting using anti-KDEL antibodies (supplemental Fig. S1*B*). Approximately 5.0 mg of FPLC-purified GRP78 protein was obtained from 400 ml of bacterial culture. Consistent with previous findings for recombinant hamster GRP78 (35), recombinant human GRP78 containing the His tag was functionally active, based on its ATPase (supplemental Fig. S1*C*) and chaperone activities (supplemental Fig. S1*D*).

Patient Samples—Blood samples were obtained from patients with prostate cancer from the Department of Urology, St. Joseph's Healthcare, Hamilton, Ontario, Canada. Written informed consent was obtained from patients and approved by the Research Ethics Board of St. Joseph's Healthcare (REB#08-3047).

Isolation of Anti-GRP78 Autoantibodies—Anti-GRP78 autoantibodies (GRP78 a-AB) were purified from the serum of prostate cancer patients by affinity chromatography on protein A-Sepharose, as previously described (36).

Cell Treatments—Ionomycin (Sigma-Aldrich) and thapsigargin (Tg, Sigma-Aldrich) stock solutions were diluted in DMSO as a transitional solvent and given in the appropriate physiological buffer to achieve a final concentration of 0.5–20 μM. Tg was used as an ER stress inducer and a positive control for the TF PCA assay. Tunicamycin (Tm, Sigma-Aldrich) stocks were diluted in DMSO, and final concentration in physiological buffers ranged from 1 to 10 μg/ml. Tm was used as an inducer of ER stress and a negative control for the TF PCA assay. Phospholipase C (PLC) inhibitor, U73123, and its nonactive analogue, U73122, were obtained from Santa Cruz Biotechnology (Santa Cruz, CA). Both chemicals were diluted to a final concentration of 5–10 μM in 1× TBS. The CNVKSDKSC peptide (GeneMed Synthesis, San Antonio, TX) was resuspended at a concentration of 60 μg/ml in 1× PBS and used to neutralize GRP78 a-AB.

Biotinylation of Cell Surface Proteins—Biotinylation of cell surface proteins was performed using the Cell Surface Protein Isolation Kit (Pierce). Briefly, four T75 flasks of T24/83 cells were grown to 95% confluency, washed twice with ice-cold 1× PBS and incubated in 0.25 mg/ml EZ-Link Sulfo-NHS-SS-Biotin for 30 min at 4 °C with rocking. Following saturation with quenching solution, the cells were scraped, pelleted at 500 × *g* for 3 min, and washed several times with 1× TBS. Cells were lysed in 500 μl of lysis buffer for 30 min on ice with vortexing every 5 min. The lysates were centrifuged at 10,000 × *g* for 2 min at 4 °C, and the biotinylated proteins were isolated from the cleared supernatant by binding to immobilized NeutrAvidin slurry for 60 min at room temperature with rotation. The slurry was washed four times with wash buffer containing protease inhibitors, and the biotinylated proteins were solubilized in 400 μl of 4× SDS-PAGE sample buffer (50 mM Tris, pH 6.8, 2% SDS, 10% glycerol, 0.01% bromphenol blue, and 50 mM DTT) for 60 min at room temperature with rotation. As a control, total cell

lysates were collected in SDS-PAGE sample buffer. Immunoblot analysis was used to identify target proteins of interest in both total and cell surface lysates.

Immunoblotting—Total cell lysates in 4× SDS-PAGE sample buffer were separated on a 10% SDS-PAGE gel under reducing conditions and transferred to nitrocellulose membranes (Bio-Rad) using the Trans-Blot Semi-Dry transfer apparatus (Bio-Rad). Membranes were blocked overnight in 5% skim milk in 1× TBST and then incubated with a primary antibody (anti-GRP78/Bip, catalog no. 610979, BD Transduction, San Jose, CA; anti-Phospho-eIF2α, catalog no. 9721S, Cell Signaling, Danvers, MA) followed by the appropriate horseradish peroxidase (HRP)-conjugated secondary antibodies (Dako, Carpinteria, CA) diluted in 1× TBST containing 1% skim milk. Membranes were visualized using the Western Lighting Chemiluminescence Reagent (PerkinElmer Life Sciences), and Kodak X-OMAT Blue XB-1 film (PerkinElmer Life Sciences) was exposed and developed using a Kodak X-OMAT 1000A processor. To control for equivalent protein loading, immunoblots were re-probed with a mouse monoclonal anti-β-actin antibody (catalog no. A5441, Sigma-Aldrich).

FACS Analysis—FACS analysis was used to detect cell surface TF and GRP78. Briefly, non-permeabilized T24/83 cells were detached from cell culture plates using 2 mM EDTA and centrifuged at 200 × *g* for 5 min at 4 °C. The cell pellet was resuspended in FACS wash buffer (1× PBS/1% FBS) and centrifuged at 200 × *g* for 3 min. To examine cell surface GRP78, cells were incubated (1:200 dilution) in the presence of anti-GRP78 monoclonal antibodies conjugated to Alexa488 (catalog no. SPA-827-488, Assay Design, Ann Arbor, MI). To examine surface TF, cells were incubated (1:100 dilution) in the presence of a rabbit anti-human TF antibody (catalog no. 4502, American Diagnostica, Stamford, CT) in FACS wash buffer for 40 min on ice. Cells were washed three times with FACS wash buffer and incubated (1:200) with the corresponding secondary antibody (catalog no. A21206, Alexa Fluor 488-conjugated donkey anti-rabbit, Molecular Probes, Carlsbad, CA) in FACS wash buffer for 30 min on ice in the dark. Cells were washed, fixed, and stored in 1% fresh formaldehyde. FACS data analysis was performed using the Cytomics FC 500 Series Flow Cytometry Systems (Beckman Coulter Canada, Mississauga, Ontario, Canada).

Indirect Immunofluorescence—T24/83 cells grown on coverslips were washed with Hanks' balanced salt solution (HBSS) (Invitrogen) containing 1 mM $CaCl_2$, 1 mM $MgCl_2$, and fixed for 30 min at room temperature in 4% fresh formaldehyde in 1× PBS. The slides were then incubated in 5% nonfat milk in 1× PBS for 90 min at room temperature. Excess blocking buffer was removed from the slide, and cells were incubated with a primary sheep anti-GRP78 antibody, goat anti-human tissue factor (catalog no. 4501, American Diagnostica), or a combination of the two in 1% nonfat milk in 1× PBS overnight at 4 °C. The cells were then washed three times in 1× PBST and incubated with a secondary antibody containing a 1:1000 dilution of an Alexa Fluor 568-conjugated donkey anti-sheep IgG, an Alexa Fluor 488-conjugated rabbit anti-goat IgG, or a mixture of the two for 90 min at 4 °C in the dark. As controls, cells were incubated with the secondary IgG alone. Finally, the cells were washed three times with 1× PBS and mounted. Images were captured using a Zeiss Axio Observer fluorescence microscope equipped with a 100×/1.4 numerical aperture Plan Apochromat oil immersion lens (Carl Zeiss, Thornwood, NY). Confocal data were collected as previously described (37), and optical sections were three-dimensionally reconstructed using an average intensity algorithm for projections of optical section stacks using ImageJ version 1.37 (National Institutes of Health, Bethesda, MD).

SPR—Potential biomolecular interactions were investigated using a Biacore 1000 biosensor system (Biacore, Amersham Biosciences). Biotinylated recombinant human GRP78 or ovalbumin, diluted in filtered and degassed Hepes-buffered saline (20 mM Hepes, 150 mM NaCl, pH 7.4) containing 2 mM $CaCl_2$ and 0.005% Tween 20 (HBS-Tw), was adsorbed to a Biacore streptavidin SA chip at a flow rate of 5 μl/min at 25 °C until 1300 response units (RU) of biotinylated GRP78 or 2500 RU of ovalbumin were adsorbed. To determine the binding of recombinant human TF (a generous gift from Dr. George P. Vlasuk, Corvas Pharmaceuticals) to GRP78, 30-μl aliquots, in concentrations ranging from 62.5 to 2000 nM, were injected over the flow cells at a flow rate of 10 μl/min for ~5 min, followed by a 5-min wash to monitor association and dissociation, respectively. It was not necessary to regenerate the flow cells between the injections. As a positive control, an anti-human GRP78 polyclonal antibody (catalog no. C20, Santa Cruz Biotechnology) was injected over the flow cells at a concentration of 4 μg/ml using the same protocol. Peak RU values determined for each recombinant TF concentration were corrected for the RU values with control ovalbumin.

Continuous Measurement of Cell Surface TF PCA—We have recently developed a continuous assay for the measurement of TF PCA on intact cancer cells (31). Briefly, cells were seeded into a 96-well tissue culture plate (1×10^4 cells/well) the day before the experiment. The culture media was then removed, and the cells were washed once with 1× TBS. A mixture containing 1 nM human FVIIa, 30 nM human FX, 10 mM $CaCl_2$, and 0.4 mM chromogenic substrate S-2765 (Diapharma, West Chester, OH) in 1× TBS was added to each well. Following addition of the test agent diluted in 1× TBS, the absorbance at 405 nm was measured every 2 min for 3 h at 37 °C. A standard curve was generated where 100 units of TF activity was defined as the amount of activity in 0.3 μl of human recombinant TF, which is equivalent to 450 μg of TF (as determined by the American Diagnostica ELISA). V_{max} was calculated using SoftMax Pro and used to determine the amount of FXa generated per 10,000 cells (units/10,000 cells).

RNA Isolation and RT-PCR—RNA was isolated using an RNeasy Mini kit (Qiagen), and cDNA was synthesized using a High Capacity cDNA Reverse Transcription kit (Applied Biosystems). Real-time RT-PCR reactions were carried out based on protocols described previously using SYBR Green MasterMix (Applied Biosystems) (38, 39) using primers listed in Table 1.

Calcium Imaging—Confluent cells (1×10^4 cells per well) grown in 96-well plates were washed in HBSS (Invitrogen) containing 20 mM HEPES. Fura-2 AM was prepared in 20% pluronic acid F127 (Invitrogen) in DMSO. A 10 μM working solu-

TABLE 1
Quantitative RT-PCR primers

Gene	Forward primer	Reverse primer
Spliced *XBP1*	5′-TTGAGAACCAGGAGTTAAG-3′	5′-CTGCACCTGCTGCGGACT-3′
CHOP	5′-AGAACCAGGAAACGGAAACAGA-3′	5′-TCTCCTTCATGCGCTGCTTT-3′
β-ACTIN	5′-TGGGCATGGGTCAGAAGGAT-3′	5′-AAGCATTTGCGGTGGACGAT-3′

tion of Fura 2-AM in HBSS was incubated on the cells at room temperature for 30 min. Cells were washed three times with HBSS and preincubated in HBSS for 15 min before experiments at 37 °C to allow for de-esterification of the dye. Plates were read at 37 °C kinetically at two wavelengths (λ), λ_1 (340 nm excitation, 515 nm emission, measuring dye bound to Ca^{2+}), and λ_2 (380 nm excitation, 515 nm emission, measuring unbound dye). Measurements were made for 5 min to establish a baseline followed by the addition of the agonist Tg (1 μM), Tm (5 μg/ml), or ionomycin (10 μM) diluted in 1× PBS. PBS was also used without test substance as a vehicle control. Plates were then read kinetically at λ_1 and λ_2 for 30 min to establish a ratio of Ca^{2+} bound over free dye representing the change in cytosolic [Ca^{2+}].

Measurement of Intracellular Calcium in Single Cells—Intracellular calcium in T24/83 cells was measured using the fluorescent indicator Fura-2 AM (40). The cells were plated on sterile coverslips in 35-mm tissue culture dishes and incubated at 37 °C for 18–24 h. On the day of the experiment, Fura-2 AM (2 mM) was added, and the dish was incubated at 37 °C for 30 min. Cell monolayers were then rinsed twice with HBSS containing 10 mM HEPES, pH 7.4, 3.5 mM $NaHCO_3$, and once with DMEM containing 0.1% BSA. Cell monolayers grown on coverslips were placed on the inverted microscope stage, and intracellular [Ca^{2+}] was measured using a Digital Imaging Microscopy system (Inovision Corp., Research Triangle Park, NC) employing dual excitation ratio imaging techniques at 37 °C. After collecting baseline data, increasing concentrations of the anti-GRP78 autoantibodies was added to the cell monolayers to determine the effect of ligand binding on calcium mobilization. A digitized video image was obtained by averaging up to 256 frames with the following filter combination: Fura-2 excitation, 340 and 380 nm; emission, >450 nm. Routinely, excitation intensity was attenuated 100- to 1000-fold before reaching the cell, and the background images were obtained. Intracellular [Ca^{2+}] was measured by subtracting the background from images on a pixel basis. To obtain the intracellular [Ca^{2+}] for an individual cell, the mean value of the pixel ratio for the cell was compared with values obtained with the same equipment using Fura-2-containing EGTA-Ca^{2+} buffers (41).

Statistical Analysis—Excel software was used to determine the standard error of the mean for each treatment. Significance of differences between control and various treatments was determined by analysis of variance. On finding significance with analysis of variance, an unpaired Student's *t* test was performed. For all analyses, $p \leq 0.05$ was considered significant.

RESULTS

T24/83 Cells Express Cell Surface GRP78 and TF—We (24, 31) as well as others (42) have demonstrated that the T24/83 human bladder carcinoma cell line displays prothrombotic characteristics due to enhanced TF expression and PCA. Based on these findings, T24/83 cells were chosen as our cancer cell model to investigate the effect of cell surface GRP78 on TF PCA.

A number of studies have identified GRP78 on the surface of a variety of human cancer cells (26–31, 43–45). To determine if GRP78 is similarly expressed on the surface of T24/83 cells, cell surface proteins were isolated using a biotin-based technique followed by immunoblotting with anti-GRP78 antibodies. GRP78 was identified in both total cell lysates and on the cell surface of T24/83 cells using this approach (Fig. 1*A*). As expected, TF was predominantly expressed on the cell surface, consistent with its localization in the plasma membrane. In contrast to GRP78 and TF, several nuclear proteins, including proliferating cell nuclear antigen and lamin B were exclusively found in the total cell lysates and not on the cell surface. Consistent with these biochemical findings, FACS analysis (Fig. 1*B*) and three-dimensional image reconstruction of optical sections captured using confocal microscopy (Fig. 1*C*) demonstrated the presence of GRP78 on the cell surface. In these reconstructions, GRP78 was observed throughout the cell surface; however, punctuate regions of high GRP78 expression were apparent above the nucleus. Indirect immunofluorescence on non-permeabilized cells showed the presence of GRP78 and TF on the surface of T24/83 cells (Fig. 1*D*). Both cell surface GRP78 and TF were expressed in a similar staining pattern over the cell surface. Negative controls with the secondary antibody alone showed little or no immunofluorescence. Taken together, these findings demonstrate that T24/83 cells actively express both GRP78 and TF on their cell surface.

GRP78 Does Not Directly Bind to TF or Modulate TF PCA—Previous studies have suggested that GRP78 can negatively regulate procoagulant activity by directly associating with TF on the cell surface of endothelial cells (25). Although anti-GRP78 antibodies were able to immunoprecipitate TF, as observed on immunoblots, anti-TF antibodies failed to pull down GRP78 (data not shown). To further assess the direct interaction between GRP78 and TF, surface plasmon resonance (SPR) was used to measure binding between immobilized recombinant human GRP78 and full-length non-lipidated recombinant human TF. As shown in Fig. 2*A* (*upper panel*), the shallow and linear slope of the dose-response curves between TF and GRP78 suggests no specific binding. As a positive control, a strong and direct interaction was observed between the immobilized GRP78 and an anti-GRP78 antibody (Fig. 2*A*, *bottom panel*). Further, treatment of quiescent T24/83 cells with increasing doses of recombinant GRP78 had no effect on TF PCA (Fig. 2*B*). Because exogenous recombinant GRP78 did not activate TF PCA on quiescent T24/83 cells, we examined whether it could modulate TF PCA induced by thapsigargin. Again, increasing doses of recombinant GRP78 had no effect on

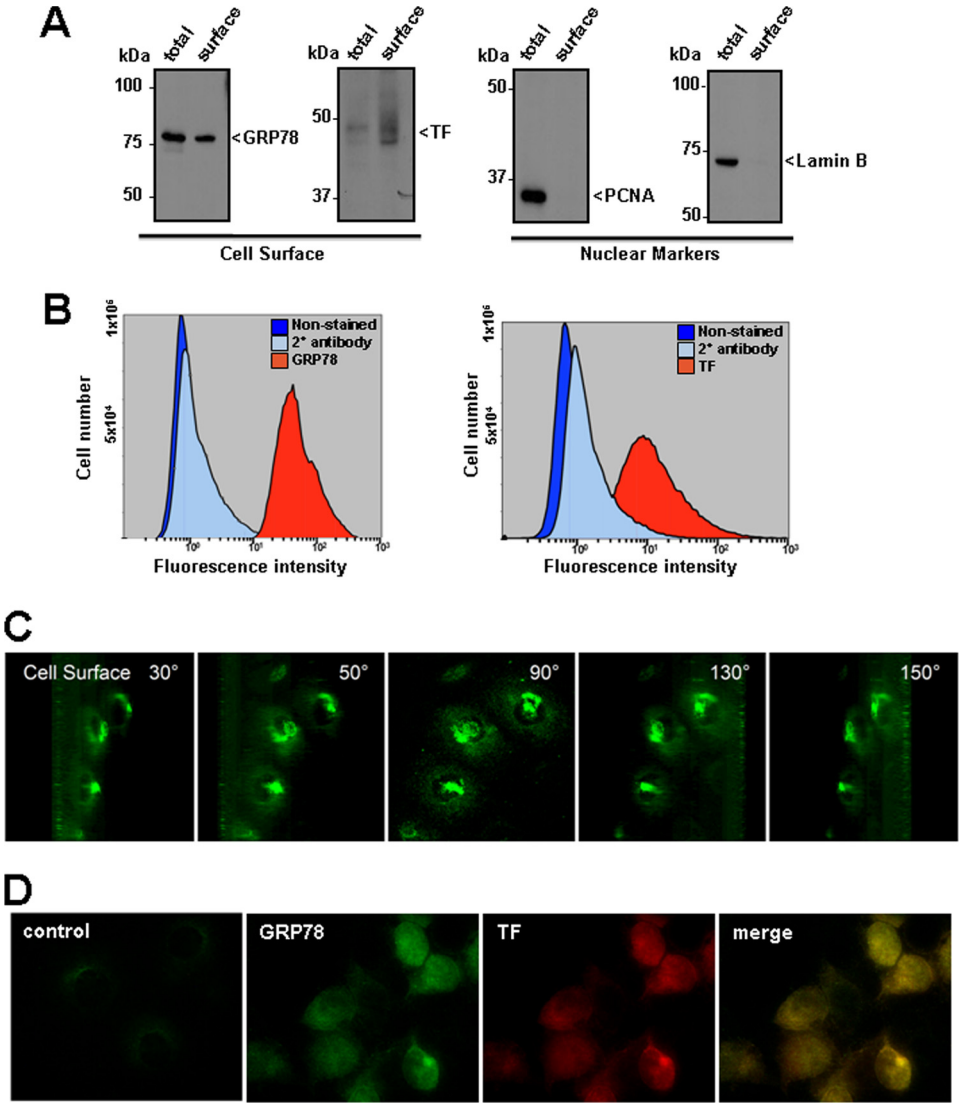

FIGURE 1. **GRP78 and TF are expressed on the surface of T24/83 cells.** *A*, cell surface proteins were biotinylated, and cell lysates were subjected to streptavidin pulldown. Cell surface proteins were eluted, separated on 10% SDS-PAGE gels, transferred to nitrocellulose membranes, and immunoblotted with antibodies to GRP78 (*GRP78*), anti-proliferating nuclear cell antigen (*PCNA*), lamin B (*lamin B*), or TF (*TF*). Cell surface fractions (*surface*) were compared with proteins in total cell lysates (*total*). The nuclear markers PCNA and Lamin B are not present in the surface fractions. *B*, cell surface GRP78 and TF were detected by FACS analysis using antibodies against GRP78 or TF, respectively. Secondary antibody staining alone and unstained cells acted as negative controls. *Histograms* were generated using the Cytomics FC 500 series flow cytometry software. *C*, T24/83 cells grown on coverslips were fixed without permeabilization, immunostained for GRP78, and subjected to confocal analysis. Optical sections of the cells were three-dimensionally reconstructed and projected using ImageJ software at rotation angles of 30, 50, 90, 130, and 150 degrees to visualize cell surface GRP78. *D*, identification of cell surface GRP78 and TF in T24/83 cells. Co-immunostaining for GRP78 and TF was performed on fixed, non-permeabilized cells and viewed by fluorescence microscopy. Regions of cell surface overlap for GRP78 and TF in the *merged image* appear as *yellow* staining.

the ability of thapsigargin to enhance TF PCA (Fig. 2*C*). These findings suggest that GRP78 does not directly bind to TF and fails to modulate TF PCA on T24/83 cells.

Increased Cytosolic [Ca^{2+}] and Not UPR Activation Induces TF PCA in T24/83 Cells—We have demonstrated recently that the ER stress-inducing agents ionomycin and thapsigargin up-regulate TF PCA by increasing cytosolic [Ca^{2+}] (24, 31). To determine whether increased TF PCA results from UPR activation or a specific elevation of cytosolic [Ca^{2+}] brought about by thapsigargin, T24/83 cells were also treated with tunicamycin, an inducer of ER stress that inhibits GlcNAc phosphotransferase activity and *N*-linked glycosylation (46) without altering cytosolic [Ca^{2+}]. Immunoblotting showed that both thapsigargin and tunicamycin caused ER stress and unfolded protein response (UPR) induction, as measured by a temporal increase in eIF2α phosphorylation and GRP78 protein levels (Fig. 3*A*). Further, quantitative RT-PCR demonstrated a similar increase in the mRNA levels for CHOP as well as the spliced form of XBP-1 in T24/83 cells treated with thapsigargin or tunicamycin (Fig. 3*B*). However, only thapsigargin was able to increase cytosolic [Ca^{2+}] (Fig. 3*C*). As expected, ionomycin treatment also caused a significant and sustained increase in cytosolic [Ca^{2+}]. Comparison of the effect of tunicamycin and thapsigargin on TF PCA revealed that only thapsigargin dose-dependently increased TF PCA in T24/83 cells (Fig. 3*D*). Given that thapsigargin depletes ER Ca^{2+} stores and increases cytosolic [Ca^{2+}], we investigated whether chelating the free cytosolic Ca^{2+} would reduce TF PCA activation. Pretreatment of cells with 1,2-bis(2-aminophenoxy)ethane-*N*,*N*,*N*′,*N*′-tetraacetic acid (BAPTA), a specific Ca^{2+} chelator (47), significantly reduced thapsigargin-mediated TF PCA (Fig. 3*E*). These findings suggest that increases in cytosolic [Ca^{2+}] induce TF PCA independent of ER stress and UPR activation.

Anti-GRP78 Autoantibodies Increase Cytosolic [Ca^{2+}] and Induce TF PCA—Previous studies have reported that anti-GRP78 autoantibodies from prostate cancer patients bind to cell surface GRP78 on several human prostate cancer cell lines and cause the release of Ca^{2+} from ER stores (26). Consistent with these findings, anti-GRP78 autoantibodies were able to dose-dependently increase cytosolic [Ca^{2+}] over a human IgG control in T24/83 cells (Fig. 4*A*). Importantly, autoantibody concentrations of 60 μg/ml caused a >6-fold increase in cytosolic [Ca^{2+}], intracellular levels that are necessary to up-regulate TF PCA (15). To elucidate the effect of anti-GRP78 autoantibodies on TF PCA, cells were treated with increasing concentrations of the anti-GRP78 autoantibody: 7 μg/ml, which corresponds to the maximum levels observed in the healthy population, and 30–60 μg/ml, which corresponds to the levels observed in prostate

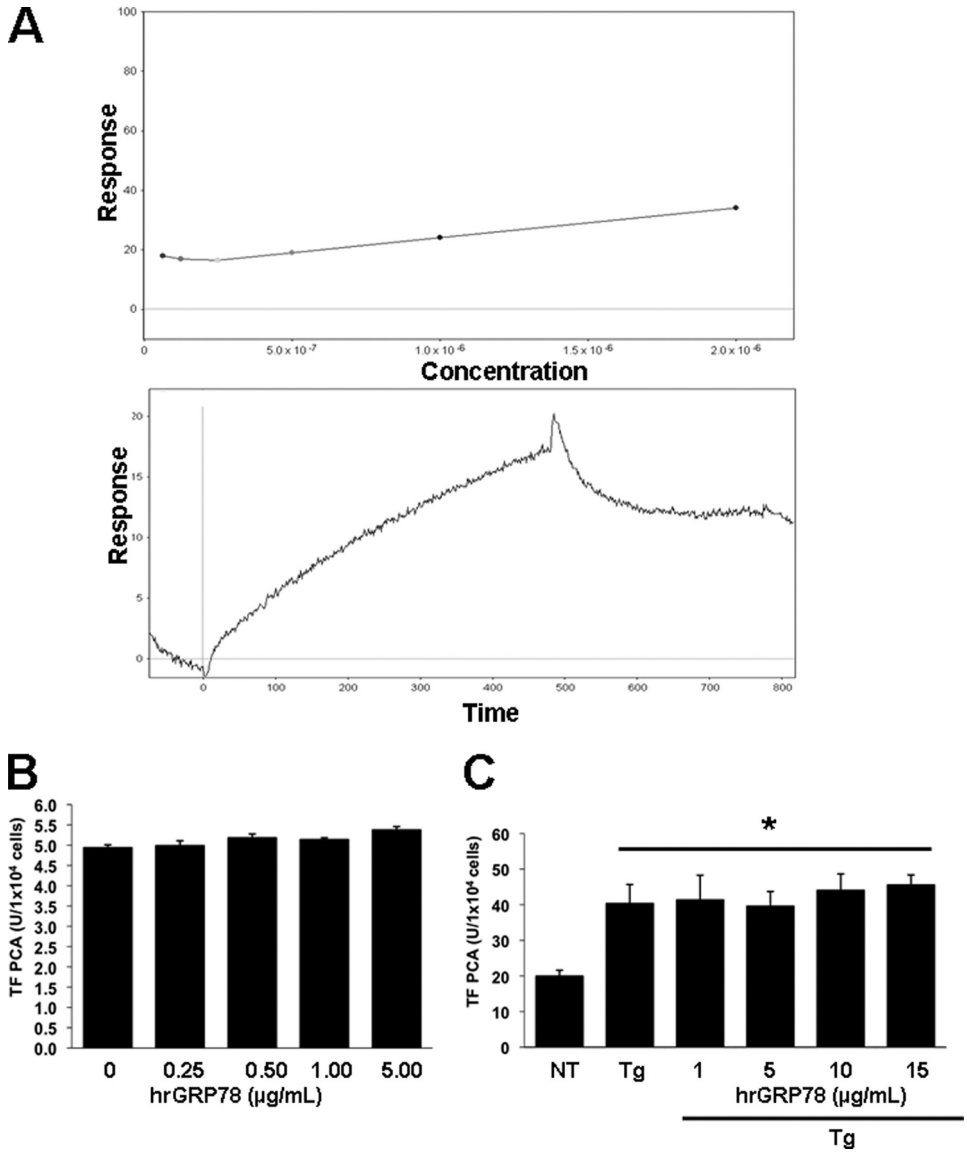

FIGURE 2. **Recombinant human GRP78 does not bind to TF and fails to modulate TF PCA.** *A*, binding of recombinant human GRP78 to TF using SPR. Biotinylated recombinant human GRP78 was adsorbed to a separate flow cell of an SA BIAcore chip containing pre-immobilized streptavidin to ~1300 RU. As a control, ovalbumin was adsorbed to a separate flow cell to ~2500 RU. Increasing concentrations of recombinant human TF (62.5–2000 nM) were injected into the flow cells at 10 μl/min, followed by a 5-min wash to monitor dissociation (*top panel*). Data indicate that the addition of increasing doses of TF do not bind to immobilized GRP78. As a positive control, robust binding was demonstrated between an anti-GRP78 antibody and the immobilized GRP78. *B*, effect of exogenous recombinant human GRP78 on TF PCA. T24/83 cells (1×10^4 cells/well) seeded in a 96-well plate were treated with increasing doses of exogenous recombinant human GRP78 (*hrGRP78*) for 3 h, and TF PCA was measured using the continuous assay ($n = 8$). *C*, effect of exogenous recombinant human GRP78 (*hrGRP78*) on TF PCA induced by thapsigargin. T24/83 cells were seeded in a 96-well plate and treated with 5 μM thapsigargin (*Tg*) in the absence or presence of increasing concentrations of exogenous recombinant human GRP78. TF PCA was measured using the continuous assay ($n = 8$). *, $p < 0.05$ *versus* non-treated cells (*NT*).

cancer patients (Fig. 4*B*) (26). Our results demonstrated that treatment of cells with 7 μg/ml of the anti-GRP78 autoantibodies had no effect on TF PCA. However, 60 μg/ml of the autoantibody caused a significant increase in TF PCA similar to that observed with thapsigargin (Fig. 4*B*). A similar enhancement in TF PCA was observed with 30 μg/ml of the autoantibody. This effect on TF PCA was abolished by preincubation with an anti-TF inhibitory antibody, implying that this effect was mediated exclusively by TF. In contrast, the nonspecific anti-GFP antibody had no significant effect on TF PCA induced by the autoantibodies. To further confirm the role of cell surface GRP78 in TF PCA following treatment with the anti-GRP78 autoantibodies, we utilized the prostate cancer cell line (PC-3) that expresses TF (31) but low levels of cell surface GRP78 (Fig. 4*C*) (26). Both T24/83 and PC-3 cells were treated with thapsigargin or anti-GRP78 autoantibodies, and TF PCA was measured (Fig. 4*D*). Thapsigargin treatment elicited a significant up-regulation of TF PCA for both cell lines. In contrast, autoantibody treatment up-regu lated TF PCA in the T24/83 but not PC-3 cells, suggesting that cell surface GRP78 is necessary for autoantibody-mediated TF PCA.

Pretreatment with the CNVKSDKSC Peptide Blocks Autoantibody-mediated TF PCA in T24/83 Cells—Anti-GRP78 autoantibodies produced by prostate cancer patients bind to a peptide containing the primary amino acid sequence CNVKSDKSC, which mimics the linear primary amino acid sequence Leu^{98}–Leu^{115} located in the N-terminal region of GRP78 (33). Based on these findings, we determined whether the CNVKSDKSC peptide inhibits TF PCA in T24/83 cells treated with the anti-GRP78 autoantibodies. As shown in Fig. 5*A*, pretreatment of the anti-GRP78 autoantibodies with the CNVKSDKSC peptide significantly inhibited TF PCA in T24/83 cells. The observation that the CNVKSDKSC peptide failed to inhibit TF PCA following thapsigargin treatment indicates that the peptide has no direct inhibitory effect on TF PCA (data not shown).

Anti-GRP78 Autoantibody Increases Cytosolic [Ca^{2+}] via Phospholipase C Activation—It has been reported that cell surface GRP78 interacts with a heterotrimeric G protein, resulting in Gqα-protein-dependent activation of phospholipase C (PLC) (48). PLC cleaves phosphatidylinositol 4,5-bisphosphate to produce diacylglycerol and IP_3. Once formed, IP_3 molecules bind specific IP_3 receptors/Ca^{2+} channels on the ER membrane (49), thereby increasing cytosolic [Ca^{2+}], which could enhance TF PCA. To evaluate the role of PLC in autoantibody-mediated TF PCA, T24/83 cells were treated with the PLC inhibitor U73122 or its non-active analogue U73343. As shown in Fig. 5*B*, treatment of cells with

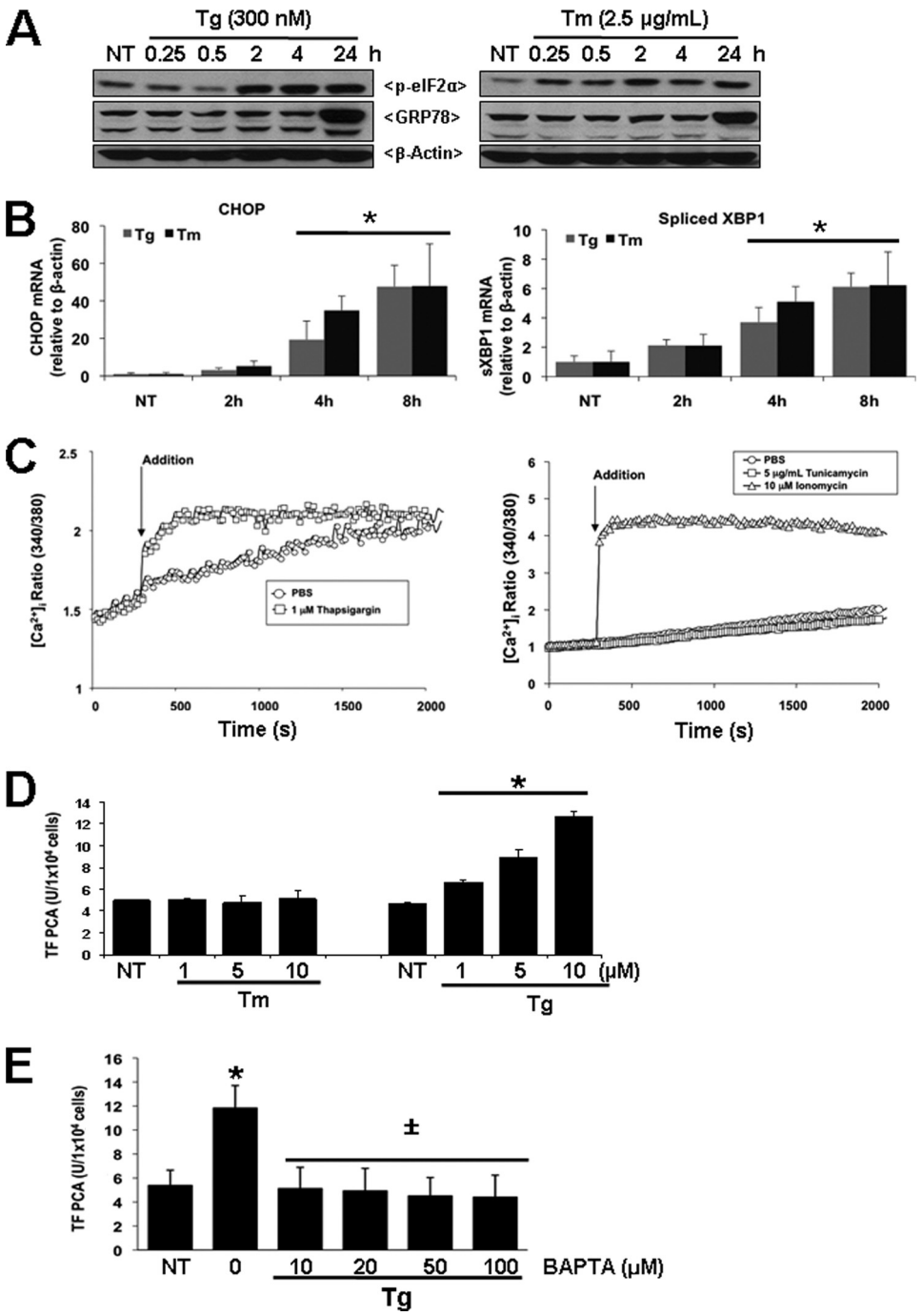

FIGURE 3. **Differential effects of ER stress agents on cytosolic [Ca^{2+}] and TF PCA in T24/83 cells.** *A*, detection of UPR markers in T24/83 cells following treatment with tunicamcyn (*Tm*) or thapsigargin (*Tg*). T24/83 cells in 6-well plates were treated with ER stress-inducers tunicamycin (2.5 μg/ml) or thapsigargin (300 nM) for 24 h. Total protein lysates solubilized in SDS-PAGE sample buffer were separated in 10% SDS-PAGE gels, transferred to nitrocellulose membranes, and immunoblotted for phospho-eIF2α (*p-eIF2*α) and GRP78. Membranes were stripped and reprobed with β-actin as a loading control. Results shown are representative of three independent experiments. *B*, quantitative RT-PCR analysis of CHOP and spliced XBP-1 mRNA in T24/83 cells treated with thapsigargin or tunicamycin for 2, 4, and 8 h. Total RNA was isolated, reverse transcribed to single-stranded cDNA, and analyzed by quantitative RT-PCR using primers specific for human CHOP or spliced XBP1. Results are expressed as -fold induction of target gene mRNA levels *versus* β-actin. *, $p < 0.05$ *versus* non-treated (*NT*) cells. *C*, effect of thapsigargin or tunicamycin on cytosolic [Ca^{2+}] in T24/83 cells. Calcium fluorometry of T24/83 cells treated with thapsigargin (1 μM), tunicamycin (5 μg/ml), ionomycin (10 μM), or drug vehicle (1× PBS), was determined utilizing the ratiometric calcium-sensitive dye Fura-2 AM. Ratiometric measurements were made for 30 min after agonist stimulation. *D*, TF PCA in T24/83 cells following treatment with increasing concentrations of thapsigargin or tunicamycin. *, $p < 0.01$ *versus* non-treated cells (*NT*). *E*, TF PCA in T24/83 cells following treatment with 5 μM thapsigargin (positive control). T24/83 cells were pre-treated for 30 min in the absence or presence of increasing doses of BAPTA. *, $p < 0.05$ *versus* non-treated cells (*NT*). $^{\pm}$, $p < 0.05$ *versus* Tg-treated cells.

U73122, but not U73343, dose-dependently inhibited the up-regulation of TF PCA induced by the anti-GRP78 autoantibodies.

Tunicamycin Pretreatment Reduces TF PCA—GRP78 is a major ER lumenal Ca^{2+}-storage protein, and its overexpression can protect cells from Ca^{2+}-induced cytotoxicity (50). Preconditioning of cells with sub-lethal doses of tunicamycin can increase GRP78 protein levels and prevent disturbances in ER Ca^{2+} (51). Based on these findings, T24/83 cells were pretreated with tunicamycin for 24 h to induce the expression of GRP78 (Fig. 3*A*) without an up-regulation of TF PCA (Fig. 3*C*). Following tunicamycin pretreatment, T24/83 cells were tested for TF PCA up-regulation in the absence or presence of either thapsigargin or anti-GRP78 autoantibodies. As shown in Fig. 5*C*, tunicamycin pretreatment significantly reduced the effects of thapsigargin or anti-GRP78 autoantibodies on TF PCA. Furthermore, tunicamycin pretreatment caused a significant repression in TF PCA in non-treated T24/83 cells.

Annexin V Inhibits TF PCA Mediated by Thapsigargin or Anti-GRP78 Autoantibodies—Increases in cytosolic [Ca^{2+}] have been shown to activate TF at the cell surface by perturbing the plasma membrane PS asymmetry leading to exposure of PS molecules (15) and the acceleration of coagulation reactions on the cell surface (16, 52–54). Treatment of T24/83 cells with increasing doses of annexin V, a specific PS-binding protein (16), resulted in a significant repression in TF PCA mediated by thapsigargin or anti-GRP78 autoantibodies (Fig. 5*D*). Unlike tunicamycin pretreatment, annexin V had no inhibitory effect on TF PCA in non-treated T24/83 cells.

DISCUSSION

The majority of tumor cells display increased TF expression and the prothrombotic state observed in cancer patients has been largely attributed to the activation of TF

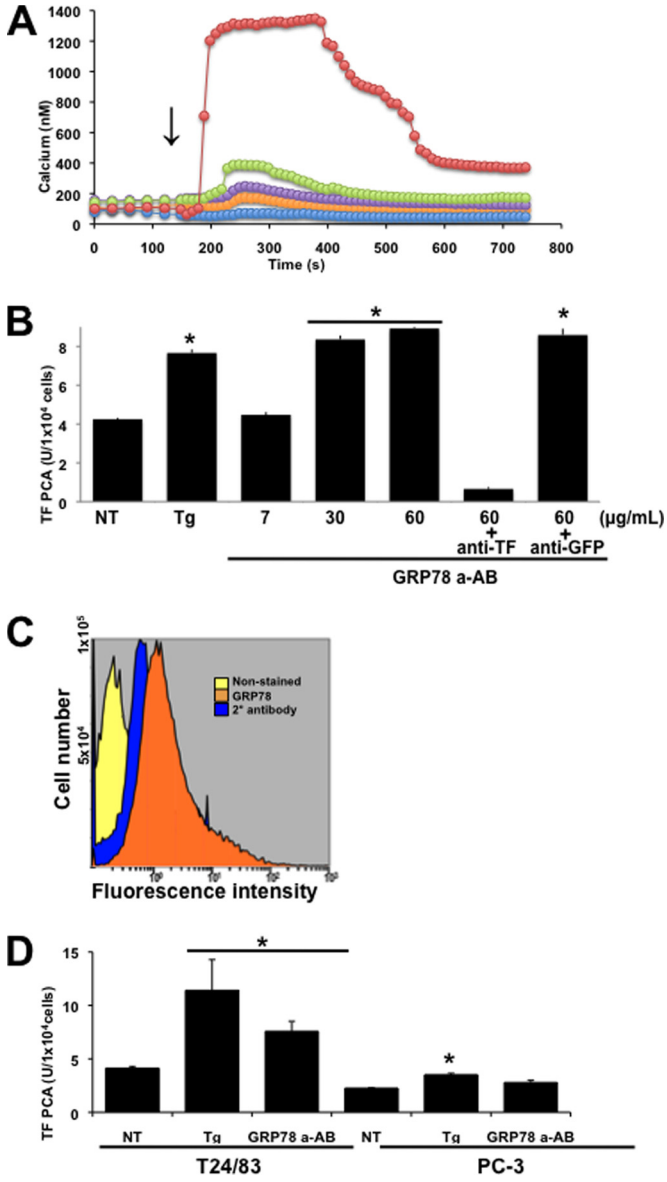

FIGURE 4. **Effect of anti-GRP78 autoantibodies on cytosolic [Ca^{2+}] and TF PCA.** *A*, T24/83 cells were loaded with Fura-2 AM (4 μM), and changes in intracellular [Ca^{2+}] were measured using digital imaging microscopy on single cells after the addition of 5 (*orange circles*), 10 (*violet circles*), 20 (*green circles*), or 60 (*red circles*) μg/ml of anti-GRP78 autoantibodies. Human IgG (*blue circles*) was used as a negative control. *B*, TF-PCA on intact T24/83 cells treated with 5 μM (Tg) thapsigargin or increasing concentrations of the anti-GRP78 autoantibody (*GRP78 a-AB*). *60+antiTF* represents cells pretreated for 1 h with 10 μg/ml of an anti-TF neutralizing antibody. *60+antiGFP* represents cells pretreated for 1 h with 10 μg/ml anti-GFP antibody. TF-PCA was measured continuously for 3 h on T24/83 cells treated with 60 μg/ml of the anti-GRP78 autoantibody (*GRP78 a-AB*). *C*, cell surface detection of GRP78 on PC-3 cells by FACS analysis using antibodies against GRP78. Secondary antibody staining alone and unstained cells acted as negative controls. *Histograms* were generated using the Cytomics FC 500 series flow cytometry software. *D*, TF-PCA was measured in T24/83, and PC-3 cells were treated in the absence or presence of 5 μM thapsigargin (*Tg*) or 60 μg/ml anti-GRP78 autoantibody (*GRP78 a-AB*). *, $p < 0.05$ *versus* non-treated cells (*NT*).

(4). Our previous studies have demonstrated that overexpression of GRP78 in the ER lumen inhibits TF PCA by protecting cells from changes in cytosolic [Ca^{2+}] and/or the generation of reactive oxygen species (24, 37). However, unlike normal cells, GRP78 is present on the cell surface of a wide variety of human cancer cells (26–31, 43–45). In this study, we investigated whether the presence of cell surface GRP78 modulates TF PCA in T24/83 cells, a well established human bladder carcinoma cell line with prothrombotic characteristics (42). Our findings suggest that the binding of anti-GRP78 autoantibodies to cell surface GRP78 causes PLC-mediated release of Ca^{2+} from ER stores, thereby increasing cytosolic [Ca^{2+}]. This in turn alters plasma membrane asymmetry resulting in enhanced TF PCA. Thus, our findings may explain how TF is activated on the surface of cancer cells and contributes to the hypercoagulable state observed in cancer patients.

Our initial experiments were designed to assess the effects of ER stress-inducing agents on cytosolic [Ca^{2+}] and TF PCA. Treatment of T24/83 cells with thapsigargin or tunicamycin, two well known ER stress-inducing agents, elicited diametrically opposed effects on TF PCA. Thapsigargin, a well defined sarco/endoplasmic reticulum Ca^{2+}-ATPase pump inhibitor, induces ER stress by depleting ER Ca^{2+} stores and increasing cytosolic [Ca^{2+}] (55). In contrast, tunicamycin induces ER stress by inhibiting *N*-linked glycosylation (46). Both tunicamycin and thapsigargin induced ER stress in T24/83 cells, as demonstrated by a similar activation of UPR markers. However, unlike thapsigargin, tunicamycin treatment did not increase cytosolic [Ca^{2+}]. Moreover, thapsigargin, but not tunicamycin treatment, dose-dependently up-regulated TF PCA suggesting that depletion of ER Ca^{2+} stores and not ER stress/UPR activation is required for the up-regulation of TF PCA. Further support for this concept comes from the additional observation that chelation of cytosolic Ca^{2+} with BAPTA-AM attenuated thapsigargin-induced TF PCA.

The ability of tunicamycin to induce the expression of GRP78 without altering cytosolic [Ca^{2+}] implies that pretreatment with this ER stress-inducing agent could potentially inhibit TF PCA. This is based on previous studies showing that GRP78 is a major ER lumenal Ca^{2+}-storage protein and protects from Ca^{2+}-induced cell death (50). In a previous study, we also reported that overexpression of GRP78 by tunicamycin reduces the release of Ca^{2+} from ER stores (37). Indeed, tunicamycin preconditioning inhibited TF PCA induced by anti-GRP78 autoantibodies or thapsigargin. These findings provide evidence that suppressing the release of ER Ca^{2+} by overexpressing GRP78, and likely other ER chaperones in the ER lumen, can block TF PCA.

Cell surface biotinylation was used to demonstrate the expression of TF as well as GRP78 on the surface of T24/83 cells, a finding consistent with other cancer cells (26–30). Indirect immunofluorescence and FACS analysis confirmed the presence of cell surface GRP78 and TF. Three-dimensional reconstructions of optical sections acquired by confocal microscopy revealed high GRP78 expression above the nucleus of T24/83 cells. Although not completely understood, localization of GRP78 expression to this region may reflect distinct focal points for the recruitment of GRP78 to the cell surface. Thus, it is interesting to note that ER-resident chaperone proteins such as GRP78, calnexin, and calreticulin can associate with focal adhesions to mediate IL-1-induced Ca^{2+} signaling (56, 57).

The cellular localization of GRP78 to the ER lumen is dictated by its C-terminal KDEL (Lys-Asp-Glu-Leu) sequence, an ER retention signal found on many ER-resident chaperones (30,

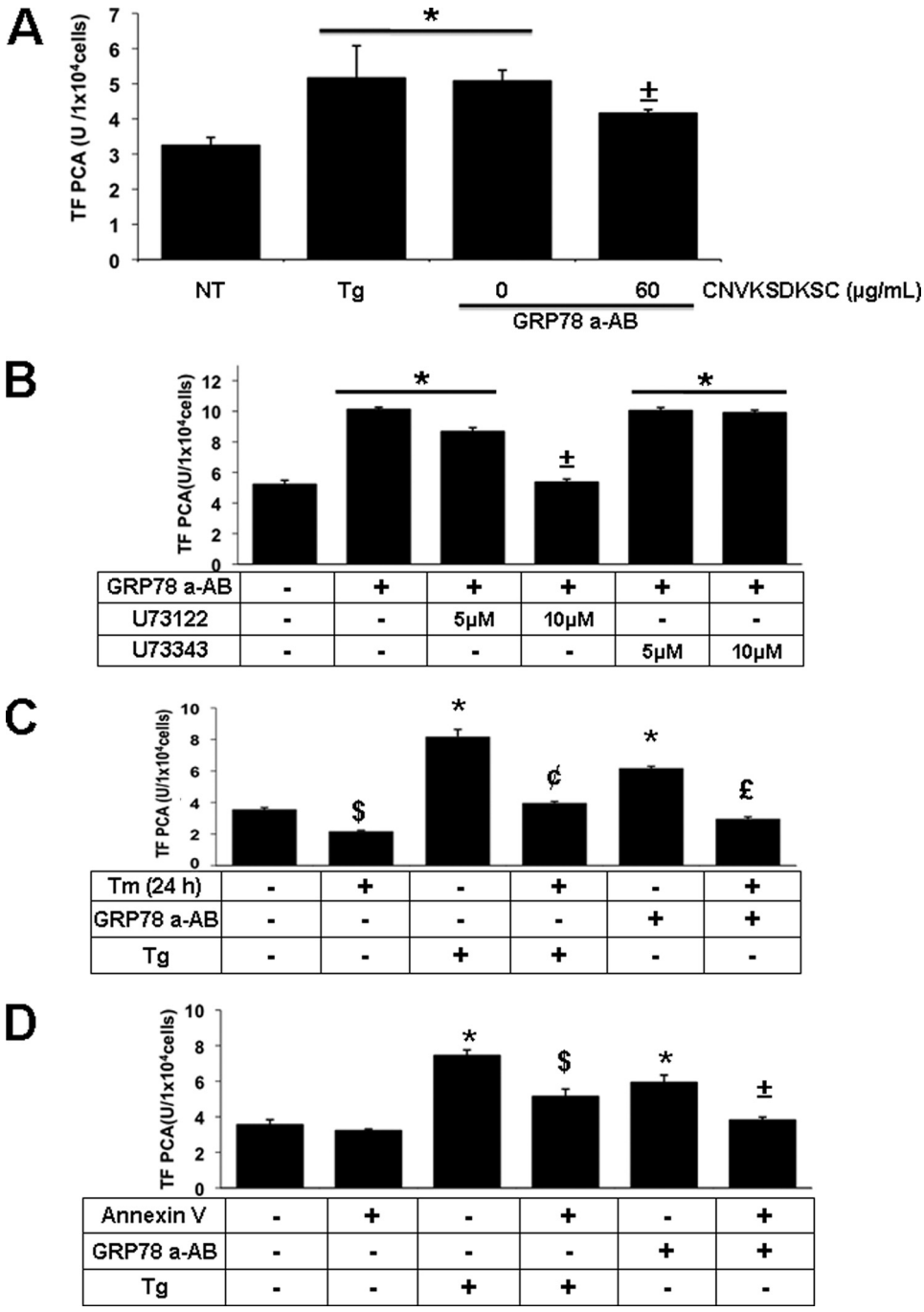

FIGURE 5. **Binding of anti-GRP78 autoantibodies to cell surface GRP78, changes in cytosolic [Ca^{2+}] or alterations in plasma membrane integrity modulate TF PCA.** *A*, effect of CNVKSDKSC peptide on TF PCA induced by anti-GRP78 autoantibodies. TF-PCA was measured on intact T24/83 cells treated with 5 μM thapsigargin (*Tg*) or 60 μg/ml anti-GRP78 autoantibodies (*GRP78 a-AB*) in the absence or presence of 60 μg/ml CNVKSDKSC peptide. *, $p < 0.05$ *versus* non-treated cells (*NT*). $^{\pm}$, $p < 0.05$ *versus* cells treated with thapsigargin or the anti-GRP78 autoantibodies. *B*, effect of PLC inhibition on TF PCA induced by anti-GRP78 autoantibodies. T24/83 cells were pretreated for 1 h in the absence or presence of 5 or 10 μM of the active or non-active PLC inhibitors, U73122 or U73343, respectively. TF-PCA was then measured on intact T24/83 cells treated with 60 μg/ml anti-GRP78 autoantibodies (*GRP78 a-AB*). *, $p < 0.005$ *versus* non-treated cells. $^{\pm}$, $p < 0.05$ *versus* cells treated with U73122 or U73343. *C*, effect of tunicamycin pre-conditioning on TF PCA induced by 5 μM thapsigargin (*Tg*) or 60 μg/ml anti-GRP78 autoantibodies. T24/83 cells were grown in the absence or presence of low-dose tunicamycin (*Tm*, 2.5 μg/ml) for 24 h. Following washing with 1× TBS, cells were placed in fresh growth media for 3 h before the addition of 5 μM thapsigargin (*Tg*) or 60 μg/ml anti-GRP78 autoantibodies. TF PCA was measured continuously for 3 h following the addition of thapsigargin or anti-GRP78 autoantibodies. *, $p < 0.05$ *versus* untreated cells (*NT*). $^{\$}$, $p < 0.05$ *versus* untreated cells (NT). $^{¢}$, $p < 0.05$ *versus* thapsigargin treated cells. $^{£}$, $p < 0.05$ *versus* autoantibody treated cells. *D*, effect of annexin V pre-treatment on TF PCA. TF PCA was measured continuously for 3 h on intact T24/83 cells treated with 5 μM thapsigargin (*Tg*) or 60 μg/ml anti-GRP78 autoantibodies (*GRP78 a-AB*) in the absence or presence of 2.5 μg/ml annexin V (2.5 μg/ml). *, $p < 0.05$ *versus* non-treated cells (*NT*). $^{\$}$, $p < 0.05$ *versus* thapsigargin treated cells. $^{\pm}$, $p < 0.05$ *versus* autoantibody treated cells.

58, 59). However, GRP78 is found on the cell surface of many cancer cells where it acts as a signaling receptor (26, 29, 32). Currently, it remains unclear how GRP78 escapes ER retrieval mechanisms mediated by the KDEL receptor, given that GRP78 isolated from the cell surface retains its KDEL sequence (30, 58). Two possible explanations are that the KDEL receptors on the ER membrane are down-regulated, modified, or saturated with other ER lumenal proteins or that the KDEL sequence on GRP78 is somehow masked by the co-chaperone MTJ-1 (60). Recent studies have also demonstrated that ER stress may mediate specific mechanisms for GRP78 surface localization and/or ER retention (58). In addition to its cell surface localization on cancer cells, the ability of GRP78 to be incorporated into the plasma membrane is of major interest. Previous studies have demonstrated a subpopulation of GRP78 that is present on the cytosolic surface of the ER membrane (61), consistent with that of a transmembrane protein. In addition to GRP78, calnexin is another ER transmembrane protein found on the cell surface (62).

Recent studies have suggested a direct GRP78/TF interaction at the surface of cultured vascular endothelial cells (25) and platelets (63), suggesting that GRP78 can directly bind TF to negatively regulate its activity (25). However, our SPR studies failed to reveal binding of functional recombinant GRP78 to TF. Although we could immunoprecipitate TF from the surface of T24/83 cells with anti-GRP78 antibodies, in reciprocal experiments we were unable to immunoprecipitate cell surface GRP78 with an anti-TF antibody. These observations suggest in cancer cells that the interaction between cell surface GRP78 and TF is weak or that an antibody-mediated conformational change occurs in cell surface GRP78 or TF that alters binding. The inability of exogenously added human recombinant GRP78 to modulate TF PCA on the sur-

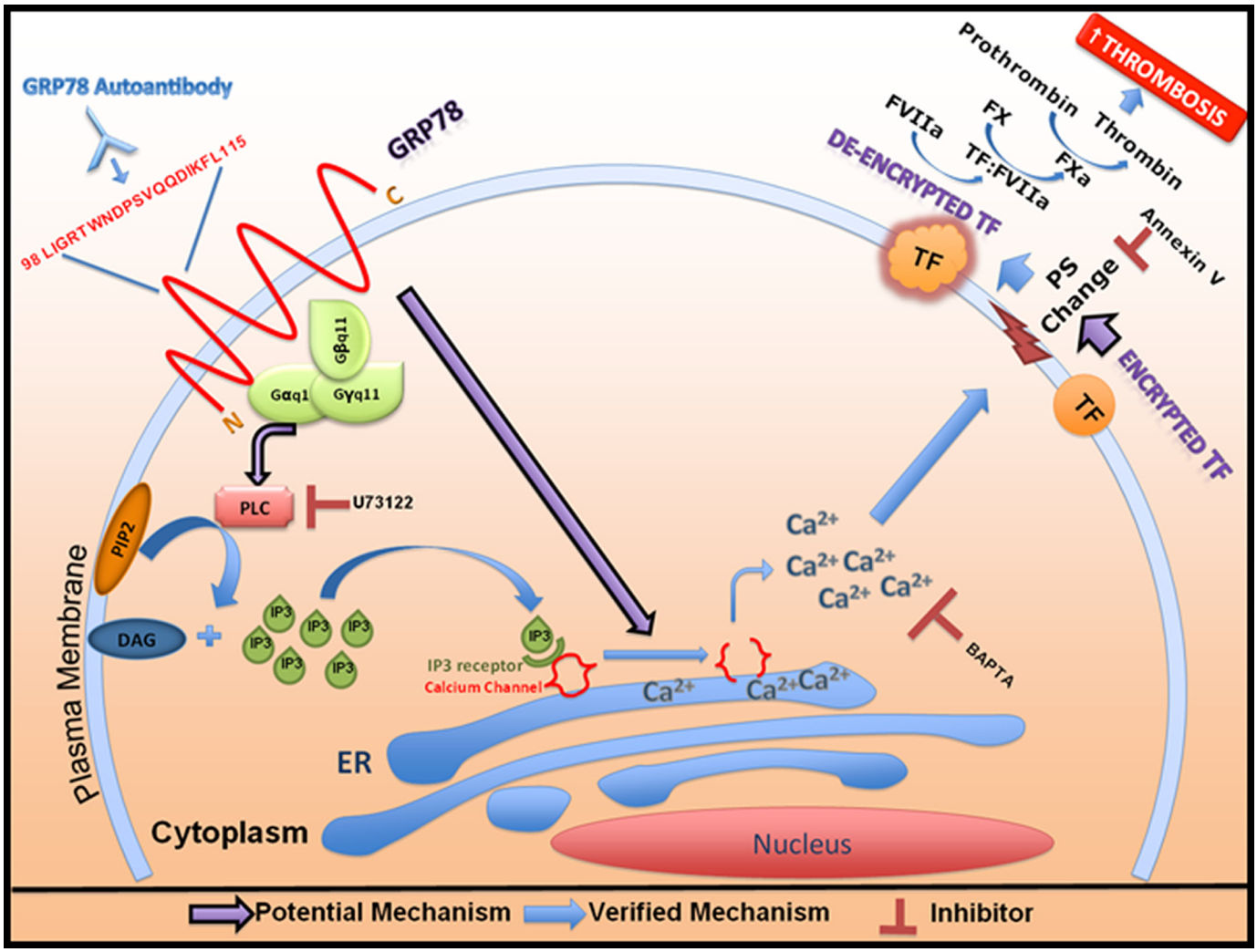

FIGURE 6. **A model for enhanced TF PCA following the binding of anti-GRP78 autoantibodies to cell surface GRP78.** Cell surface GRP78 forms a putative complex with the G-protein-11 (G-α,β,γ-11) complex. Anti-GRP78 autoantibodies bind to the Leu^{98}–Leu^{115} N-terminal domain of GRP78 exposed on the cell surface. Upon binding, a signaling cascade involving $G\alpha_{q11}$ is activated, leading to enhanced PLC activation and inositol 1,4,5-trisphosphate (IP_3) production. IP_3 molecules can readily diffuse through the cytosol where they bind to their specific receptors on the ER, leading to the opening of Ca^{2+} channels on the ER membrane and elevating cytosolic [Ca^{2+}]. This increase in cytosolic [Ca^{2+}] can result in TF de-encryption by disrupting plasma membrane asymmetry and leading to the exposure of PS on the cell surface. TF de-encryption triggers an increase in TF PCA, resulting in increased thrombosis.

face of resting or activated T24/83 cells again implies no direct interaction. This finding is consistent with a recent report demonstrating that exogenously added recombinant GRP78 does not bind to the cell surface (58). Although our findings suggest that GRP78 and TF do not form a direct complex, at least in the context of purified components, we cannot rule out the possibility that GRP78 and TF form transient multiprotein complexes on the cell surface, in different cell types or under varying stress conditions, such as ER or oxidative stress. Clearly, additional studies are required to further clarify the cellular factors or stress conditions that affect GRP78/TF interactions on the cell surface.

The topography of cell surface GRP78 and its adaptation to function as a signaling receptor can somehow affect its immunogenicity (26, 32, 33). Autoantibodies to GRP78 have been identified in the serum from patients with prostate, ovarian, or gastric cancer (32, 33). In virtually all these cancers, these autoantibodies recognize the linear GRP78 primary amino acid sequence Leu^{98}–Leu^{115}, implying that this region in the N-terminal domain of cell surface GRP78 is highly immunogenic. In terms of clinical significance, the presence of anti-GRP78 autoantibodies in human plasma correlates with accelerated cancer progression, enhanced metastatic potential, and reduced survival (33). In this study, we showed that treatment of T24/83 cells with levels of anti-GRP78 autoantibodies (60 μg/ml) comparable to those found in the plasma of prostate cancer patients caused a significant increase in cytosolic [Ca^{2+}] and enhanced TF PCA. In contrast, exposure of the cells to lower concentrations of these anti-GRP78 autoantibodies (7 μg/ml) found in the plasmas of healthy individuals failed to affect cytosolic [Ca^{2+}] or up-regulate TF PCA (26). As confirmation for a role of cell surface GRP78 in activating TF PCA, we utilized the PC-3 prostate cancer cell line that expresses TF but little or no GRP78 on the cell surface (26). Here, we were able to show that treatment with anti-GRP78 autoantibodies did not enhance TF PCA; however, a significant increase in TF PCA was still observed when PC-3 cells were treated with thapsigargin. Taken together, these findings suggest that, in addition to

GRP78 exposure on the cell surface, the TF PCA response also requires the presence of a certain threshold level of circulating anti-GRP78 autoantibodies.

The receptor function of cell surface GRP78 has been demonstrated in respect to α_2M signaling (64) and as a co-receptor for the COX A9 virus (65, 66). Additionally, immunoprecipitation studies of plasma membrane fractions from activated α_2M stimulated macrophages demonstrated cell surface GRP78 coupled to the pertussis toxin-insensitive G-protein, $G\alpha_{q11}$ (48). Studies have demonstrated that anti-GRP78 autoantibodies bind to the same tertiary epitope on GRP78 (Leu^{98}–Leu^{115}) as α_2M (26), suggesting that similar signaling mechanisms with anti-GRP78 autoantibodies may be similar to those with α_2M. Treatment with the PLC inhibitor, U73122, but not its non-active analogue, U73343, inhibited TF PCA elicited by the anti-GRP78 autoantibodies. Activation of PLC increases cytosolic inositol 1,4,5-trisphosphate (IP_3), which then binds to specific receptors on ER Ca^{2+} channels and causes ER Ca^{2+} release (49). These results are consistent with a mechanism of increased cytosolic [Ca^{2+}] mediating the effect of GRP78 autoantibodies on TF PCA (Fig. 6), similar to that observed for thapsigargin (31).

The binding of anti-GRP78 autoantibodies to cell surface GRP78 can increase cytosolic [Ca^{2+}] at levels sufficient to disturb flippase activity (15, 16) and therefore may cause exposure of PS molecules on the cell surface. Previous studies have shown that PS expression on the cell surface de-encrypts TF and facilitates its interaction with its co-factor FVIIa (15). Based on our findings, we present a model in Fig. 6 showing that engagement of GRP78 autoantibodies with cell surface GRP78 activates PLC, which triggers an increase in [IP_3] and subsequent ER Ca^{2+} release. This in turn leads to PS exposure, TF de-encryption, and enhanced TF PCA, which culminates in a fibrin-rich clot. In addition to its role in thrombosis, enhanced TF PCA is also linked to increased tumor cell survival, angiogenesis, and metastasis (17–20, 67–69). Thus, strategies aimed at blocking cell surface GRP78 signaling have the potential of decreasing the risk of cancer-related thrombotic events as well as tumor growth.

REFERENCES

1. Sousou, T., and Khorana, A. A. (2009) *Arterioscler. Thromb. Vasc. Biol.* **29,** 316–320
2. Sud, R., and Khorana, A. A. (2009) *Thromb. Res.* **123,** Suppl. 4, S18–S21
3. Boccaccio, C., Sabatino, G., Medico, E., Girolami, F., Follenzi, A., Reato, G., Sottile, A., Naldini, L., and Comoglio, P. M. (2005) *Nature* **434,** 396–400
4. Yu, J. L., May, L., Lhotak, V., Shahrzad, S., Shirasawa, S., Weitz, J. I., Coomber, B. L., Mackman, N., and Rak, J. W. (2005) *Blood* **105,** 1734–1741
5. Mackman, N. (2004) *Arterioscler. Thromb. Vasc. Biol.* **24,** 1015–1022
6. Bach, R. R., and Moldow, C. F. (1997) *Blood* **89,** 3270–3276
7. Conway, E. M., Bach, R., Rosenberg, R. D., and Konigsberg, W. H. (1989) *Thromb. Res.* **53,** 231–241
8. Erlich, J., Fearns, C., Mathison, J., Ulevitch, R. J., and Mackman, N. (1999) *Infect. Immun.* **67,** 2540–2546
9. Bombeli, T., Karsan, A., Tait, J. F., and Harlan, J. M. (1997) *Blood* **89,** 2429–2442
10. Greeno, E. W., Bach, R. R., and Moldow, C. F. (1996) *Lab. Invest.* **75,** 281–289
11. Kobayashi, Y., Yoshimura, N., Nakamura, K., Yamagishi, H., and Oka, T. (1998) *Transplantation* **66,** 708–716
12. Carson, S. D., Perry, G. A., and Pirruccello, S. J. (1994) *Blood* **84,** 526–534
13. Consonni, R., and Bertina, R. M. (1995) *Thromb. Haemost.* **74,** 904–909
14. Bach, R., and Rifkin, D. B. (1990) *Proc. Natl. Acad. Sci. U.S.A.* **87,** 6995–6999
15. Bach, R. R. (2006) *Arterioscler. Thromb. Vasc. Biol.* **26,** 456–461
16. Wolberg, A. S., Monroe, D. M., Roberts, H. R., and Hoffman, M. R. (1999) *Blood Coagul. Fibrinolysis* **10,** 201–210
17. Kasthuri, R. S., Taubman, M. B., and Mackman, N. (2009) *J. Clin Oncol.* **27,** 4834–4838
18. Milsom, C., and Rak, J. (2008) *Pathophysiol. Haemost. Thromb.* **36,** 160–176
19. Rak, J., Milsom, C., Magnus, N., and Yu, J. (2009) *Best Pract. Res. Clin. Haematol.* **22,** 71–83
20. Rak, J., Milsom, C., and Yu, J. (2008) *Curr. Opin. Hematol.* **15,** 522–528
21. Abdulkadir, S. A., Carvalhal, G. F., Kaleem, Z., Kisiel, W., Humphrey, P. A., Catalona, W. J., and Milbrandt, J. (2000) *Hum. Pathol.* **31,** 443–447
22. Kaushal, V., Mukunyadzi, P., Siegel, E. R., Dennis, R. A., Johnson, D. E., and Kohli, M. (2008) *Appl. Immunohistochem. Mol. Morphol.* **16,** 1–6
23. Al-Nedawi, K., Meehan, B., Micallef, J., Lhotak, V., May, L., Guha, A., and Rak, J. (2008) *Nat. Cell. Biol.* **10,** 619–624
24. Watson, L. M., Chan, A. K., Berry, L. R., Li, J., Sood, S. K., Dickhout, J. G., Xu, L., Werstuck, G. H., Bajzar, L., Klamut, H. J., and Austin, R. C. (2003) *J. Biol. Chem.* **278,** 17438–17447
25. Bhattacharjee, G., Ahamed, J., Pedersen, B., El-Sheikh, A., Mackman, N., Ruf, W., Liu, C., and Edgington, T. S. (2005) *Arterioscler. Thromb. Vasc. Biol.* **25,** 1737–1743
26. Gonzalez-Gronow, M., Cuchacovich, M., Llanos, C., Urzua, C., Gawdi, G., and Pizzo, S. V. (2006) *Cancer Res.* **66,** 11424–11431
27. Pozza, L. M., and Austin, R. C. (2005) *Arterioscler. Thromb. Vasc. Biol.* **25,** 1529–1531
28. Shin, B. K., Wang, H., Yim, A. M., Le Naour, F., Brichory, F., Jang, J. H., Zhao, R., Puravs, E., Tra, J., Michael, C. W., Misek, D. E., and Hanash, S. M. (2003) *J. Biol. Chem.* **278,** 7607–7616
29. Misra, U. K., Gonzalez-Gronow, M., Gawdi, G., Hart, J. P., Johnson, C. E., and Pizzo, S. V. (2002) *J. Biol. Chem.* **277,** 42082–42087
30. Xiao, G., Chung, T. F., Pyun, H. Y., Fine, R. E., and Johnson, R. J. (1999) *Brain Res. Mol. Brain Res.* **72,** 121–128
31. Caldwell, J. A., Dickhout, J. G., Al-Hashimi, A. A., and Austin, R. C. (2010) *Lab. Invest.* **90,** 953–962
32. Gonzalez-Gronow, M., Selim, M. A., Papalas, J., and Pizzo, S. V. (2009) *Antioxid Redox Signal* **11,** 2299–2306
33. Mintz, P. J., Kim, J., Do, K. A., Wang, X., Zinner, R. G., Cristofanilli, M., Arap, M. A., Hong, W. K., Troncoso, P., Logothetis, C. J., Pasqualini, R., and Arap, W. (2003) *Nat. Biotechnol.* **21,** 57–63
34. Junop, M. S., Modesti, M., Guarné, A., Ghirlando, R., Gellert, M., and Yang, W. (2000) *EMBO J.* **19,** 5962–5970
35. Wei, J., and Hendershot, L. M. (1995) *J. Biol. Chem.* **270,** 26670–26676
36. Mavropoulos, J. C., Cuchacovich, M., Llanos, C., Aguillón, J. C., Gatica, H., Pizzo, S. V., and Gonzalez-Gronow, M. (2005) *J. Rheumatol.* **32,** 2116–2124
37. Dickhout, J. G., Sood, S. K., and Austin, R. C. (2007) *Antioxid Redox Signal* **9,** 1863–1873
38. Bookout, A. L., and Mangelsdorf, D. J. (2003) *Nucl. Recept. Signal* **1,** e012
39. Bustin, S. A., Benes, V., Garson, J. A., Hellemans, J., Huggett, J., Kubista, M., Mueller, R., Nolan, T., Pfaffl, M. W., Shipley, G. L., Vandesompele, J., and Wittwer, C. T. (2009) *Clin. Chem.* **55,** 611–622
40. Gonzalez-Gronow, M., Gawdi, G., and Pizzo, S. V. (1993) *J. Biol. Chem.* **268,** 20791–20795
41. Grynkiewicz, G., Poenie, M., and Tsien, R. Y. (1985) *J. Biol. Chem.* **260,** 3440–3450
42. López-Pedrera, C., Jardí, M., Inglés-Esteve, J., Muñoz-Cánoves, P., Dorado, G., Velasco, F., and Félez, J. (1997) *Am. J. Hematol.* **56,** 71–78
43. Davidson, D. J., Haskell, C., Majest, S., Kherzai, A., Egan, D. A., Walter, K. A., Schneider, A., Gubbins, E. F., Solomon, L., Chen, Z., Lesniewski, R., and Henkin, J. (2005) *Cancer Res.* **65,** 4663–4672
44. Wiest, D. L., Bhandoola, A., Punt, J., Kreibich, G., McKean, D., and Singer, A. (1997) *Proc. Natl. Acad. Sci. U.S.A.* **94,** 1884–1889

45. Delpino, A., and Castelli, M. (2002) *Biosci. Rep.* **22,** 407–420
46. Price, N. P., and Tsvetanova, B. (2007) *J. Antibiot. (Tokyo)* **60,** 485–491
47. Sergeev, I. N. (2005) *J. Steroid. Biochem. Mol. Biol.* **97,** 145–151
48. Misra, U. K., and Pizzo, S. V. (2008) *J. Cell. Biochem.* **104,** 96–104
49. van Rossum, D. B., and Patterson, R. L. (2009) *Cell. Calcium* **45,** 535–545
50. Lièvremont, J. P., Rizzuto, R., Hendershot, L., and Meldolesi, J. (1997) *J. Biol. Chem.* **272,** 30873–30879
51. Hung, C. C., Ichimura, T., Stevens, J. L., and Bonventre, J. V. (2003) *J. Biol. Chem.* **278,** 29317–29326
52. Zwaal, R. F., and Schroit, A. J. (1997) *Blood* **89,** 1121–1132
53. Kunzelmann-Marche, C., Satta, N., Toti, F., Zhang, Y., Nawroth, P. P., Morrissey, J. H., and Freyssinet, J. M. (2000) *Thromb. Haemost.* **83,** 282–289
54. Lentz, B. R. (2003) *Prog. Lipid Res.* **42,** 423–438
55. Inesi, G., Hua, S., Xu, C., Ma, H., Seth, M., Prasad, A. M., and Sumbilla, C. (2005) *J. Bioenerg. Biomembr.* **37,** 365–368
56. Wang, Q., Rajshankar, D., Branch, D. R., Siminovitch, K. A., Herrera Abreu, M. T., Downey, G. P., and McCulloch, C. A. (2009) *J. Biol. Chem.* **284,** 20763–20772
57. Wang, Q., Herrera Abreu, M. T., Siminovitch, K., Downey, G. P., and McCulloch, C. A. (2006) *J. Biol. Chem.* **281,** 31093–31105
58. Zhang, Y., Liu, R., Ni, M., Gill, P., and Lee, A. S. (2010) *J. Biol. Chem.* **285,** 15065–15075
59. Andres, D. A., Rhodes, J. D., Meisel, R. L., and Dixon, J. E. (1991) *J. Biol. Chem.* **266,** 14277–14282
60. Misra, U. K., Gonzalez-Gronow, M., Gawdi, G., and Pizzo, S. V. (2005) *J. Immunol.* **174,** 2092–2097
61. Reddy, R. K., Mao, C., Baumeister, P., Austin, R. C., Kaufman, R. J., and Lee, A. S. (2003) *J. Biol. Chem.* **278,** 20915–20924
62. Okazaki, Y., Ohno, H., Takase, K., Ochiai, T., and Saito, T. (2000) *J. Biol. Chem.* **275,** 35751–35758
63. Molins, B., Peña, E., Padro, T., Casani, L., Mendieta, C., and Badimon, L. (2010) *Arterioscler. Thromb. Vasc. Biol.* **30,** 1246–1252
64. Misra, U. K., Gonzalez-Gronow, M., Gawdi, G., Wang, F., and Pizzo, S. V. (2004) *Cell. Signal* **16,** 929–938
65. Triantafilou, K., Fradelizi, D., Wilson, K., and Triantafilou, M. (2002) *J. Virol.* **76,** 633–643
66. Triantafilou, M., Wilson, K. M., and Triantafilou, K. (2001) *Cytometry* **43,** 279–289
67. Zhang, Y., Deng, Y., Luther, T., Müller, M., Ziegler, R., Waldherr, R., Stern, D. M., and Nawroth, P. P. (1994) *J. Clin. Invest.* **94,** 1320–1327
68. Hembrough, T. A., Swartz, G. M., Papathanassiu, A., Vlasuk, G. P., Rote, W. E., Green, S. J., and Pribluda, V. S. (2003) *Cancer Res.* **63,** 2997–3000
69. Rak, J., Milsom, C., May, L., Klement, P., and Yu, J. (2006) *Semin. Thromb. Hemost.* **32,** 54–70

Supplementary Figure 1: Production and purification of recombinant human GRP78 from bacteria.

A) Coomassie stained SDS-polyacrylamide gel of fractions containing recombinant human GRP78 protein. Following induction with IPTG, transformed Rosetta (DE3) cells were pelleted (*lane 1*), resuspended in 20mM Tris (pH 8.5), 0.5M KCl, 0.03% lauryldimethylamine oxide (LOAD), 10% glycerol supplemented with protease inhibitors (PMSF, leupeptin, pepstin and benzamidine) and lysed by passage though a French pressure cell at 8000 p.s.i. After clarification by centrifugation at 40,000 rpm for 40 min (*lanes 2,3*), GRP protein was purified by nickel affinity- fast protein liquid chromatography (FPLC) system. The Ni column was washed with the same above buffer and the cell lysate was injected into the column. Samples were eluted with a gradient of imidazole by increasing the salt concentration of the wash buffer (0-100%). *Lanes 4* and *5* represent flow through. *Lanes 6* to *9* represent pooled fractions containing human GRP78. M, molecluar mass markers.

B) Immunoblot analysis of human GRP78 in bacterial lysates. Total lysates from transformed Rosetta (DE3) cells treated in the absence (*lane 1*) or presence of IPTG (*lane 2*) to induce GRP78 expression were separated on 10% SDS-polyacrylamide gels, transferred to nitrocellulose membrane and immunoblotted for human GRP78 using anti-KDEL antibodies. *Lane 3* contains FPLC-purified human GRP78. Results indicate that intact human GRP78 can be successfully produced and purified using a bacterial expression system.

C) ATPase activity assay. The ATPase activity of hrGRP78 was analyzed by quantitating the free P_i liberated during ATP hydrolysis using the method of Seals et al. (1). Briefly, reactions were initiated by adding hrGRP78 to an assay mixture containing: 35.7 mM Tris-HCl (pH 7.4), 0.7 mM [$\gamma-^{32}$P]ATP, 1.4 mM $MgCl_2$, and 0.385 µM hrGRP78 in a final volume of 140 µL. After incubation at 37˚C for 30 min, 20 µL of 6% SDS was added to the reaction mixture to terminate the reaction. After adding 60 µL of fresh phosphate reagent (10 N sulfuric acid, 2 vol; 10% ammonium molybdate, 2 vol; and 0.1 M silicotungstic acid, 1 vol), 1 mL of 65:35 xylene:isobutyl alcohol (v/v) was added, and the samples were vortexed vigorously. The aqueous and organic phases were then separated by centrifugation for 5 min at 14,000 rpm in a microcentrifuge. The organic phase (1 mL) was removed, mixed with 10 mL of toluene:omnifluor:ethanol, and counted in a liquid scintillation counter to determine [^{32}P]P_i released. The data were obtained from three independent experiments.

D) Protein-peptide interaction studies with hrGRP78 and peptide pp38. Functional studies on the interaction of native hrGRP78 and pp38, a synthetic octa-peptide that mimics the unfolded regions of target proteins in the ER were carried out using Surface Plasmon Resonance (SPR). Peptide pp38 binds to GRP78 with high affinity and stimulates the ATPase activity of the protein (2). All binding experiments were performed at 20^{o}C using a Biacore 3000 system (Biacore AB, Uppsala, Sweden) in which biosensor chips were covalently coupled with hrGRP78. Prior to hrGRP78 immobilization, the flow cells of the chip were thoroughly washed with three pulses each of 50 mM NaOH and 50 mM HCl. After priming the system, the hrGRP78 was immobilized by amine-coupling chemistry using the Biacore wizard. HBS-P buffer, pH7.4 containing 0.15M NaCl and 0.005% surfactant P-20 was used as running buffer for immobilization and for performing binding assays. hrGRP78 (equivalent to 13,800 RU) was immobilized in Fc-2, while Fc-1 was treated similarly without hrGRP78 to serve as a reference flow cell. Before running the actual experiment the system was primed twice to remove any residual immobilization reagents. For binding assays the octa-peptide solution was prepared in water and various dilutions of the stock

solutions were made in running buffer in the range of 1-100 μM. All of the samples were briefly centrifuged at 5,000 rpm for 2 min to remove any trapped air bubbles. Various concentrations of peptide analyte were injected in Fc1 and Fc2 (Fc2-Fc1 format) at a flow-rate of 30 μL/min for 3 min. The binding of pp38 to immobilized hrGRP78 was measured in arbitrary resonance units (RU). The interaction association (K_A) and dissociation rate constants (K_D) between native hrGRP78 and pp38 were 16.7 M^{-1} and 0.0597 M, respectively.

Reference:

1. Seals, J. R., McDonald, J. M., Bruns, D., and Jarett, L. (1978) *Anal Biochem* **90**, 785-795.
2. Fourie, A. M., Sambrook, J. F., and Gething, M. J. (1994) *J Biol Chem* **269**, 30470-30478.

Supplementary Figure 1 – Al-Hashimi *et al.* – JBC 2010

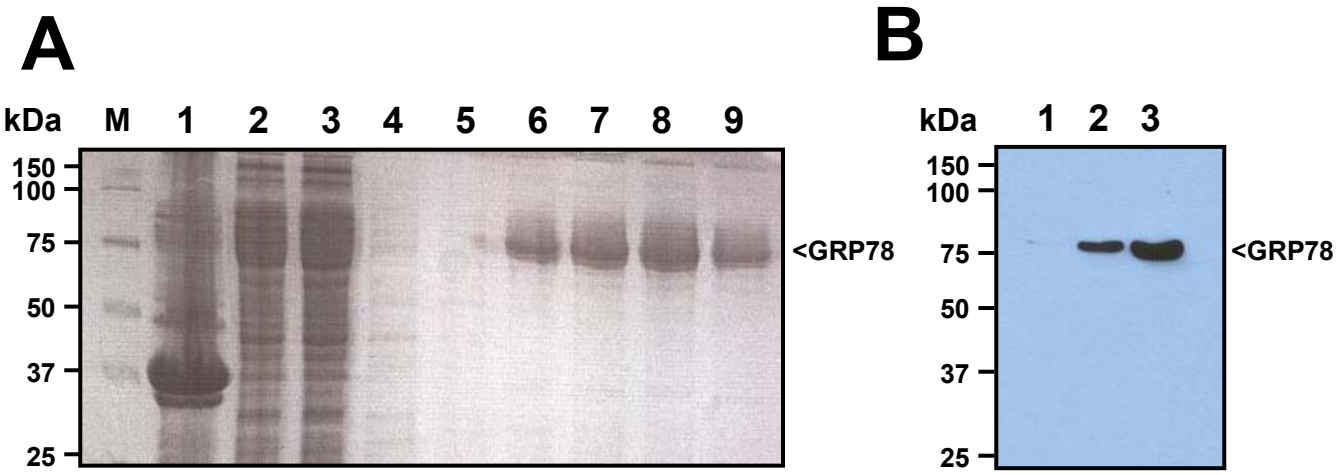

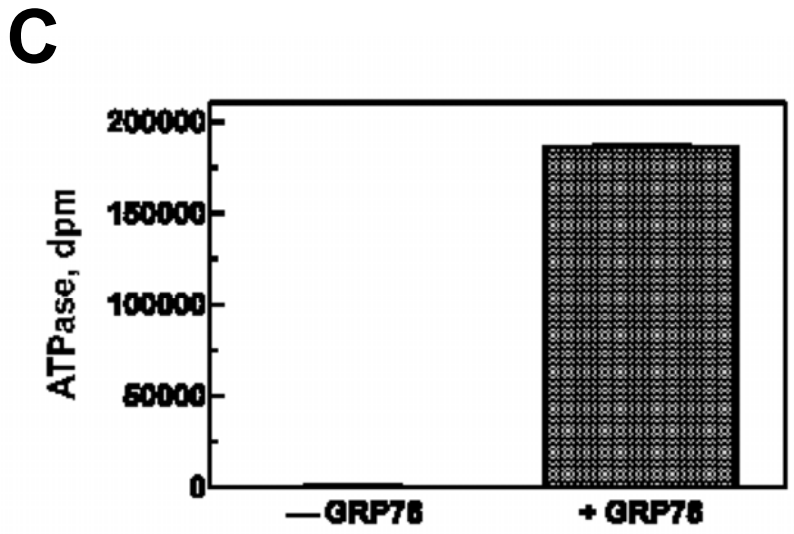

D

Surface	k_a (s^{-1} M^{-1})	k_d (s^{-1})	K_A(M^{-1})	K_D (M)
hrGRP78	0.598	0.0357	16.7	0.0597

CHAPTER 4

CANCER CELL SUBMISSION 2016

Preamble

This chapter is an orginal submitted for publication to the Cancer Cell journal.

Authors' Contribution A. Al-Hashimi and R.C. Austin designed the study. A. Al-Hashimi performed all the cell culture, animal and clinical investigations and related analyses, performed Western blotting, conducted the animal study, and assisted in tissue collection and analysis. S. Lhotak assisted in tissue collection, and provided technical assistance in histology and immunohistochemistry. A. Al-Hashimi wrote and prepared the manuscript. Co-authors provided intellectual input. A. Al-Hashimi and R.C. Austin reviewed and edited the manuscript and all authors approved of the final submission.

Cell Surface GRP78 Activation by Anti-GRP78 Autoantibodies Confers Tumor Growth via Tissue Factor

Ali A. Al-Hashimi[1], Paul Lebeau[1], Fadwa Majeed[1], Enio Polena[1], Šárka Lhotak[1], Celeste A.F. Collins[1], Jehonathan H. Pinthus[1], Mario Gonzalez-Gronow[2], Jen Hoogenes[1], Edward D. Masumoto[1], Salvatore Pizzo[2], Mark Crowther[1], Anil Kapoor[1], Janusz Rak[3], Gabriel Gyulay[1], Bobby Shayegan[1] and Richard C. Austin[1,*]

[1]Department of Medicine, McMaster University and St. Joseph's Healthcare Hamilton, Hamilton, Ontario, Canada.

[2]Department of Pathology, Duke University, Durham, NC, 27708, USA

[3]Department of Pediatrics, Division of Experimental Medicine, Faculty of Medicine, McGill University

*Correspondence: austinr@taari.ca

Summary:

Anti-GRP78 autoantibodies (anti-GRP78 autoAbs) derived from the blood of prostate cancer (PCa) patients can increase tissue factor (TF) activity *in vitro* by binding to cell surface GRP78. In this study, we report a direct association of anti-GRP78 autoAbs with PCa grade, and demonstrate a TF-dependent mechanism whereby anti-GRP78 autoAbs significantly increase the growth of DU145-derived tumors in NOD/SCID mice. This TF-dependent effect on tumor growth was blocked using enoxaparin, a low molecular weight heparin that disrupts the autoAb/cell surface GRP78 complex. These findings support a model in which TF activation via the engagement of anti-GRP78 autoantibodies to surface GRP78 confers tumor growth and represents a novel therapeutic target for the management of PCa.

Significance (MAX 120 words):

The mechanism of PCa progression, beyond castration resistance, is not fully characterized and this contributes to poor PCa management and patient treatment. We have identified a new mechanism that highlights the importance of anti-GRP78 autoAbs in promoting cancer progression. This mechanism is orchestrated by TF, the major initiator of the coagulation cascade. We further showed that heparin and low molecular weight heparin can block the binding of anti-GRP78 autoantibodies to tumor cells thereby reducing tumor growth in mice. PCa patients diagnosed with elevated anti-GRP78 autoantibodies levels may benefit from LMWH treatment.

Introduction

Prostate cancer (PCa) is the most frequently diagnosed cancer in men and accounts for 15% of all new cancer cases (Center, Jemal et al. 2012). Age-adjusted incidence rates of PCa have increased dramatically, largely due to the increased availability of screening for prostate-specific antigen (PSA) and earlier detection (Center, Jemal et al. 2012). Although patients with organ confined disease have favorable prognoses, metastatic disease remains incurable (Lippi, Montagnana et al. 2009). Furthermore, secondary thrombotic complications can increase the risk of disease progression and mortality in PCa patients. Current evidence indicates that this prothrombotic state occurs on the surface of cancer cells and involves the enhanced expression of tissue factor (TF) and/or its procoagulant activity (Abdulkadir, Carvalhal et al. 2000, Akashi, Furuya et al. 2003, Milsom and Rak 2008). In addition to its critical role in hemostasis and clot formation, TF also promotes tumor growth and metastasis (Rak, Milsom et al. 2006, Milsom and Rak 2008, Milsom, Yu et al. 2008). A growing body of genetic and pharmacological evidence suggests that activation of tumor cell-expressed TF contributes to tumor growth byinducing an array of proangiogenic and immune modulating cytokines, chemokines and growth factors (Ruf, Disse et al. 2011; Rak et al. 2006; Garnier et al. 2010).

We reported previously a novel mechanism whereby anti-GRP78 autoantibodies (anti-GRP78 autoAbs) modulate TF activity via release of Ca^{2+} from the endoplasmic reticulum (ER) compartment to the cytosol (Al-Hashimi, Caldwell et al. 2010). Mintz and colleagues originally reported that circulating anti-GRP78 autoantibodies

(autoAbs) in the blood of PCa patients could bind to a peptide with the amino acid sequence CNVKSDKSC (Mintz et al. 2003) which contains a tertiary structure that resembles the linear N-terminal domain (Leu_{98}-Leu_{115}) of cell surface GRP78 (Gonzalez-Gronow et al. 2006). PCa patients were shown to have pathological levels of anti-GRP78 autoAbs (≥60 μg/mL), compared to age matched healthy controls (~5μg/mL) (Gonzalez-Gronow et al. 2006). Furthermore, we, and others have reported that GRP78 is expressed on the surface of cells derived from a wide variety human cancers, including prostate, ovarian, leukemia, and lung cancers (Shin, Wang et al. 2003, Gonzalez-Gronow et al., 2006; Watson, Chan et al. 2003, Pozza and Austin 2005, Al-Hashimi, Caldwell et al. 2010, Lee 2014). GRP78 is a member of the HSP70 family of proteins and is considered an ER-resident molecular chaperone that facilitates the correct folding and assembly of newly synthesized proteins (Ron and Walter 2007). However, current studies indicate that when expressed on the surface of tumor cells, GRP78 functions as a unique signaling receptor to promote cell proliferation and survival (Gonzalez-Gronow, Selim et al. 2009). Exposure of GRP78 on the surface of tumor cells is linked to the production of anti-GRP78 autoAbs in PCa patients (Mintz et al. 2003). The majority of these circulating anti-GRP78 autoAbs target the N-terminal domain of GRP78 at Leu_{98}-Leu_{115} and are correlated with accelerated cancer progression, enhanced metastatic potential and reduced survival (Gonzalez-Gronow, Cuchacovich et al. 2006).

In this study, we used a NOD/SCID mouse xenograft mouse model to investigate whether the binding of anti-GRP78 autoAb to cell surface GRP78 potentiated tumor growth in a TF-dependent and –independent manner. Given that the anti-GRP78 autoAb epitope binding domain on surface GRP78 contains a heparin binding domain (Gonzalez-Gronow et al., 2006), we examined whether the LMWH, enoxaparin, could abolish the effect of the anti-GRP78 autoAb on tumor growth. Results of our study validate the anti-GRP78 autoAb/cell surface GRP78 complex as a viable cellular target for the treatment of PCa.

Results

Cell Surface GRP78 Expression Correlates with PCa Grade

Cell surface expression of GRP78 has been reported to be increased in a wide range of cultured tumor cell lines, including prostate, ovarian, and lung (Al-Hashimi et al., 2010; Pozza and Austin, 2005; Shin, Wang et al. 2003). To assess changes in cell surface and total GRP78 expression with increasing PCa disease grade, tumor sections from the Human Protein Atlas were immunostained for GRP78 at grade I, III and IV. Figure 1A demonstrates low level immunostaining for total and cell surface GRP78 in Grade 1 PCa. In Grade II PCa, cell surface GRP78 expression is increased in most tumor cells (Figure 1B). Finally, in grade IV PCa, there was very strong immunostaining for GRP78, including the cell surface (Figure 1C). These findings suggest that increases in total and cell surface GRP78 correlate with the progression of PCa.

Anti-GRP78 AutoAb Titres Correlate with PSA Levels in PCa patients

Given that cell surface GRP78 expression increases with disease grade, we assessed whether anti-GRP78 autoAbs correlated with more advanced disease. Serum samples from PCa patients were obtained from the Ontario Tumour Bank. Anti-GRP78 autoAb titers were subsequently measured and correlated with blood PSA levels. A recent report has suggested that PSA levels can be used to estimate prostate cancer grade (Teeter, Presti et al. 2013). Using a Pearson correlation test,

we demonstrated a significant ($p<0.05$) and positive correlation coefficient ($r=0.38$) between anti-GRP78 autoAb titres and PSA levels (n=48) (Figure 2A). To further examine this correlation, patient samples were redistributed into four groups based on their blood PSA concentrations: Low PSA (<2 ng/mL), Low to medium PSA (2-7 ng/mL), High PSA (7-12 ng/mL), and Very high PSA (>12 ng/mL), (adapted from the D'Amico PCa risk categories; D'Amico, Whittington et al. 1998). Malignancy free, aged-matched males that were not diagnosed with PCa were used as controls (Figure 2B). This analysis demonstrated that increased anti-GRP78 autoAb titres correlated with higher blood PSA levels; all samples had significantly higher anti-GRP78 autoAb titres compared to the control group.

Sustaining consistent antigen presentation can enhance the production of specific IgG-type antibodies, since the half-life of antigen specific antibodies is less than 3 weeks (Vieira and Rajewsky 1988). Two cohorts of patients diagnosed with PCa that were prescribed prostatectomies were examined at pre-operative and 24-weeks post-operative stages for anti-GRP78 autoAb titres (Figure 2C). A significant decrease in anti-GRP78 autoAb titres was observed in patients post-operatively (mean=90.88 μg/mL, $p<0.0001$), compared to pre-operative levels (mean= 124.2 μg/mL). Currently, these post-operative patients have negligible PSA levels (PSA<1 ng/mL, data not shown) and are in remission.

Engagement of Anti-GRP78 AutoAbs to Surface GRP78 Activates the Unfolded Protein Response (UPR)

We have previously shown that binding of anti-GRP78 autoAbs to cell surface GRP78 results in ER Ca^{2+} efflux and UPR activation, a pro-survival pathway initiated by ER stress (Al-Hashimi, Caldwell et al. 2010). Consistent with these findings, treatment of DU145 cells with pathological concentrations (60 μg/mL) of the anti-GRP78 autoAbs increased the expression of a number of UPR markers at both the protein (Figure 3A) and RNA levels (Figure 3B). This included an increase in expression of PDI, IRE1α, GRP78 and spliced XBP1. In contrast, expression levels of CHOP, an ER stress-induced apoptosis marker, did not change in response to the anti-GRP78 autoAb (Figure 3). These findings suggest that induction of the UPR is a reliable and robust marker for assessing the engagement of anti-GRP78 autoAbs to cell surface GRP78 on PCa cells.

TF is Required for Tumor Growth Induced by Anti-GRP78 AutoAbs

De Ridder and colleagues had previously shown that a humoral response to GRP78 can promote tumor growth and proliferation (de Ridder, Gonzalez-Gronow et al. 2011). Furthermore, treatment of DU145 cells with anti-GRP78 autoAbs results in increased TF expression and activation (Al-Hashimi, Caldwell et al. 2010), thereby contributing to tumor growth (Milsom and Rak 2008). Based on these previous studies, we evaluated the contribution of anti-GRP78 autoAbs to tumor growth *in*

vivo. Wild type DU145 cells were implanted subcutaneously into the flank of NOD/SCID mice. Animals were assigned to three groups and each group was administered an intraperitoneal injection at the site of the tumor with 1) PBS (vehicle control), 2) control human IgG (control antibody), or 3) anti-GRP78 autoAbs. Ten weeks post-injection, anti-GRP78 autoAbs significantly accelerated the rate of tumor growth in mice, compared to vehicle and human IgG control groups (Figure 4A). This accelerated tumor growth continued for twelve weeks post-injection until termination of the experiment. Treatment with anti-GRP78 autoAbs resulted in increased TF immunostaining within the tumors, compared to tumors obtained from the human IgG group (Figure 4B), a finding consistent with increased mRNA expression of TF (Figure 4C). As observed for cultured DU145 cells, tumors treated with anti-GRP78 autoAbs had significantly higher expression levels of both UPR (GRP78, ATF4, spliced XBP-1) and proliferation markers (Ki67, VEGFR2), compared to control tumors treated with human IgG (Figure 4C). Consistent with these findings, gene expression analysis using NanoString® identified numerous UPR markers, including PERK, calnexin, calreticulin, ATF4, ATF6, GRP78 and total XBP1 that were significantly upregulated in the anti-GRP78 autoAb treated samples (Figure 4D; complete heat map for gene expression is available in Supplemental Figure 1). Finally, a 48% increase in Ki67 positive cells were observed in the anti-GRP78 autoAb treated tumors, compared to those treated with human IgG (Figure 4E).

Our findings show that treatment of wild type DU145 derived tumors in mice with anti-GRP78 autoAbs resulted in increased TF expression at both the mRNA and protein level (Figure 4B and 4C). Thus, to determine whether there is a direct role of TF in mediating the effect of anti-GRP78 autoAbs on increased tumor progression, TF protein expression in DU145 cells was stably knocked down using a TF shRNA lenti-viral vector (Figure 5A). A lenti-viral vector encoding GFP acted as a control ($DU145^{GFP}$). Western blot analysis of four clones revealed a variable decrease in TF expression post antibiotics selection (Figure 5A) Since DU145-clone 4 ($DU145^{KD}$) had undetectable levels of endogenous TF expression, we determined whether this reduction in TF expression correlated with reduced TF activity. Treatment of $DU145^{KD}$ with anti-GRP78 autoAb did not increase TF activity (Figure 5B), compared to the $DU145^{GFP}$ and the DU145-clone 1 cell line having reduced TF expression. To elucidate the contribution of TF to tumor progression, $DU145^{GFP}$ or $DU145^{KD}$ cells were implanted in NOD/SCID mice, and tumor progression was monitored. Eight-week post injection, $DU145^{KD}$ tumors grew at a slower rate than control $DU145^{GFP}$ tumors (Figure 5C, left panel). Staining for TF confirmed decreased TF expression in $DU145^{KD}$ tumors, compared to control $DU145^{GFP}$ tumors (Figure 5C, right panel). To define the contribution of TF to tumor growth mediated by anti-GRP78 autoAbs, $DU145^{KD}$ were implanted in NOD/SCID mice. One group of mice received a weekly injection of anti-GRP78 autoAbs and a control group received a weekly injection of human IgG at the tumor site. No difference in tumor growth was observed between human IgG control and anti-GRP78 autoAb treated groups (Figure 5D). These

findings suggest that the increase in tumor growth induced by anti-GRP78 autoAb was dependent on TF.

Immunodepletion or Neutralization of Anti-GRP78 AutoAbs Inhibits TF Activity

Given our findings that engagement of purified anti-GRP78 autoAbs with cell surface GRP78 increases TF expression and activity, we sought to determine whether blood from PCa patients contained additional factors that could also activate TF on the surface of tumor cells. Anti-GRP78 autoAbs were immunodepleted from the serum of patients diagnosed with PCa, as described previously (Al-Hashimi et al. 2010). As expected, TF procoagulant activity was significantly increased in cultured DU145 cells treated with either purified anti-GRP78 autoAbs (60 μg/ml) or undiluted patient serum containing 60 μg/mL of anti-GRP78 autoAbs (Figure 6A). In contrast, no increase in TF activity was observed in DU145 cells treated with serum immunodepleted for anti-GRP78 autoAbs, a finding comparable to untreated cells. Thapsigargin was used as a positive control due to its ability to increase cytosolic intracellular Ca^{2+} and activate TF (Figure 6A). Furthermore, pretreatment of different patient sera with human recombinant GRP78 (hrGRP78, 60 μg/mL) significantly reduced TF activity elicited by the anti-GRP78 autoAb. As expected, the addition of hrGRP78 to cells treated with thapsigargin did not block the increase in TF activity (Figure 6B). These findings indicate that anti-GRP78 autoAbs are the major activator of TF in the blood of PCa patients and contains no additional factors that were able to enhance TF activity.

Heparin and LMWH Block the Binding of Anti-GRP78 AutoAbs to Cell Surface GRP78 and Reduce Tumor Growth *In Vivo*

Previous studies have demonstrated that GRP78 possesses a heparin-binding domain that consists in part of Leu_{98}-Thr_{102} (Hansen, O'Leary et al. 1995). This heparin binding domain is present within the N-terminal autoantibody binding site (Leu_{98}-Thr_{102}) of GRP78. Based on this finding, we examined the ability of heparin to block the binding of anti-GRP78 autoAbs to cell surface GRP78. Pre-treatment of intact DU145 cells with heparin (50 IU/mL) was shown to block the activation of TF by the anti-GRP78 autoAb (Figure 7A). As expected, heparin pre-treatment did not affect thapsigargin-induced TF activity (Figure 7A). In addition to standard heparin, the LMWH enoxaparin was tested to examine its ability to block the interaction of anti-GRP78 autoAbs with cell surface GRP78. Consistent with the findings for heparin, enoxaparin was also effective in abolishing the binding of anti-GRP78 autoAbs to cell surface GRP78 (Figure 7B). Furthermore, DU145 cells pre-treated with enoxaparin showed significantly lower fluorescence intensity of GRP78 staining compared to untreated cells (Figure 7C). These findings suggest that enoxaparin interferes with the binding of anti-GRP78 autoAbs to cell surface GRP78. Based on these observations, we examined the ability of enoxaparin to alleviate the effect of anti-GRP78 autoAbs on tumor progression *in vivo*. NOD/SCID mice were randomly divided into two groups, PBS (control) and enoxaparin. Wild type DU145 cells were implanted into each group of mice followed by weekly

injections of either anti-GRP78 autoAbs or control human IgG at the site of the tumor. One week after the administration of anti-GRP78 autoAbs, mice from the anti-GRP78 autoAb and IgG groups received a secondary treatment of enoxaparin (6 mg/kg/week), with the remaining mice treated with PBS (control). While animals treated with anti-GRP78 autoAbs had accelerated tumor growth compared to IgG treated animals, the enoxaparin group showed a significant and marked reduction in tumor growth induced by anti-GRP78 autoAbs (Figure 7D). However, tumor growth, although much slower, was similar in mice treated with enoxaparin alone compared to PBS treated mice. These findings suggest that enoxaparin treatment blocks tumor growth elicited by the anti-GRP78 autoAbs but does not in itself have anti-tumor properties in this model system.

Gene expression was assessed using NanoString® in tumors treated with control IgG or anti-GRP78 autoAbs that were subjected to the enoxaparin intervention (complete heat map for gene expression is available in Supplemental Figure 1). In contrast to treatment of tumors with anti-GRP78 autoAbs (Figure 4D), no significant induction in UPR gene expression was noted between either groups (Figure 7E). These findings suggest that the effect of anti-GRP78 autoAbs on UPR activation via cell surface GRP78 was abolished by enoxaparin.

Discussion

In this study, we present data that supports an intriguing and important role for anti-GRP78 autoAbs as potentiators of PCa growth and proliferation. Experimental cell culture and tumor models as well as clinical samples from PCa patients were used to demonstrate anti-GRP78 autoAbs as a determinant of tumor growth. Mechanistically, anti-GRP78 autoAbs purified from the blood of PCa patients bind to cell surface GRP78 on tumor cells, thereby causing increased expression and activation of TF, the critical mediator of the coagulation pathway. Moreover, this effect was solely dependent on these anti-GRP78 autoAbs as immunodepleting/neutralizing these autoAbs revealed no other factors in the plasma of PCa patients capable of inducing TF expression/activity. Using a NOD/SCID mouse xenograft model of tumor growth, we show for the first time that anti-GRP78 autoAbs directed against the N-terminal domain of GRP78 (Leu_{98}-Leu_{115}) significantly increased tumor growth in a TF-dependent manner. Importantly, the LMWH enoxaparin blocked accelerated tumor growth potentiated by the anti-GRP78 autoAbs. Taken together, our results support a model (Figure 8) whereby the activation of TF via the engagement of anti-GRP78 autoantibodies to GRP78 on the surface of cancer cells represents a critical mechanistic switch for tumor growth.

GRP78 is widely recognized as a molecular chaperone that aids in the folding and assembly of newly synthesized proteins within the ER (Ni et al. 2011; Ron and Walter 2007; Gonzalez-Gronow et al. 2009; Austin 2009). In addition, ER luminal GRP78 is

known to redirect misfolded proteins for ER-associated degradation, regulate ER calcium homeostasis and control the activation of the UPR following ER stress. However, a wide range of human tumor cell lines show that GRP78 can function in a manner distinct from its chaperone activity; GRP78 can be actively translocated to the cell surface and function as a modulator of signaling, proliferation, invasion and immunity (Lee 2014; Gonzalez-Gronow et al. 2009; Al-Hashimi et al. 2010). Furthermore, a humoral response against surface GRP78 is correlated with poor prognosis in PCa (Mintz et al. 2003) and anti-GRP78 autoAbs derived from PCa patients demonstrate mitogenic potential when exposed to a variety of PCa cell lines, including 1-LN and DU145 (Gonzalez-Gronow et al. 2006). These findings imply that anti-GRP78 autoAbs directed against GRP78 on the surface of tumor cells represent a marker of cancer progression as well as a potentiator of tumor growth and proliferation. Although recent *in vivo* studies have suggested that immunity against GRP78 accelerates tumor growth *in vivo* (deRidder et al. 2011), the direct contribution of these anti-GRP78 autoAbs to tumor growth as well as the underlying mechanism which supports this enhanced tumorigenicity was not defined.

Using archived tumor tissue as well as plasma samples taken from a patient cohort diagnosed with different stages of PCa, we demonstrated a significant increase in cell surface GRP78 expression that was correlated with more advanced disease. Furthermore, there was a positive correlation between PSA blood levels and anti-GRP78 autoAb titres in a cohort of PCa patients having advanced disease but prior

to receiving surgical treatment. Circulating anti-GRP78 autoAbs are also detected in other cancers, including colorectal cancer (Raiter et al. 2014), hepatocellular carcinoma (Shao et al. 2012), and ovarian carcinoma (Chinni et al. 1997). Furthermore, the presence of anti-GRP78 autoAbs in the blood of cancer patients is now considered to be a serological diagnostic marker for early cancer detection (Raiter et al. 2014; Quinones et al. 2008). It is well-documented that an increase in antigen presentation on the surface of cancer cells can drive antibody production (Mintz et al. 2003; Reuschenbach et al. 2009; Vieira and Rajewsky 1988, Steinman and Hemmi 2006). Thus, we compared anti-GRP78 autoAb titres in the pre-prostatectomy stage (patients with active PCa) with the post-prostatectomy stage (PCa patients who are deemed cancer-free). Post-operative patients demonstrated significantly lower levels of anti-GRP78 autoAbs, compared to pre-operative patients. This finding supports the concept that the expression of GRP78 on the surface of prostate tumors could stimulate the expression of anti-GRP78 autoAbs. It is worth noting that while post-operative patients had significantly lower anti-GRP78 autoAb titres compared to patients with active disease, these titres were not reduced to the levels observed in control patients. We are currently investigating whether anti-GRP78 autoAb titres would eventually fall to normal levels over time.

The correlation of anti-GRP78 autoAbs with PCa disease grade suggests a contributory role in mediating disease progression. We examined mechanisms by which anti-GRP78 autoAbs can enhance tumor cell survival and growth. Previously, the binding of anti-GRP78 autoAbs to cell surface GRP78 resulted in depletion of ER

Ca^{2+} stores (Al-Hashimi et al. 2010). This process is key in activating the UPR pro-survival pathway (Misra, Gonzalez-Gronow et al. 2004, Al-Hashimi, Caldwell et al. 2010). Interestingly, only pathological doses of anti-GRP78 autoAbs observed in patients with PCa resulted in the induction of several UPR markers at the protein and RNA levels. However, there was no change in the expression of the pro-apoptotic marker CHOP, a bZIP transcription factor induced by the ATF6 and PERK pathways (Rutkowski, Arnold et al. 2006).

UPR activation enables cells to either manage current stress conditions, or activate apoptosis. Mild activation of the UPR leads to an adaptation to cellular stresses by means of increased chaperone expression (Rutkowski, Arnold et al. 2006). In terms of a mechanism, Rutkowski suggested that mild UPR activation was linked to selective intrinsic instabilities of apoptotic proteins, such as CHOP, thereby creating a strong pro-survival bias (Rutkowski, Arnold et al. 2006). It is worth noting that increased GRP78 expression was linked to chemoresistance, leading to therapeutic failures in response to chemotherapy (Gifford, Huang et al. 2016). We are currently investigating whether activation of the UPR following the binding of anti-GRP78 autoAbs to cell surface GRP78 can confer protection against apoptotic cell death and thus in part contribute to tumor growth and metastasis.

We have previously reported that the binding of anti-GRP78 autoAbs to cell surface GRP78 can increase TF expression and activity (Al-Hashimi, Caldwell et al. 2010). It is well established that TF expression and activation are correlated with increased tumor progression (Milsom et al., 2009; Rak, Milsom et al. 2006, de Ridder et al.,

2010). It is worth noting that while the risk of thrombosis among PCa patients is relatively low; TF expression/activation can also increase inflammation and angiogenesis resulting in improved proliferative capacity of the tumor (Abdulkadir, Carvalhal et al. 2000, Akashi, Furuya et al. 2003, Milsom and Rak 2008). Based on these studies, tumor growth was measured in an *in vivo* model system, the immunodeficient NOD/SCID mice, that allows for the growth of human tumor cells in the presence of a complete repertoire of coagulation factors (Fang, Lin et al. 1996, Emeis, Jirouskova et al. 2007). Our studies showed that only tumors derived from WT DU145 cells, and not DU145 cells stably knocked down for TF, enhanced tumor growth when treated with anti-GRP78 autoAb. In addition, autoAb treated tumors demonstrated activation of the UPR as well as increased levels of the cell proliferation marker Ki67. Therefore our findings show that other pathways that influence cell proliferation and viability can be activated following the binding of anti-GRP78 autoAbs to surface GRP78.

Impaired TF expression and/or function can potentially limit tumor progression, however, direct modification of TF expression is clinically unfeasible considering the imminent risk of bleeding complications (Khorana 2009). Therefore, we explored approaches to block the interaction of anti-GRP78 autoAbs with cell surface GRP78 on PCa cells. Previous studies have reported that GRP78 contains a heparin binding site consisting of Leu_{98}-Arg_{101} (Hansen, O'Leary et al. 1995), which resides within the N-terminal region of GRP78 that is known to contain the epitope for anti-GRP78 autoAb binding. Although studies by Mousa and colleagues have

suggested that heparin and enoxaparin can function as anti-cancer agents, the underlying mechanism has not been characterized (Mousa, Linhardt et al. 2006, Mousa and Petersen 2009, Vlodavsky, Ilan et al. 2007). Our *in vitro* data show that heparin and LMWH are sufficient to disrupt the binding of anti-GRP78 autoAbs to cell surface GRP78 and reduce TF activity. As expected, heparin treatment did not affect the induction of TF activity by thapsigargin, indicating that heparin does not impair the release of ER Ca^{2+} that contributes to TF activation (Al-Hashimi et al. 2010). Additionally, we demonstrated via immunofluorescence that enoxaparin pre-treatment inhibited anti-GRP78 autoAb binding to the surface DU145 cells. This data indicates that heparin or enoxaparin pre-treatment can successfully prevent the binding of anti-GRP78 autoAbs to the surface of cancer cells, thereby inhibiting TF activity. Furthermore, these findings provide a novel mechanism by which heparin reduces local anti-coagulant effects independent of its ability to inactivate thrombin and Xa via antithrombin.

Based on these findings, we designed an interventional study to assess the ability of enoxaparin to block the growth of DU145-derived tumors in NOD/SCID mice, both in the presence or absence of anti-GRP78 autoAbs. It is worth mentioning that the intervention approach in this experiment was adapted to test the ability of enoxaparin to block the binding of anti-GRP78 autoAbs in the presence of a complete coagulation system. Treatment with enoxaparin abolished the effect of anti-GRP78 autoAbs on accelerated tumor growth in these mice. Furthermore, analysis of tumors treated with anti-GRP78 autoAbs and enoxaparin demonstrated

no activation of the UPR, compared to tumors treated with only anti-GRP78 autoAbs. Based on these results, our studies suggest that agents like enoxaparin which can interfere with the autoantibody/surface GRP78 complex could represent a potential new strategy for the treatment of PCa or other cancers that are impacted by the presence of anti-GRP78 autoAb. However, the benefits of using enoxaparin or heparin must be balanced with the potential for bleeding in these patients.

In summary, our findings support the treatment of PCa with heparin or heparin-like molecules in patients having elevated levels of anti-GRP78 autoAbs. Whether this strategy would benefit other cancers in which anti-GRP78 autoAbs are elevated is worthy of investigation.

EXPERIMENTAL PROCEDURES

Human Protein Atlas

Protein immunohistochemistry images from normal and cancer tissue were downloaded from the publicly available data base of the Human Protein Atlas (http://www.proteinatlas.org). Representative samples were downloaded from Adenocarcinoma, NOS (M-81403, patient id: 3040), Low grade (M-814031, Patient id: 3957), and High grade (M-814033, Patient id: 3978). Images were analyzed for total and cell surface GRP78 immunostaining.

PSA and Anti-GRP78 Autoantibody Titres

Biological materials were obtained from the Ontario Tumour Bank, which is funded by the Ontario Institute for Cancer Research. Blood samples were taken from a patient cohort diagnosed with PCa prior to treatment administration. PSA values were provided by the Ontario Tumour Bank. anti-GRP78 autoAb titres were measured using an established ELISA protocol as described previously (Al-Hashimi, Caldwell et al. 2010).

Cell Culture

Cancer cell lines were purchased from the American Type Culture Collection (Manassas, VA). The human prostate cancer cell line, DU145, was cultured in MEM+GLUTAMAX media (Invitrogen, Carlsbad, CA). All media were supplemented with 10% fetal bovine serum (Sigma-Aldrich, St. Louis, MO) containing 100 U/ml

penicillin and 100 μg/ml streptomycin (Invitrogen). Cells were maintained at 37°C in a humidified atmosphere of 5% CO_2.

Patient Samples

Blood samples from patients with PCa were obtained from the Department of Urology, St. Joseph's Healthcare, Hamilton, ON, Canada. Written informed consent was obtained from each patient and approved by the Research Ethics Board of St. Joseph's Healthcare (REB#08-3047).

Isolation of anti-GRP78 autoAbs

Anti-GRP78 autoAbs were purified from the serum of PCa patients by affinity chromatography on Protein A-Sepharose, as previously described (Al-Hashimi, Caldwell et al. 2010).

Cell Treatments

Thapsigargin (Sigma-Aldrich) stock solutions were diluted in DMSO as a vehicle solvent and given in the appropriate physiological buffer to achieve a final concentration of 5 μM. Tg was used as an ER stress inducer and a positive control for the TF activity assay. The hrGRP78 peptide was resuspended at a concentration of 60 μg/ml in PBS and used to neutralize GRP78 autoantibodies.

Immunoblotting

Cells were lysed in 4X SDS-PAGE sample buffer and total protein lysates were separated on a 10% SDS-PAGE gel under reducing conditions. Following separation

on SDS-polyacrylamide gels, proteins were transferred to nitrocellulose membranes (Bio-Rad, Richmond, CA) using a Trans-Blot Semi-Dry transfer apparatus (Bio-Rad). Membranes were blocked overnight in 5% skim milk in 1X TBST and then incubated with primary antibody (anti-GRP78/Bip: Cat#610979, BD Transduction, San Jose, CA, USA; anti-Phospho-eIF2α: Cat#9721S, and the VEGF pathway sampler kit #8696, Cell Signaling, Danvers, MA, anti-TF #4502, American Diagnostica, anti-CHOP, #B3, Santa Cruz) followed by the appropriate horseradish peroxidase (HRP)-conjugated secondary antibodies (Dako, Carpinteria, CA, USA) diluted in 1X TBST containing 1% skim milk. Membranes were visualized using the Western Lighting Chemiluminescence Reagent (Perkin-Elmer, Boston, MA) and Kodak X-OMAT Blue XB-1 film (Perkin-Elmer) was exposed and developed using a Kodak X-OMAT 1000A Processor. To control for equivalent protein loading, immunoblots were stripped and re-probed with anti-β-actin antibody (Cat# A5441, Sigma-Aldrich).

Continuous Measurement of Cell Surface TF PCA

We previously developed a continuous assay for the measurement of TF PCA on intact cancer cells (Caldwell, Dickhout et al. 2010). Briefly, cells were seeded into a 96-well tissue culture plate ($1x10^4$ cells/well) the day before the experiment. The culture media was removed and the cells were washed once with 1X TBS. A cocktail containing 1 nM human FVIIa, 30 nM human FX, 10 mM $CaCl_2$ and 0.4 mM chromogenic substrate S-2765 (Diapharma, West Chester, OH) in 1X TBS was added to each well. Following addition of the test agent diluted in 1X TBS, the absorbance

at 405 nm was measured every 2 min for 3 h at 37°C. A standard curve was generated where 100 units of TF activity was defined as the amount of activity in 0.3 μL of human recombinant TF, which is equivalent to 450 μg of TF (as determined by the American Diagnostica ELISA). V_{max} was calculated using SoftMax Pro and used to determine the amount of FXa generated per 10,000 cells (U/10,000 cells).

RNA Isolation and RT-PCR

RNA was isolated using the Qiagen RNeasy Mini kit (Qiagen) and cDNA synthesized using the Applied Biosystem High Capacity cDNA Reverse Transcription kit (Applied Biosystems). Real time RT-PCR reactions were carried out based on protocols described previously using Sybr-Green MasterMix (Applied Biosystems) (Bookout and Mangelsdorf 2003, Bustin, Benes et al. 2009) using primers listed in Table I.

Table I: quantitative RT-PCaR Primers

Human Genes	**Forward Primers (5'-3')**	**Reverse Primer (5'-3')**
ATF4	GGGACAGATTGGATGTTGGAGA	ACCCAACAGGGCATCCAAGT
GRP78	CATCACGCCGTCCTATGTCG	CGTCAAAGACCGTGTTCTCG
Ki67	GGGCCAATCCTGTCGCTTAAT	GTTATGCGCTTGCGAACCT
XBP1s	CCGCAGCAGGTGCAGG	GAGTCAATACCGCCAGAATCCA
TF	GCCAGGAGAAAGGGGAAT	CAGTGCAATATAGCATTTGCAGTAGC
VEGFR	GAGGAGCAGTTACGGTCTGTG	TCCTTTCCTTAGCTGACACTTGT
β-Actin	TCACCCACACTGTGCCCATCTACGA	CAGCGGAACCGCTCATTGCCAATGG
18S	GGCCCTGTAATTGGAATGAGTC	CCAAGATCCAACTACGAGCTT

Generation of TF Knock Down DU145 Cells

DU145 cells grown to 50% confluency in a 12-well plate were infected with lenti-viral particles containing human TF shRNA vector (Santa Cruz Biotechnology, Santa Cruz, CA) based on manufacturer protocols. After 48 hrs, colonies were selected using complete MEM media containing 5 μg/mL of puromycin (Santa Cruz). Colonies were assessed for TF expression and activity using Western bloting and the continuous assay, respectively. As a control, DU145 were infected with lenti-viral particles containing a GFP or scrambled shRNA vectors. Infected colonies were selected by incubating the cells with puromycin selection media.

TF-Dependent Tumor Growth in NOD/SCID Mice

All mouse experiments were approved and performed following the guidelines of the McMaster University ethics board as outlined in the Animal Utilization Protocol (Hamilton, ON, Canada). Control DU145 orTF knock down ($DU145^{KD}$) cells were injected subcutaneously into the flank of 7-week old NOD/SCID mice (Jackson Laboratory). A total volume of 0.1 mL of matrigel and $5x10^5$ cells was injected subcutaneously into the flank of mice. Tumor formation was monitored and measured weekly. When tumors reached 5% of normal body weight, mice were sacrificed and tumor tissue was collected. Tumor volume was determined based on the following equation: Tumor Volume=Length x $Width^2$ x 0.52. Mice had unlimited access to food and water.

Anti-GRP78 AutoAb Treatment and Tumor Growth

Twenty-four NOD/SCID mice (Jackson Laboratory, 8-week old) were injected with 0.1 mL of matrigel containing $10x10^5$ cells subcutaneously into the left flank. Mice were divided into treatment groups as follows: 1) PBS (0.1 mL, weekly injection), 2) control human IgG (168 μg IgG in 0.1 mL PBS, weekly injection), or 3) anti-GRP78 autoAb (168 μg anti-GRP78 autoAb in 0.1 mL PBS, weekly injection). anti-GRP78 autoAbs were isolated from twenty-four PCa patients and pooled to produce the source of anti-GRP78 autoAb. Tumor formation was monitored and measured weekly. When tumors reached 5% of normal body weight, mice were sacrificed and tumor tissue was processed for mRNA analysis.

Enoxaparin intervention: The intervention study utilized the same protocol as shown above. The intervention group (n=5) cohort received an additional injection of enoxaparin sodium (Lovenox, Sanofi Aventis) two weeks after tumor implantation, a control group (n=5) received 100 μL of PBS injection. Enoxaparin was diluted in 0.9% sterile saline at a concentration of 1 mg/mL and administered at 6 mg/kg/week intravenously into the tumor site.

RNA Isolation and NanoString® Analysis

Total RNA was isolated from flash frozen mouse tumor tissue using the RNeasy Lipid Tissue Mini Kit (Cat. No. 74804). Only RNA with RIN> 5 was used in our NanoString® analyses. NanoString® data was normalized against 7 housekeeping genes, IPO8, GUSB, TBP, YWHAZ, ACTB, GAPDH and RPLP2. *p* values were corrected for multiple comparisons using the Benjamin-Hochberg procedure in nsolver® programming and heatmaps were produced using Java Treeview software.

Hierarchical gene clustering was performed on heatmaps using Euclidean distance and complete linkage.

GRP78 Immunoflurescence

Wild type DU145 cells were grown in chamber slides. Upon 50% confluence, cells were left untreated or treated with 10 mg/mL of enoxaparin for 4 hours. Cells were fixed with 4% paraformaldehyde solution and either incubated with anti-GRP78 autoAbs (60 μg/mL) or PBS control for 1 hour. Anti-human ALEXA 488 secondary antibody (Molecular Probes) were used to detect with anti-GRP78 autoAb. DAPI stain (Sigma) was used to identify the nucleus. Slides were imaged using the Olympus DSU microscope.

Immunohistochemical Staining

Tumor tissue isolated from mice was fixed in formalin and paraffin embedded. Four micrometer sections were deparaffinized and blocked with 5% normal goat (Ki67 antibody) or rabbit serum (TF antibody). Sections were incubated with primary antibody for 1 hour at room temperature, followed by goat anti-rabbit or rabbit anti-goat biotinylated secondary antibodies (Vector Laboratories), diluted 1/500 in 0.05 mol/L Tris buffer, pH 7.5, for 30 minutes, and streptavidin-peroxidase (Zymed Laboratories), diluted 1/20, for 5 minutes. Sections were developed in Nova Red peroxidase substrate (Vector Laboratories) and counterstained with hematoxylin. ImageJ (Rasband, W.S., ImageJ, U. S. National Institutes of Health, Bethesda, Maryland, USA, http://imagej.nih.gov/ij/, 1997-2015) was used to determine the number of Ki67 positive cells.

Statistical Analysis

Graphpad Prism software (Ver 6.07) was used to analyze quantitative data. Correlation studies using clinical data were analyzed based on the Pearson correlation test. Significance of differences between control and various treatments were determined by analysis of variance (ANOVA). On finding significance with ANOVA, an unpaired Student's t-test was performed. For all analyses, $p \leq 0.05$ was considered significant.

Figure Legends:

Figure. 1. PCa Disease Grade Correlates with Increased Cell Surface GRP78 Expression.

Prostate specimens from PCa patients were graded pathologically and stained for GRP78 protein. Scale bar, 100 μm.

(A) Grade I PCa specimen demonstrating a limited number of cells stained for cell surface GRP78.

(B) Grade II PCa specimen demonstrating an increase in cells positive for cell surface GRP78. An increase in endogenous GRP78 is also observed.

(C) Grade IV PCa specimen demonstrating a marked increase in endogenous and cell surface GRP78 expression throughout the specimen.

Arrows denote cells stained for cell surface GRP78. Regions highlighted in red represent clusters of cells with high expression of cell surface GRP78.

Figure. 2. Correlation of Circulating Anti-GRP78 AutoAb Titres with Serum PSA Concentrations in a Clinical Population Diagnosed with PCa.

(A) Anti-GRP78 autoAb levels positively correlate with PSA concentrations in a clinical population diagnosed with PCa. The Pearson correlation indicated a significant positive correlation. $p<0.05$, r = 38.4%, n=48.

(B) Patients grouped in Low PSA (1-2 ng/mL, n=12), Medium PSA (3-7 ng/mL, n=14), High PSA (8-19 ng/Ml, n=13), or Very High (20+ ng/mL, n=8) demonstrate

increasing anti-GRP78 autoAb titres as PSA levels increase. Controls: age-matched individuals (n=9) who were not diagnosed with PCa. $^{**}p<0.01$; $^{**}p<0.001$.

(C) PCa patient cohort recovering from the prostatectomy procedure (24 weeks postoperative) demonstrate significantly lower anti-GRP78 autoAb tires (90.88 μg/mL, $^{***}p<0.0001$) compared to titres observed in the pre-operative cohort (124.2 μg/mL).

Figure. 3. Treatment of Wild Type DU145 Cells with Anti-GRP78 AutoAbs Increases the Expression of TF and UPR markers.

(A) Pathological doses of anti-GRP78 autoAbs (60 μg/ml) increase protein expression of TF as well as markers of UPR activation (PDI, IRE1, and phospho-eIF2α), compared to non-treated (NT) cells; or cells treated with a normal-dose of anti-GRP78 autoAb titres (5 μg/mL). As a loading control, immunoblots were probed for β-actin.

(B) Quantitative RT-PCR analysis of GRP78 and spliced XBP-1 mRNA expression in DU145 cells treated with a pathological dose of anti-GRP78 autoAbs (60 μg/mL). Results are expressed as fold induction versus β-actin. $^{*}p<0.05$ versus non-treated (NT) cells, n=3.

Figure. 4. Anti-GRP78 AutoAbs Accelerate Tumor Growth in Mice and Increase Protein Expression of TF and UPR Markers.

(A) Treatment of wild type DU145 derived tumors in NOD/SCID mice with anti-GRP78 autoAbs significantly increased the rate of tumor growth compared to PBS or human IgG treated mice. NS, non-significant. *p<0.05, **p<0.001 versus IgG and PBS treatment, n=8 per group.

(B) Immunohistochemical analysis of tumors treated with anti-GRP78 autoAbs demonstrated an increase in TF expression, compared to human IgG-treated tumors. Scale bar, 100 μm.

(C) Quantitative RT-PCR analysis of tumors treated with anti-GRP78 autoAb demonstrated increased mRNA expression of TF, VEGR, Ki67, spliced XBP-1, ATF4, and GRP78. *p<0.05 compared to IgG group, n=3.

(D) Heat map showing gene expression levels of seven UPR markers using NanoString®. Colors represent the fold changes in gene expression with control human IgG or anti-GRP78 autoAb treatment. p values are indicated for each gene, n=3 per treatment.

(E) Immunohistochemical analysis of the proliferation marker Ki67 demonstrates a 48% increase in stained cells in the anti-GRP78 autoAb treated group, compared to mice treated with control human IgG. Representative images of five sections are shown. ImageJ was used to count the number of Ki67 positive cells. Scale bar, 100 μm.

Figure. 5. TF Knock Down in DU145 Cells Inhibits Anti-GRP78 AutoAb-Mediated TF Activity and Accelerates Tumor Progression.(A) Western blot analysis of

TF expression in cells treated with lenti-viral particles encodingTF shRNA. As a control, cells were treated with control lenti-viral particles encoding GFP. As a loading control, immunoblots were probed for β-actin. Clone 4 demonstrates very low TF protein expression and is referred to as $DU145^{KD}$.

(B) Treatment of $DU145^{KD}$ cells with anti-GRP78 autoAb demonstrates no change in TF activity, compared to control cells and clone 1. *p<0.05 compared to non-treated (NT) cells, n=5.

(C) $DU145^{KD}$ derived tumors demonstrate decreased tumor growth rate, compared to control DU145 tumors (left panel). Significant p values are shown on the graph. Immunohistochemical analysis demonstrated decreased TF expression in $DU145^{KD}$ derived tumors, compared to control DU145 tumors (right panel). *p<0.05. Scale bar, 100 μm, n=5 per group.

(D) Anti-GRP78 autoAbs do not alter the rate of tumor growth in $DU145^{KD}$ derived tumors. Human IgG treatment was used as a control for anti-GRP78 autoAb. n=5 per group.

Figure. 6. Immunodepletion of Anti-GRP78 AutoAbs From Serum Reduces TF Activity.

(A) Treatment of intact wild type DU145 cells with thapsigargin (Tg, 5 μM), anti-GRP78 autoAb (60 μg/mL), or patient sera significantly increases TF activity. * p<0.05, n=5 per group. Sera samples that were immunodepleted of anti-GRP78 autoAbs ($Serum_{dep}$) demonstrate TF activity levels similar to control

non-treated (NT) cells. # $p<0.05$ compared to non-depleted serum (Serum), n=5 per group

(B) Treatment of sera from PCa patients with human recombinant GRP78 (hrGRP78, 60 μg/mL) demonstrate lower TF activity compared to their respective native sera on intact wild type DU145 cells. #$p<0.05$, n=5 per group; *$p<0.05$ compared to non-treated (NT) cells, n=5 per group.

Figure. 7. Heparin and the LMWH, Enoxaparin, Block the Binding of Anti-GRP78 AutoAb to DU145 Cells and Inhibit Tumor Growth

(A) Heparin pre-treatment (50 IU/mL) inhibited the effect of anti-GRP78 autoAbs on TF activity in intact wild type DU145 cells. Heparin pre-treatment did not affect TF activity on non-treated (NT) or thapsigargin-induced (Tg, 5μM) cells. *$p<0.05$, compared to non-treated cells (NT), n=5; #$p<0.05$ compared to cells treated with anti-GRP78 autoAB only, n=5 per group.

(B) Heparin (50-100 IU/mL) and enoxaparin (5-40 mg/mL) inhibited the anti-GRP78 autoAb-mediated increase in TF activity in intact DU145 cells. *$p<0.05$ compared to non-treated (NT) cells, n=5. #$p<0.05$, decrease in TF activity with heparin or enoxaparin pretreatment, n=5.

(C) GRP78 immunostaining (green) using anti-GRP78 autoAb (left image) on intact DU145 cells. Pre-treating cells with enoxaparin (10 mg/mL) inhibited cell surface GRP78 staining by the anti-GRP78 autoAb (middle image). Cells treated with only secondary antibody were used to assess background

fluorescence (right image). DAPI was used to stain the nucleus (blue). Scale bar, 20 μm.(D) Left panel: wild type DU145 derived tumors in NOD/SCID mice were either treated with anti-GRP78 autoAbs or human IgG (control). Both groups received a secondary treatment of PBS (intervention control). Tumors treated with anti-GRP78 autoAbs demonstrated an significant increase in tumor growth rate compared to IgG treated mice. $^{**}p<0.001$ versus IgG, n=6 per group. Right Panel: wild type DU145 derived tumors in NOD/SCID mice were either treated with anti-GRP78 autoAb or human IgG (control). Both groups received a secondary treatment of enoxaparin (6 mg/kg/week) (intervention group, n=6 per group). Tumors treated with anti-GRP78 autoAb demonstrated no change in tumor growth rate compared to IgG treated tumors and compared to results shown in the left panel.

(E) Heat map showing gene expression levels of seven UPR markers using NanoString®. Colors represent the fold changes in gene expression with control human IgG, or anti-GRP78 autoAb treatment (60 μg/mL); both groups received the enoxaparin (6 mg/kg/week) treatment. *p* values are indicated for each gene, n=3 per treatment.

Figure. 8. Anti-GRP78 AutoAbs Increase Tumor Growth by Binding to Cell Surface GRP78 and activating TF. Anti-GRP78 autoAbs bind to cell surface GRP78; this interaction can be interrupted by heparin or enoxaparin. Binding of anti-

GRP78 autoAb to cell surface GRP78 induces elevated cytosolic Ca^{2+} concentrations that can activate the pro-survival UPR pathway and increase TF activity. Overall, this interaction leads to increased rate of tumor growth, improved angiogenesis, and potentially, enhanced survival via UPR activation.

Supplemental Figures:

Figure 1: Heat map showing expression levels of genes. Fold changes represent the changes in gene expression with control human IgG, or anti-GRP78 autoAb treatment.

Left panel; both groups received the enoxaparin treatment. Right Panel: no additional treatments were administered.

Reference:

Abdulkadir, S. A., G. F. Carvalhal, Z. Kaleem, W. Kisiel, P. A. Humphrey, W. J. Catalona and J. Milbrandt (2000). "Tissue factor expression and angiogenesis in human prostate carcinoma." Hum Pathol 31(4): 443-447.

Al-Hashimi, A. A., J. Caldwell, M. Gonzalez-Gronow, S. V. Pizzo, D. Aboumrad, L. Pozza, H. Al-Bayati, J. I. Weitz, A. Stafford, H. Chan, A. Kapoor, D. W. Jacobsen, J. G. Dickhout and R. C. Austin (2010). "Binding of anti-GRP78 autoantibodies to cell surface GRP78 increases tissue factor procoagulant activity via the release of calcium from endoplasmic reticulum stores." J Biol Chem 285(37): 28912-28923.

Bookout, A. L. and D. J. Mangelsdorf (2003). "Quantitative real-time PCR protocol for analysis of nuclear receptor signaling pathways." Nucl Recept Signal 1: e012.

Caldwell, J. A., J. G. Dickhout, A. A. Al-Hashimi and R. C. Austin (2010). "Development of a continuous assay for the measurement of tissue factor procoagulant activity on intact cells." Lab Invest 90(6): 953-962.

Center, M. M., A. Jemal, J. Lortet-Tieulent, E. Ward, J. Ferlay, O. Brawley and F. Bray (2012). "International variation in prostate cancer incidence and mortality rates." Eur Urol 61(6): 1079-1092.

D'Amico, A. V., R. Whittington, S. B. Malkowicz, D. Schultz, K. Blank, G. A. Broderick, J. E. Tomaszewski, A. A. Renshaw, I. Kaplan, C. J. Beard and A. Wein (1998). "Biochemical outcome after radical prostatectomy, external beam radiation therapy, or interstitial radiation therapy for clinically localized prostate cancer." JAMA 280(11): 969-974.

de Ridder, G. G., M. Gonzalez-Gronow, R. Ray and S. V. Pizzo (2011). "Autoantibodies against cell surface GRP78 promote tumor growth in a murine model of melanoma." Melanoma Res 21(1): 35-43.

Fang, C. H., T. C. Lin, A. Guha, Y. Nemerson and W. H. Konigsberg (1996). "Activation of factor X by factor VIIa complexed with human-mouse tissue factor chimeras requires human exon 3." Thromb Haemost 76(3): 361-368.

Gifford, J. B., W. Huang, A. E. Zeleniak, A. Hindoyan, H. Wu, T. R. Donahue and R. Hill (2016). "Expression Of GRP78, Master Regulator Of The Unfolded Protein Response, Increases Chemoresistance In Pancreatic Ductal Adenocarcinoma." Mol Cancer Ther.

Gonzalez-Gronow, M., M. Cuchacovich, C. Llanos, C. Urzua, G. Gawdi and S. V. Pizzo (2006). "Prostate cancer cell proliferation in vitro is modulated by antibodies against glucose-regulated protein 78 isolated from patient serum." Cancer Res 66(23): 11424-11431.

Gonzalez-Gronow, M., M. A. Selim, J. Papalas and S. V. Pizzo (2009). "GRP78: a multifunctional receptor on the cell surface." Antioxid Redox Signal 11(9): 2299-2306.

Hansen, L. K., J. J. O'Leary, A. P. Skubitz, L. T. Furcht and J. B. McCarthy (1995). "Identification of a homologous heparin binding peptide sequence present in fibronectin and the 70 kDa family of heat-shock proteins." Biochim Biophys Acta 1252(1): 135-145.

Khorana, A. A. (2009). "Cancer and thrombosis: implications of published guidelines for clinical practice." Ann Oncol 20(10): 1619-1630.

Lee, A. S. (2014). "Glucose-regulated proteins in cancer: molecular mechanisms and therapeutic potential." Nat Rev Cancer 14(4): 263-276.

Lippi, G., M. Montagnana, G. C. Guidi and M. Plebani (2009). "Prostate-specific antigen-based screening for prostate cancer in the third millennium: useful or hype?" Ann Med 41(7): 480-489.

Milsom, C. and J. Rak (2008). "Tissue factor and cancer." Pathophysiol Haemost Thromb 36(3-4): 160-176.

Misra, U. K., M. Gonzalez-Gronow, G. Gawdi, F. Wang and S. V. Pizzo (2004). "A novel receptor function for the heat shock protein Grp78: silencing of Grp78 gene expression attenuates alpha2M*-induced signalling." Cell Signal 16(8): 929-938.

Mousa, S. A., R. Linhardt, J. L. Francis and A. Amirkhosravi (2006). "Anti-metastatic effect of a non-anticoagulant low-molecular-weight heparin versus the standard low-molecular-weight heparin, enoxaparin." Thromb Haemost 96(6): 816-821.

Rak, J., C. Milsom, L. May, P. Klement and J. Yu (2006). "Tissue factor in cancer and angiogenesis: the molecular link between genetic tumor progression, tumor neovascularization, and cancer coagulopathy." Semin Thromb Hemost 32(1): 54-70.

Ron, D. and P. Walter (2007). "Signal integration in the endoplasmic reticulum unfolded protein response." Nat Rev Mol Cell Biol 8(7): 519-529.

Ruf, W., J. Disse, T. C. Carneiro-Lobo, N. Yokota and F. Schaffner (2011). "Tissue factor and cell signalling in cancer progression and thrombosis." J Thromb Haemost 9 Suppl 1: 306-315.

Rutkowski, D. T., S. M. Arnold, C. N. Miller, J. Wu, J. Li, K. M. Gunnison, K. Mori, A. A. Sadighi Akha, D. Raden and R. J. Kaufman (2006). "Adaptation to ER stress is mediated by differential stabilities of pro-survival and pro-apoptotic mRNAs and proteins." PLoS Biol 4(11): e374.

Shin, B. K., H. Wang, A. M. Yim, F. Le Naour, F. Brichory, J. H. Jang, R. Zhao, E. Puravs, J. Tra, C. W. Michael, D. E. Misek and S. M. Hanash (2003). "Global profiling of the cell surface proteome of cancer cells uncovers an abundance of proteins with chaperone function." J Biol Chem 278(9): 7607-7616.

Teeter, A. E., J. C. Presti, Jr., W. J. Aronson, M. K. Terris, C. J. Kane, C. L. Amling and S. J. Freedland (2013). "Do nomograms designed to predict biochemical recurrence (BCR) do a better job of predicting more clinically relevant prostate cancer outcomes than BCR? A report from the SEARCH database group." Urology 82(1): 53-58.

Vieira, P. and K. Rajewsky (1988). "The half-lives of serum immunoglobulins in adult mice." Eur J Immunol 18(2): 313-316.

Vlodavsky, I., N. Ilan, Y. Nadir, B. Brenner, B. Z. Katz, A. Naggi, G. Torri, B. Casu and R. Sasisekharan (2007). "Heparanase, heparin and the coagulation system in cancer progression." Thromb Res 120 Suppl 2: S112-120.

Figure 1. Al-Hashimi *et al.*, 2016

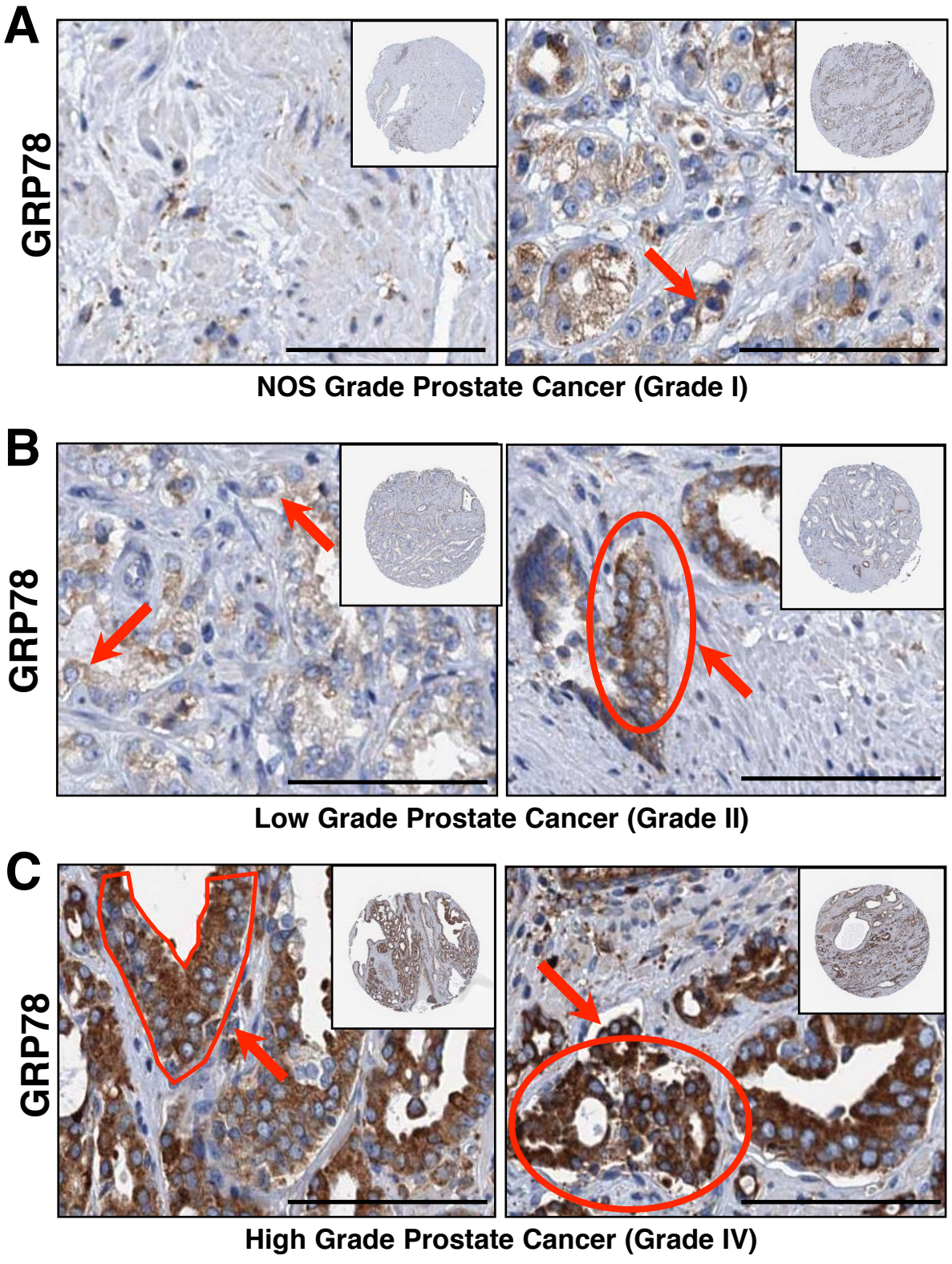

Figure 2. Al-Hashimi *et al.*, 2016

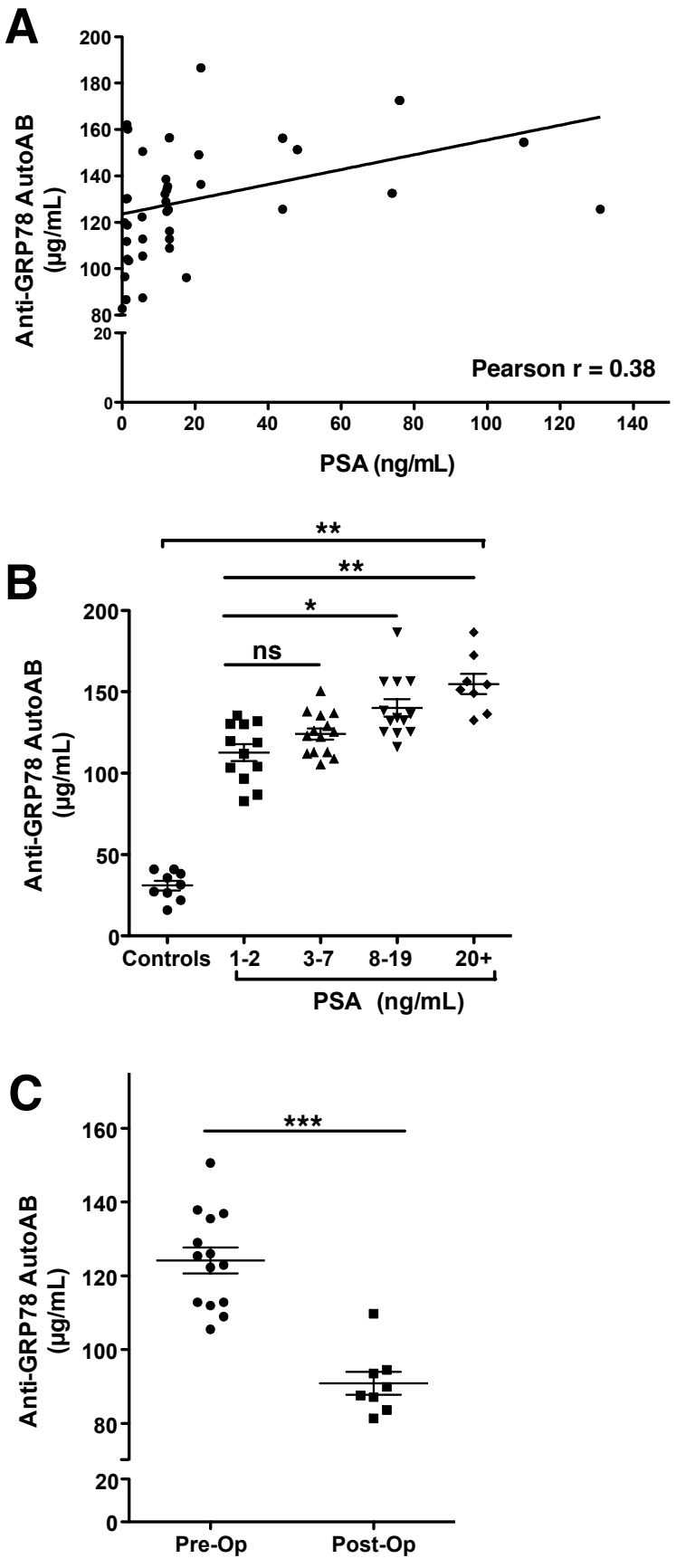

Figure 3. Al-Hashimi *et al.*, 2016

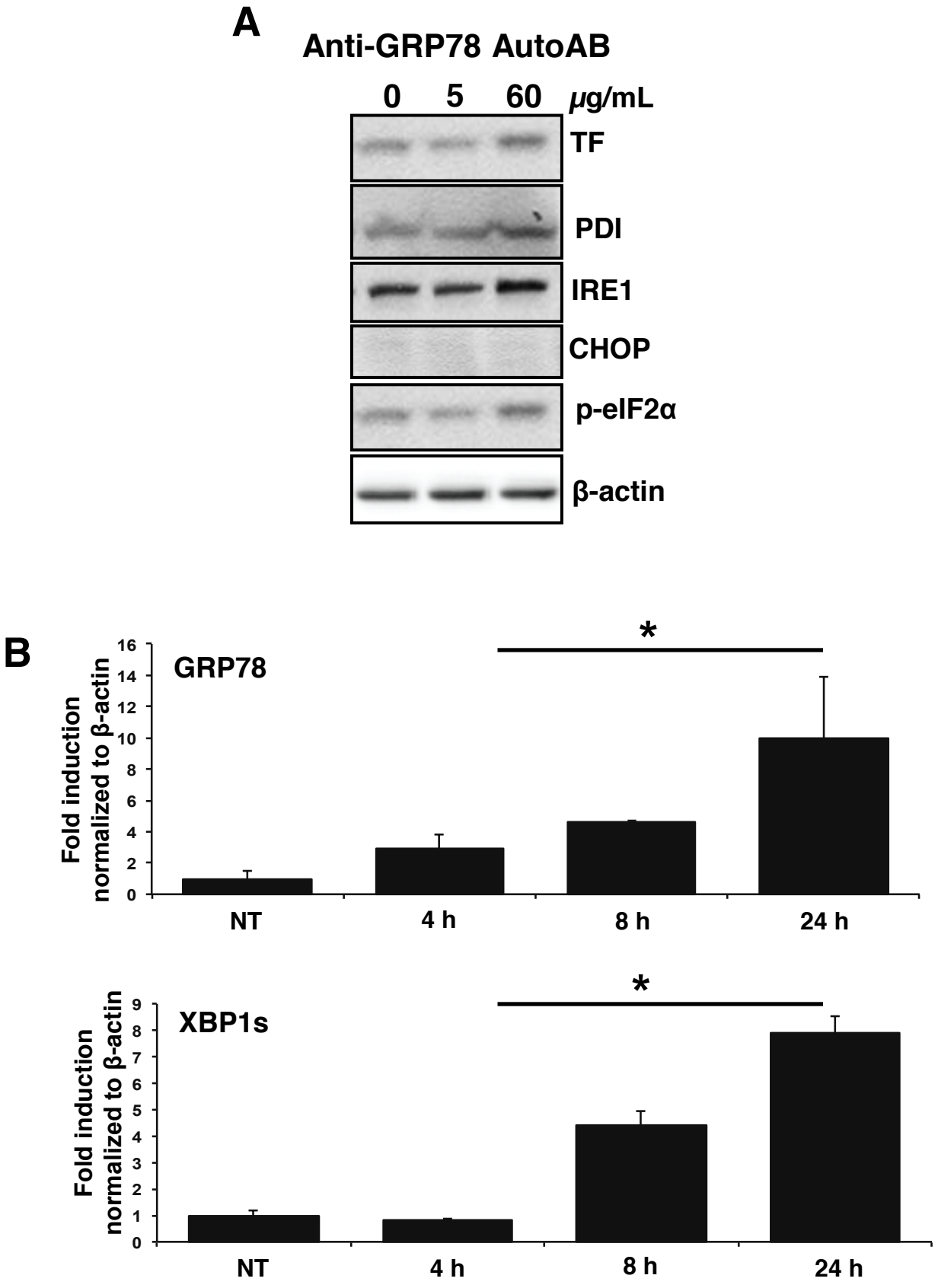

Figure 4. Al-Hashimi *et al.*, 2016

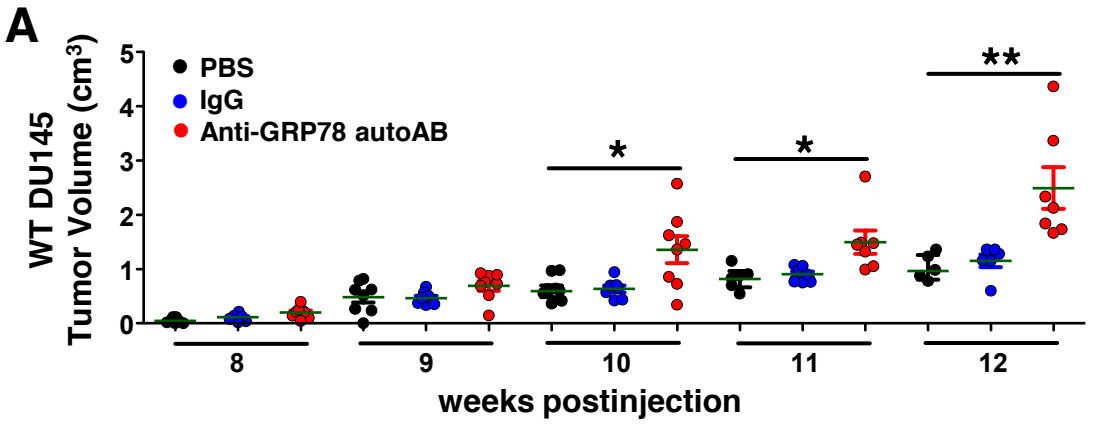

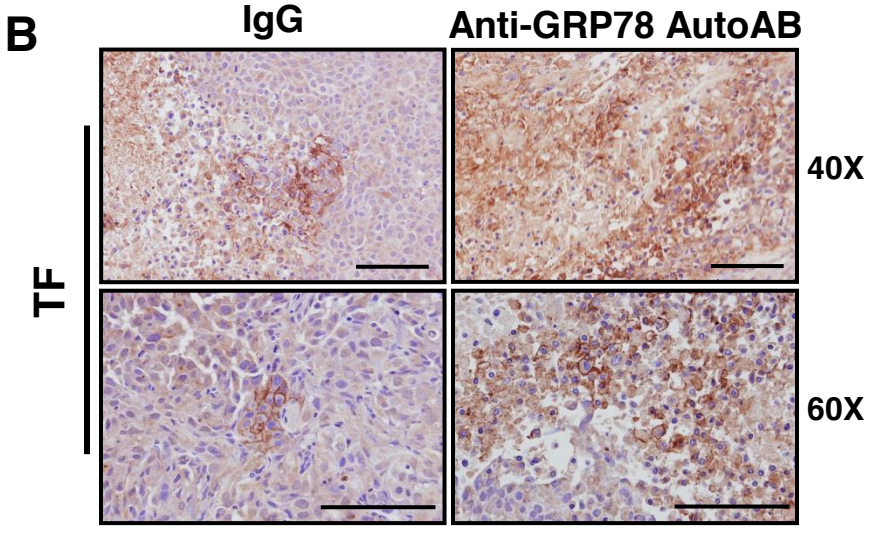

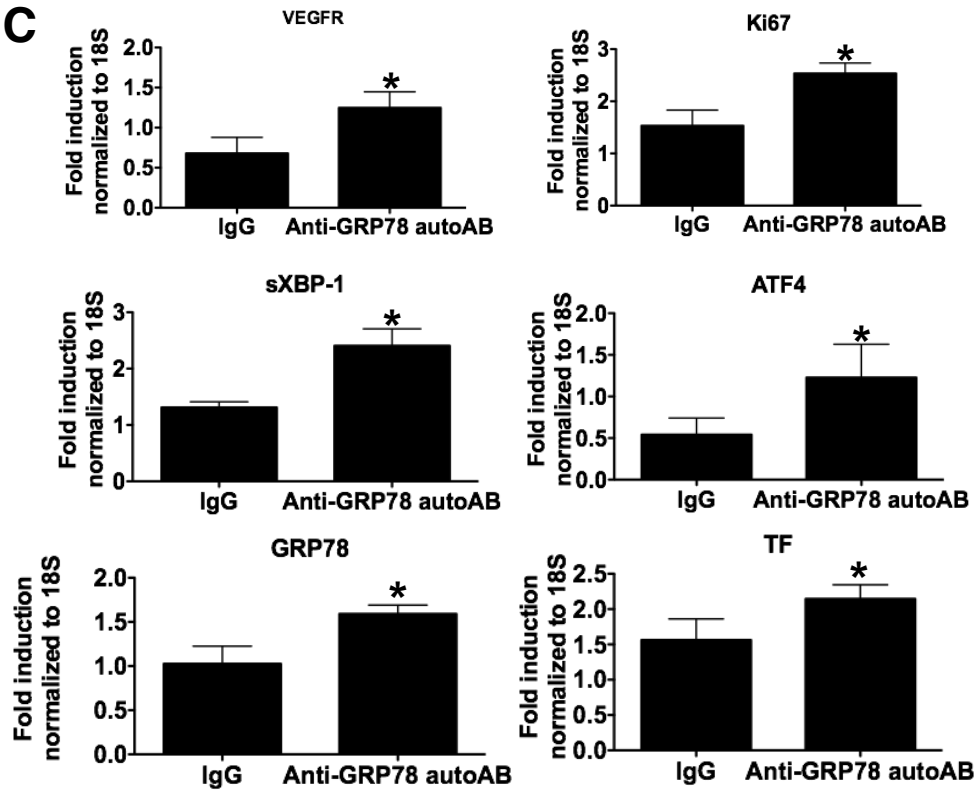

Figure 4. Al-Hashimi *et al.*, 2016

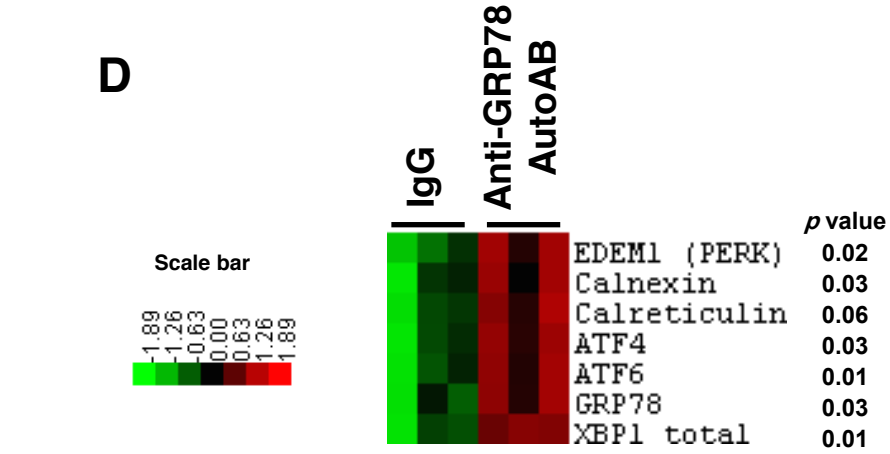

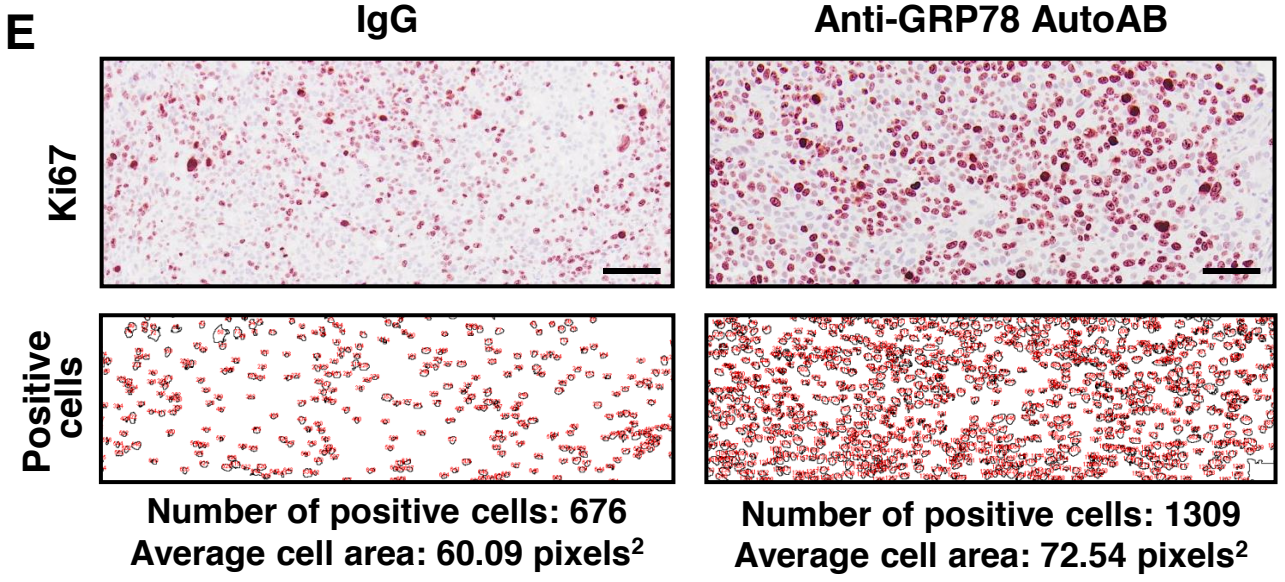

Figure 5. Al-Hashimi *et al.*, 2016

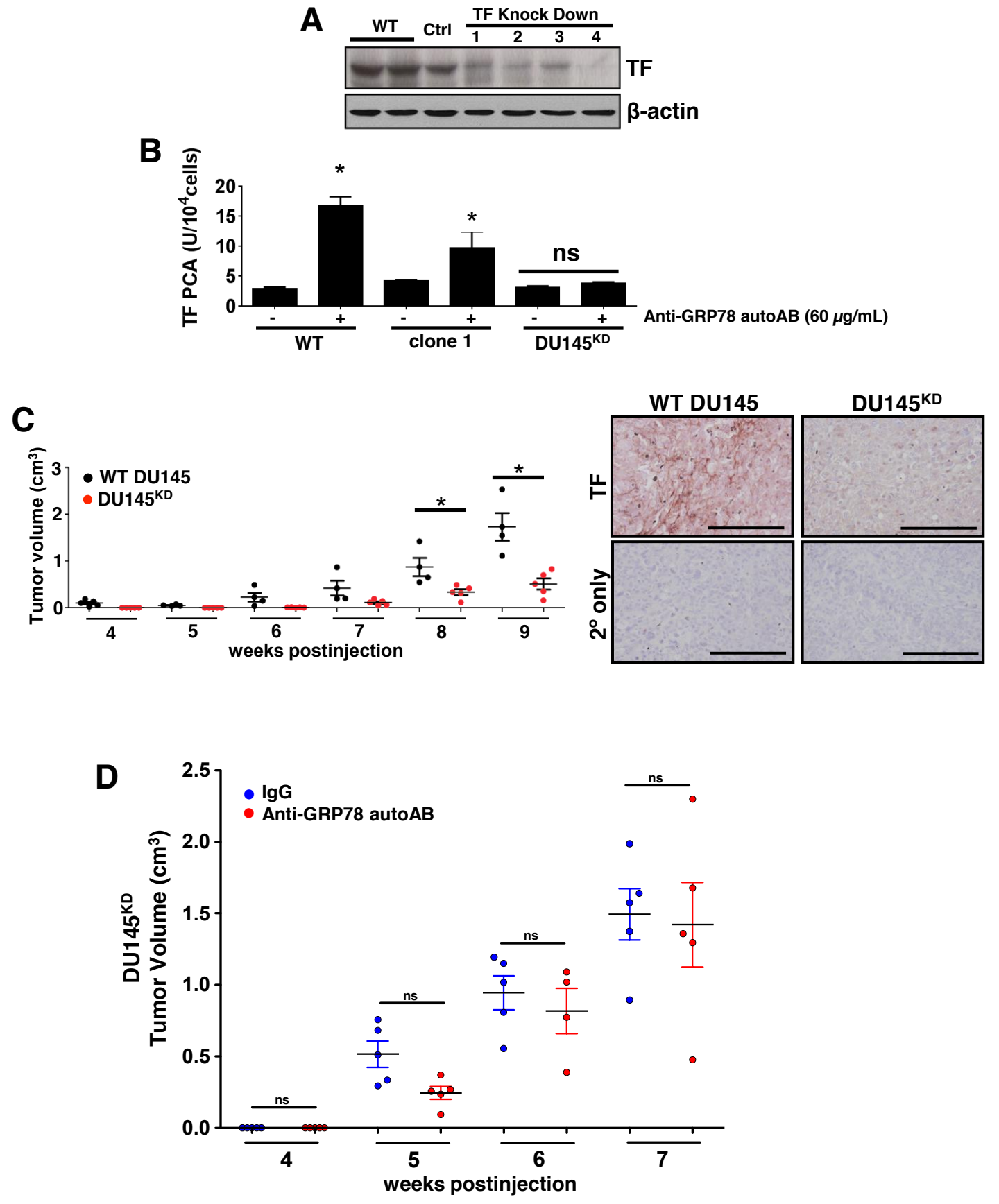

Figure 6. Al-Hashimi *et al.*, 2016

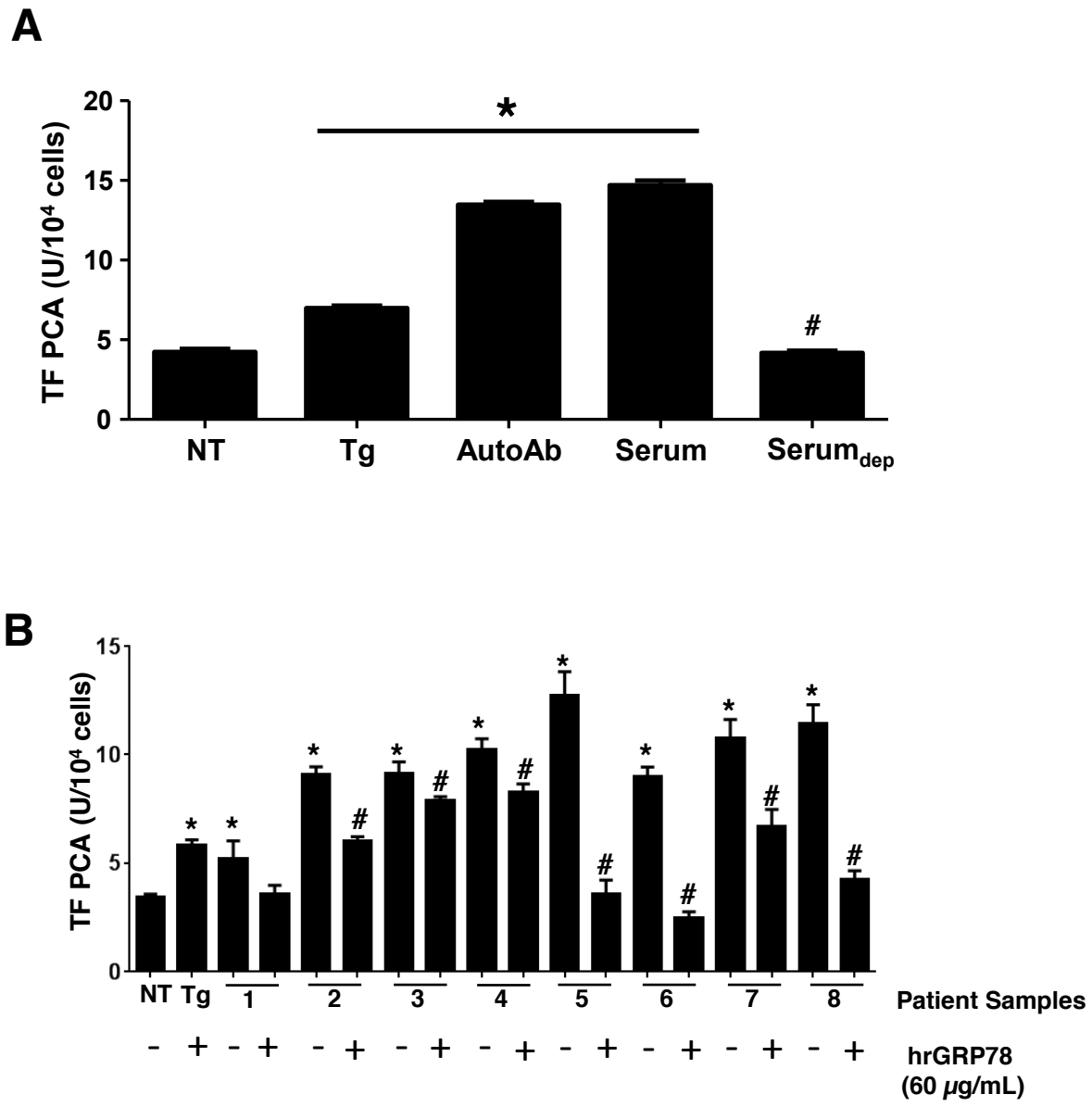

Figure 7. Al-Hashimi *et al.*, 2016

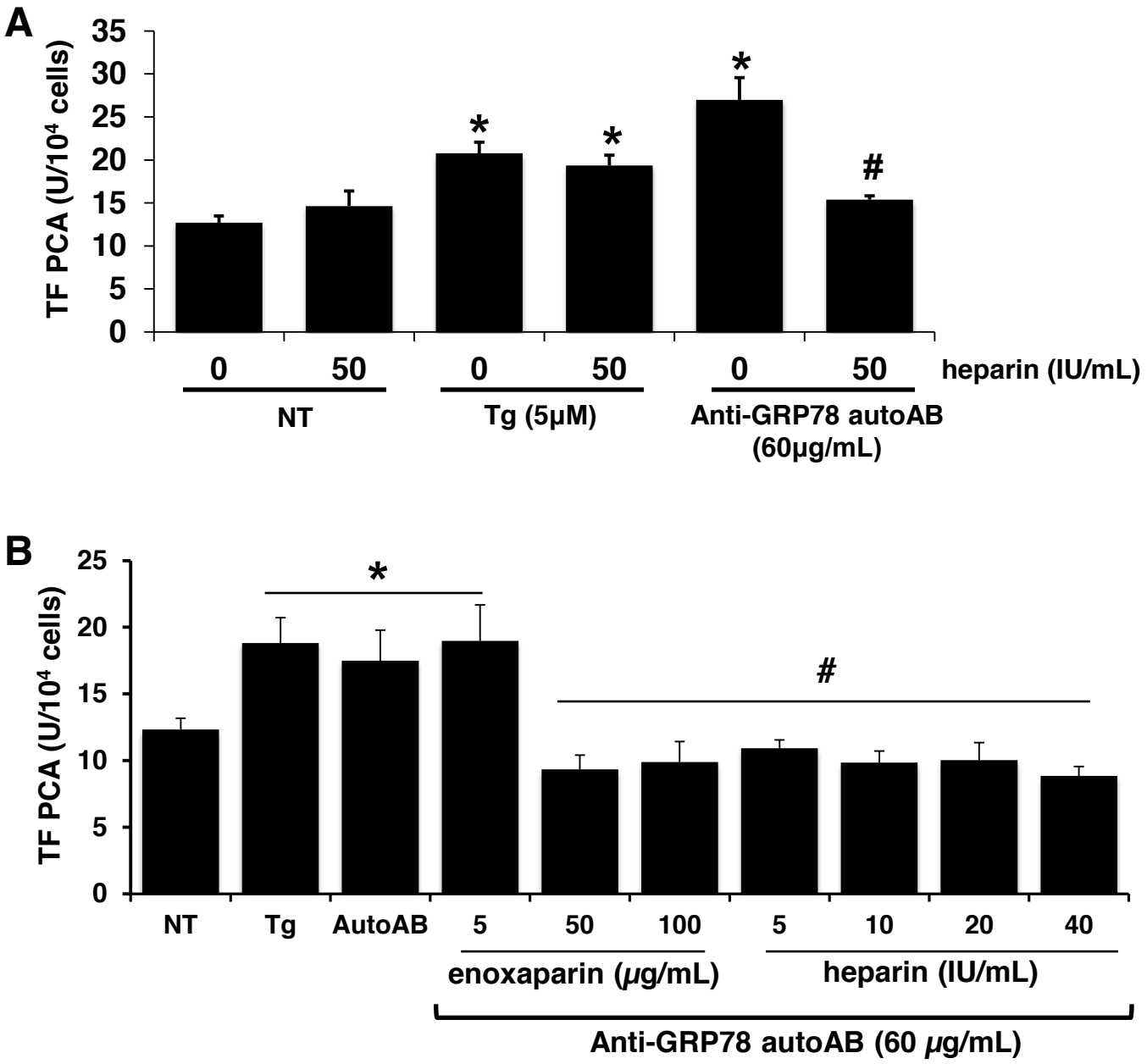

Figure 7. Al-Hashimi *et al.*, 2016

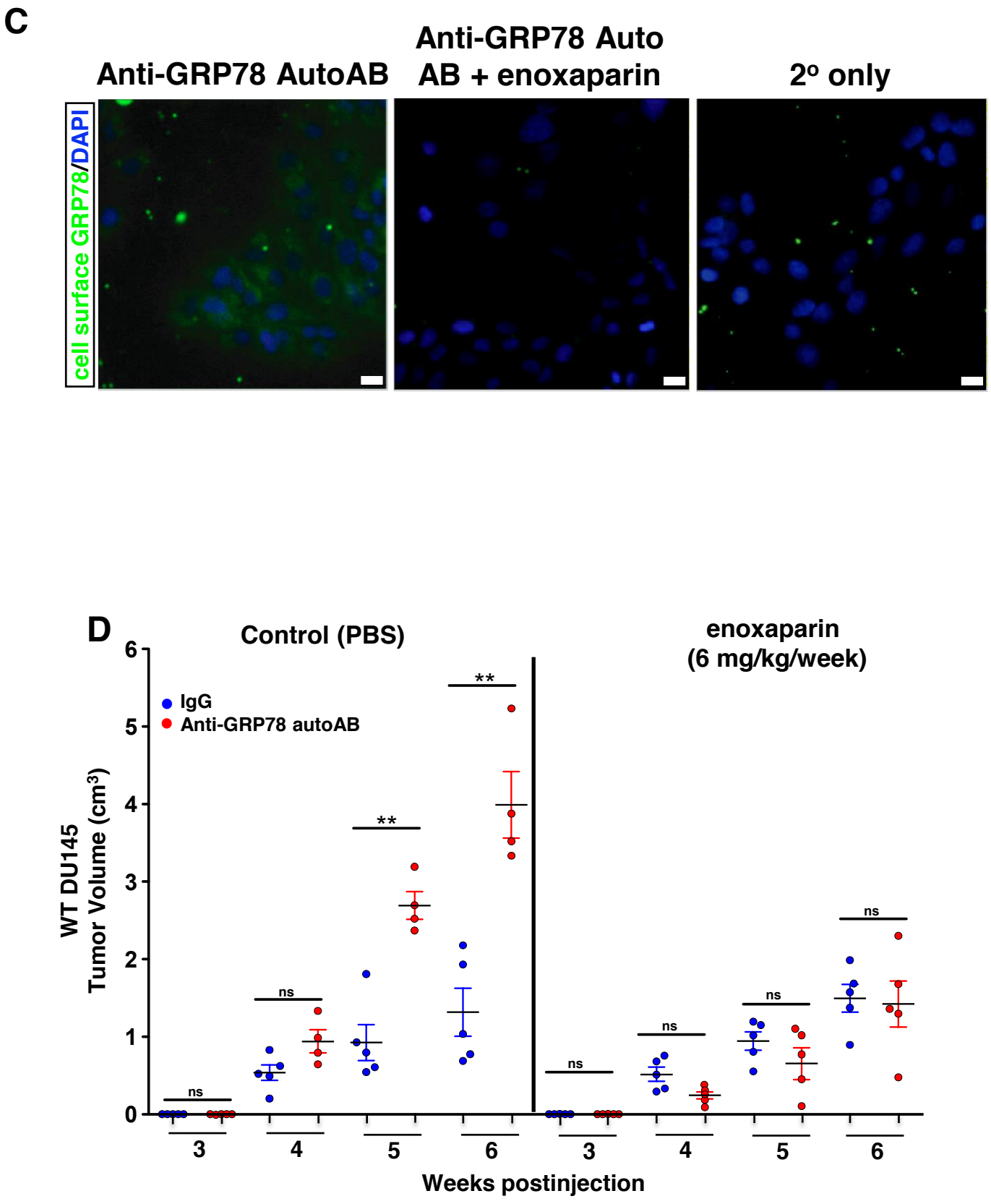

Figure 7. Al-Hashimi *et al.*, 2016

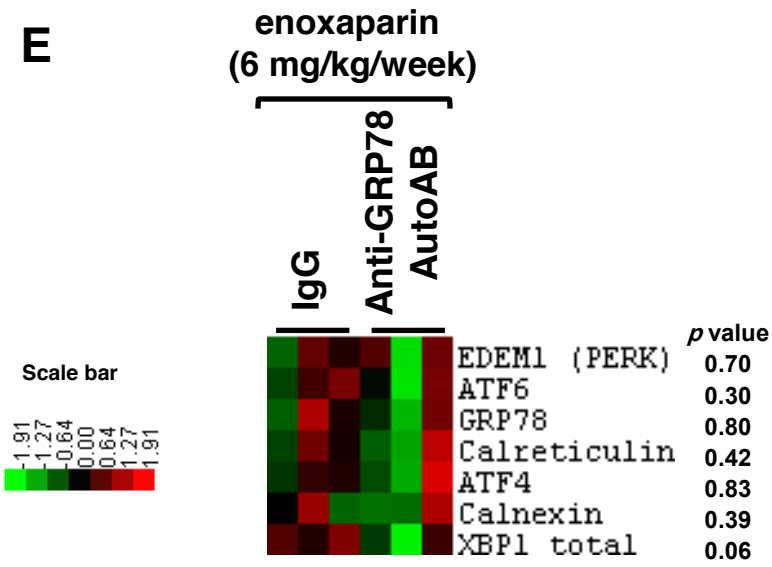

Figure 8. Al-Hashimi *et al.*, 2016

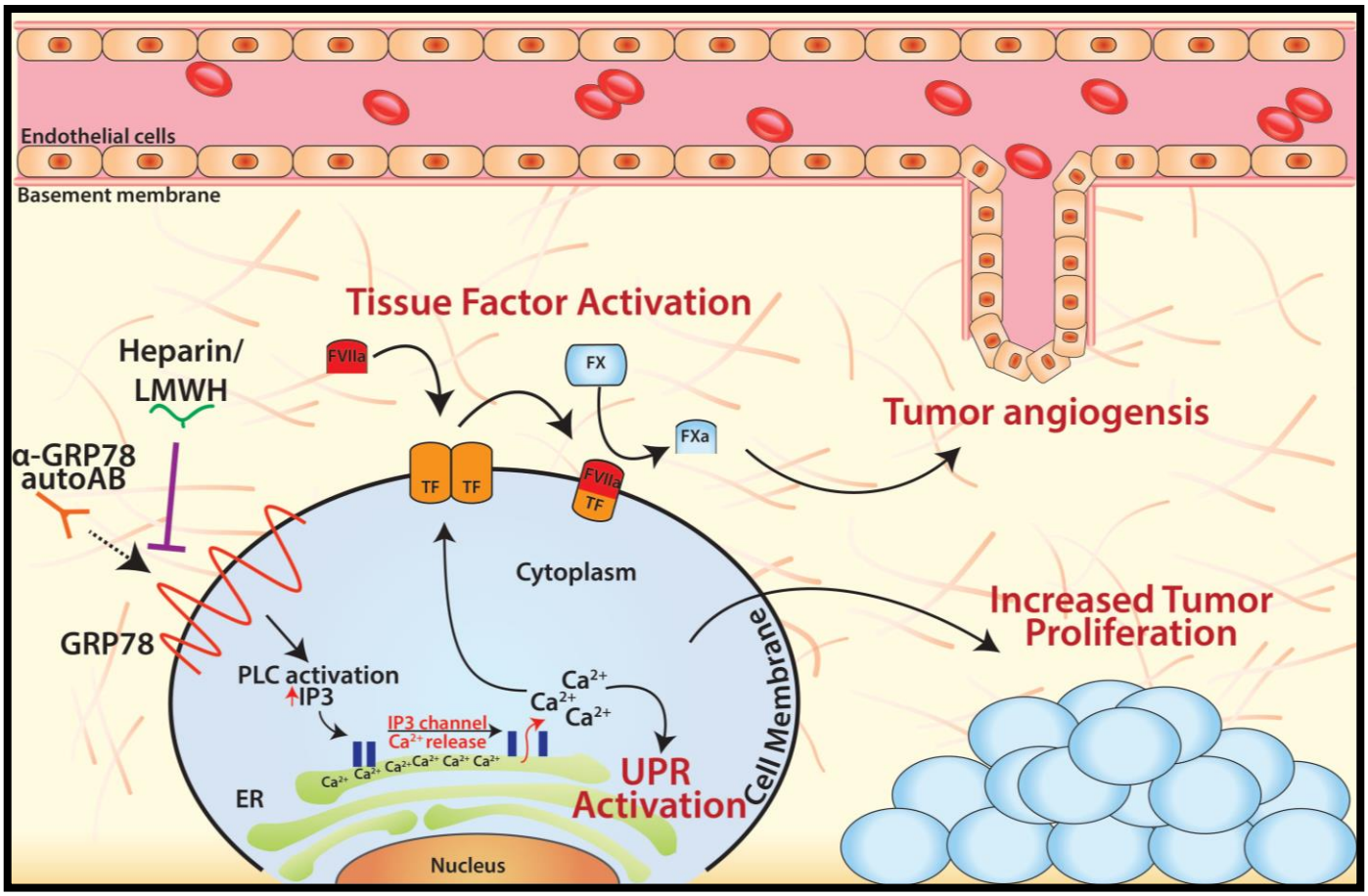

Figure S1

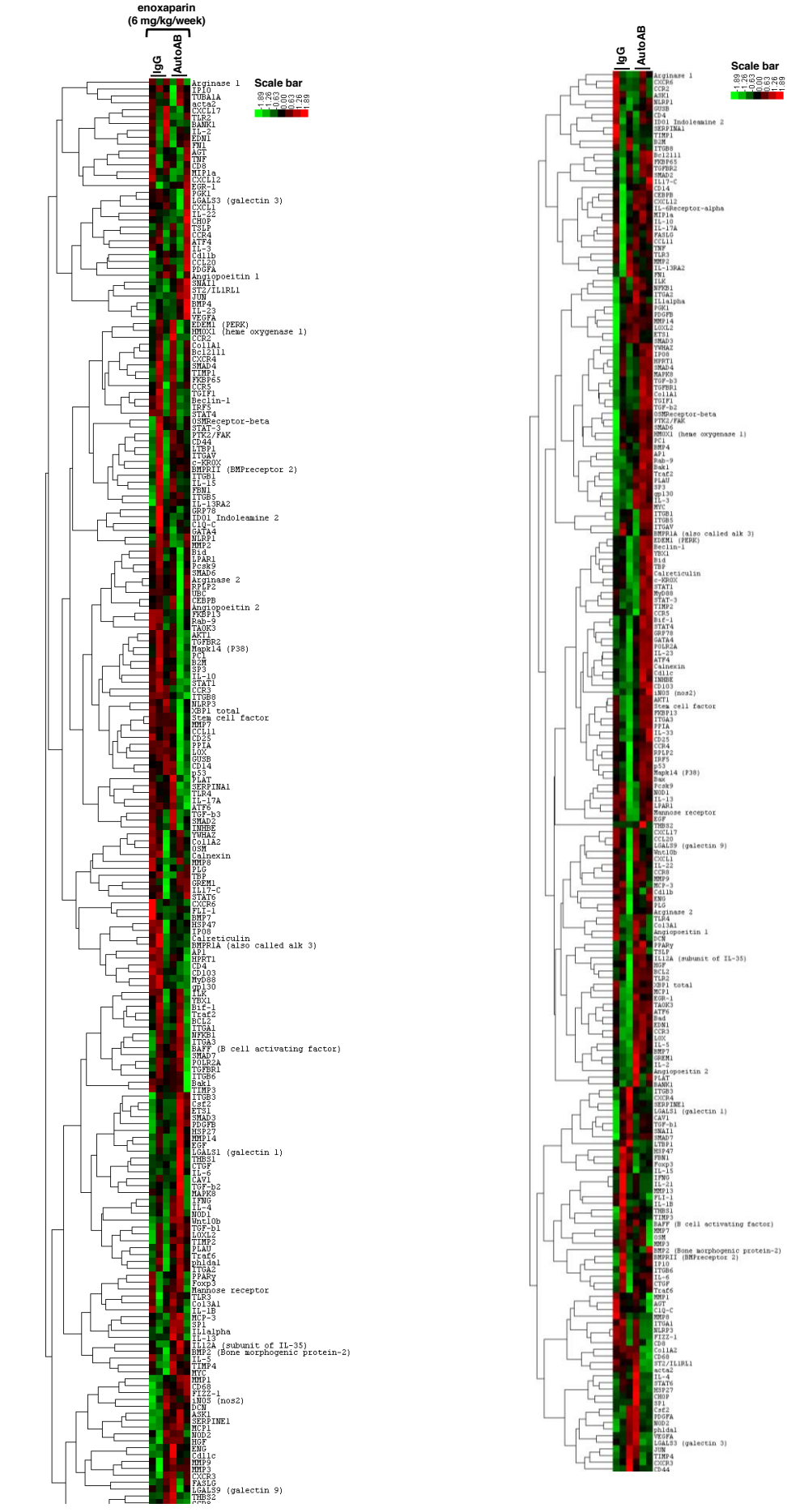
enoxaparin
(6 mg/kg/week)
IgG
AutoAB
Scale bar
-1.89
-1.26
-0.63
0.00
0.63
1.26
1.89
Arginase 1
TP10
TUBA1A
acta2
CXCL17
TLR2
BANK1
IL-2
EDN1
FN1
AGT
TNF
CD8
MIP1a
CXCL12
EGR-1
PGK1
LGALS3 (galectin 3)
CXCL1
IL-22
CHOP
TSLP
CCR4
ATF4
IL-3
Cd11b
CCL20
PDGFA
Angiopoeitin 1
SNAI1
ST2/IL1RL1
JUN
BMP4
IL-23
VEGFA
EDEM1 (PERK)
HMOX1 (heme oxygenase 1)
CCR2
Col1A1
Bcl2l11
CXCR4
SMAD4
TIMP1
FKBP65
CCR5
TGIF1
Beclin-1
IRF5
STAT4
GSMReceptor-beta
STAT-3
PTK2/FAK
CD44
LTBP1
ITGAV
c-KROX
BMPRII (BMPreceptor 2)
ITGB1
IL-15
FBN1
ITGB5
IL-13RA2
GRP78
ID01 Indoleamine 2
C1Q-C
GATA4
NLRP1
MMP2
Bid
LPAR1
Pcsk9
SMAD6
Arginase 2
RPLP2
UBC
CEBPB
Angiopoeitin 2
FKBP13
Rab-9
TAOK3
AKT1
TGFBR2
Mapkl4 (P38)
P61
B2M
SP3
IL-10
STAT1
CCR3
ITGB8
MLPP3
XBP1 total
Stem cell factor
MMP7
CCL11
CD25
PPIA
LOX
GUSB
CD14
p53
PLAT
SERPINA1
TLR4
IL-17A
ATP5
TGF-b3
SMAD2
LMNBE
YWHAZ
Col1A2
U2M
Calnexin
MMP8
PLG
TBP
GREM1
IL17-C
STAT6
CXCR6
FLI-1
BMP7
HSP47
IP08
Calreticulin
BMPRIA (also called alk 3)
AP1
HPRT1
CD4
CD103
MyD88
gp130
TLR
YBX1
Bif-1
Traf2
BCL2
ITGA1
NFKB1
ITGA3
BAFF (B cell activating factor)
SMAD7
POLR2A
TGFBR1
ITGB6
Bak1
TIMP3
ITGB3
Cse2
ETS1
SMAD3
PDGFB
HSP27
MMP14
EGF
LGALS1 (galectin 1)
TNBS1
LTGF
IL-6
CAV1
TGF-b2
MAPK8
IFNG
IL-4
NOD1
Wntl0b
TGF-b1
LOXL2
TIMP2
PLAU
Traf6
phlda1
ITGA2
PPARy
Foxp3
Mannose receptor
TLR3
Col3A1
IL-1B
MCP-3
SP1
ILlalpha
IL-13
IL12A (subunit of IL-35)
BMP2 (Bone morphogenic protein-2)
IL-5
TIMP4
MYC
MMP1
CD68
PIZZ-1
iNOS (nos2)
DCN
ASK1
SERPINE1
MCP1
NOD2
HGF
ENG
Cd11c
MMP9
MMP3
CXCR3
FASLG
LGALS9 (galectin 9)
TNBS2
CCR8
IgG
AutoAB
Scale bar
-1.89
-1.26
-0.63
0.00
0.63
1.26
1.89
Arginase 1
CXCR6
CCR2
ASK1
NLRP1
GUSB
CD4
ID01 Indoleamine 2
SERPINA1
TIMP1
B2M
ITGB8
Bcl2l11
FKBP65
TGFBR2
SMAD2
IL17-C
CD14
CEBPB
CXCL12
IL-6Receptor-alpha
MIP1a
IL-10
IL-17A
FASLG
CCL11
TNF
TLR3
MMP2
IL-13RA2
FN1
ILK
NFKB1
ITGA2
ILlalpha
PGK1
PDGFB
MMP14
LOXL2
ET31
SMAD3
YWHAZ
IP08
HPRT1
SMAD4
MAPK8
TGF-b3
TGFBR1
Col1A1
TGIF1
TGF-b2
GSMReceptor-beta
PTK2/FAK
SMAD6
HMOX1 (heme oxygenase 1)
FC1
BMP4
AP1
Rab-9
Bak1
Traf2
PLAU
SP3
gp130
IL-3
MYC
ITGB1
ITGB5
ITGAV
BMPR1a (also called alk 3)
EDEM1 (PERK)
Beclin-1
YEC1
Bid
TBP
Calreticulin
c-KROX
STAT1
MyD88
STAT-3
TIMP2
CCR5
Bif-1
STAT4
GRP78
GATA4
POLR2A
IL-23
ATP4
Calnexin
Cd11c
HNDBE
Cd103
iNOS (nos2)
AKT1
Stem cell factor
FKBP13
ITGA3
PPIA
IL-33
CD25
CCR4
RPLP2
IRF5
p53
Mapk14 (P38)
Rae
Pcsk9
NOD1
IL-13
LPAR1
Mannose receptor
EGF
TNBS2
CXCL17
CCL20
LGALS9 (galectin 9)
Wntl0b
CXCL1
IL-22
CCR8
MMP9
MCP-3
Cd11b
ENG
PLG
Arginase 2
TLR4
Col3A1
Angiopoeitin 1
DCN
PPARy
TSLP
IL12A (subunit of IL-35)
HGF
BCL2
TLR2
XBP1 total
MCP1
EGR-1
TAOK3
ATP6
Bad
EDN1
CCR3
LOX
IL-5
BMP7
GREM1
IL-2
Angiopoeitin 2
PLAT
BANK1
ITGB3
CXCR4
SERPINE1
LGALS1 (galectin 1)
CAV1
TGF-b1
SNAI1
SMAD7
LTBP1
HSP47
FBN1
Foxp3
IL-15
IFNG
IL-21
MMP13
FLI-1
IL-1B
TNBS1
TIMP3
BAFF (B cell activating factor)
MMP7
U2M
MMP3
BMP2 (Bone morphogenic protein-2)
BMPRII (BMPreceptor 2)
IP10
ITGB6
IL-6
CTGF
Traf6
MMP1
AGT
C1Q-C
MMP8
ITGA1
NLRP3
FIZZ-1
CD8
Col1A2
CD68
ST2/IL1RL1
actaa2
IL-4
STAT6
HSP27
CHOP
SP1
Cse2
PDGFA
NOD2
phlda1
VEGFA
LGALS3 (galectin 3)
JUN
TIMP4
CXCR3
CD44

CHAPTER 5

SUPPLEMENTARY FIGURES

Supplementary Figure 1: Immunoprecipitation of cell surface GRP78 and TF.

Background: Bhattacharjee and colleagues had demonstrated that cell surface GRP78 can modulate TF on the cell surface by direct physical contact (Bhattacharjee, Ahamed et al. 2005). This interaction was shown when TF was overexpressed. Bhattacharjee concluded that an antibody abolishing this interaction lead to increased activation of TF PCA in endothelial cells.

Objectives: To assess TF:GRP78 interaction as means to modulate TF PCA, under normal condition.

Methods: Four T75 flasks containing T24/83 cells were grown to 90% confluence. The immunoprecipitation of cell surface GRP78 and TF on intact T24/83 cells was carried out based on the Abcam immunoprecipitation protocol (Abcam, Cambridge, MA, USA) using anti-GRP78 antibodies (Cat#610979, BD Transduction), mouse IgG (negative control, Cat#sc-2078, Santa Cruz Biotechnology), anti-human TF antibodies (Cat#4501, American Diagnostica), or rabbit IgG (negative control, cat#sc-2090, Santa Cruz Biotechnology). Protein lysates containing cell surface proteins were solubilized in SDS-PAGE sample buffer, separated in 7% SDS-PAGE gels, transferred to nitrocellulose membranes and immunoblotted for GRP78 (Cat#610979, BD Transduction) or TF (Cat#4501, American Diagnostica).

Results and Discussion: Results of pull-down experiments using anti-GRP78 antibody indicate that TF was immunoprecipitated from the surface of T24/83 cells. Reciprocal experiments we were unable to immunoprecipitate cell surface GRP78 with an anti-TF antibody. These observations suggest that the interaction

between cell surface GRP78 and TF is weak or that an antibody-mediated conformational change occurs in cell surface GRP78 or TF that alters binding.

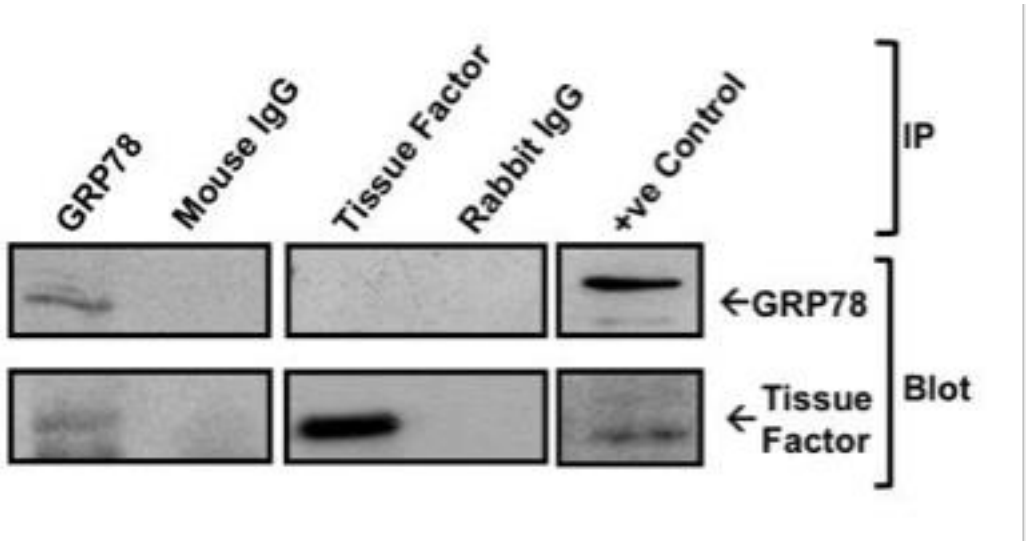

Supplementary Figure 2: Effect of PCa versus healthy controls-purified anti-GRP78 autoantibodies.

Background: Dr. Gonzalez-Grownow and colleagues have determined that anti-GRP78 autoantibodies purified from patients diagnosed with prostate cancer are highly glycosylated, compared to control healthy individuals (Gonzalez-Gronow, Cuchacovich et al. 2006).

Objectives: We and others have demonstrated that patients diagnosed with PCa have higher titres of anti-GRP78 autoantibodies (~60μg/mL), compared to healthy controls (~5-7μg/mL). The objective of this experiment was to examine the activity of anti-GRP78 autoantibodies purified from healthy controls at pathological doses (60μg/mL).

Methods: DU145 cells were seeded in 96-well plate. Upon 90% confluences, cells were left untreated, or treated with thapsigargin (positive control, 5μM), PCa purified anti-GRP78 autoantibodies (AutoAb High Gly, 60μg/mL), or healthy individuals purified autoantibodies (AutoAB Low Gly, 60μg/mL). TF PCA was measured using the continuous tissue factor assay.

Results and Discussion: Treating cells with the positive control, thapsigargin (5 μM), or anti-GRP78 autoantibodies (60μg/mL) derived from PC patients were shown to significantly increase TF PCA. Conversely, treating cells with anti-GRP78 autoantibodies (60μg/mL) derived healthy controls did not cause a TF PCA response. In fact TF PCA was significantly decreased in comparison to non-treated cells (NT). This indicates that glycosylation of anti-GRP78 autoantibody is required for its function as an activator of TF PCA. These results suggest that without hyper-

glycoylations, high concentrations of anti-GRP78 autoantibodies are not sufficient to to activate TF PCA. It will be interesting to investigate how tumour cells communication with the immune system to dictate how these autoantibodies are manufactured.

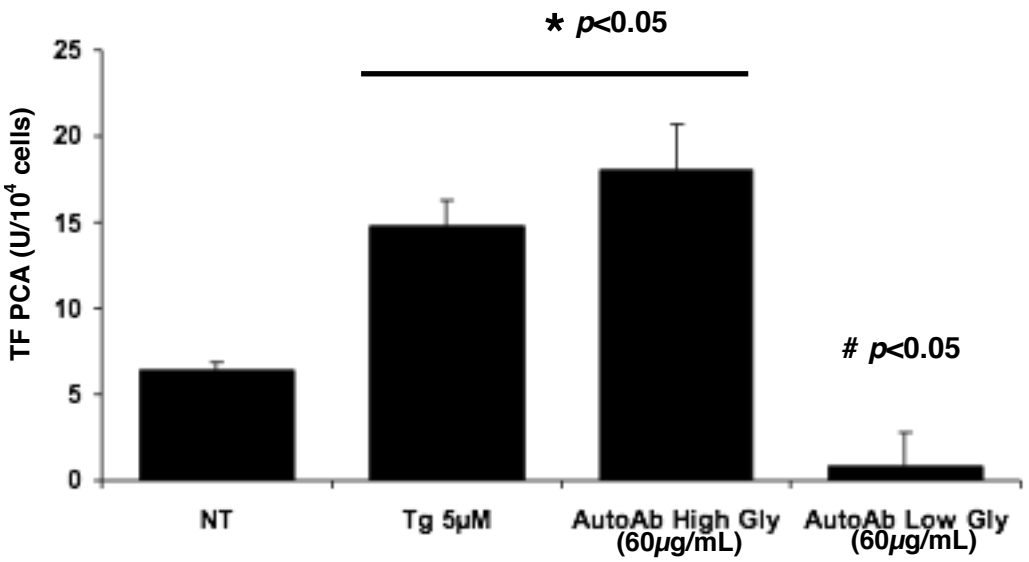

Supplementary Figure 3: Anti-GRP78 autoantibodies increase microvesicle production.**

This work was done in collaboration with Dr. K. Al-Nedawi.

Background: Anti-GRP78 autoantinodies were shown to activate TF on the cell surface of PC cells through a mechanism involving Ca^{2+} release from the ER to the cytoplasm (Al-Hashimi et. al. 2010). It is well-documented that an increase in cytosolic Ca^{2+} can trigger tumor-associated microvesicles release (Yu, Harris et. al. 2011). It is well-documented that microvesicles are considered a transport vehicle that can carry cargo proteins and other genetic information from one cell to another. The surface receptors of microvesicles allow their targeting and capture by recipient cells, this allows them to incorporate into the proteic, lipidic, and even genetic messages carried by the vesicles, resulting in modifications of their physiological state of the target cell (Yáñez-Mó M et. al. 2015, Buzas EI et. al. 2014et al., van der Pol E et. al. 2012).

Objectives: To elucidate other functions of anti-GRP78 autoantibodies, we investigated whetherthese autoantibodies can facilitate modification of cellular functions by increasing microvesicle production from tumour cells.

Method: DU145 cells were cultured in minimum essential medium (MEM; Gibco) supplemented with 10 % (v/v) fetal bovine serum and antibiotics (50 U/mL penicillin, 50 mg/mL streptomycin). Cells were seeded into 100 mm culture dishes at 50-60 % confluency. Twenty-four hours prior to treatment with auto-antibody preparation, cells were incubated in serum-free MEM. Cells were then treated with

60 mg/mL auto-antibody or PBS for 24 h before conditioned medium was harvested for microvesicle isolation.

Conditioned medium was harvested from cells and subjected to two successive centrifugations at 300 x *g* and 12,000 x *g* for 10 min and 20 min, respectively to remove dead cells and cellular debris. Microvesicles were isolated from the pre-cleared conditioned medium by centrifugation at 100,000 x g for 2 h using a Beckman Type 70.1 Ti rotor. The microvesicle pellet was resuspended in phosphate-buffered saline and protein content was determined using the BioRad Detergent-Compatible (DC) Protein Assay after lysing microvesicles with 2 % (w/v) sodium dodecylsulphate.

Whole cell extracts or microvesicles were fractionated by SDS-PAGE on a 10% acrylamide gel and transferred to a nitrocellulose membrane. After blocking with 5 % (w/v) skim milk in TBS-T for 60 min at room temperature, the membrane was probed with primary antibodies against tissue factor (American Diagnostica), GRP78 (BD Transduction), CD63 (BioLegend), or b-actin (Cell Signaling) overnight at 4°C. Membranes were was four times with TBS-T (1x15 min and 3x5 min) and probed with appropriate HRP-linked secondary antibody (Cell Signaling) for 60 min at room temperature. Blots were washed four times with TBS-T (1x15 min and 3x5 min) and developed using the ECL system (Amersham Biosciences).

Results and Discussion: Microvesicles were shown to contribute to improved cancer survival, their mechanism of action included transfer of genetic material and other cargo proteins that target specific cells (Yu et. al. 2011). In fact, Di Vizio and

colleagues had shown that microvesilces isolated from the prostate cancer cell line, DU145, are capable of stimulating the proliferation and migration of tumourcells in association with AKT pathway signalling (Di Vizio et. al. 2009). Treatment of anti-GRP78 autoantibodies on wild type DU145 showed increased overall shedding of microvesicles, compared to PBS control treated cells. Western blot analysis had shown that anti-GRP78 autoantibodies increase overall GRP78 expression in cells, and TF expression in microvesicles. This data indicates that anti-GRP78 autoantibodies drive microvesicls production with the goal of improving survival. An increase in TF-enriched microviscles production can hint to the possibility of an increase in thrombotic complications, or improved proliferation of tumour cells. Future directions include identifying differences in genetic and protein cargo of microvesicles isolated from autoantibodies or PBS treated cells.

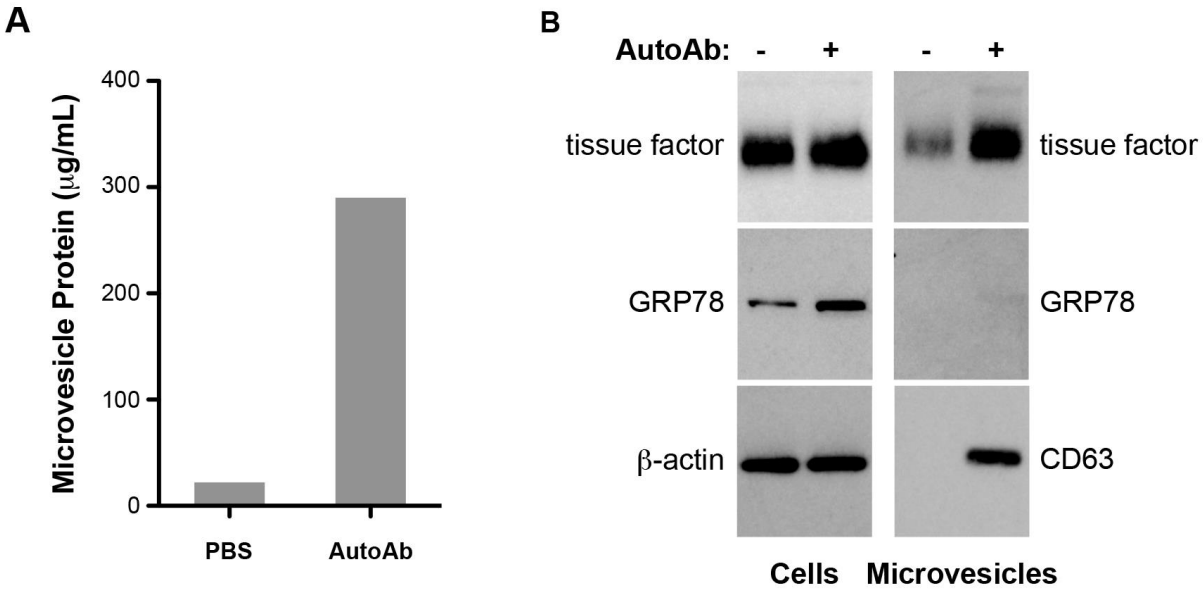
A
Microvesicle Protein (μg/mL)
400
300
200
100
0
PBS
AutoAb
B
AutoAb: - + - +
tissue factor
tissue factor
GRP78
GRP78
β-actin
CD63
Cells
Microvesicles

CHAPTER 6

GLOBAL DISCUSSION

PC is a highly heterogeneous disease, often coupled with a lengthy and complex developmental stage. Diagnosis of PC can be performed using a combination of blood tests to examine PSA levels, and a biopsy to confirm disease manifestation and its pathological stage (Siegel, Naishadham et al. 2013). The interplay of thrombotic factors and disease progression emerges as a recurring and central theme in prostate cancer. The identification of cell surface GRP78 as cellular receptor that can modulate proliferation and its potential interaction with TF has suggested a new method of regulating TF activity (Bhattacharjee, Ahamed et al. 2005). Abolishing this TF:GRP78 interaction using antibodies against GRP78 could lead to increased TF PCA(Bhattacharjee, Ahamed et al. 2005). Further, previous studies had demonstrated the expression of GRP78 on the cell surface of PC cells and was associated with production of antibodies that bind to cell surface GRP78 (Arap et al., 2004; Mintz, Kim et al. 2003). This suggests a potential mechanism where anti-GRP78 autoantibodies could be linked to modulation of TF activity (Mintz et al. 2003). Increased TF expression and/or activity is a newly discovered function that drives PC disease progression (Milsom and Rak, Milsom et al. 2006).

In the first part of my PhD research project, I elucidated the mechanism by which anti-GRP78 autoantibodies modulate TF expression and PCA. Although both TF and GRP78 are expressed on the cell surface, there was no evidence of a stable interaction between human recombinant GRP78 and TF (Al-Hashimi, Caldwell et al. 2010); immunoprecipitation experiments demonstrated similar conclusions

(Supplemental Figure 1). This suggested the presence and activation of an intracellular pathway leading to increased TF PCA. Previously, we had demonstrated that agents that deplete ER calcium stores, namely thapsigargin, can increase TF PCA (Pozza and Austin 2005). Consistent with these findings, anti-GRP78 autoantibodies elicited a dose-dependent increase in cytoplasmic calcium concentration and enhanced TF PCA (Al-Hashimi, Caldwell et al. 2010). It was previously shown that an increase in cytoplasmic calcium efflux from the ER results in the inactivation of the flippase membrane enzyme. This leads to exposure of the phosphotidyl serine molecule on the cell surface, and enhances TF de-encryption and, thus increases PCA. We have demonstrated that stabilizing cytosolic calcium concentration using BAPTA, or blocking the expression of phosphotidyl serine molecules using annexin V, can reduce the effect of anti-GRP78 autoantibodies on TF PCA. This novel observation where TF activity on cancer cells is modulated by agents produced by the immune system suggests the immune system can modulate thrombosis, indirectly, and potentially contribute to PC progression. We investigated the effect of anti-GRP78 autoantibodies on cellular fucntions to identify mechanisms that contribute to disease progression.

Our findings suggested that these autoantibodies could have a more pertinent role in terms of altering tumour biology. Upon examining the effects of these autoantibodies on cells *in vitro*, we have identified them as inducers of ER stress leading to activation of the UPR pathway (Chapter 4). This is similar to the established ER stress inducer, thapsigargin, which activates the UPR by depleting

ER calcium. This is in line with our hypothesis where anti-GRP78 autoantibodies are thought to contribute to ER stress considering their ability to deplete ER calcium stores, similar to thapsigargin (Chapter 3). The UPR augments the cell's ER protein folding capacity in the face of physiological insults, such as when nutrients are limited in the cell environment (Tameire, Verginadis et al. 2015), protecting cells against cell death. Our findings suggest that at the cellular level, anti-GRP78 autoantibodies may help cells handle physiological stresses that can lead to improved survival.

Activation of the UPR can augment the cell's ability to handle proteotoxic stress. However, this very pathway that leads to activation of the UPR can also result in TF activation. The connection between increased TF activity and enhanced tumorigenesis suggests a new function for anti-GRP78 autoantibodies as mediators of tumour growth. To test this, we utilized an immunodeficient animal model, the NOD/SCID mouse strain. This model was selected given that human TF can bind to murine Factor VIIa with high affinity, an essential step for the activation of the coagulation cascade (Peterseon et. al. 2005). Here, we demonstrated that DU145 cell-derived tumours receiving anti-GRP78 autoantibody injections demonstrated accelerated tumour growth rate, compared to control cohorts that received human IgG or PBS injections. Further, tumour tissue NanoString gene array analysis indicated that the UPR was up-regulated in tumours treated with anti-GRP78 autoantibodies, consistent with *in vitro* data. This observation is likely due to the ability of anti-GRP78 autoantibodies to elicit ER calcium leakage into the cytosol,

as reported previously (Al-Hashimi et al. 2010). In this setting, UPR activation would be beneficial for tumour cells, as it is designed to enable cells to manage both oxidative and proteotoxic stress conditions. Rutkowski and colleagues demonstrated a potential mechanism where mild activation of the UPR leads to cellular adaption to environmental stresses by means of increased chaperone expression (Rutkowski, Arnold et al. 2006). Such stresses include newly implanted cancer cells that did not have access to consistent blood supply, and thus have limited access to nutrients in their microenvironment. In addition to its role in augmenting survival, UPR activation was linked to chemoresistance leading to therapeutic failure in response to chemotherapy (Gifford, Huang et al. 2016). Results from similar experiments that were carried out using DU145 TF knock-down cells suggested that TF is required for the effect of anti-GRP78 on accelerated tumour growth.

Identifying the contribution of anti-GRP78 autoantibodies to increased cell surface TF PCA and enhanced tumour growth allowed us to investigate means of reducing or eliminating their effect on cells. Immunodepletion of anti-GRP78 autoantibodies from patients' serum, or neutralizing the antibodies with human recombinant GRP78 were shown to be viable approaches to alleviate their effects on increased TF PCA. However, the clinical application of such approaches has many challenges; injecting a foreign peptide into patients can signal to the immune system to mount an unwanted response. Further, dialyzing anti-GRP78 autoantibodies out of patients blood, for example using a dialysis cartridge, may not be effective

considering the rate of autoantibody generation is not known. Identification of the binding site (Leu_{98}-Leu_{115}) where anti-GRP78 autoantibodies bind to cell surface GRP78 allowed us to investigate agents that would have the capability of competing for this binding site. The HSP70 family of proteins, to which GRP78 belongs, were shown to contain a conserved heparin binding site at the N-terminal domain, Leu_{98}-Arg_{101} (Hansen, O'Leary et al. 1995). Not only is heparin a clinically approved drug, but studies by Mousa and colleagues have suggested that heparin and the LMWH, enoxaparin, function as anti-cancer agents; increased tumor necrosis and enhanced gemcitabine response in the mouse cancer models. It is worth noting that some studies suggested that the anti-cancer effects of heparin can take place independent of its anti-coagulant properties (Mousa, Linhardt et al. 2006, Mousa and Petersen 2009). . In this study, we were able to show that heparin and enoxaparin can interfere with binding of anti-GRP78 autoantibodies to cell surface GRP78, which subsequently eliminates the antibody effect on increased TF PCA. Furthermore, we demonstrated the ability of enoxaparin to eliminate the effect of anti-GRP78 antibodies on increased tumour growth in NOD/SCID mice. Our data suggests a new mechanism for enoxaparin as an anti-cancer agent, by preventing the binding of anti-GRP78 autoantibodies. Another interpretation of this data suggests that heparin can act as an anti-coagulant upstream of TF. Under normal conditions, heparin functions by inactivating thrombin and activated factor X (factor Xa) through an antithrombin-dependent mechanism (Hirsh, Anand et al. 2001). However, our data suggests that heparin may have more of a localized role in

terms of indirectly blocking TF PCA and coagulation through its ability to block the autoantibody-cell surface GRP78 interaction.

In conclusion, our data suggests that titres of anti-GRP78 autoantibodies increase with PSA, which points to their contribution of increased risk of thrombotic complications, in addition to enhancing tumour growth. Taken together, expression of cell surface GRP78 can drive the production of anti-GRP78 autoantibodies. Engagement of anti-GRP78 autoantibodies to cancer cells can induce the UPR which can lead to increased GRP78 expression. It is possible that increase total GRP78 expression coincides with increased cell surface expression of the protein. Thus, targeting anti-GRP78 antibodies may provide a method to decrease the rate of tumour growth.

CHAPTER 7

CLINICAL IMPLICATION

The heterogeneity of PC, combined with potential shortcomings in current prognostic determinants is a challenge to physicians who are unable to discriminate between metastatic and non-metastatic forms of the disease. A clear understanding of the molecular basis of PC has important clinical implications including the identification of molecular prognostic factors that allow the prediction of the course and the outcome of PC. This study unveils a new mechanism by which the patients' immune response initiates production of anti-GRP78 autoantibodies. These antibodies were shown to accelerate tumour growth and correlate with stages of disease. In addition, the finding that heparin and LMWH molecules can interfere with the binding of anti-GRP78 autoantibodies to cell surface GRP78 and delay tumour growth emphasizes that these molecules may have a positive impact on cancer management. While heparin and LMWH are clinically used to prevent and treat thrombotic complications associated with cancer, however, researchers had made the observation that these anti-coagulant molecules can control cancer growth (Mousa and Petersen 2009). This study is first to demonstrate a mechanism by which LMWH limits increased cancer growth mediated by anti-GRP78 autoantibodies. This highlights the need to investigate the impact of heparin and LMWH on PC progression in a patient population with confirmed high titres of anti-GRP78 autoantibodies.

Another important clinical implication of this project is the potential for anti-GRP78 autoantibodies to predict PC grade. In Chapter 4 of this report, I have demonstrated a correlation between increased GRP78 expression and PC grade.

Further, anti-GRP78 autoantibodies were correlated with serum PSA concentrations. This suggests that anti-GRP78 autoantibodies can be examined as a potential new diagnostic test to determine PC grade. Measuring serum anti-GRP78 autoantibodies to determine PC grade would be a major advancement in the diagnostic field of PC. Moreover, a blood test approach has the potential to limit the number of false negatives compared to a needle biopsy. A false negative from a needle biopsy can occur when the biopsy needle misses the malignant area in the prostate. Our data sets the stage to investigate anti-GRP78 autoantibody as a novel biomarker which can aid in appropriate diagnosis of PC.

CHAPTER 8

ANALYSIS, FUTURE DIRECTION, AND LIMITATIONS

In Chapter 3, we examined the effect of anti-GRP78 autoantibodies on promoting TF PCA. We hypothesized that cell surface GRP78 is likely the antigen that leads to the production of anti-GRP78 autoantibodies. Under normal physiological conditions, GRP78 molecules are retained in the ER due to its KDEL retention sequence (Corbett, Oikawa et al. 1999; Michalak et al., 1999). This raises the question of how GRP78 can escape ER retention and translocate to the cell surface. Examining different pathophysiological mechanisms in disorders such as cancer revealed that a variety of intrinsic or extrinsic cellular stresses evoke perturbations that lead to ER stress and activation of the UPR pathway (Tameire, Verginadis et al. 2015). Activation of the UPR leads to increased expression of ER chaperones, and it is thought that the KDEL receptors within the ER become overwhelmed and allow some of the proteins to escape the ER retention system. In fact, Wiersma and colleagues have demonstrated that GRP78, protein disulfide isomerase (PDI), and calreiculin are expressed on the cell surface under conditions of ER stress (Wiersma, Michalak et al. 2015). Another mechanism that can contribute to the translocation of GRP78 from the ER to the cell surface is via its interaction with the Dnaj3 protein, the murine tumour cell Dnaj-like protein 1 (MTJ-1). It has been reported that MTJ-1 can assist protein translocation by blocking access to the KDEL receptor on GRP78 (Gonzalez-Gronow et al., 2009; Shen and Hendershot 2005). However, further research is required to properly elucidate this mechanism. It is possible that overwhelmed KDEL receptors on the ER, combined with blocked

KDEL receptors on GRP78, leads to the translocation of GRP78 from the ER to the cell surface.

Another interesting observation that Dr. Gonzalez-Gronow and collegues has made was the presence of anti-GRP78 autoantibodies in healthy individuals (~5 μg/mL)(Gonzalez-Gronow, Cuchacovich et al. 2006). Dr. Gonzalez-Gronow determined that anti-GRP78 autoantibodies purified from cancer patients are highly-glycosylated, compared with autoantibodies isolated from control individuals (Gonzalez-Gronow et. al. 2006). Thus, we investigated the potential of the low-glycosylated and highly-glycosylated autoantibodies, at 60 μg/mL, to activate TF PCA (Supplemental Figure 2). Our data indicate that the low-glycosylated autoantibodies do not activate TF PCA, while the highly-glycosylated autoantibodies do increase TF activity using the 60 μg/mL concentration. Our data provides evidence that the glycosylation of anti-GRP78 autoantibodies mediates its pathological function. Selim and colleagues had determined that anti-GRP78 purified from melanoma patients show that Fab and Fc regions increase in their glycosylation (Selim, Burchette et al. 2011); one out of two Fab were shown to be glycosylated (55 to 65 kDa) and the Fc fragment was shown to be aberrantly glycosylated (27 to 33 kDa). This suggests that anti-GRP78 IgG is asymmetrically glycosylated at the Fab region and aberrantly glycosylated at the Fc. In terms of functionality, the asymmetrical glycosylation was shown to induce induce phosphorylation of Akt (Selim, Burchette et al. 2011).

In addition to their role as activators of TF activity, we have evidence that anti-GRP78 can modulated production of microcvesicles. Recent studies suggest that microvesicles can play a significant role in horizontal communication between tumour cells and other parts of the body, such as the immune system (Muralidharan-Chari, Clancy et al. 2010). Shedding of microvesicles is a highly regulated process that occurs in a spectrum of cell types and, including tumour cells. Microvesicles have been widely detected in various biological fluids, including peripheral blood, and facilitate the horizontal transfer of bioactive molecules, such as proteins, RNAs, and microRNAs. They are now thought to have vital roles in tumour invasion and metastasis, inflammation, and coagulation (Cossette et al., 2010; Milsom, Yu et al. 2008). In this investigation, we demonstrated that anti-GRP78 autoantibodies increase shedding of microvesicles in DU145 cells (Supplemental Figure 3). Immunoblot analysis from these experiments indicate that TF and GRP78 are present in these vesicles. Increased shedding of microvesicles (loaded with TF and GRP78) can act to help sensitize the immune system and aid in the production of anti-GRP78 autoantibodies. TF located on microvesicles can have a role in angiogenesis progression at the site of the tumour and other site of the body.

The pathological role of anti-GRP78 autoantibodies in caner highlights the need to identify new means to reverse their effects on improved cancer progression. Examination of means to neutralize anti-GRP78 autoantibodies revealed that heparin pre-treatment could prevent the binding of anti-GRP78 autoantibodies to

TF. The HSP70 family of proteins were shown to have a heparin binding site at the N-terminal domain by the primary amino acid sequence, Leu_{98}-$The_{102,}$ (Hansen, O'Leary et al. 1995). This interaction with heparin is sufficient to block the binding site of cell surface GRP78, Leu_{98}-Leu_{115} (Gonzalez-Gronow et al. 2006). Previous studies had suggested that heparin can function as an anti-cancer agent, however, the underlying mechanism has not been characterized (Mousa, Linhardt et al. 2006, Mousa and Petersen 2009, Vlodavsky, Ilan et al. 2007). Our data (chapter 4) indicate that heparin diminished the effects of anti-GRP78 autoantibodies on increased tumour progression and TF activity. Furthermore, these findings provide a novel mechanism by which heparin reduces local anti-coagulant effects independent of its ability to inactivate thrombin and Xa via antithrombin. The use of heparin in the clinic still pose a risk of bleeding in patients (Cossette, Pelletier et al. 2010). Thus, we plan on examining modified heparin molecules (with no or modified anti-coagulant activity) as inhibitors of binding of anti-GRP78 autoantibodies to cell surface GRP78. This can be tested in a small pilot clinical study to examine the effects of these molecules on accelerated tumour progression, mediated by anti-GRP78 autoantibodies.

Finally, our clinical data have demonstrated a correlation between anti-GRP78 autoantibodies and PSA in a cohort of patients diagnosed with PC. To investigate whether anti-GRP78 autoantibodies can be used as a marker of PC progression, a follow-up study could be established where changes in anti-GRP78 autoantibody concentration are examined in a longitudinal study. Another clinical trial of

importance would be to investigate anti-GRP78 autoantibody titres and glycosylation status in a population with recurring prostate cancer. Anti-GRP78 autoantibody titres and glycosylation status may not only alert to the presence of PC but they may also hint at the stage of cancer progression (i.e. early, intermediate or advanced disease). If true, this could help physicians minimize the risk of over- or under-treating patients. One final investigation pertains to the fact that anti-GRP78 autoantibodies exist in other cancer types, including melanoma and ovarian cancer (Gonzalez-Gronow, Hershfield et al. 2004). This indicates that this mechanism can be applicable to other malignancies where a similar autoantibody-mediated mechanism is being used to promote disease progression. It will be informative to investigate whether anti-GRP78 autoantibodies from different cancers can activate TF and increase tumour growth.

CHAPTER 9

CONCLUSION

We have utilized a diverse and multi-faceted approach in order to study the impact of anti-GRP78 autoantibodies in PC growth and proliferation. We elucidated the pathway by which anti-GRP78 autoantibodies activate TF PCA, and identified their contribution and correlation to PC progression. We have obtained a reliable mechanism of how anti-GRP78 autoantibodies modulate PC progression, and potentially contribute to cancer-related thrombosis. We have demonstrated the significance of these autoantibodies *in vitro*, *in vivo*, and in a clinical setting of PC diagnosis. Thus, anti-GRP78 autoantibodies can be viewed as a potential novel target for future treatment and prognosis strategies. Further research in this area has the potential to improve the diagnosis of PC and may enable physicians to administer more appropriate and efficacious treatments. Future directions from this investigation have the potential to contribute to our understanding of cross-talk between the tumour cell and other systems in the body, moreover, this project have the potential to contribute to the establishment of a novel and accurate diagnostic technique for PC grade.

CHAPTER 10

REFERENCES

Abdulkadir, S. A., G. F. Carvalhal, Z. Kaleem, W. Kisiel, P. A. Humphrey, W. J. Catalona and J. Milbrandt (2000). "Tissue factor expression and angiogenesis in human prostate carcinoma." Hum Pathol 31(4): 443-447.

Abe, K., Shoji, M., Chen, J., Bierhaus, A., Danave, I., Micko, C., Casper, K., Dillehay, D. L., Nawroth, P. P., Rickles, F. R. (1999). Regulation of vascular endothelial growth factor production and angiogenesis by the cytoplasmic tail of tissue factor. Proc Natl Acad Sci U S A. 96: 8663-8668.

Ahamed, J., Ruf, W. (2004). Protease-activated receptor 2-dependent phosphorylation of the tissue factor cytoplasmic domain. J Biol Chem. 279: 23038-23044.

Ahamed, J., Versteeg, H. H., Kerver, M., Chen, V. M., Mueller, B. M., Hogg, P. J., Ruf, W. (2006). Disulfide isomerization switches tissue factor from coagulation to cell signalling. PNAS. 103(38): 13932-13937.

Alberts, B., Bray, D., Lewis, J., Raff, M., Roberts, K., Watson, J. D. Molecular Biology of the Cell, 3rd edition. New York: Garland Publishing, Inc. 1994. 620-621.

Albrecht, S., Kotzsch, M., Siegert, G., Luther, T., Grossman, H., Grosser, M., Muller, M. (1996). Detection of circulating tissue factor and factor VII in a normal population. Thromb Haemost. 75: 772-777.

Albrektsen, T., Sorensen, B. B., Hjorto, G. M., Fleckner, J., Rao, L. V., Petersen, L. C. (2007). Transcriptional program induced by factor VIIa–tissue factor, PAR1 and PAR2 in MDA-MB-231 cells. J Thromb Haemost. 5: 1588-1597.

Al-Hashimi, A. A., J. Caldwell, M. Gonzalez-Gronow, S. V. Pizzo, D. Aboumrad, L. Pozza, H. Al-Bayati, J. I. Weitz, A. Stafford, H. Chan, A. Kapoor, D. W. Jacobsen, J. G. Dickhout and R. C. Austin (2010). "Binding of anti-GRP78 autoantibodies to cell surface GRP78 increases tissue factor procoagulant activity via the release of calcium from endoplasmic reticulum stores." J Biol Chem 285(37): 28912-28923.

Amarzguioui, M., Peng, Q., Wiiger, M. T., Vasovic, V., Babaie, E., Holen, T., Nesland, J. M., Prydz, H. (2006). Ex vivo and in vivo delivery of anti-tissue factor short interfering RNA inhibits mouse pulmonary metastasis of B16 melanoma cells. Clin Cancer Res. 12: 4055-4061.

Aoki, M., Tamatani, M., Taniguchi, M., Yamaguchi, A., Bando, Y., Kasai, K., Miyoshi, Y., Nakamura, Y., Vitek, M. P., Tohyama, M., Tanaka, H., Sugimoto, H. (2001). Hypothermic treatment restores glucose regulated protein 78 (GRP78) expression in ischemic brain. Mol. Brain. Res. 95: 117-128.

Arap, M. A., Lahdenranta, J., Mintz, P. J., Hajitou, A., Sarkis, A. S., Arap, W., et al. (2004). Cell surface expression of the stress response chaperone GRP78 enables tumourtargeting by circulating ligands. Cancer Cell. 6: 275-284.

Bach, R. R. (2006). Tissue factor encryption. Arterioscler. Thromb. Vasc. Biol. 26: 456-461.

Bach, R. R., & Moldow, C. F. (1997). Mechanism of tissue factor activation on HL-60 cells. Blood. 89(9): 3270-3276.

Bach, R., Konigsberg, W. H., Nemerson, Y. (1988). Human tissue factor contains thioester-linked palmitate and stearate on the cytoplasmic half-cystine. Biochemistry. 27: 4227- 4231.

Bach, R., Rifkin, D. B. (1990). Expression of tissue factor procoagulant activity: regulation by cytosolic calcium. Proc Natl Acad Sci US., 87: 6995-6999.

Bakanay, S., Key, N. S., Bach, R. R. (2001). Both capacitative and non-capacitative Ca2+ entry are required for disruption of phosphatidylserine asymmetry and de-ecryption of tissue factor procoagulant activity on the HL-60 cell surface (Abstract). Blood. 501(98).

Banfi, C., Camera, M., Giandomenico, G., Toschi, V., Arpaia, M., Mussoni, L., Tremoli, E., Colli, S. (2003). Vascular thrombogenicity induced by progressive LDL oxidation: protection by antioxidants. Thromb. Haemost. 89: 544-553.

Banner, D. W., D'Arcy, A., Chene, C., Winkler, F. K., Guha, A., Konigsberg, W. H., Nemerson, Y., Kirchhofer, D. (1996) The crystal structure of the complex of blood coagulation factor VIIa with soluble tissue factor. Nature. 380: 41-46.

Barrowclife, T. W., Fabregas, P., Jardi, M., Cancelas, J., Rabaneda, M., Felez, J. (2002). Procoagulant activity of T lymphoblastoid cells due to exposure of negatively charged phospholipid. Thromb. Haemost. 87: 442-449.

Belting, M., Dorrell, M. I., Sandgren, S., Aguilar, E., Ahamed, J., Dorfleutner, A., Carmeliet, P., Mueller, B. M., Friedlander, M., Ruf, W. (2004). Regulation of angiogenesis by tissue factor cytoplasmic domain signalling. Nat Med. 10: 502-509.

Berckmans, R. J., Nieuwland, R., Boing, A. N., Romijn, F. P., Hack, C. E., Sturk, A. (2001). Cell-derived microparticles circulate in healthy humans and support low grade thrombin generation. Thromb Haemost. 85: 639-646.

Berg, J. M., Tymoczko, J. L., & Stryer, L. (Eds.). (2002). Biochemistry (5th ed.)W.H. Freeman and Company.

Bhattacharjee, G., Ahamed, J., Pedersen, B., El-Sheikh, A., Mackman, N., Ruf, W., et al. (2005). Regulation of tissue factor-mediated initiation of the coagulation cascade by cell surface GRP78. Arteriosclerosis, Thrombosis and Vascular Biology. (1737), 1743.

Bjørklid, E., Storm, E. (1977). Purification and some properties of the protein component of tissue thromboplastin from human brain. Biochem J. 165: 89-96.

Bläss, S., Union, A., Raymackers, J., Schumann, F., Ungethüm, U., Müller-Steinbach, S., et al. (2001). The stress protein BiP is overexpressed and is a major B and T cell target in rheumatoid arthritis. Arthritis & Rheumatism. 44(4): 761-771.

Blond-Elgundi, S., Cwirla, S. E., Dower, W. J., Lipshutz, R. J., Sprang, S. R., Sambrook, J. F., Gething, M. J. (1993). Affinity panning of a library of peptides displayed on bacteriophages reveals the binding specificity of BiP. Cell. 75: 717-728.

Bluff, J. E., Brown, N. J., Reed, M. W. R., Staton, C. A. (2008). Tissue factor, angiogenesis and tumour progression. Breast Cancer Research. 10: 204.

Bluff, J. E., Mangera, A., Brown, N. J., Reed, M. W. R., Staton, C. A. (2006). Tissue factor and vascular endothelial growth factor in breast cancer [abstract]. Angiogenesis. 9: P31.

Bochkov, V. N., Mechtcheriakova, D., Lucerna, M., Huber, J., Malli, R., Graier, W., Hofer, E., Binder, B. R., Leitinger, N. (2002). Oxidized phospholipids stimulated TF expression in human endothelial cells via activation of ERK/EGR-1 and Ca2+/NFAT. Blood. 99: 199-206.

Bogdanov, V. Y., Balasubramanian, V., Hathcock, J., Vele, O., Lieb, M., Nemerson, Y. (2003). Alternatively spliced human tissue factor: a circulating, soluble, thrombogenic protein. Nat Med. 9: 458-462.

Booden, M. A., Eckert, L. B., Der, C. J., Trejo, J. (1999). Persistent signalling by dysregulated thrombin receptor trafficking promotes breast carcinoma cell invasion. Mol Cell Biol. 24: 1990-1999.

Breider, M. A., & Yang, Z. (1994). Tissue factor expression in bovine endothelial cells induced by pasteurella haemolytica lipopolysaccharide and interleukin-1. Vet. Pathol. 1: 55-60.

Bromberg, M. E., Konigsberg, W. H., Madison, J. F., Pavashe, A., Garen, A. (1995). Tissue factor promotes melanoma metastasis by a pathway independent of blood coagulation. Proc Natl Acad Sci USA. 92: 8205-8209.

Bugge, T. H., Xiao, Q., Kombrinck, K. W., Flick, M. J., Holmback, K., Danton, M. S., Colbert, M. C., Witte, D., P., Fujikava, K., Davie, E. W., Degen, J. L. (1996). Fatal embryonic bleeding events in mice lacking tissue factor, the cell-associated initiator of blood coagulation. Proc Natl Acad Sci USA. 93: 6258-6263.

Cabre, A., Girona, J., Vallve, J. C., Masana, L. (2004). Aldehydes mediate tissue factor induction: A possible mechanism linking lipid peroxidation to thrombotic events. J. Cell. Physiol. 198: 230-236.

Callander, N. S., N. Varki and L. V. Rao (1992). "Immunohistochemical identification of tissue factor in solid tumors." Cancer 70(5): 1194-1201.

Camerer, E., Rottingen, J. A., Gjernes, E., Larsen, K., Skartlien, A. H., Iversen, J. G., Prydz, H. (1999). Coagulation factors VIIa and Xa induce cell signalling leading to up-regulation of the egr-1 gene. J Biol Chem. 274: 32225-32233.

Carlsson, S. and A. Vickers (2015). "Spotlight on prostate cancer: the latest evidence and current controversies." BMC Med 13: 60.

Carmeliet, P., Mackman, N., Moons, L., Luther, T., Gressens, P., Van Vlaenderen, I., Demunck, H., Kasper, M., Breier, G., Evrard, P., Muller, M., Risau, W., Edgington, T., Collen, D. (1996). Role of tissue factor in embryonic blood vessel development. Nature. 383: 73-75.

Carson, S. D. (1996). Manifestation of cryptic fibroblast tissue factor occurs at detergent contractions which dissolve the plasma membrane. Blood Coag. Fibrinl. 7: 303-313.

Carson, S. D., Bromberg, M. E. (2000). Tissue factor encryption/de-ecryption is not altered in the absence of the cytoplasmic domain. Thromb. Haemost. 84: 657-663.

Carson, S. D., Perry, G. A., & Pirruccello, S. J. (1994). Fibroblast tissue factor: Calcium and ionophore induce shape changes, release of membrane vesicles, and

redistribution of tissue factor antigen in addition to increased procoagulant activity. Blood. 84: 526-534.

Carvalhal, G. F., S. N. Daudi, D. Kan, D. Mondo, K. A. Roehl, S. Loeb and W. J. Catalona (2010). "Correlation between serum prostate-specific antigen and cancer volume in prostate glands of different sizes." Urology 76(5): 1072-1076.

Chen, V. M., Ahamed, J., Versteeg, H. H., Berndt, M. C., Ruf, W., Hogg, P. J. (2006). Evidence for activation of tissue factor by allosteric disulfide bond. Biochemistry. 45: 12020-12028.

Cheng, C. Y., Grima, J., & Stahler, M. S. (1990). Sertoli cell synthesizes and secretes a protease inhibitor, alpha2-macroglobulin. Biochemistry. 4: 1063-1068.

Chevalier, M., Rhee, H., Elguindi, E. C., & Blond, S. Y. (2000). Interaction of murine BiP/GRP78 with the DnaJ homologue MTJ1. The Journal of Biological Chemistry. 275: 19620.

Chung, K. T., Shen, Y., Hendershot, L. M. (2002). BAP, a mammalian BiP-associated protein, is a nucleotide exchange factor that regulates the ATPase activity of BiP. J. Biol. Chem. 277: 47557-47563.

Consonni, R., & Bertina, R. M. (1995). Antigen and functional expression of tissue factor in endotoxin stimulated U937 cells: Regulation of activity by calcium ionophore A23187. Thromb Haemost. 74: 904-909.

Conway, E. M., Bach, R., Rosenberg, R. D., & Konigsberg, W. H. (1989). Tumor necrosis factor enhances expression of tissue factor mRNA in endothelial cells. Thrombosis Research. 53: 231-241.

Corbett, E. F., K. Oikawa, P. Francois, D. C. Tessier, C. Kay, J. J. Bergeron, D. Y. Thomas, K. H. Krause and M. Michalak (1999). "Ca2+ regulation of interactions between endoplasmic reticulum chaperones." J Biol Chem 274(10): 6203-6211.

Corbett, E. F., K. Oikawa, P. Francois, D. C. Tessier, C. Kay, J. J. Bergeron, D. Y. Thomas, K. H. Krause and M. Michalak (1999). "Ca2+ regulation of interactions between endoplasmic reticulum chaperones." J Biol Chem 274(10): 6203-6211.

Corbett, E. F., Oikawa, K., Francois, P., Tessier, D. C., Kay, C., Bergeron, J. J. M., Thomas, D. Y., Krause, K. H., Michalak, M. (1999). Ca2+ regulation of interactions between endoplasmic reticulum chaperones. J. Biol. Chem. 274: 6203-6211.

Corrigall, V. M., Bodman-Smith, M. D., Fife, M. S., Canas, B., Myers, L. K., Wooley, P. H., et al. (2001). The human endoplasmic reticulum molecular chaperone BiP is an autoantigen for rheumatoid arthritis and prevents the induction of experimental arthritis. The Journal of Immunology. 166: 1492-1498.

Cossette, B., M. E. Pelletier, N. Carrier, M. Turgeon, C. Leclair, P. Charron, D. Echenberg, T. Fayad and P. Farand (2010). "Evaluation of bleeding risk in patients exposed to therapeutic unfractionated or low-molecular-weight heparin: a cohort study in the context of a quality improvement initiative." Ann Pharmacother 44(6): 994-1002.

Crawley, J., Lupu, F., Westmuchett, A. D., Severs, N. J., Kakka, V. V., Lupu, C. (2000). Espression, localization and activity of tissue factor pathway inhibitor in normal and atherosclerotic human vessels. Arterioscler. Throm. Vasc. Biol. 20: 1362-1373.

Crutchley, D. J., Que, B. G. (1995). Copper-induced tissue factor expressionin human monocytic THP-1 cells and its inhibition by antioxidants. Circulation. 92: 238-243.

Cunnea, P. M., Miranda-Vizuete, A., Bertoli, G., Simmen, T., Damdimopoulos, A. E., Hermann, S., Leinonen, S., Huikko, M. P., Gustafsson, J. A., Sitia, R., Spyrou, G. (2003). ERdj%, an endoplasmic reticulum (ER)-resident protein containing DnaJ and thioredoxin domains, is expressed in secretory cells or following ER stress. J. Biol. Chem. 278: 1059-1066.

Davidson, D. J., Haskell, C., Majest, S., Kherzai, A., Egan, D. A., Walter, K. A., et al. (2005). Kringle 5 of human plasminogen induces apoptosis of endothelial and tumourcells through surface-expressed glucose-regulated protein 78. Cancer Research. 65: 4663-4672.

Delpino, A., & Castelli, M. (2002). The 78 kDa glucose-regulated protein (GRP78/BIP) is expressed on the cell membrane, is released into cell culture medium and is also present in human peripheral circulation. Bioscience Reports. 22: 407-420.

Diamant, M., Nieuwland, R., Pablo, R. F., Sturk, A., Smit, J. W., Radder, J. K. (2002). Elevated numbers of tissue-factor exposing microparticles correlate with components of the metabolic syndrome in uncomplicated type 2 diabetes mellitus. Circulation. 106: 2442-2447.

Diaz, C., Schroit, A. J. (1996). Role of translocases in the generation of phosphatidylserine assymetry. J. Memb. Biol. 151: 1-9.

Dickhout, J. G., Sood, S. K., Austin, R. C. (2007). Role of the endoplasmic reticulum calcium disequilibria in the mechanism of homocysteine-induced ER stress. Antioxid Redox Signal. 11: 1863-1873.

Dickson, R. B., Willingham, M. C., Gallo, M., & Pastan, I. H. (1981). Inhibition by bacitracin of high affinity binding of 125I-alpha2M to plasma membranes. FEBS Letters. 126(2): 265-268.

Dietzen, D. J., Jack, G. G., Page, K. L., Tezloff, T. A., Hall, C. L., Mast, A. E. (2003). Localization of tissue factor pathway inhibitor to lipid rafts is not required for the inhibition of factor VIIa/tissue factor activity. Throm. Haemost. 89: 65-73.

Dimmeler, S., Zeiher, A. M. (2000). Endothelial cell apoptosis in angiogenesis and vessel regression. Circ Res. 87: 434-439.

Donate, F., Kelly, C. R., Ruf, W., Edgington, T. S. (2000). Dimerization of tissue factor supports solution-phase autoactivation of factor VII without influencing proteolytic activation of factor X. Biochemistry. 39: 11467-11476.

Dong, D., Ko, B., Baumeister, P., Swenson, S., Costa, F., Markland, F., Stiles, C., Paterson, J. B., Bates, S. E., Lee, A. S. (2005). Vascular targeting and antiangiogenesis agents induce drug resistance effector GRP78 within the tumourmicroenvironment. Cancer Res. 65: 5785-5791.

Dorfleutner, A., Ruf, W. (2003). Regulation of tissue factor cytoplasmic domain phosphorylation by palmitoylation. Blood. 102: 3998-4005.

Dorner, A. J., Boyle, D. G., Kaufman, R. J. (1987). The relationship of N-linked glycosylation and heavy chain-binding protein associated with the secretion of glycoproteins. J. Cell. Biol. 105: 2665-2674.

Drake, T. A., Morrissey, J. H., & Edgington, T. S. (1989)(b). Selective cellular expression of tissue factor in human tissues. Implications for disorders of hemostasis and thrombosis. American Journal of Pathology. 134(5): 1087-1097.

Drake, T. A., Ruf, W., Morrissey, J. H., Edgington, T. S. (1989)(a). Functional tissue factor is entirely cell surface expressed on lipopolysaccharide-stimulated human blood monocytes and a constitutively tissue factor-producing neoplastic cell line. J Cell Biol. 109: 389-395.

Dykens, J. A. (1994). Isolated cerebral and cerebellar mitochondria produce free radicals when exposed to elevated Ca2+ and Na+: implications for neurodegeneration. J. Neurochemistry. 63: 584-591.

Eddleston, M., De La Torre, J. C., Oldstone, M. B., Loskutoff, D. J., Edginton, T. S., Mackman, N. (1993). Astrocytes are the primary source of tissue factor in the murine central nervous system – a role for astrocytes in cerebral hemostasis. J Clin Invest. 92: 349-358.

Eilertsen, K. E., Bjarne, O. (2004). Tissue factor: (patho)physiology and cellular biology. Blood Coagul Fibrinolysis. 15: 521-538.

Ellgaard, L., Helenius, A. (2003). Quality control in the endoplasmic reticulum. Nature Rev. Mol. Cell Biol. 4: 181-191.

Fadok, V. A., Veolker, D., Campbell, P. A., Cohen, J. J., Bratton, D. L., Henson, P. M. (1992). Exposure of phosphatidylserine on the surface of apoptotic lymphocytes triggers specific recognition and removal by macrophages. J Immunol. 148: 2207-2216.

Fang, S., J. Dropkin, R. Herbert, D. Triola and P. Landsbergis (2007). "Workers' compensation experiences of computer users with musculoskeletal disorders." Am J Ind Med 50(7): 512-518.

Faria, E. F., G. F. Carvalhal, R. B. dos Reis, M. Tobias-Machado, R. A. Vieira, L. O. Reis, L. Nogueira, R. D. Machado, C. H. Freitas, Jr., W. J. Magnabosco, E. C. Mauad and A. L. Carvalho (2012). "Use of low free to total PSA ratio in prostate cancer screening: detection rates, clinical and pathological findings in Brazilian men with serum PSA levels <4.0 ng/mL." BJU Int 110(11 Pt B): E653-657.

Faulk, W. P., Labarrere, C. A., Carson, S. D. (1990). Tissue factor: identification and characterization of cell types in human placentae. Blood. 76: 86-96.

Fielding, C. J., Fielding, P. E. (2000). Cholesterol and caveolae: structural and functional relationships. Biochem, Biophys. Acta. 1529: 210-222.

Flaherty, K. M., DeLuca-Flaherty, C., McKay, D. B. (1990). Three-dimensional structure of the ATPase fragment of a 70K heat-shocl cognate protein. Nature. 346: 623-628.

Fleck, R. A., Rao, L. V., Rapaport, S. I., Varkin, N. (1990). Localization of human tissue factor antigen by immunostaining with monospecific, polyclonal anti-human tissue factor antibody. Thromb Res. 57: 765-781.

Flossel, C., Luther, T., Muller, M., Albrecht, S., Kasper, M. (1994). Immunohistochemical detection of tissue factor (TF) on paraffin sections of routinely fixed human tissue. Histochemistry. 101: 449-453.

Flucher, B. E., Franzini-Armstrong, C. (1996). Formation of junctions involved in excitation-contraction coupling in skeletal and cardiac muscle. Proc Natl Acad Sci. 93(15): 8101-8106.

Flynn, G. C., Pohl, J., Flocco, M. T., Rothman, J. E. (1991). Peptode-binding specificity of the molecular chaperone BiP. Nature 353: 726-730.

Folkman, J. (1990). What is the evidence that tumors are angiogenesis dependent? J Natl Cancer Inst. 82: 4-6.

Freedman, R. B. (1989). Protein disulfide isomerase: multiple roles in the modification of nascent secretory proteins. Cell. 57: 1069-1072.

Fryer, R. H., Wilson, B. D., Gubler, D. B., Fitzgerald, L. A., & Rodgers, G. M. (1993). Homocysteine, a risk factor for premature vascular disease and thrombosis, induces tissue factor activity in endothelial cells. Arteriosclerosis, Thrombosis and Vascular Biology. 13(9): 1327-1333.

Furie, B., & Furie, B. C. (1992). Molecular and cellular biology of blood coagulation. The New England Journal of Medicine. 326: 800-806.

Ge, L., Ly, Y., Hollenberg, M., DeFea, K. (2003). A beta-arrestin-dependent scaffold is associated with prolonged MAPK activation in pseudopodia during protease-activated receptor-2-induced chemotaxis. J Biol Chem. 278: 34418-34426.

Gething, M. J. (1999). Role and regulation of the ER chaperone BiP. Sem. Cell Develop. Biol. 10: 465-472.

Gething, M. J., Sambrook, J. (1992). Protein folding in the cell. Nature. 355: 33-45.

Gettins, P. G. (1995). Thiol ester cleavage-dependent conformational change in human alpha 2-macroglobulin. influence of attacking nucleophile and of Cys949 modification. Biochemistry. 34(38): 12233-12240.

Giesen, P. L., Nemerson, Y. (2000). Tissue factor on the loose. Semin Thromb Hemost. 26: 379-384.

Gifford, J. B., W. Huang, A. E. Zeleniak, A. Hindoyan, H. Wu, T. R. Donahue and R. Hill (2016). "Expression Of GRP78, Master Regulator Of The Unfolded Protein Response, Increases Chemoresistance In Pancreatic Ductal Adenocarcinoma." Mol Cancer Ther.

Goldhaber, S. Z. (2005). Tamoxifen: preventing breast cancer and placing the risk of deep vein thrombosis in perspective. Circulation. 111: 539-541.

Gonzalez-Gronow, M., Cuchacovich, M., Llanos, C., Urzua, C., Gawdi, G., & Pizzo, S. V. (2006). Prostate cancer cell proliferation in vitro is modulated by antibodies against glucose-regulated protein 78 isolated from patient serum. Cancer Research. 66(23): 11424-11431.

Gonzalez-Gronow, M., Kaczowka, S.J., Payne, S., Wang, F., Gawdi, G., & Pizzo, S. V. (2007). Plasminogen structural domains exhibit different functions when associated with cell surface GRP78 of the voltage-dependent anion channel. The Journal of Biological Chemistry. 282(45): 32811-32820.

Gonzalez-Gronow, M., M. A. Selim, J. Papalas and S. V. Pizzo (2009). "GRP78: a multifunctional receptor on the cell surface." Antioxid Redox Signal 11(9): 2299-2306.

Gonzalez-Gronow, M., M. Cuchacovich, C. Llanos, C. Urzua, G. Gawdi and S. V. Pizzo (2006). "Prostate cancer cell proliferation in vitro is modulated by antibodies against glucose-regulated protein 78 isolated from patient serum." Cancer Res 66(23): 11424-11431.

Gonzalez-Gronow, M., M. S. Hershfield, F. X. Arredondo-Vega and S. V. Pizzo (2004). "Cell surface adenosine deaminase binds and stimulates plasminogen activation on 1-LN human prostate cancer cells." J Biol Chem 279(20): 20993-20998.

Goretzki, L., & Mueller, B. M. (1998). Low-density-lipoprotein-receptor-related protein (LRP) interacts with a GTP-binding protein. Biochemistry Journal. 336(2): 381-386.

Grabner, M., Dirksen, R. T., Beam, K. G. (1998). Tagging woth green fluorescent protein reveals a distinct subcellular distribution of L-type and non-L-type Ca 2+ channels expressed in dysgenic myotubues. Proc Natl Acad Sci. 95(4): 1903-1908.

Greeno, E. W., Bach, R. R., Moldow, C. F. (1996). Apoptosis is associated with increased cell surface tissue factor procoagulant activity. Lab. Invest. 75: 281-289.

Griffin, C. T., Srinivasan, Y., Zheng, Y. W., Huang, W., Coughlin, S. R. (2001). A role for thrombin receptor signalling in endothelial cells during embryonic development. Science. 293: 1666-1670.

Guba, M., Yezhelyev, M., Eichhorn, M. E., Schmid, G., Ischenko, I., Papyan, A., Graeb, C., Seeliger, H., Geissler, E. K., Jauch, K. W., Bruns, C. J. (2005). Rapamycin induces tumor-specific thrombosis via tissue factor in the presence of VEGF. Blood. 105: 4463-4469.

Hamada, K., Kuratsu, J., Saitoh, Y., Takeshima, H., Nishi, T., Ushio, Y. (1996). Expression of tissue factor in glioma. Noshuyo Byori. 13: 115-118.

Hamamoto, T., Tamamoto, M., Nordfang, O., Peterson, J. G. L., Foster, D. C., Kisiel, W. (1993) Inhibitory properties of full-length and truncated recombinant tissue factor pathway inhibitor (TFPI). J. Biol. Chem. 268: 8704-8710.

Hamik, A., Setiadi, H., Bu, G., McEver, R. P., Morrissey, J. H. (1999). Down-regulation of monocyte tissue factor mediated by tissue factor pathway inhibitor and the low density lipoprotein receptor-related protein. J. Biol. Chem. 274: 4962-4969.

Hamilton, A. S., P. C. Albertsen, T. K. Johnson, R. Hoffman, D. Morrell, D. Deapen and D. F. Penson (2011). "Trends in the treatment of localized prostate cancer using supplemented cancer registry data." BJU Int 107(4): 576-584.

Hanover, J. A., Cheng, S., Willingham, M. C., & Pastan, I. H. (1983). Alpha 2-macroglobulin binding to cultured fibroblasts. solubilization and partial purification of binding sites. The Journal of Biological Chemistry. 258(1): 370-377.

Hanover, J. A., Willingham, M. C., & Pastan, I. H. (1983). Receptor-mediated endocytosis of alpha 2-macroglobulin: Solubilization and partial purification of the fibroblast alpha 2-macroglobulin receptor. Annals of the New York Academy of Sceinces. 421(1): 410-423.

Hansen, C. B., van Deurs, B., Peterson, L. C., Rao, L. V. M. (1999). Discordant expression of tissue factor and its activity in polarized epithelial cells. Asymmetry in anionic phospholipids availability as a possible explanation. Blood. 94: 1657-1664.

Hansen, L. K., J. J. O'Leary, A. P. Skubitz, L. T. Furcht and J. B. McCarthy (1995). "Identification of a homologous heparin binding peptide sequence present in fibronectin and the 70 kDa family of heat-shock proteins." Biochim Biophys Acta 1252(1): 135-145.

Harlos, K., Martin, D. M. A., O'Brian, D. P., Jones, E. Y., Stuart, D. I., Polikarpov, I., Miller, A., Tuddenham, E. G. D., Boys, C. W. G. (1994) Crystal structure of the extracellular region of human tissue factor. Nature. 370: 662-666.

Hatakeyama, K., Asada, Y., Marutsuka, K., Kataoka, H., Sato, Y., & Sumiyoshi, A. (1998). Expression of tissue factor in the rabbit aorta after balloon injury. Atherosclerosis. 139: 265-271.

Hathcock, J. J., Nemerson, Y. (2004). Platelet deposition inhibits tissue factor activity: in vitro clots are impermeable to factor Xa. Blood. 104: 123-127.

Hembrough, T. A., Swartz, G. M., Papathanassiu, A., Vlasuk, G. P., Rote, W. E., Green, S. J., Pribluda, V. S. (2003). Tissue factor/factor VIIa inhibitors block angiogenesis and tumourgrowth through a nonhemostatic mechanism. Cancer Res. 63: 2997-3000.

Hendershot, L. M., Wei, J., Gaut, J., Melnick, J., Aveil, S., Argon, Y. (1996). Inhibition of immunoglobulin folding and secretion by dominant negative BiP ATPase mutants. Proc. Natl. Acad. Sci. 93: 5269-5274.

Herket, O., Diebold, I., Brandes, R. P., Hess, J., Busse, R., Gorlach, A. (2002). NADPH oxidase mediates tissue factor-dependent surface procoagulant activity by thrombin in human vascular smooth muscle cells. Circulation. 105: 2030-2036.

Hirsh, J., S. S. Anand, J. L. Halperin and V. Fuster (2001). "Mechanism of action and pharmacology of unfractionated heparin." Arterioscler Thromb Vasc Biol 21(7): 1094-1096.

Hjortoe, G. M., Petersen, L. C., Albrektsen, T., Sorensen, B. B., Norby, P. L., Mandal, S. K., Pendurthi, U. R., Rao, L. V. (2004). Tissue factor–factor VIIa specific up-regulation of IL-8 expression in MDA-MB-231 cells is mediated by PAR-2 and results in increased cell migration. Blood. 103: 3029-3037.

Hofer, A. M., Brown, E. M. (2003). Extracellular calcium sensing and signalling. Nature Rev. Mol. Cell Biol. 4: 530-538.

Howard, G. C., Misra, U. K., DeCamp, D. L., & Pizzo, S. V. (1996). Altered interaction of cis-dichlorodiammineplatinum(II)-modified 2-macroglobulin (2M) with the low density lipoprotein receptor-related protein/ 2M receptor but not the 2M signalling receptor. Journal of Clinical Investigation. 97(5): 1193-1203.

Howard, G. C., Yamaguchi, Y., Misra, U. K., Gawdi, G., Nelsen, A., DeCamp, D. L., et al. (1996). Selective mutations in cloned and expressed -macroglobulin receptor binding fragment alter binding to either the 2-macroglobulin signalling receptor or the low density lipoprotein receptor-related Protein/2-macroglobulin receptor The Journal of Biological Chemistry. 271(24): 14105-14111.

Hron, G., Kollars, M., Weber, H., Sagaster, V., Quehenberger, P., Eichinger, S., Kyrle, P. A., Weltermann, A. (2007). Tissue factor-positive microparticles: cellular origin and association with coagulation activation in patients with colorectal cancer. Thromb Haemost. 97: 119-123.

Hu, T., Bach, R. R., Horton, R., Konigsberg, W. H., Todd, M. B. (1994). Procoagulant activity in cancer cells is dependent on tissue factor expression. Oncol Res. 6: 321-327.

Iakhiaev, A., Pendurthi, U. R., Voigt, J., Exban, M., Rao, L. V. M. (1999) Catabolism of factor VIIa bound to tissue factor in fibroblasts in the presence and absence of tissue factor pathway inhibitor. J. Biol. Chem. 274: 36995-37003.

Jemal, A., R. Siegel, E. Ward, Y. Hao, J. Xu and M. J. Thun (2009). "Cancer statistics, 2009." CA Cancer J Clin 59(4): 225-249.

Jiang, X., Bailly, M. A., Panetti, T. S., Cappello, M., Konigsberg, W. H., Bromberg, M. E. (2004). Formation of tissue factor–factor VIIa–factor Xa complex promotes cellular signalling and migration of human breast cancer cells. J Thromb Haemost. 2: 93-101.

Jiang, X., Guo, Y. L., Bromberg, M. E. (2006). Formation of tissue factor–factor VIIa–factor Xa complex prevents apoptosis in human breast cancer cells. Thromb Haemost. 96: 196-201.

Kato, K., Elsayed, Y. A., Namoto, M., Nakagawa, K., & Sueishi, K. (1996). Enhanced expression of tissue factor activity in the atherosclerotic aortas of cholesterol-fed rabbits. Thrombosis Research. 82: 335-347.

Khorana, A. A., Ahrendt, S. A., Ryan, C. K., Francis, C. W., Hruban, R. H., Hu, Y. C., Hostetter, G., Harvey, J., Taubman, M. B. (2007). Tissue factor expression, angiogenesis, and thrombosis in pancreatic cancer. Clin Cancer Res. 13: 2870-2875.

Kobayashi, Y., Yoshimura, N., Nakamura, K., Yamagishi, H., & Oka, T. (1998). Expression of tissue factor in hepatic ischemic-reperfusion injury of the rat. Transplantation. 66: 708-716.

Konigsberg, W., Kirchofer, D., Riederer, M. A., Nemerson, Y. (2001). The TF:VIIa complex: clinical significance, structure-function relationships and its role in signalling and metastasis. Thromb. Haemost. 86: 757-771.

Koomagi, R., Volm, M. (1998). Tissue-factor expression in human non-small-cell lung carcinoma measured by immunohistochemistry: correlation between tissue factor and angiogenesis. Int J Cancer. 79: 19-22.

Kowaltowski, A. J., Castilho, R. F., Vercesi, A. E. (1995) Ca2+-induced mitochondrial membrane permeabilization: role of coenzyme Q redox state. Am. J. Physiol. 269: C141-C147.

Koyama, T., Nishida, K., Ohdama, S., Savada, M., Murakami, N., Hirosava, S., Kuriyama, R., Matsuzava, K., Hasegava, R., Aoki, N. (1994). Determination of plasma tissue factor antigen and its clinical significance. Br J Haematol. 87: 343-347.

Kruman, I., Guo, Q., Mattson, M. P. (1998). Calcium and reactive oxygen species mediate staurosporin-induced mitochondrial dysfunction and apoptosis in PC12 cells. J. Neurosci. Res. 51: 293-308.

Kunzelmann-Marche, C., Satta, N., Toti, F., Zhang, Y., Nawroth, P. P., Morrissey, J. H. et al. (2000). The influence exerted by a restricted phospholipid microenvironment on the expression of tissue factor activity at the cell plasma membrane surface. Thromb Haemost. 83: 282-289.

Lamb, H. K., Mee, C., Xu, W., Liu, L., Blond, S., Cooper, A., Charles, I. G., Hawkins, A. R. (2006). The affinity of a major Ca2+ binding site on GRP78 is differentially enhanced by ADP and ATP. J. Biol. Chem. 281: 8796-8805.

Le, D. T., Rapaport, S. I., & Rao, L. V. (1992). Relations between factor VIIa binding and expression of factor VIIa/tissue factor catalytic activity on cell surfaces. The Journal of Biological Chemistry. 267(22): 15447-15454.

Lee, A. S. (2001). The glucose-regulated proteins: Stress induction and clinical applications. Trends in Biochemical Sciences. 26: 504-510.

Lee, A. Y., & Levine, M. N. (2003). Venous thromboembolsm and cancer: Risk and outcomes. Circulation. 107: 17-21.

Lewis, J. C., Bennet-Cain, A. L., DeMars, C. S., Doellgast, G. J., Grant, K. W., Jones, N. L., Gupta, M. (1995). Procoagulant activity after exposure of monocyte-derived macrophages to minimally oxidized low density lipoprotein. Co-localization of tissue factor antigen and nascent fibrin fibres at the cell surface. Am. J. Pathol. 147: 1029-1040.

Li, C., Colman, L. M., Collier, M. E., Dyer, C. E., Greenman, J., Ettelaie, C. (2006). Tumour-expressed tissue factor inhibits cellular cytotoxicity. Cancer Immunol Immunother. 55: 1301-1308.

Lievremont, J. P., Rizzuto, R., Hendershot, L., Meldolesi, J. (1997). BiP, a major chaperone protein of the endoplasmic reticulum lumen, plays a direct and important role in the storage of the rapidly exchanging pool of Ca2+. J. Biol. Chem. 272: 30873-30879.

Liu, C., Bhattacharjee, G., Boisvert, W., Dilley, R., & Edgington, T. (2003). In vivo interrogation of the molecular display of atherosclerotic lesion surfaces. American Journal of Pathology. 163: 1859-1871.

Liu, H., Bowes, R. C., van de Water, B., Sillence, C., Nagelkerke, J. F., & Stevens, J. L. (1997). Endoplasmic reticulum chaperones GRP78 and calreticulin prevent oxidative stress, Ca2+ disturbances, and cell death in renal epithelial cells. The Journal of Biological Chemistry. 272: 21751-21759.

Liu, H., Miller, E., van de Water, B., & Stevens, J. L. (1998). Endoplasmic reticulum stress proteins block oxidant-induced Ca2+ increases and cell death. The Journal of Biological Chemistry. 273: 12858-12862.

Lodish, H. F., Kong, N. (1990). Perturbation of cellular calcium blocks exit of secretory proteins from the rough endoplasmic reticulum. J. Biol. Chem. 265:10893-10899.

Lopez-Pedera, C., Jardi, M., Ingles-Esteve, J., Munoz-Canoves, P., Dorado, G., Velasco, F., Felez, J. (1997). Characterization of tissue factor expression on the human endothelial cell line ECV304. Am. J. Hematol. 56: 71-78.

Lucero, H. A., Lebeche, D., Kaminer, B. (1994). ER calcistorin/protein disulfide isomerase (PDI). Sequence determination and expression of a cDNA clone encoding

a calcium storage protein with PDI activity from endoplasmic reticulum of the sea urchin egg. J. Biol. Chem. 269: 23112-23119.

Lupu, C., Goodwin, C. A., Westmuckett, A. D., Emeis, J. J., Scully, M. F., Kakkhar, V. V., Lupu, F. (1997). Tissue factor pathway inhibitor in endothelial cells colocalizes with glycolipid microdomains/caveolae. Regulatory mechanism(s) of the anticoagulant properties of the endothelium. Arterioscler. Throm. Vasc. Biol. 17: 2964-2974.

Lupu, C., Hu, X., Lupu, F. (2005). Caveolin-1 enhances tissue factor pathway inhibitor exposure and function on the cell surface. J. Biol. Chem. 280: 22308-22317.

Luther, T., Flossel, C., Mackman, N., Bierhaus, A., Kasper, M., Albrecht, S., Sage, E. H., Iruelaarispe, L., Grossmann, H., Strohlein, A., Zhang, Y., Navroth, P. P., Carmeliet, P., Loskutoff, D. J., Muller, M. (1996). Tissue factor expression during human and mouse development. Am J Pathol. 149: 101-113.

Lykke, J., Nielsen, H. J. (2003). The role of tissue factor in colorectal cancer. Eur J Surg Oncol. 29: 417-422.

Lysov Z., Dwivedi, D. J., Gould, T. J., Liaw, P. C. (2016) Procagulant effects of lung cancer chemotherapy: impact on microparticles and cell-free DNA. Blood Coagul Fibrinolysis. E-publication ahead of print; PMID: 26919453.

Ma, L., Francia, G., Viloria-Petit, A., Hicklin, D. J., du Manoir, J., Rak, J., Kerbel, R. S. (2005). In vitro procoagulant activity induced in endothelial cells by chemotherapy and antiangiogenic drug combinations: modulation by lower-dose chemotherapy. Cancer Res. 65: 365-373.

Ma, Y., Hendershot, L. M. (2004). The role of the unfolded protein response in tumour development: friend or foe? Nature. 4: 966-977.

Mackman, N., Morrisey, J. H., Fowler, B., Edginton, T. S. (1989). Complete sequence of the human tissue factor gene, a highly regulated cellular receptor that initiates the coagulation cascade. Biochemistry. 28: 1755-1762.

Mackman, N., Sawdey, M. S., Keeton, M. R., Loskutoff, D. J. (1993). Murine tissue factor gene expression in vivo: Tissue and cell specificity and regulation by lipopolysaccharide. Am J Pathol. 143: 76-84, 1993.

Mallat, Z., Hugel, B., Ohan, J., Leseche, G., Freyssinet, J. M., Tedgui, A. (1999). Shed membrane microparticles with procoagulant potential in human atherosclerotic plaques: a role for apoptosis in plaque thrombogenicity. Circulation. 99: 348-353.

Maly, M. A., Tomasov, P., Hajek, P., Blasko, P., Hrachovinova, I., Salaj, P., Veselka, J. (2007). The role of tissue factor in thrombosis and hemostasis. Physiol. Res. 56: 685-695.

Mandal, S. K., Iakhiaev, A., Pendurthi, U. R., Rao, L. V. M. (2005). Acute cholesterol depletion impairs functional expression of tissue factor in fibroblasts: Modulation of tissue factor activity by membrane cholesterol. Blood. 105: 153-160.

Marmur, J. D., Rossikhina, M., Guha, A., Fyfe, B., Friedrich, V., Mendlowitz, M., et al. (1993). Tissue factor is rapidly induced in arterial smooth muscle after balloon injury. Journal of Clinical Investigation. 91(5): 2253-2259.

Marmur, J. D., Thiruvikraman, S. V., Fyfe, B. S., Guha, A, Sharma, S. K., Ambrose, J. A., Falkon, J. T., Nemerson, Y., Taubman, M. B. (1996). Identification of active tissue factor in human coronary atheroma. Circulation. 94: 1226-1232.

Martin, D. M., Boys, C. W., & Ruf, W. (1995). Tissue factor: Molecular recognition and cofactor function. FASEB J. 9(10): 852-859.

Martin, S. J., Reutelingsperger, C. P. M., McGahon, A. J., Rader, J. A., van Schie, R. C. A. A., LaFace, D. M., Green, D. R. (1995). Early redistribution of plasma membrane phosphatidylserine is a general feature of apoptosis regardless of the initiating stimulus: inhibition by overexpression of Bcl-2 and Abl. J. Exp. Med. 182: 1545-1556.

Martinelli, I. (2001). Risk factors in venous thromboembolism. Thromb Haemost. 86: 395-403.

Marx, G. M., Steer, C. B., Harper, P., Pavlakis, N., Rixe, O., Khayat, D. (2002). Unexpected serious toxicity with chemotherapy and antiangiogenic combinations: time to take stock! J Clin Oncol. 20: 1446-1448.

Maynard, J. R., Heckman, C. A., Pitlick, F. A., Nemerson, Y. (1975). Association of tissue factor activity with the surface of cultured cells. J Clin Invest. 55: 814-824.

McKay, D. B. (1993). Structure and mechanism of 70-kDa heat-shock-relate proteins. Advances in Protein Chemistry. 44: 67.

Mechtcheriakova, D., Wlachos, A., Holzmuller, H., Binder, B. R., & Hofer, E. (1999). Vascular endothelial cell growth factor-induced tissue factor expression in endothelial cells is mediated by EGR-1. Blood. 93: 3811-3823.

Meerovitch, K., Wing, S., Goltzman, D. (1998). Proparathyroid hormone-related protein is associated with the chaperone protein BiP and undergoes proteosome-mediated degradation. J. Biol. Chem. 273:21025-21030.

Meunier, L., Usherwood, Y. K., Chung, K. T., Hendershot, L. M. (2002). A subset of chaperones and folding enzymes form multiprotein complexes in endoplasmic reticulum to bind nascent proteins. Mol. Biol. Cell. 13: 4456-4469.

Michalak, M., Corbett, E. F., Mesaeli, N., Nakamura, K., Opas, M. (1999). Calreticulin: one protein, one gene, many functions. Biochem. J. 344: 281-292.

Michalak, M., E. F. Corbett, N. Mesaeli, K. Nakamura and M. Opas (1999). "Calreticulin: one protein, one gene, many functions." Biochem J 344 Pt 2: 281-292.

Milsom, C. and J. Rak (2008). "Tissue factor and cancer." Pathophysiol Haemost Thromb 36(3-4): 160-176.

Milsom, C., J. Yu, L. May, N. Magnus and J. Rak (2008). "Diverse roles of tissue factor-expressing cell subsets in tumourprogression." Semin Thromb Hemost 34(2): 170-181.

Mintz, A., D. M. Gibo, A. B. Madhankumar and W. Debinski (2003). "Molecular targeting with recombinant cytotoxins of interleukin-13 receptor alpha2-expressing glioma." J Neurooncol 64(1-2): 117-123.

Mintz, P. J., J. Kim, K. A. Do, X. Wang, R. G. Zinner, M. Cristofanilli, M. A. Arap, W. K. Hong, P. Troncoso, C. J. Logothetis, R. Pasqualini and W. Arap (2003). "Fingerprinting the circulating repertoire of antibodies from cancer patients." Nat Biotechnol 21(1): 57-63.

Misra, U. K., & Pizzo, S. V. (2002). Regulation of cytosolic phospholipase A2 activity in macrophages stimulated with receptor-recognized forms of 2-macroglobulin. The Journal of Biological Chemistry. 277(6): 4069-4078.

Misra, U. K., Chu, C. T., Gawdi, G., & Pizzo, S. V. (1994)(a). Evidence for a second alpha2-macroglobulin receptor. The Journal of Biological Chemistry. 269(17): 12541-12547.

Misra, U. K., Chu, C. T., Gawdi, G., & Pizzo, S. V. (1994)(b). The relationship between low density lipoprotein-related protein/alpha 2-macroglobulin (alpha 2M) receptors and the newly described alpha 2M signalling receptor. The Journal of Biological Chemistry. 269(28): 18303-18306.

Misra, U. K., Gonzalez-Gronow, M., Gawdi, G., & Pizzo, S. V. (2005). The role of MTJ-1 in cell surface translocation of GRP78, a receptor for alpha2-macroglobulin-dependent signalling. The Journal of Immunology. 174: 2092-2097.

Misra, U. K., Pizzo, S. V. (2008). Heterotrimetic Galphaq11 co-immunoprecipitates with surface-anchored GRP78 from plasma membranes of alpha2M*-stimulated marophages. J Cell Biochem. 104: 96-104.

Miyake, H., Hara, I., Arakawa, S., Kamidono, S. (2000). Stress protein GRP78 prevents apoptosis induced by calcium ionophore, ionomycin, but not by glycosylation inhibitor, tunicamycin, in human prostate cancer cells. J. Cell. Biochem. 77: 396-408.

Morris, D. R., Ding, Y., Ricks, T. K., Gullapalli, A., Wolfe, B. L., Trejo, J. (2006). Protease-activated receptor-2 is essential for factor VIIa and Xa induced signalling, migration, and invasion of breast cancer cells. Cancer Res. 66: 307-314.

Morrissey, J. H. (2001) Tissue Factor: an enzyme cofactor and a true receptor. Thromb. Haemost. 86: 66-74.

Mousa, S. A. and L. J. Petersen (2009). "Anti-cancer properties of low-molecular-weight heparin: preclinical evidence." Thromb Haemost 102(2): 258-267.

Mousa, S. A., R. Linhardt, J. L. Francis and A. Amirkhosravi (2006). "Anti-metastatic effect of a non-anticoagulant low-molecular-weight heparin versus the standard low-molecular-weight heparin, enoxaparin." Thromb Haemost 96(6): 816-821.

Mueller, B. M., Reisfeld, R. A., Edgington, T. S., Ruf, W. (1992). Expression of tissue factor by melanoma cells promotes efficient hematogenous metastasis. Proc Natl Acad Sci U S A. 89: 11832-11836.

Mueller, B. M., Ruf, W. (1998). Requirement for binding of catalytically active factor VIIa in tissue factor-dependent experimental metastasis. J Clin Invest. 101: 1372-1378.

Mulder, A. B., Smit, J. W., Bom, V. J. J., Blom, N. R., Ruiters, M. H. J., Halie, M. R., van der Meer, J. (1996)(a). Association of smooth muscle cell tissue factor with caveolae. Blood. 88: 1306-1313.

Muller, Y. A., Ultsch, M. H., Kelley,R.F., de Vos, A. M. (1994) Structure of the extracellular domain of human tissue factor:location of the factor VIIa binding site. Biochemistry. 33: 10864-10870.

Munro, S., Pelham, H. R. (1987). A C-terminal signal prevents secretion of luminal ER proteins. Cell. 48: 899-907.

Muralidharan-Chari, V., J. W. Clancy, A. Sedgwick and C. D'Souza-Schorey (2010). "Microvesicles: mediators of extracellular communication during cancer progression." J Cell Sci 123(Pt 10): 1603-1611.

Ngo, C. V., Picha, K., McCabe, F., Millar, H., Tawadros, R., Tam, S. H., Nakada, M. T., Anderson, G. M. (2007), CNTO 859, a humanized anti-tissue factor monoclonal antibody, is a potent inhibitor of breast cancer metastasis and tumourgrowth in xenograft models. Int J Cancer. 120: 1261-1267.

Nieuwland, R., Berckmans, R. J., McGregor, S., Boing, A. N., Romijn, M., Westendorp, R. G., Hack, C. E., Sturk, A. (2000). Cellular origin and procoagulant properties of microparticles in meningococcal sepsis. Blood. 95: 930-935, 2000.

Odom, A. R., Misra, U. K., & Pizzo, S. V. (1997). Nickel inhibits binding of alpha2-macroglobulin-methylamine to the low-density lipoprotein receptor-related protein/alpha2-macroglobulin receptor but not the alpha2-macroglobulin signalling receptor. Biochemistry. 36(41): 12395-12399.

Ollivier, V., Bentolila, S., Chabbat, J., Hakim, J., de Prost, D. (1998). Tissue factor-dependent vascular endothelial growth factor production by human fibroblasts in response to activated factor VII. Blood. 91: 2698-26703.

Orrenius, S., McConkey, D. J., Bellomo, G., Nicotera, P. (1989). Role of Ca2+ in toxic cell killing. Trends Pharmacol. Sci. 10: 281-285.

Ott, I., Fischer, E. G., Miyagi, Y., Mueller, B. M., Ruf, W. (1998). A role for tissue factor in cell adhesion and migration mediated by interaction with actin-binding protein 280. J Cell Biol. 140: 1241-1253.

Ott, I., Weigand, B., Michl, R., Seitz, I., Sabbari-Erfani, N., Neumann, F. J., Schomig, A. (2005) Tissue factor cytoplasmic domain stimulates migration by activation of the GTPase Rac1 and the mitogen-activated protien kinase p38. Circulation. 111: 349-355.

Ott, M., Robertson, J. D., Gogvadze, V., Zhivotovsky, B., Orrenius, S. (2002). Cytochrome c release from mitochondria proceeds by a two-step process. Proc. Natl. Acad. Sci. 99: 1259-1263.

Paborsky, L. R., Caras, I. W., Fisher, K. L., Gorman, C. M. (1991) Lipid association, but not the transmembrane domain, is required for tissue factor activity. Substitution of the transmembrane domain with a phosphatidylinositol anchor. The Journal of Biological Chemistry. 266: 21911-21916.

Pahl, H. L. (1999). Signal transduction from the endoplasmic reticulum to the cell nucleus. physiology review. 79: 683-701.

Palumbo, J. S., Talmage, K. E., Massari, J. V., La Jeunesse, C. M., Flick, M. J., Kombrinck, K. W., Hu, Z., Barney, K. A., Degen, J. L. (2007). Tumor cell-associatedtissue factor and circulating hemostatic factors cooperate to increase metastatic potential through natural killer cell-dependent and-independent mechanisms. Blood. 110: 133-141.

Paredes, N., Xu, L., Berry, L. R., Chan, A. K. C. (2003). The effects of chemotherapeutic agents on the regulation of thrombin on cell surfaces. Br. J. Haematol. 120: 315-324.

Parry, G. C. N., Erlich, J. H., Carmeliet, P., Luther, T., Mackman, N. (1998). Low levels of tissue factor are compatible with development and hemostasis in mice. J. Clin. Invest. 101: 560-569.

Pawlinski, R., Fernandes, A., Kehrle, B., Pedersen, B., Parry, G., Erlich, J., Pyo, R., Gutstein, D., Zhang, J., Castellino, F., Melis, E., Carmeliet, P, Baretton, G., Luther, T., Taubman, M., Rosen, E., Mackman, N. (2002). Tissue factor deficiency causes cardiac fibrosis and left ventricular dysfunction. Proc. Natl. Acad. Sci. 99: 15333-15338.

Pawson, T., Scott, J. D., (1997). Signaling through scaffold, anchoring and adaptor proteins. Science. 278: 2075-2080.

Pendurthi, U. R., Ghosh, S., Mandal, S. K., Rao, L. M. V. (2007). Tissue factor activation: is disulfide bond switching a regulatory mechanism? Blood. 110: 3900-3908.

Penn, M. S., Mei-Zhen, C., Winokur, A. L., Bethea, J., Hamilton, T. A., DiCorleto, P. E., Chisolm, G. M. (2000) Smooth muscle cell surface tissue factor pathway activation by oxidized low-density lipoprotein requires cellular lipid peroxidation. Blood. 96: 3056-3063.

Penn, M. S., Patel, C. V., Cui, M. Z., DiCorleto, P. E., & Chisolm, G. M. (1999). LDL increases inactive tissue factor on vascular smooth muscle cell surfaces: Hydrogen peroxide activates latent cell surface tissue factor. Circulation. 99: 1753-1759.

Petersen, L. C., P. L. Norby, S. Branner, B. B. Sorensen, T. Elm, H. R. Stennicke, E. Persson and S. E. Bjorn (2005). "Characterization of recombinant murine factor VIIa and recombinant murine tissue factor: a human-murine species compatibility study." Thromb Res 116(1): 75-85.

Pozza, L. M., & Austin, R. C. (2005). Getting a GRP on tissue factor activation. Arteriosclerosis, Thrombosis and Vascular Biology. 25: 1529-1531.

Prandoni, P., Lensing, A. W. A., Piccioli, A., Bernardi, E., Simioni, P., Girolami, B., Marchiori, A., Sabbion, P., Prins, M. H., Noventa, F., Girolami, A. (2002). Recurrent venous thromboembolism and bleeding complications during anticoagulant treatment in patients with cancer and venous thrombosis. Blood. 100(10): 3484-3488.

Rak, J., C. Milsom, L. May, P. Klement and J. Yu (2006). "Tissue factor in cancer and angiogenesis: the molecular link between genetic tumor progression, tumor neovascularization, and cancer coagulopathy." Semin Thromb Hemost 32(1): 54-70.

Rao, L. V. M. (1992). Tissue factor as a tumourprocoagulant. Cancer Metastasis Review. 11: 249-266.

Rao, L. V. M., Pendurthi, U. R. (2003). Regulation of tissue factor-factor VIIa expression on cell surfaces: a role for tissue factor-factor VIIa endocytosis. Mol. Cell. Biochem. 253: 131-140.

Rao, L.V. M., Pendurthi, U. R. (2005). Tissue factor–factor VIIa signalling. Arterioscler Thromb Vasc Biol. 25: 47-56.

Rao, R. V., Peel, A., Logvinova, A., del Rio, G., Hermel, E., Yokota, T., Goldsmith, P. C., Ellerby, L. M., Ellerby, H. M., Bredesen, D. E. (2002). Coupling endoplasmic reticulum stress to the cell death program: role of the ER chaperone GRP78. FEBS Lett. 514: 122-128.

Reddy, R. K., Mao, C., Baumeister, P., Austin, R. C., Kaufman, R. J., Lee, A. S. (2003). Endoplasmic reticulum chaperone protein GRP78 protects cells from apoptosis induced by topoisomerase inhibitors. Role of ATP binding site in suppression of caspase-7 activation. J. Biol. Chem. 278: 20915-20924.

Rehemtulla, A., Ruf, W., Edgington, T. S. (1991) The integrity of the cysteine 186-cysteine 209 bond of the second disulfide loop of tissue factor is required for binding of factor VII. The Journal of Biological Chemistry. 266(16): 10294-10299.

Rickles, F. R., Hair, G. A., Zeff, R. A., Lee, E., & Bona, R. D. (1995). Tissue factor expression in human leukocytes and tumourcells. Thromb Haemost. 74: 391-395.

Rizzuto, R., Pinton, P., Ferrari, D., Chami, M., Szabadkai, G., Magalhaes, P. J., Di Virgilio, F., Pozzan, T. (1993). Calcium and apoptosis: facts and hypothesis. Oncogene. 22: 8619-8627.

Roivainen, M., Piirainen, L., Hovi, T., Virtanen, I., Riikonen, T., Heino, J., et al. (1994). Entry of coxsackievirus A9 into host cells: Specific interactions with avb3 integrin, the vitronectin receptor. Virology. 203: 307-312.

Roivanen, M., Knip, M., Hyoty, H., Kulmala, P., Hiltunen, M., Vahasalo, P., et al. (1998). Several different enterovirus serotypes can be associated with prediabetic autoimmune episodes and onset of overt IDDM. childhood diabetes in finland (DiMe) study group. Journal of Medical Virology. 56: 74-78.

Roivanen, M., Rasilainen, S., Ylipaasto, P., Nissinen, R., Ustinov, J., Bouwens, L., et al. (2000). Mechanisms of coxsackievirus-induced damage to human pancreatic b-cells. Journal of Clinical Endocrinology and Metabolism. 85: 432-440.

Rong, Y., Post, D. E., Pieper, R. O., Durden, D. L., Van Meir, E. G., Brat, D. J. (2005). PTEN and hypoxia regulate tissue factor expression and plasma coagulation by glioblastoma. Cancer Res. 65: 1406-1413.

Rota, S., McWilliam, N. A., Baglin, T. P., Bryne, C. D. (1998). Atherogenic lipoproteins support assembly of the prothrombinase complex and thrombin generation: modulation by oxidation and vitamine E. Blood. 91: 508-515.

Roy, S., Paborsky, L. R., & Vehar, G. A. (1991). Self-association of tissue factor as revealed by chemical crosslinking. The Journal of Biological Chemistry. 266(8): 4665-4668.

Ruddon, R. W., Bedows, E. (1997). Assisted protein folding. J. Biol. Chem. 272: 3125-3128.

Ruf, W., & Dickinson, C. D. (1998). Allosteric regulation of the cofactor-dependent serine protease coagulation factor VIIa. Trends in Cardiovascular Medicine. 8(8): 350-356.

Ruf, W., Rehemtulla, A., Edgington, T. S. (1991). Phospholipid-independent and dependent interactions required for tissue factor receptor and cofactor function. J. Biol. Chem. 266: 2158-2166.

Rutkowski, D. T., S. M. Arnold, C. N. Miller, J. Wu, J. Li, K. M. Gunnison, K. Mori, A. A. Sadighi Akha, D. Raden and R. J. Kaufman (2006). "Adaptation to ER stress is mediated by differential stabilities of pro-survival and pro-apoptotic mRNAs and proteins." PLoS Biol 4(11): e374.

Saraste, A., Pulkki, K. (2000). Morphological and biochemical hallmarks of apoptosis. Cardiovasc. Res. 45: 528-537.

Sato, H., Konishi, Y., Tanaka, H., Takahashi, O., Tanaka, T. (2004). Annexin V inhibits lipopolysaccharide-induced procoagulant activity on human monocytes. Thromb. Res. 114: 45-49.

Selim, M. A., J. L. Burchette, E. V. Bowers, G. G. de Ridder, L. Mo, S. V. Pizzo and M. Gonzalez-Gronow (2011). "Changes in oligosaccharide chains of autoantibodies to GRP78 expressed during progression of malignant melanoma stimulate melanoma cell growth and survival." Melanoma Res 21(4): 323-334.

Sevinsky, J. R., Rao, L. V., Ruf, W. (1996). Ligand-induced protease receptor translocation into caveolae: a mechanism for regulating cell surface proteolysis of the tissue factor-dependent coagulation pathway. J Cell Biol. 133: 293-304.

Shen, Y. and L. M. Hendershot (2005). "ERdj3, a stress-inducible endoplasmic reticulum DnaJ homologue, serves as a cofactor for BiP's interactions with unfolded substrates." Mol Biol Cell 16(1): 40-50.

Shen, Y., Meunier, L., Hendershot, L. M. (2002). Identification and characterization of a novel endolasmic reticulum (ER) DnaJ homologue, which stimulates ATPase activity of BiP in vitro and is induced by ER stress. J. Biol. Chem. 277: 15947-15956.

Shin, B. K., Wang, H., Yim, A. M., Le Naour, F., Brichory, F., Jang, J. H., et al. (2003). Global profiling of the cell surface proteome of cancer cells uncovers an abundance of proteins with chaperone function. The Journal of Biological Chemistry. 278: 7607-7616.

Siddiquif, A., Desai, H., Amirkhosravi, A., Amaya, M., Francis, J. L. (2002). The presence and release of tissue factor from human platelets. Platelets. 13: 247-253.

Siegbahn, A., Johnell, M., Rorsman, C., Ezban, M., Heldin, C. H., Ronnstrand, L. (2000). Binding of factor VIIa to tissue factor on human fibroblasts leads to activation of phospholipase C and enhanced PDGF-BB-stimulated chemotaxis. Blood. 96: 3452-3458.

Siegel, R., D. Naishadham and A. Jemal (2013). "Cancer statistics, 2013." CA Cancer J Clin 63(1): 11-30.

Sitia, R., Braakman, I. (2003). Quality control in the endoplasmic reticulum protein factory. Nature. 426: 891-894.

Slater, A. F. G., Stefan, C., Nobel, I., van den Dobbelsteen, D. J., Orrenius, S. (1995). Signaling mechanisms and oxidative stress in apoptosis. Toxicol. Lett. 82/83: 149-153.

Solovey, A., Gui, L., Key, N. S., & Hebbel, R. P. (1998). Tissue factor expression by endothelial cells in sickle cell anemia. Journal of Clinical Investigation. 101(9): 1899-1904.

Sorensen, B. B., Rao, L. V. M., Tornehave, D., Gammeltoft, S., Petersen, L. C. (2003). Antiapoptotic effect of coagulation factor VIIa. Blood. 102: 1708-1715.

Sousou, T. and A. Khorana (2009). "Identifying cancer patients at risk for venous thromboembolism." Hamostaseologie 29(1): 121-124.

Spicer, E. K., Horton, R., Bloem, L., Bach, R., Williams, K. R., Guha, A., Kraus, J., Lin, T. C., Nemerson, Y., Konigsberg, W. H. (1987) Isolation of cDNA clones coding for human tissue factor: primary structure of the protein and cDNA. Proc. Natl. Acad. Sci. 84: 5148-5152.

Spiro, R. G., Zhu, Q., Bhoyroo, V., Soling, H. D. (1996). Definition of the lectin-like properties of the molecular chaperone, calreticulin, and demonstration of its copurification with endomannosidease from rat liver Golgi. J. Biol. Chem. 271: 11588-11594.

Steffel, J., Luscher, T. F., & Tanner, F. C. (2006). Tissue factor in cardiovascular diseases: Molecular mechanisms and clinical implications. Circulation. 113: 722-731.

Stevens, J. L., Liu, H., Halleck, M., Bowes, R. C., Chen, Q. M., van de Water, B. (2000). Linking gene expression to mechanisms of toxicity. Toxicol. Lett. 112-113: 479-486.

Strickland, D. K., Ashcom, J. D., Williams, S., Burgess, W. H., Migliorini, M., & Argraves, W. S. (1990). Sequence identity between the alpha 2-macroglobulin receptor and low density lipoprotein receptor-related protein suggests that this

molecule is a multifunctional receptor. The Journal of Biological Chemistry. 265(29): 17401-17404.

Sud, R. and A. A. Khorana (2009). "Cancer-associated thrombosis: risk factors, candidate biomarkers and a risk model." Thromb Res 123 Suppl 4: S18-21.

Sunnerhagen, M., Forsen, S., Hoffren, A. M., Drakenberg, T., Teleman, O., Stenflo, J. (1995). Structure of the Ca2+-free Gla domain sheds light on membrane binding of blood coagulation proteins. Nature Struct. Biol. 2: 504-509.

Tameire, F., Verginadis, II and C. Koumenis (2015). "Cell intrinsic and extrinsic activators of the unfolded protein response in cancer: Mechanisms and targets for therapy." Semin Cancer Biol 33: 3-15.

Taniguchi, T., Kakkar, A. K., Tuddenham, E. G., Williamson, R. C., Lemoine, N. R. (1998). Enhanced expression of urokinase receptor induced through the tissue factor–factor VIIa pathway in human pancreatic cancer. Cancer Res. 58: 4461-4467.

Tesselaar, M. E., Romijn, F. P., Van Der Linden, I. K., Prins, F. A., Bertina, R. M., Osanto, S. (2007). Microparticle-associated tissue factor activity: a link between cancer and thrombosis? J Thromb Haemost. 5: 520-527.

Thastrup, P., Cullen, P. J., Drobak, B. K., Hanley, M. R., & Dawson, A. P. (1990). Thapsigargin, a tumourpromoter, discharges intracellular Ca2+ stores by specific inhibition of the endoplasmic reticulum Ca2+-ATPase. Proc. Natl. Acad Sci. 87: 2466-2470.

Thiagarajan, P., Tait, J. F. (1991). Collagen-induced exposure of anionic phospholipid in platelets and platelet-derived microparticles. J Biol Chem. 266: 24302-24307.

Thiruvikraman, S. V., Guha, A., Roboz, J., Taubman, M. B., Nemerson, Y., Fallon, J. T. (1996). In situ localization of tissue factor in human atherosclerotic plaques by binding of digoxigenin-labeled factor VIIa and X. Lab Invest. 75: 451-461.

Tilley, R., & Mackman, N. (2006). Tissue factor in hemostasis and thrombosis. Sem. Thromb. Hemost. 32: 5-10.

Triantafilou, K., Fradelizi, D., Wilson, K., & Triantafilou, M. (2002). GRP78, a coreceptor for coxsackievirus A9, interacts with major histocompatibility complex class I molecules WHich mediate virus internalization. Journal of Virology. 76(2): 633-643.

Triantafilou, M., Fradelizi, D., Triantafilou, K. (2001). Major histocompatibility class one molecule associates with glucose regulated protein (GRP) 78 on the cell surface. Human Immunol. 62: 764-770.

Triantafilou, M., Triantafilou, K., & Wilson, K. M. (2000). A 70 kDa MHC-class-I associated protein (MAP-70), identified as a receptor molecule for coxsackievirus A9 cell attachment. Human Immunology. 61: 867-878.

Turano, C., Coppari, S., Altieri, F., Ferraro, A. (2002). Proteins of the PDI family: unpredicted non-ER localizations and functions. J Cell. Physiol. 193: 154-163.

Uno, K., Homma, S., Satoh, T., Nakanishi, K., Abe, D., Matsumoto, K., Oki, A., Tsunoda, H., Yamaguchi, I., Nagasawa, T., Yoshikawa, H., Aonuma, K. (2007). Tissue factor expression as a possible determinant of thromboembolism in ovarian cancer. Br J Cancer. 96: 290-295.

Uramoto, H., Sugio, K., Oyama, T., Nakata, S., Ono, K., Yoshimatsu, T., Morita, M., Yasumoto, K. (2005). Expression of endoplasmic reticulum molecular chaperone GRP78 in human lung cancer and its clinical significance. Lung Cancer. 49:55-62.

Vassilakos, A., Michalak, M. Lehrman, M. A., Williams, D. B. (1998). Oligosaccharide binding characteristics of the molecular chaperones calnexin and calreticulin. Biochemistry. 37: 3480-3490.

Versteeg, H. H., Hoedemaeker, I., Diks, S. H., Stam, J. C., Spaargaren, M., van Bergen, E. N., Henegouwen, P. M., van Deventer, S. J., Peppelenbosch, M. P. (2000). Factor VIIa/tissue factor-induced signalling via activation of Src-like kinases, phosphatidylinositol 3-kinase, and Rac. J Biol Chem. 275: 28750-28756.

Versteeg, H. H., Peppelenbosch, M. P., Spek, C. A. (2003). Tissue factor signal transduction in angiogenesis. Carcinogenesis. 24: 1009-1013.

Versteeg, H. H., Schaffner, F., Kerver, M., Petersen, H. H., Ahamed, J., Felding-Habermann, B., Takada, Y., Mueller, B. M., Ruf, W. (2008). Inhibition of tissue factor signalling suppresses tumourgrowth. Blood. 111: 190-199.

Versteeg, H. H., Spek, C. A., Richel, D. J., Peppelenbosch, M. P. (2003). Coagulation factors FVIIa and Xa inhibits apoptosis and anoikis. Oncogene. 23: 410-417.

Versteeg, H. H., Spek, C. A., Slofstra, S. H., Diks, S. H., Richel, D. J., Peppelenbosch, M. P. (2004). FVIIa:TF induces cell survival via G12/G13-dependent Jak/STAT activation and BclXL production. Circ Res. 94: 1032-1040.

Vrana, J. A., Stang, M. T., Grande, J. P., Getz, M. J. (1996). Expression of tissue factor in tumourstroma correlates with progression to invasive human breast cancer:

paracrine regulation by carcinoma cell-derived members of the transforming growth factor beta family. Cancer Res. 56: 5063-5070.

Wang, J., Weiss, I., Svoboda, K., Kwaan, H. C. (2001). Thrombogenic role of cells undergoing apoptosis. Br. J. Haematol. 115: 382-391.

Watson, L. M., Chan, A. K. C., Berry, L. R., Li, J., Sood, S. K., Dickhout, J. G., et al. (2003). Overexpression of the 78-kDa glucose-regulated protein/ immunoglobulin-binding protein (GRP78/BiP) inhibits tissue factor procoagulant activity. The Journal of Biological Chemistry. 278: 17438-17447.

Weinstein, E. A., Li, H., Lawson, J. A., Rokach, J., Fitzgerald, G. A., Axelsen, P. H. (2000). Prothrombinase acceleration by oxidatively damaged phospholipids. J. Biol. Chem. 275: 22925-22930.

Westmuckett, A. D., Lupu, C., Roquefeuil, S., Krausz, T., Kakkar, V. V., Lupu, F. (2000). Fluid flow induces upregulation of synthesis and release of tissue factor pathway inhibitor in vivo. Arterioscler. Thromb. Vasc. Biol. 20: 2474-2482.

White, R. H. (2003). The epidemiology of venous thromboembolism. Circulation. 107, 14-18.

Wiersma, V. R., M. Michalak, T. M. Abdullah, E. Bremer and P. Eggleton (2015). "Mechanisms of Translocation of ER Chaperones to the Cell Surface and Immunomodulatory Roles in Cancer and Autoimmunity." Front Oncol 5: 7.

Wiersma, V. R., M. Michalak, T. M. Abdullah, E. Bremer and P. Eggleton (2015). "Mechanisms of Translocation of ER Chaperones to the Cell Surface and Immunomodulatory Roles in Cancer and Autoimmunity." Front Oncol 5: 7.

Wiertz, E. J., Tortorella, D., Bogyo, M., Yu, J., Mothes, W., Jones, T. R., Rapoport, T. A., Ploegh, H. L. (1996). Sec61-mediated transfer of a membrane protein from the endoplasmic reticulum to the proteosome for destruction. Nature. 384: 432-438.

Wiest, D. L., Bhandoola, A., Punt, J., Kreibich, G., McKean, D., Singer, A. (1997). Incomplete endoplasmic reticulum (ER) retention in immature thymocytes as revealed by surface expression of "ER-resident" molecula chaperones. Proc. Natl. Acad. Sci. 94: 1884-1889.

Wilcox, J.N., Smith, K. M., Schwartz, S. M., Gordon, D. (1989). Localization of tissue factor in the normal vessel wall and in the atherosclerotic plaque. Proc Natl Acad Sci USA. 86: 2839-2843.

Wolberg, A. S., Kon, R. H., Monroe, D. M., Ezban, M., Roberts, H. R., Hoffman, M. (2000). Deencryption of cellular tissue factor is independent of its cytoplasmic domain. Biochem. Biophys. Res. Comm. 272: 332-336.

Wolberg, A. S., Monroe, D. M., Roberts, H. R., Hoffman, M. R. (1999). Tissue factor de-encryption: ionophore treatment induces changes in tissue factor activity by phosphatidylserine-dependent and -independent mechanisms. Blood Coagulation & Fibrinolysis. 10: 201-210.

Xiao, G., Chung, T. F., Fine, R. E., Johnson, R. J. (1999)(b). Calreticulin is transported to the surface of NG108-15 cells where it forms surface patches and is partially degraded in an acidic compartment. J. Neurosci. Res. 58: 652-662.

Xiao, G., Chung, T. F., Pyun, H. Y., Fine, R. E., Johnson, R. J. (1999)(a). KDEL proteins are found on the surface of NG108-15 cells. Mol. Brain Res. 72: 121-128.

Yu, J. L., May, L., Lhotak, V., Shahrzad, S., Shirasawa, S., Weitz, J. I., Coomber, B. L., Mackman, N., Rak, J. W. (2005). Oncogenic events regulate tissue factor expression in colorectal cancer cells: implications for tumourprogression and angiogenesis. Blood. 105: 1734-1741.

Yu, Z., Luo, H., Hu, W., Mattson, M. P. (1999). The endoplasmic reticulum stress-resoinsive protein GRP78 protects neurons against excitotoxicity and apoptosis: suppression of oxidative stress and stabilization of calcium homeostasis. Exp. Neurol. 155: 302-314.

Zacharias, D. A., Violin, J. D., Newton, A. C., Tsien, R. Y. (2002). Partitioning of lipidmodified monomeric GFPs into membrane microdomains of live cells. Science. 296: 913-916.

Zangari, M., Barlogie, B., Anaissie, E., Saghafifar, F., Eddlemon, P., Jacobson, J., Lee, C. K., Thertulien, R., Talamo, G., Thomas, T., Van Rhee, F., Fassas, A., Fink, L., Tricot, G. (2004). Deep vein thrombosis in patients with multiple myeloma treated with thalidomide and chemotherapy: effects of prophylactic and therapeutic anticoagulation. Br J Haematol. 126: 715-721.

Zhang, J., Ding, J., Zhang, X., Shao, X., Hao, Z. (2005). Regulation of vascular endothelial growth factor (VEGF) production and angiogenesis by tissue factor (TF) in SGC-7901 gastric cancer cells. Cancer Biol Ther. 4: 769-772.

Zhang, Y., Deng, Y., Luther, T., Muller, M., Ziegler, R., Waldherr, R., Stern, D. M., Nawroth, P. P. (1994). Tissue factor controls the balance of angiogenic and antiangiogenic properties of tumourcells in mice. J Clin Invest. 94: 1320-1327.

Zhou J., Lhotak, S., Hilditch, B. A., Austin, R. C. (2005). Activation of the unfolded protein response occurs at all stages of atherosclerotic lesion development in apolipoprotein E-deficient mice. Circulation. 111: 1814-1821.

Zwaal, R. F., Comfurius, P., Bevers, E. M. (2005). Surface exposure of phosphatidylserine in pathological cells. Cell Mol Life Sci. 62: 971-988.

Zwaal, R. F., Schroit, A. J. (1997). Pathophysiologic implications of membrane phospholipid asymmetry in blood cells. Blood. 89: 1121-1132.